

THE CELLULAR AND MECHANISTIC STUDY OF NISIN
INHIBITION OF *BACILLUS ANTHRACIS* SPORE OUTGROWTH, NISIN
ALTERATION OF INFECTION, AND NATIVE PRODUCER IMMUNITY

BY

IAN M. GUT

DISSERTATION

Submitted in partial fulfillment of the requirements
for the degree of Doctor of Philosophy in Microbiology
in the Graduate College of the
Univeristy of Illinois at Urbana Champaign, 2011

Urbana, Illinois

Doctoral Committee:

Professor Steven R. Blanke, Director of Research
Professor Wilfred A. van der Donk, Chair
Professor James A. Imlay
Professor Gary J. Olsen
Associate Professor Brenda A. Wilson

ABSTRACT

A critical step during *Bacillus anthracis* infection is the outgrowth of germinated spores into vegetative bacilli that proliferate and disseminate rapidly within the host. An important challenge exists for developing chemotherapeutic agents that act upon and kill *B. anthracis* immediately after germination initiation when antibiotic resistance is lost, but prior to the outgrowth into vegetative bacilli, which is accompanied by toxin production. Chemical agents must also function in a manner refractive to the development of antimicrobial resistance. In this thesis we have identified the lantibiotics as a class of chemotherapeutics that are predicted to satisfy these two criteria. The objective of this thesis was to evaluate the efficacy of nisin, a prototypical lantibiotic, in prevention of outgrowth of germinated *B. anthracis* spores. Like all lantibiotics, nisin is a ribosomally translated peptide that undergoes post-translational modification to form (methyl)lanthionine rings that are critical for antimicrobial activity. Our studies indicate that nisin rapidly inhibits the *in vitro* outgrowth of germinated *B. anthracis* Sterne 7702 spores. Although germination initiation was shown to be essential for nisin-dependent antimicrobial activity, nisin did not inhibit or promote germination initiation. Nisin irreversibly killed germinated spores by blocking the establishment of a membrane potential and oxidative metabolism, while not affecting the dissolution of the outer spore structures. The membrane permeability of the spore was increased by nisin, but germinated spores did not undergo full lysis. Nisin was demonstrated to localize to lipid II, which is the penultimate precursor for cell wall biogenesis. This localization suggests two

possible independent mechanisms of action, membrane pore formation and inhibition of peptidoglycan synthesis. Structure-activity studies with a truncated form of nisin lacking the two C-terminal (methyl)lanthionine rings and with non-pore forming mutants indicated that membrane disruption is essential for nisin-dependent inhibition of spore outgrowth to prevent membrane potential establishment. Finally, utilizing an *in vitro* infection model, it was shown that nisin reduced the viability of *B. anthracis* spores within an infection resulting in increased survival of immune cells while reducing infection-mediated cytokine expression. Fluorescence microscopy indicated that nisin localizes with spores within phagosomes of peritoneal macrophages in germinating conditions. These data demonstrate the effectiveness of nisin, as a model lantibiotic, for preventing spore outgrowth. It is speculated that nisin targeting of lipid II, resulting in membrane perturbations, may be effective at inhibiting the outgrowth of spores prepared from bacteria across a number of species.

ACKNOWLEDGEMENTS

First and foremost, I would like to demonstrate immense gratitude to my advisors Professors Steven R. Blanke and Wilfred A. van der Donk. Both advisors have been extremely supportive and nurturing in effort to instill good laboratory practice, analytical skills, and a drive to investigate all scientific questions and problems thoroughly. The combination of microbiology and chemistry advisors has fostered a grasp of biology, chemistry, and biochemistry that would otherwise be impossible. I am truly honored and humbled to be a member of both laboratories and appreciate the tremendous opportunity to work with both of these men.

Thank you to my dissertation committee, Professors Brenda A. Wilson, James A. Imlay, and Gary J. Olsen, for their support and encouragement during my graduate research. I appreciate their challenging questions that require a strong knowledge of both lantibiotics and bacterial pathogenesis fields as well as a broad understanding of microbiology and chemistry as a whole. I appreciate their commitment to excellence, and I am proud to be a member of the microbiology graduate program at the University of Illinois at Urbana-Champaign.

The National Institutes of Health, National Institutes of Allergy and Infectious Disease, and the Howard Hughes Medical Institute generously funded my projects. It was my great privilege to be selected for the Predoctoral Chemistry-Biology Interface Training Program and the James R. Beck Microbiology Graduate Fellowship.

A great thank you goes out Dr. Barbara Pilas and Ben Montez from the R. J. Carver Biotechnology Center at the University of Illinois – Urbana/Champaign (UIUC) for assistance with flow cytometry. Furthermore, I would like to acknowledge the assistance of Lou Ann Miller from the Center for Microscopic Imaging, within Material Sciences at the UIUC for assistance with TEM. I would also like to thank the members of Mass Spectrometry, J. Carver Metabolomics, and Protein Science facilities in conjunction with those already listed because without their help and training my research would not have been possible.

I would like to thank past and present members of the Blanke laboratory particularly Dr. Angela Prouty, Dr. Michael Prouty, Dr. Tamilselvam Batcha, Amandeep Gargi, and Prashant Jain. I greatly appreciate the patience and understanding shown during my early research years. All the lessons learned have helped shaped the research that I performed. Also, the laboratory would never be as enjoyable without the laughs that came from working with friends.

I would like to thank past and present members of the van der Donk laboratory particularly Dr. Matthew Levensgood and Kevin Clark for helping a microbiologist do some chemistry. I greatly appreciate the help that Neha Garg provided in the construction and purification of nisin variants. Furthermore, I would like to thank Dr. Leigh Ann Furgerson Ihnken, Trent Oman, and Juan Velasquez for their insight and a good discussion. I would also like to thank Dr. Christopher Thibodeaux for his interpretation of Nisl parameters. Lastly, I would like to include John Hung, Patrick Knerr, Dr. Gabby Thibodeaux, and Noah Bindmann with those already listed for providing a great work environment that

made it enjoyable to perform research. Lab would not be the same without good stories and many laughs.

I would like to extend a special thanks to Martha Freeland who was always there to help with any administrative detail and kept the laboratory and CBI program running smoothly as possible. Further more I would like to thank Deb LeBaugh and Diane Tsevelekos for their hard work and dependability as the staff of the microbiology department. These ladies did a wonderful job of making my graduate career run smoothly, limiting and preventing administrative headaches accompanying graduate research.

I greatly appreciate the hard work put forth by Brett Chrabot, Paul Dilfer, and Stephanie Czeschin who are wonderful undergraduates that I mentored during my graduate career. They performed as exemplary undergraduate researchers who successfully completed challenging research goals, and they were always ready to provide an extra helping hand when asked. I always enjoyed and appreciated the discussions we had, which included academic, research, and extra curricular topics that stimulated the mind and many laughs.

An immense amount of gratitude and appreciation goes out to my family particularly my parents for always caring and providing an ear to vent my frustration when things did not work in the laboratory. Without their support and encouragement, I would have never been able to achieve the goal that I have attained. I would also like to thank the my grandmothers, Anna and Rozalia, for always pointing out that a good education was the number one tool to having a successful professional life, and their unconditional support has always been

welcomed and appreciated. To Erik, Marnie, Gus, and Mary Jane, thank you for always showing interest and providing encouragement because it truly takes a whole family to help raise a child.

Finally, I would like to bestow my deepest and most heart felt gratitude to Bojana, my wife. She was the rock to stand on when times were tough, and she was the first one to smile and provide congratulations when successes were achieved. I greatly value her ability to make me smile no matter the situation and the critical review of my ideas, rationale, and papers. She instilled an intense drive within me to achieve all my goals while keeping me humble and grounded. Her support and love has been immeasurable, and she makes me want to improve every part of myself. Thank you from the bottom of my heart for everything.

TABLE OF CONTENTS

LIST OF FIGURES	xviii
LIST OF TABLES	xxiv
CHAPTER 1: THE PATHOGEN <i>BACILLUS ANTHRACIS</i> AND THE LANTIBIOTIC NISIN.....	1
1.1 <i>Bacillus anthracis</i> endospore	1
1.2 <i>Bacillus anthracis</i> spore germination.....	5
1.3 <i>B. anthracis</i> spore infection of immune cells	6
1.4 Virulence factors of <i>B. anthracis</i>	8
1.5 Antibiotic resistance and current treatments of <i>B. anthracis</i>	13
1.6 Inhibition of bacterial spores.....	14
1.7 Lantibiotics	16
1.8 Nisin biosynthesis	19
1.9 Nisin target and mode of action.....	22
1.10 Nisin and subtilin immunity and regulation of biosynthesis	26
1.11 Antimicrobial resistance to nisin	30
1.12 Studies described in this thesis.....	31
1.13 References.....	32
CHAPTER 2: INHIBITION OF <i>BACILLUS ANTHRACIS</i> SPORE OUTGROWTH BY NISIN	46
2.1 Introduction	46
2.2 Results	48
2.2.1 Purification of nisin	48
2.2.2 Growth inhibition by nisin	49

2.2.3	Nisin does not inhibit germination initiation	52
2.2.4	Germination initiation is required for the inhibitory action of nisin	54
2.2.5	Nisin prevents spore development into vegetative bacilli	56
2.2.6	Spores incubated with nisin do not produce lethal toxin	59
2.2.7	The action of nisin prevents spores from becoming metabolically active	61
2.2.8	The effects of nisin action on membrane integrity	65
2.2.9	Nisin does not prevent spore remodeling during germination	67
2.2.10	Structural evaluation of nisin inhibition of bacilli and protoplasts	68
2.2.11	Structural evaluation of nisin inhibition of spores	71
2.2.12	Effect of delayed addition of nisin on growth	72
2.2.13	pH effects on <i>B. anthracis</i> spore germination	73
2.3	Discussion	74
2.4	Materials and Methods	78
2.4.1	Spore preparations	78
2.4.2	Nisin purification	78
2.4.3	Culturing <i>B. anthracis</i> spores	79
2.4.4	Determination of IC ₅₀ and IC ₉₀ values of nisin against endospores	80
2.4.5	CFU quantification	81
2.4.6	Spore hydration	81
2.4.7	Heat resistance	81

2.4.8	Differential interference contrast microscopy	82
2.4.9	Immunoblot analysis	82
2.4.10	Oxidative metabolism.....	83
2.4.11	Membrane potential	83
2.4.12	Membrane integrity	84
2.4.13	Quantification of dipicolinic acid (DPA; 2,6-pyridinecarboxylic acid).....	84
2.4.14	Transmission electron microscopy (TEM).....	85
2.4.15	Scanning electron microscopy (SEM).....	85
2.4.16	Statistics	85
2.5	References.....	86
CHAPTER 3: MECHANISM OF NISIN INHIBITION OF <i>BACILLUS ANTHRACIS</i> SPORE OUTGROWTH		92
3.1	Introduction	92
3.2	Results	94
3.2.1	Fluorescently-labeled nisin analogs bind to lipid II and have similar properties as wild type nisin	94
3.2.2	Nisin binds to lipid II of germinated spores.....	96
3.2.3	Lipid II binding is not sufficient to inhibit outgrowth	108
3.2.4	Lipid II binding is associated with nisin-dependent loss of membrane potential	112
3.2.5	Lipid II binding is associated with nisin-dependent alterations in membrane integrity	114
3.2.6	Modification of the nisin hinge region, but not Dha5, results in the loss of outgrowth inhibition.....	116
3.2.7	Membrane depolarization inhibits spore outgrowth	119

3.3 Discussion.....	121
3.4 Materials and Methods.....	121
3.4.1 Spore preparations.....	121
3.4.2 Nisin purification.....	122
3.4.3 Labeling of nisin and vancomycin	122
3.4.4 Truncation of nisin with chymotrypsin	124
3.4.5 Culturing <i>B. anthracis</i> spores	125
3.4.6 Characterization of antibiotic effects on germination and outgrowth	126
3.4.7 Differential interference contrast (DIC) and epi- fluorescence microscopy.....	126
3.4.8 Functional competition assay.....	127
3.4.9 Competition binding assay	127
3.4.10 Site-directed mutagenesis	128
3.4.11 Over expression of <i>nisA</i> and mutants with <i>in vivo</i> posttranslational modifications	130
3.4.12 Cleavage of modified prenisin with trypsin and purification of nisin variants.....	132
3.5 References.....	134
 CHAPTER 4: CHARACTERIZATION OF NISIN-MEDIATED MEMBRANE DISRUPTION UTILIZING <i>BACILLUS ANTHRACIS</i> SPORES	 137
4.1 Introduction	137
4.2 Results	138
4.2.1 Nisin induces the flow of ions across the spore membrane.....	138

4.2.2	Nisin mediates small molecule movement across the spore membrane	141
4.2.3	Nisin does not induce spore lysis	142
4.2.4	Nisin renders the germinating spore metabolically inactive	144
4.2.5	Blocking nisin-mediated membrane disruption with ionic channel inhibitors	145
4.2.6	Blocking nisin-mediated membrane disruption with PEGs	149
4.2.7	Blocking the nisin pore does not alter spore viability or outgrowth	153
4.3	Discussion.....	154
4.4	Materials and Methods	156
4.4.1	Spore preparations.....	156
4.4.2	Nisin purification.....	157
4.4.3	Culturing <i>B. anthracis</i> spores	157
4.4.4	CFU quantification.....	157
4.4.5	Spore hydration.....	158
4.4.6	Heat resistance	158
4.4.7	Oxidative metabolism.....	158
4.4.8	Membrane integrity	159
4.4.9	Potassium release.....	159
4.4.10	Chloride release	160
4.4.11	Cell lysis - glucose-6-phosphate dehydrogenase (G6PD) release	160
4.4.12	Cell lysis - DNA release	161

4.4.13 Statistics	161
4.5 References.....	162
CHAPTER 5: <i>BACILLUS ANTHRACIS</i> SPORE INTERACTIONS WITH MAMMALIAN CELLS: EFFECTS OF MEDIUM COMPOSITION ON THE OUTCOME OF AN <i>IN VITRO</i> INFECTION	
5.1 Introduction	164
5.2 Results	167
5.2.1 The composition of cell culture medium influences the germination and outgrowth of <i>B. anthracis</i> spores	167
5.2.2 Effects of pre-conditioned culture medium on the germination state of <i>B. anthracis</i> spores	176
5.2.3 Mammalian cells remain viable and functional for at least 4 h in FBS-free culture medium	179
5.2.4 Germination state of spores does not alter the uptake by mammalian cells.....	181
5.2.5 Germination state of spores influences the number of viable, intracellular <i>B. anthracis</i>	183
5.2.6 Germination state of <i>B. anthracis</i> spores influences the viability of RAW264.7 cells during <i>in vitro</i> infection	185
5.3 Discussion.....	187
5.4 Materials and Methods.....	189
5.4.1 Spore preparations and fluorescent labeling.....	189
5.4.2 Mammalian cell culture	189
5.4.3 Evaluation of <i>B. anthracis</i> spore germination in cell culture media.....	190
5.4.4 Pre-conditioning of cell culture media	191
5.4.5 Mammalian cell viability	191
5.4.6 Flow cytometry.....	192

5.4.7 Cell cycle assay	192
5.4.8 Mammalian cell metabolism assay.....	193
5.4.9 <i>In vitro</i> infection of mammalian cells with <i>B. anthracis</i>	193
5.4.10 Quantification of <i>B. anthracis</i> uptake by mammalian cells.....	194
5.4.11 Quantification of viable, intracellular <i>B. anthracis</i>	196
5.4.12 Statistics	196
5.5 References.....	197
CHAPTER 6: NISIN MODULATION OF <i>BACILLUS ANTHRACIS</i> SPORE AND IMMUNE CELL INTERACTIONS AND SURVIVAL	202
6.1 Introduction	202
6.2 Results	205
6.2.1 Nisin induced dose dependent clearance of viable <i>B. anthracis</i>	205
6.2.2 Nisin prevents <i>B. anthracis</i> proliferation in post infection treatments.....	208
6.2.3 Nisin increased the survival of immune cells.....	212
6.2.4 The presence of nisin during infection reduced spore association and internalization	215
6.2.5 Nisin interacted with spores during an infection	229
6.2.6 Nisin reduced cytokine release during an infection	230
6.3 Discussion.....	234
6.4 Materials and Methods.....	238
6.4.1 Spore preparations and fluorescent labeling.....	238
6.4.2 CFU quantification.....	239
6.4.3 Heat resistance	239

6.4.4	Nisin purification.....	239
6.4.5	Labeling of nisin	239
6.4.6	Cell culture	240
6.4.7	Spore interactions and uptake by mammalian cells	240
6.4.8	Mammalian cell viability	242
6.4.9	Fluorescence quenching of Alexa Fluor AF488-spores.....	242
6.4.10	Flow cytometry.....	242
6.4.11	Quantification of cell-associated viable <i>B. anthracis</i>	242
6.4.12	Epi-Fluorescence microscopy	243
6.4.13	Cytokine release - cytometric array assay	243
6.4.14	Cytokine release - ELISA.....	244
6.4.15	Statistics	244
6.5	References.....	244
CHAPTER 7: NISIN INTERACTION WITH IMMUNITY PROTEINS AND LOCALIZATION		249
7.1	Introduction	249
7.2	Results	251
7.2.1	Cloning and tagging of immunity genes	251
7.2.2	GST purification of Nisl Δ 1-19 and Spal Δ 1-22	252
7.2.3	Nickel affinity purification of Spal Δ 1-22	254
7.2.4	Circular dichroism of nisin and Nisl Δ 1-19.....	254
7.2.5	Oligomerization analysis of Nisl Δ 1-19.....	256
7.2.6	Lipid II localization within <i>B. subtilis</i> ATCC 6633.....	257

7.2.7 Purification of subtilin from <i>B. subtilis</i> ATCC 6633	260
7.3 Discussion.....	261
7.4 Materials and Methods.....	264
7.4.1 Cloning of immunity genes.....	264
7.4.2 Transformation of <i>Bacillus subtilis</i> : starvation	275
7.4.3 GST purification of Nisl Δ 1-19 and Spal Δ 1-22	276
7.4.4 Nickel affinity purification of Spal Δ 1-22	278
7.4.5 Purification of nisin and subtilin.....	280
7.4.6 Labeling of nisin and vancomycin	281
7.4.7 Epi-Fluorescence microscopy	281
7.4.8 Circular dichroism	282
7.4.9 Oligomerization analysis - size exclusion chromatography native gel electrophoresis.....	282
7.4.10 Immunoblot analysis	283
7.4.11 Structure prediction.....	284
7.4.12 Statistics	284
7.5 References.....	284
CHAPTER 8: CONCLUSIONS AND FUTURE DIRECTIONS	287
8.1 Introduction	287
8.2 Summary of Results.....	288
8.2.1 Characterization of the consequences of <i>Bacillus anthracis</i> exposure to nisin	288
8.2.2 Nisin inhibits outgrowth via membrane disruption	290
8.2.3 Nisin is protective with respect to <i>in vitro</i> infection of mammalian immune cells.....	291

8.2.4 Localization and activity of immunity proteins for protection against lantibiotics in producing organisms	292
8.3 Conclusions and Future Directions	292
8.4 References.....	295
CURRICULUM VITAE.....	297

LIST OF FIGURES

FIGURE	PAGE
Figure 1.1. <i>Bacillus anthracis</i> endospore structure	4
Figure 1.2. Events of germination	6
Figure 1.3. Model of cellular toxin effects.....	12
Figure 1.4. Common non-canonical amino acids found in lantibiotics	18
Figure 1.5. Representative lantibiotic structures	19
Figure 1.6. Formation of (methyl)lanthionine rings	21
Figure 1.7. Biosynthesis of nisin.....	21
Figure 1.8. Modes of action for nisin	25
Figure 1.9. Schematic representation illustrating nisin biosynthesis, regulation, and immunity within a bacterial cell	29
Figure 2.1. Nisin Purification	48
Figure 2.2. Nisin inhibition of <i>B. anthracis</i> growth	51
Figure 2.3. DIC microscopy of nisin inhibition of <i>B. anthracis</i> bacilli....	51
Figure 2.4. Effect of nisin on the loss of optical density.....	53
Figure 2.5. Effect of nisin on the loss of heat resistance	54
Figure 2.6. Germination is required for the inhibitory action of nisin....	55
Figure 2.7. The inhibitory action of nisin is irreversible.....	56
Figure 2.8. <i>B. anthracis</i> spores do not develop into vegetative bacilli in the presence of nisin	57
Figure 2.9. Effect of nisin on toxin expression.....	60
Figure 2.10. Toxin association with organism and nisin induced precipitation of toxin	61

Figure 2.11. Effect of nisin and ciprofloxacin on oxidative metabolism establishment.....	63
Figure 2.12. Effect of nisin and ciprofloxacin on membrane potential establishment.....	64
Figure 2.13. Effect of nisin and ciprofloxacin on membrane integrity	66
Figure 2.14. Effects of nisin on spore remodeling during germination...	68
Figure 2.15. Structural evaluation of nisin inhibition of bacilli and protoplasts	70
Figure 2.16. Structural evaluation of nisin inhibition of spores	71
Figure 2.17. Effect of delayed addition of nisin on growth.....	73
Figure 2.18. pH effects on <i>B. anthracis</i> spore germination	74
Figure 3.1. Structures of nisin, vancomycin, and lipid II	93
Figure 3.2. Effect of vancomycin on germination	95
Figure 3.3. Localization of labeled nisin and vancomycin on <i>B. anthracis</i> vegetative cells.....	96
Figure 3.4. Nisin and vancomycin localization on spores.....	98
Figure 3.5. Quantification of nisin and vancomycin co-localization by Pearson's coefficient	99
Figure 3.6. Localization of Lipid II in sub-inhibitory concentration of nisin.....	100
Figure 3.7. Effect of fluorescent label on antibiotic localization	101
Figure 3.8. Conditional effects on antibiotic localization.....	102
Figure 3.9. Competition assays with nisin and vancomycin	105
Figure 3.10. Cortex hydrolase mutants do not alter nisin and vancomycin co-localization at lipid II	107
Figure 3.11. Utilizing biotin or fluorescently labeled nisin to identify or isolate a covalent protein target	108

Figure 3.12. Lipid II binding is not sufficient for outgrowth inhibition - growth curves.....	110
Figure 3.13. Lipid II binding is not sufficient for outgrowth inhibition - microscopy.....	111
Figure 3.14. Lipid II binding is not sufficient to inhibit membrane potential establishment via membrane disruption	113
Figure 3.15. C-terminal region of nisin is essential for preventing a membrane potential, spore outgrowth, and membrane disruption	114
Figure 3.16. Lipid II binding is not sufficient to disrupt metabolic function during germination.....	115
Figure 3.17. A flexible hinge region, not Dha5, is essential for preventing a membrane potential, spore outgrowth, and membrane disruption	118
Figure 3.18. Outgrowth inhibition results from membrane depolarization.....	120
Figure 3.19. Fluorescent labeling of nisin and vancomycin.....	123
Figure 3.20. Chymotrypsin cleavage nisin and purification of c-nisin	125
Figure 3.21. Cleavage of modified nisin and purification of h-nisin variants	133
Figure 4.1. Nisin induced ion efflux from germinating spores.....	141
Figure 4.2. Nisin induced PicoGreen TM uptake	142
Figure 4.3. Nisin does not induce G6PD release	143
Figure 4.4. Nisin does not induce DNA release.....	144
Figure 4.5. Nisin prevents the establishment of an oxidative metabolism.....	145
Figure 4.6. DIDS blocks nisin-mediated ion and small molecule movement across the spore membrane.....	148
Figure 4.7. DIDS reduced nisin inhibition of oxidative metabolism.....	149

Figure 4.8.	PEGs block nisin-mediated ion and small molecule movement across the spore membrane.....	152
Figure 4.9.	PEGs did not reduce nisin inhibition of oxidative metabolism.....	153
Figure 4.10.	Channel blockers and PEGs do not increase <i>B. anthracis</i> viability in the presence of nisin.....	154
Figure 5.1.	FBS in cell culture media promotes germination and outgrowth of <i>B. anthracis</i> spores.....	169
Figure 5.2.	Rich media and amino acids promote germination and outgrowth of <i>B. anthracis</i> spores.....	171
Figure 5.3.	<i>B. anthracis</i> spore germination and outgrowth in FBS-free cell culture media.....	173
Figure 5.4.	The effects of pre-conditioned culture medium on the germination state of <i>B. anthracis</i> spores	178
Figure 5.5.	Viability, cell cycle progression, and metabolic activity of RAW264.7 cells cultured under germinating or non-germinating conditions	180
Figure 5.6.	Uptake of <i>B. anthracis</i> spores into mammalian cells cultured under germinating or non-germinating conditions.....	182
Figure 5.7.	The germination state of spores influences the viability of intracellular <i>B. anthracis</i>	184
Figure 5.8.	The germination state of spores influences the viability of <i>B. anthracis</i> -infected cells	186
Figure 6.1.	Nisin induced dose dependent clearance of viable <i>B. anthracis</i>	206
Figure 6.2.	Nisin induced dose dependent clearance of viable <i>B. anthracis</i> vegetative cells.....	207
Figure 6.3.	Nisin mediated greater clearance of viable <i>B. anthracis</i> than gentamicin.....	208
Figure 6.4.	Nisin prevented <i>B. anthracis</i> proliferation in post infection treatments	210

Figure 6.5.	Nisin prevented <i>B. anthracis</i> proliferation when added prior to, during or post spore infection of macrophages	211
Figure 6.6.	Nisin increased the short term survival of immune cells....	213
Figure 6.7.	Nisin increased the short term survival of immune cells when infected by vegetative cells.....	213
Figure 6.8.	Nisin increased the short term survival of immune cells when added prior to, during or post spore infection of macrophages	214
Figure 6.9.	Nisin increased the long term survival of immune cells.....	214
Figure 6.10.	Nisin reduced spore interaction with immune cells.....	217
Figure 6.11.	Quantification of spore per infected macrophages.....	217
Figure 6.12.	Nisin altered spore interaction with immune cells when added prior to, during or post spore infection of macrophages	218
Figure 6.13.	Nisin effect on spore fluorescence	218
Figure 6.14.	Nisin does not alter spore interactions with nisin added after infection of RAW264.7 cells.....	219
Figure 6.15.	Addition of nisin altered the interaction between inert beads and immune cells	220
Figure 6.16.	Nisin reduced bacilli interaction with immune cells.....	220
Figure 6.17.	Nisin reduced spore infection of immune cells within the population	222
Figure 6.18.	Nisin does not spore interaction with nisin post immune cell infection	222
Figure 6.19.	Nisin altered spore interaction with immune cells when added prior to, during or post spore infection of macrophages	223
Figure 6.20.	Nisin reduced bacilli infection of immune cells within the population	224

Figure 6.21. Addition of nisin altered immune cells internalization of inert beads	225
Figure 6.22. Nisin altered spore binding to immune cells	227
Figure 6.23. Nisin altered spore binding to immune cells - cytochalasin D infection	228
Figure 6.24. Effect of antibiotics on spore binding - cytochalasin D infection.....	228
Figure 6.25. Nisin interacted with spores during an infection	230
Figure 6.26. Effect of nisin on infection induced cytokine expression - constant infection.....	232
Figure 6.27. Effect of nisin on infection induced cytokine expression - gentamicin protection.....	233
Figure 6.28. Effect of nisin on LPS induced cytokine expression - gentamicin protection.....	234
Figure 7.1. Expression and purification of Nisl Δ 1-19.....	253
Figure 7.2. Expression and purification of Spal Δ 1-22	253
Figure 7.3. Expression and purification of Spal Δ 1-22	254
Figure 7.4. Circular dichroism of nisin and Nisl Δ 1-19.....	256
Figure 7.5. Oligomerization analysis of Nisl Δ 1-19.....	257
Figure 7.6. Optimized lipid II localization within <i>B. subtilis</i> 6633.....	259
Figure 7.7. Purification of subtilin from <i>B. subtilis</i> ATCC 6633	261
Figure 8.1. Model of nisin mode of action	294

LIST OF TABLES

TABLE	PAGE
Table 2.1. IC ₅₀ and IC ₉₀ values of nisin against <i>B. anthracis</i> spores..	50
Table 2.2. Comparison of nisin and ciprofloxacin on the outgrowth of spores	59
Table 3.1. Comparison of nisin and c-nisin outgrowth inhibition	110
Table 3.2. Comparison of outgrowth inhibition by nisin and vancomycin	111
Table 3.3. IC ₅₀ and IC ₉₉ of nisin variants against <i>Micrococcus flavus</i>	117
Table 3.4. Comparison of outgrowth inhibition by nisin variants	119
Table 3.5. Comparison of nisin and FCCP outgrowth inhibition.....	120
Table 3.6. Primer sequences used for mutagenesis	129
Table 3.7. <i>E.coli</i> BL21(DE3) expression plasmids	132
Table 4.1. Effect of indicator dyes on <i>B. anthracis</i> spore germination and viability	139
Table 4.2. Effects of channel blockers, polyethylene glycols, and nisin on phenotypic indicator fluorescence.....	140
Table 4.3. Channel blocker inhibition of the listed phenotypic event as a function of nisin pore formation	147
Table 4.4. PEG inhibition of the several phenotypic events as a function of nisin membrane disruption.....	151
Table 5.1. FBS and cell culture media effects on germination and outgrowth of <i>B. anthracis</i> spores.....	175
Table 5.2. Concentration dependence of FBS induced germination ..	176
Table 7.1. Secondary structure characterization of NisIΔ1-19 and SpaIΔ1-22	255
Table 7.2. Primer sequences cloning LanI immunity proteins	267

Table 7.3.	Cloning of <i>B. subtilis</i> ATCC 6633 SpaI and addition of a C-terminal tag.....	269
Table 7.4.	Cloning of <i>B. subtilis</i> ATCC 6633 SpaF and addition of a C-terminal tag.....	270
Table 7.5.	Cloning of <i>B. subtilis</i> ATCC 6633 SpaI and addition of a fluorescent C-terminal tag	272
Table 7.6.	Cloning of <i>B. subtilis</i> ATCC 6633 SpaF and addition of a fluorescent C-terminal tag	272
Table 7.7.	Cloning of <i>B. subtilis</i> ATCC 6633 SpaI and addition of a fluorescent C-terminal tag	274
Table 7.8.	Cloning of <i>B. subtilis</i> ATCC 6633 SpaF and addition of a fluorescent C-terminal tag	275

CHAPTER 1: THE PATHOGEN *BACILLUS ANTHRACIS* AND THE LANTIBIOTIC NISIN

1.1 *Bacillus anthracis* endospore

B. anthracis is a Gram-positive, endospore forming rod-shaped bacterium and the causative agent of the zoonotic disease anthrax that affects mammals. *B. anthracis* exists both as actively replicating bacilli and as dormant endospores (30, 85). The endospore structure provides resistance to a wide range of chemical and physical assaults, which include but are not limited to chemical treatment, radiation, desiccation, heat, and extremes in pH (83, 99, 112). The endospore is formed in nutrient-deprived conditions allowing survival over extended periods of time, which otherwise would not be possible as bacilli (30). Despite the ability of *B. anthracis* to germinate and exist in soil (108), *B. anthracis* prefers to germinate and grow within a mammalian host gaining access to nutrient rich environments within the host via inhalation, ingestion, or skin abrasions (45). As an endospore, *B. anthracis* has the potential for long-term storage and mass dispersal as a bio-terrorist agent.

Bacterial endospores are formed during nutrient deprivation, and the molecular composition and structure of the endospore is vastly different when compared to the vegetative cell (95). Since *B. anthracis* is a Gram-positive bacterium, the external structure of the bacilli consists of a cell membrane and a peptidoglycan cell wall (109). *B. anthracis* bacilli are also surrounded by a proteinaceous S-layer followed by a poly-D-glutamic acid capsule in virulent strains such as Ames and New Hampshire (Figure 1.1A). These structures provide protection from environmental insults, and in the case of the poly-D-

glutamic acid capsule, it provides anti-phagocytic properties (64). The endospore external structure consists of a dual membrane that is separated by a thick peptidoglycan cell wall consisting of two distinct layers collectively known as the cortex (Figure 1.1B & C) (20, 76, 98, 121). The first layer of the cortex originates from the same repeating sugar subunits, N-acetylglucosamine and N-acetylmuramic acid, and protein cross linkers, L-Ala - D-Glu - Dap -D-Ala - D-Ala, as the bacilli cell wall. The second thicker and outer portion of the cortex includes additional sugars, muramic acid σ -lactam or muramic acid-alanine, within the sugar repeat of the glycan layers (Figure 1.1D) (20, 31, 40, 56, 70, 76, 98). The outer structure of the spore continues with two proteinaceous layers, the inner and outer spore coats, consisting of over 60 proteins, and all of the outer spore structures encapsulate the inner core containing the DNA (41). The core of the spore is a highly dehydrated environment and is crystalline in nature due to the high concentration of dipicolinic acid (DPA) chelated to Ca^{2+} , which ultimately renders the spore metabolically inactive (62, 121). In addition, the DNA is wrapped within small acid soluble proteins (SASP) to protect the DNA from damage and mutagenesis from chemical agents or radiation (86, 119, 121, 122). In pathogenic *Bacillus* strains such as *B. anthracis* and *B. cereus*, the outer most layer is the glycopeptide-composed exosporium, which is loosely anchored to the outer spore coat (30, 121). These dramatic morphological differences between endospores and bacilli confer upon the former resistance to chemical, enzymatic, and mechanical assaults (86, 122). Endospores also contain membrane bound protein receptors to identify the presence of a

favorable growth environment by identifying the presence of L-Ala, which alone can induce germination, or by detecting a combination of amino acids, nucleotides, and sugars for germination induction. Inactive lytic enzymes, which are required for spore coat and cortex hydrolysis, are activated during germination (86, 87, 121). In the case of cortex hydrolysis, the lytic enzymes recognize the σ -lactam within the repeating sugar units (Figure 1.1D), so that only the outer portion of the cortex is degraded leaving the innermost primordial cell wall. This selective degradation of the cortex provides the germinated and outgrowing spore shape and resistance to osmotic stress (31, 40, 56, 70).

Spores are metabolically dormant, lack any detectable enzymatic activity, and are devoid of any high energy molecules such as ATP and NADH (24, 116, 120). As a consequence of the lack of enzymatic activity, the structure of the spore, as discussed above, is designed to protect the DNA that can only be repaired once the spore has returned to life (114, 117-119, 134). Consequently, the particularly formidable structure of the spore and the lack of enzymatic activity renders the spore exceptionally difficult to kill or permanently inhibit (86, 117, 118, 121).

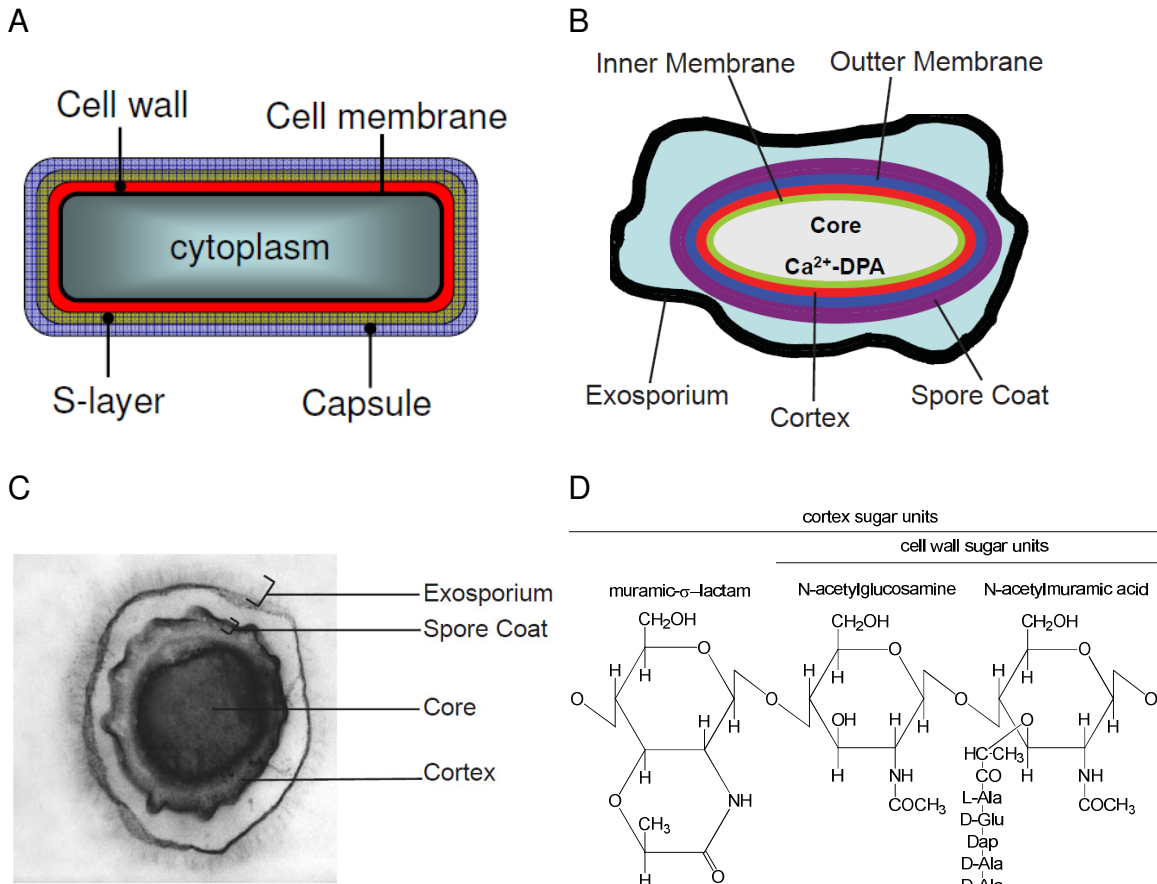


Figure 1.1. *Bacillus anthracis* endospore structure. A. Illustration of *B. anthracis* cells

structure. B. Illustration of *B. anthracis* endospore structure. C. TEM image of dormant *B. anthracis* endospore. Image were taken by Dr. Angela Prouty at 60,000x magnification. B&C. A dormant endospore consists of a core surrounded by a dual membrane, which are separated by a peptidoglycan cortex. The endospore coat is comprised of an inner coat and outer coat, which anchors the outer most layer, the exosporium. The exosporium loosely encapsulates the spore providing significant space between it and the inner structure of the spore (B: light blue). D. Structure of modified hexose sugars utilized within the cell wall (cells and spores) and the cortex (spores) of *B. anthracis*.

1.2 *Bacillus anthracis* spore germination

The series of morphological and biochemical changes that allow for the transition from an endospore to a replicating bacilli are known as germination (Figure 1.2). Germination can be divided into two phases: (1) the loss of dormancy and resistance and (2) reactivation of metabolism (85, 121). This process initiates with binding of germinant to a germination receptor in the membrane of an endospore, and once germination has been initiated, there is an irreversible commitment to progress through the series of events leading to the production of replicative bacilli (86, 121). Germinant binding will initiate a cascade of events beginning with the release of H^+ , monovalent cations Na^+ and K^+ , and Zn^{2+} , followed by the release of dipicolinic acid (DPA) in complex with Ca^{2+} , the establishment of a membrane potential, and the influx of water to hydrate the core. As a consequence of these initial events, endospores become sensitive to heat, desiccation, and chemical treatment and display a loss in refractility within seconds to minutes. Subsequent to core hydration, endospores undergo enzyme-catalyzed cortex hydrolysis and enzymatic degradation of the spore coats thereby providing the germinating endospore with amino acids and sugars for growth. Endospores then establish metabolic processes, break free from the cortex and spore coats, and outgrow into replicating bacilli in approximately 3 hours after germinant binding (86, 87, 98, 121). Furthermore, the spore outgrow is believed to be directionally from one pole shedding the unhydrolyzed cortex, spore coat, and particularly exosporium in the "bottle cap model" (97, 129). It is the act of germination that is essential for spore forming

bacteria to establish an infection within a host since the universal infectious particle is the spore (45, 46).

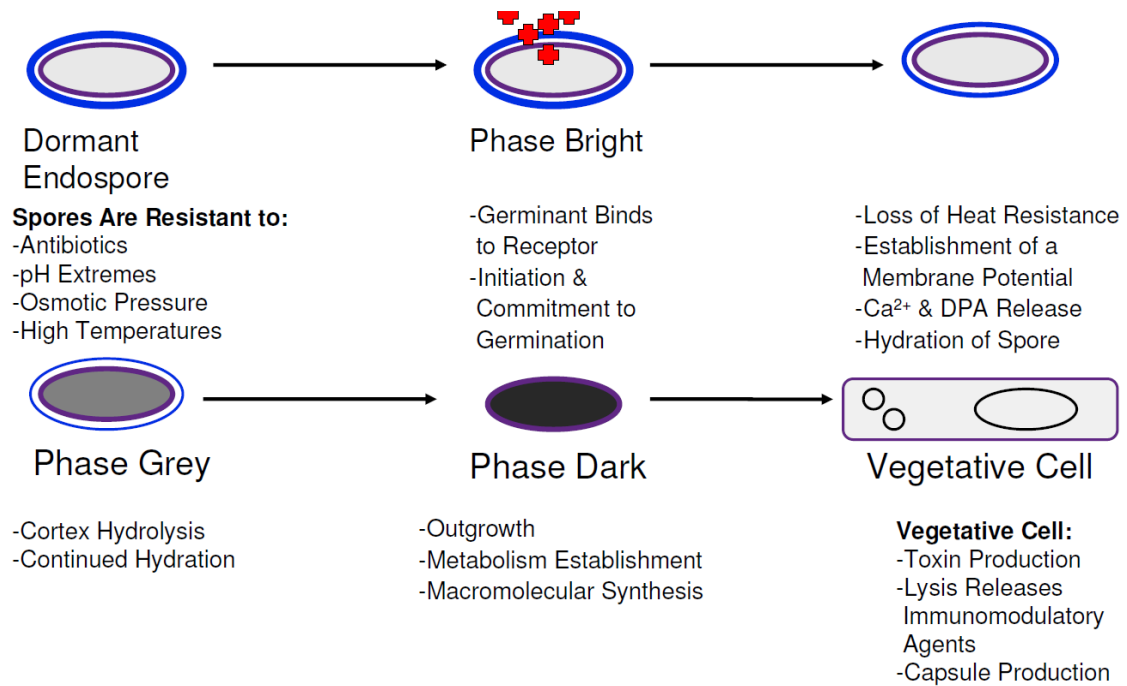


Figure 1.2. Events of germination. The phase bright dormant endospore is resistant to a variety of chemical and physical assaults. Upon binding of a germinant (red), endospores will undergo a series of morphological and chemical changes that allow for the transformation into a metabolically active and replicating vegetative cell. Key events are permanent commitment to germination, establishment of a membrane potential, release of Ca²⁺ and DPA, hydration, cortex hydrolysis, and outgrowth. The result of germination initiation is the loss of heat resistance and refractility.

1.3 *B. anthracis* spore infection of immune cells

Host immune cells play an important role in inhalational anthrax, which is a complex, multistep disease that begins with the deposition of inhaled *Bacillus anthracis* spores within the alveolar space of the lungs. Histopathological studies using several animal infection models revealed that subsequent to spore

inhalation, *B. anthracis* breaches the alveolar epithelial barrier without any clinical evidence of lung injury (131, 135, 137). Interaction between immune cells and *B. anthracis* spores is essential for infection and dissemination of disease within a host especially within an inhalation infection, which is contingent upon spore-immune cell interaction that results in phagocytosis of inhaled spores by alveolar macrophages or dendritic cells sampling the alveolar space. In several animal models, dissemination of infection into the spleen and liver begins with trafficking of spore-containing immune cells to regional lymph nodes followed by the release of *B. anthracis* spores or bacilli into the bloodstream (45, 48, 135). Recent studies have also pointed to the use of alveolar epithelial cells as a potential route of entry into the bloodstream (106). Without medical intervention, the establishment of a systemic infection will result in bacteremia, toxemia, and ultimately death of the host (30, 135).

In addition to the inhalation route of infection, which is the most likely to result in a systemic infection and death of the host, *B. anthracis* can also gain entry into a host via abrasions or open wounds on the skin or through the gastrointestinal tract (30). Infections through either of these portals of entry are significantly less deadly and will manifest themselves through a black eschar or necrotic sore and through hemolytic diarrhea, respectively (6, 30). Furthermore, an untreated cutaneous infection will result in localized swelling followed by regional edema that may affect for example an entire limb (30, 110). In both cases, replicating bacilli will invade the local epithelium resulting in access to the blood stream, and infected host immune cells will also shuttle spores to the

regional lymph nodes providing an additional mechanism by which *B. anthracis* can establish a systemic infection once the blood stream is reached (6, 30, 110). A systemic infection leading to death can be prevented with antibiotic therapy (110).

1.4 Virulence factors of *B. anthracis*

Upon germination and outgrowth, *B. anthracis* utilizes 3 primary virulence factors to establish an infection within a host, which are lethal toxin (LT), edema toxin, and capsule. The two anthrax toxins comprise 3 different proteins: (i) 2 enzymatic proteins - lethal factor (LF) and edema factor (EF) and (ii) a protective moiety - protective antigen (PA) - that allows for interaction and adhesion to target cells for intoxication. This toxin is a classical representation of a multimeric AB toxin, illustrated as A₃B₇. Several enzymatic (A) subunits will utilize the binding proteins (B) as a platform for host cell interaction and entry into the cytosol. LF is a zinc-dependent metalloprotease that cleaves mitogen-activated protein (MAP) kinase kinases, which are cytoplasmic. EF is a calmodulin dependent adenylate cyclase that requires entry into the cytoplasm for activity (Figure 1.3) (3, 147). The results of cellular intoxication by EF and LF are very distinct, which in some cases work in opposite fashion to each other. First, LF intoxication results in reduced antibody production, cytokine expression, and cell proliferation while inducing cell death. In addition to inducing fluid accumulation in tissues as a consequence of the production of cyclic AMP, EF actually activates cell rescue mechanisms such as activating protein kinase A (PKA) and

the CREB transcription factor while inhibiting cytokine expression (135, 136). Lastly, lethal and edema toxins are responsible for receptor mediated toxin killing of immune cells (4, 45-47).

EF and LF reach the cytoplasm of target cells through their interaction with PA, which interestingly induces a controlled and rapid internalization of the toxin oligomer. PA binds specifically to two anthrax toxin receptors, tumor endothelial marker 8 (TEM8, also called ANTXR1) and capillary morphogenesis gene 2 (CMG2, or ANTXR2). These two proteins are type I membrane proteins, which share extensive sequence similarity in both their extracellular and intracellular domains (111, 142). PA, which is produced by *B. anthracis* as an 83 kDa protein (PA83), is cleaved into an 63 kDa form (PA63) by host enzymes such as the furin endoprotease (147). PA63 will subsequently heptamerize into a ring-like structure, which serves as a platform for the binding of any combination of 3 EF and LF subunits (Figure 1.3) (84). The hetero-oligomeric complex, PA-EF/LF and receptors, is phagocytized by the cell and delivered to early endosomes, where the PA oligomer undergoes a conformational change due to the acidification of the endosome that leads to PA loop insertion into the endosomal membrane and pore-formation (147). EF and LF are also sensitive to the acidic pH of endosomes that leads to partial unfolding allowing them to translocate through the lumen of the PA channel entering the host cytoplasm on the other side of the endosomal membrane (23). The processing and oligomerization of PA is required for anthrax toxin internalization, which requires the use of host kinases and ubiquitin ligase. This control of endocytosis is performed by inducing Tyr

phosphorylation of the PA receptors, TEM8 and CMG2, via the eukaryotic src-like kinases, src and fyn. Phosphorylation of the target protein is followed by ubiquitination via the E3 ubiquitin ligase resulting in clathrin-mediated endocytosis (Figure 1.3) (1, 2). Once released from *B. anthracis*, LT and ET exert their cellular effects independent of the bacterium, indicating that inhibition of bacterial growth alone is not sufficient when treating an anthrax infection. In the absence of bacterial growth, toxigenic effects will still lead to toxemia and death, and treatment must prevent toxin expression or inhibit toxin activity (30, 110).

The second major virulence factor of *B. anthracis* is the γ -linked poly-D-glutamic acid capsule. This negatively charged D-amino acid layer surrounds the cell, which can be easily visualized with acid or methylene blue staining, and is directly anchored to the cell wall as linear polymers providing resistance to phagocytosis (72, 110). Moreover, this polymer is weakly immunogenic (42, 104). In addition, *B. anthracis* also has a proteinaceous S-layer to prevent antibody interaction with the bacilli (35, 82), and the cell wall is modified with teichoic or teichuronic acid, in phosphate limiting conditions, to alter the overall charge of the cell wall to a net neutral charge to prevent the attraction of cell membrane disrupting non-specific cationic peptides of the host immune system (38). Consequently, these morphological features more than any other are implicated in bacteremia in conjunction with high growth rates in a nutrient rich environment such as mammalian host sera and blood (30, 110).

The genes for the toxins and the capsule reside on two independent plasmids, pX01 and pX02, respectively. AtxA, a pXO1-encoded protein, is a

global regulator of transcription in *B. anthracis* (65) that strongly activates the expression of the toxin genes, *pagA*, *cya*, and *lef*, and the capsule biosynthetic operon, *capBCADE*, while altering the expression of many other genes contained on the plasmids and in the chromosome (11, 33, 49, 58, 128). The expression of virulence factors requires the presence of CO₂ or bicarbonate, as an *in vitro* surrogate, in conjunction with either elevated temperatures (37 °C) or production of cytochrome C within a host (27, 66, 146). This virulence gene expression is repressed during exponential growth by the growth phase regulator AbrB (107). The presence of both an activator and suppressor allows for tight control of toxin and capsule expression specifically when *B. anthracis* is within a mammalian host (65).

Additional virulence factors and the unique spore structures are utilized to evade or inactivate host reactive oxygen (26, 52, 92) and nitrogen species (101, 144), host phospholipases (96, 102, 127), and other innate immune cell responses particularly within the phagolysosome (61). Upon spore germination within an endosome, superoxide dismutases are utilized in the protection against reactive oxygen species (26, 92). Interestingly, *B. anthracis* synthesizes its own reactive nitrogen species in conjunction with the neutralizing properties of the exosporium to protect itself against host-derived reactive nitrogen species, which disable the Fenton reaction within *B. anthracis* (50, 125). Furthermore, *B. anthracis* utilizes membrane disrupting proteins and enzymes, such as anthrolysin O (54, 123) and phospholipases (54, 55), to facilitate host invasion, disruption of the endosome, and killing of host cells. Lastly, it has been

demonstrated that edema factor also inhibits the activity of host phospholipases, particularly phospholipase A2 (96, 102, 127).

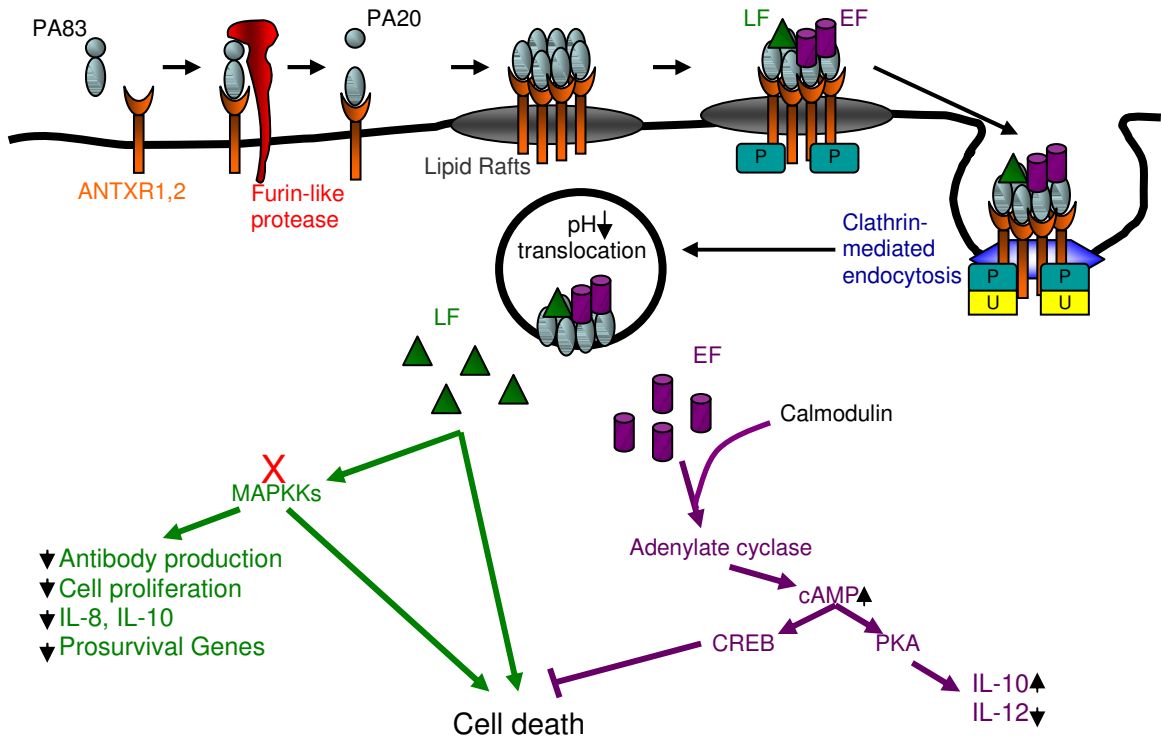


Figure 1.3. Model of cellular toxin effects (135, 136). PA83 interacts with two cellular receptors (ANTXR1/2) and is cleaved by a furin-like protein to form PA63. PA63 assembles into a heptameric oligomer that allows the binding of EF and LF and facilitates endocytosis via sequential phosphorylation and ubiquitination of the protein receptors and the entry of the catalytic subunits of the toxin into the cytosol. LF is a zinc-dependent metalloprotease that cleaves MAP kinase kinases. EF is a calcium- and calmodulin-dependent adenylate cyclase that increases intracellular cAMP concentration. P: phosphorylation. U: Ubiquitination. ↓: down regulation of expression. ↑: up regulation of expression.

1.5 Antibiotic resistance and current treatments of *B. anthracis*

The inherent resistance of *B. anthracis* to several antibiotics and the capacity to acquire resistance to currently used antibiotics underscores the importance of identifying new antimicrobials and therapies that can be utilized against anthrax. *B. anthracis* demonstrates resistance to bacitracin, cephalosporin, streptomycin, and sulfomethoxazole (unpublished results)(14, 15), compounds that target undecaprenol pyrophosphate recycling, cell wall biogenesis, the 16S ribosome, and folic acid metabolism, respectively (143). Currently employed antibiotic treatments, primarily ciprofloxacin and doxycycline, cause adverse side effects such as severe gastrointestinal symptoms including diarrhea, pain, and vomiting. Additional and more severe side effects have also been reported: seizures, syncope, myalgia, hallucinations, and anaphylaxis. All of these symptoms were observed during 60 day post-exposure prophylaxis after exposure to aerosolized *B. anthracis* endospores (77, 126). Furthermore, the misuse of antibiotics during post exposure treatment has been linked to the increase of antibiotic resistant strains. *B. anthracis* demonstrated reduced susceptibility to the quinolones when incubated in the presence of sub-inhibitory concentrations of ofloxacin or ciprofloxacin (138). Current treatments of endemic anthrax outbreaks in developing countries have resulted in penicillin resistant *B. anthracis* by activating the dormant β -lactamase present in all tested isolates (21). The acquisition of antibiotic resistance gene(s) through horizontal gene transfer is of great concern, originating in part from the ability of *B. anthracis* to become competent for transformation when experiencing nutrient

limited conditions (90). Moreover, *B. anthracis* has the ability to germinate and transfer resistance genes in soil (108).

Current antibiotic treatments require that the endospore be fully germinated into a vegetative cell with a functional metabolism as current antibiotics target protein synthesis, cell wall biosynthesis, specific metabolic pathways, or DNA replication. Cell wall biosynthesis and DNA replication inhibition will prevent bacteremia by preventing growth. It is notable that these drugs will not eliminate the effects of bacterial produced toxins on the host. Therefore, ribosomal inhibitors are required in conjunction with growth inhibiting antimicrobials to prevent toxin synthesis to eliminate toxemia (77, 126). In summary, the adverse side effects associated with the treatment of anthrax infections and the ability of *B. anthracis* to acquire antibiotic resistance underscores the critical need for the development of alternative treatments.

1.6 Inhibition of bacterial spores

When considering the options for killing or inhibiting proliferation of spore forming bacteria, one can attempt to kill the organism either as a dormant spore, germinating spore, or replicating vegetative cell. As discussed above, there are several antibiotics that can be utilized to inhibit replicating bacteria, which have become more limited with the onset of antibiotic resistance (22, 37). These methods can be utilized simultaneously with toxin neutralizing antibodies, toxin inhibitors, and supportive care to allow clearance of the spore mediated infection while counteracting toxigenic effects (22). Moreover, the Centers of Disease

Control and Prevention (CDC) suggested antibiotic treatment with pharmacological agents such as ciprofloxacin and vancomycin do not inhibit outgrowth of spores or toxin production (51).

The killing or permanent inhibition of spores is significantly more difficult because spores are extremely resistant to acids, bases, oxidizing agents, and organic solvents (122). Spore germination can be inhibited by changing the pH of the spore environment to either acidic (below pH 6) or alkaline (above pH 8) conditions (9, 100). In addition, L-amino interaction with germination receptors is inhibited in the presence of D-amino acids. The presence of both D-Ala and D-His will prevent germination even in rich media (36, 51). However, inhibition of germination with D-amino acids and pH extremes are both reversible (86, 121) and difficult to achieve within the host. In cases of strong acid treatment, spores can be killed permanently due to the rupturing of the inner membrane (113). Other permanent methods of spore inhibition *ex vivo* include treatment with formaldehyde, nitrous acids, and alkylating agents which induce DNA damage to kill spores (73, 115, 134). Glutaraldehyde and ortho-phthalaldehyde also utilize a DNA damage mechanism to kill spores (134). The spore coat provides significant resistance to most oxidizing agents including chlorine dioxide, hypochlorite, ozone and peroxyxynitrite, however spores can be killed by these agents when sufficient concentrations are used (39, 81, 148-150). Most oxidizing agents kill spores by altering the spore inner membrane, which induces membrane fragility, and rupture during germination (39, 74, 81, 124, 148-150). Furthermore, a combination of pressure to mechanically germinated spores

followed by heat to kill the heat sensitive germinated spores can be utilized to sterilize liquids and waste as performed by an autoclave (28, 44). In the food industry pasteurization is used to sterilize food, but this is only effective when spores are in a nutrient rich environment conducive for germination. Obviously, when treating a mammalian host, none of these methods are viable. Identifying pharmacological agents that inhibit germinated spores and understanding the mechanisms by which these agents inhibit organisms such as *B. anthracis* has become particularly pertinent since spore forming organisms are at their weakest during germination. Since spores no longer have antibiotic resistance associated with spore dormancy and have not begun virulence factor expression, germination is an ideal point in the spore forming bacterial life cycle for antibiotic intervention to eliminate or prevent infection.

1.7 Lantibiotics

Lantibiotics are a unique class of bacteriocins that are predominantly produced by Gram positive bacteria (8). Recent studies have also identified the production of lantibiotics in cyanobacteria (71) and proposed production by Gram-negative bacteria due to presence of the necessary genes in their genomes (43). Lantibiotics display a wide diversity with regards to structure, size, biological activity, and posttranslational modifications (Figures 1.4 & 1.5). The three unifying aspects for all lantibiotics to date are: (i) all lantibiotics are ribosomally synthesized (8), (ii) all lantibiotics contain (methyl)lanthionine rings in addition to a variety of other posttranslational modifications (Figures 1.4 & 1.5)

(8, 18), and (iii) all lantibiotic are translated as a precursor peptide with a leader sequence that is utilized by the tailoring enzyme(s) for substrate recognition (Figure 1.7) (8, 18, 91). The vast majority of these posttranslational modifications are enzymatically installed (8, 18), however, some reports have documented non-enzymatic modifications (7, 13, 34, 139, 140).

Lantibiotics have been divided into two groups according to the biosynthetic enzymes. Class I lantibiotics utilizes two enzymes, LanBC, to catalyze the dehydration of Ser and Thr, and subsequent thioether ring formation between a dehydrated residue and Cys (Figure 1.6) (93). On the other hand, class II lantibiotics use a single multi-functional enzyme, LanM, to catalyze both of these posttranslational events (Figure 1.6) (18). For both classes, the biosynthetic genes are arranged in a gene cluster, which contains the structural gene, biosynthetic tailoring enzymes, immunity genes, and a two-component regulatory system (18, 93). The biosynthetic enzymes (cyclase, dehydratase, transporter, and protease) are predominately integral membrane or membrane associated proteins. In some instances, the expression and synthesis of the lantibiotic is activated by the presence of the lantibiotic itself (8, 18, 93), and in the case of nisin the presence of the N-terminal portion containing the A and B rings is sufficient to induce production of nisin (68).

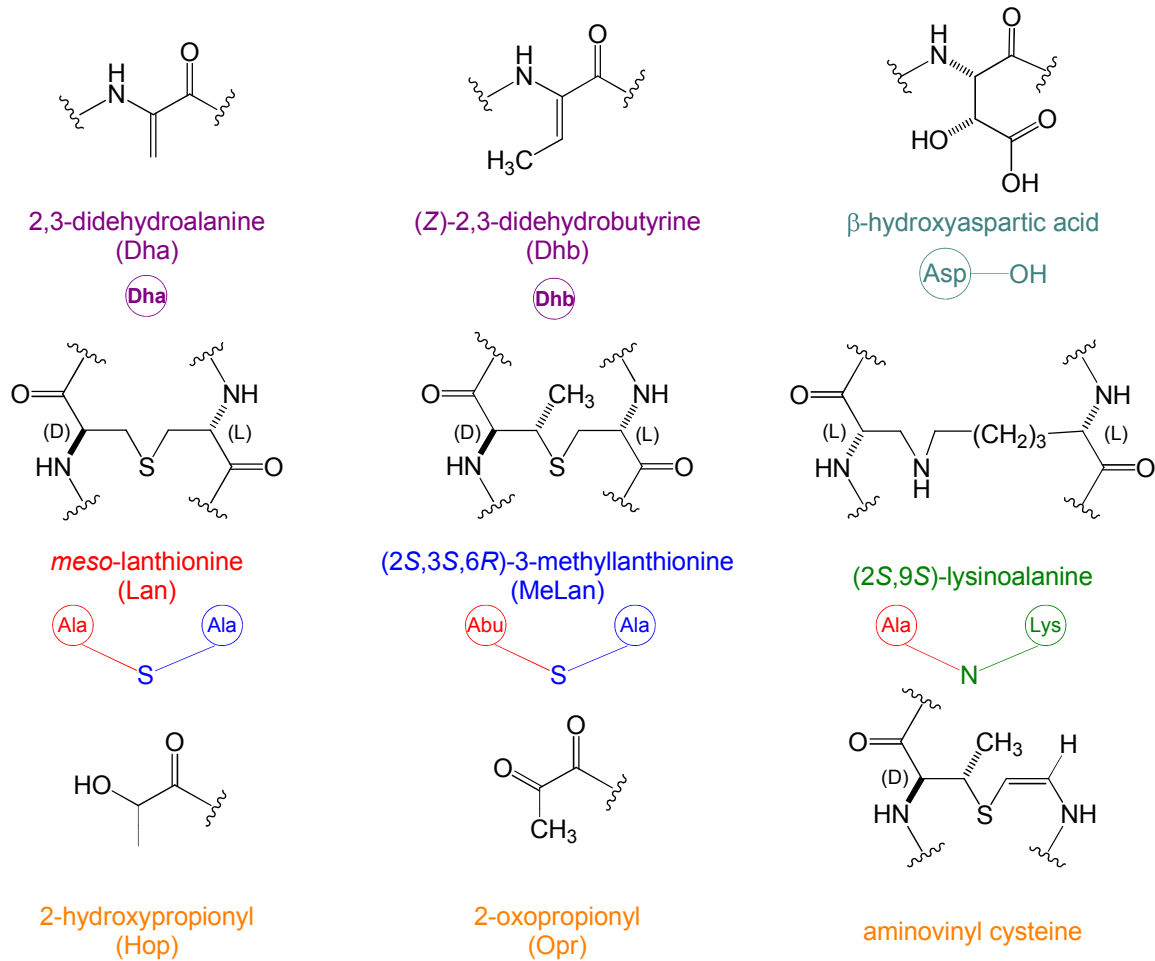


Figure 1.4. Common non-canonical amino acids found in lantibiotics. The short hand notation for each residue that will be used in this thesis is shown in color below the chemical structure.

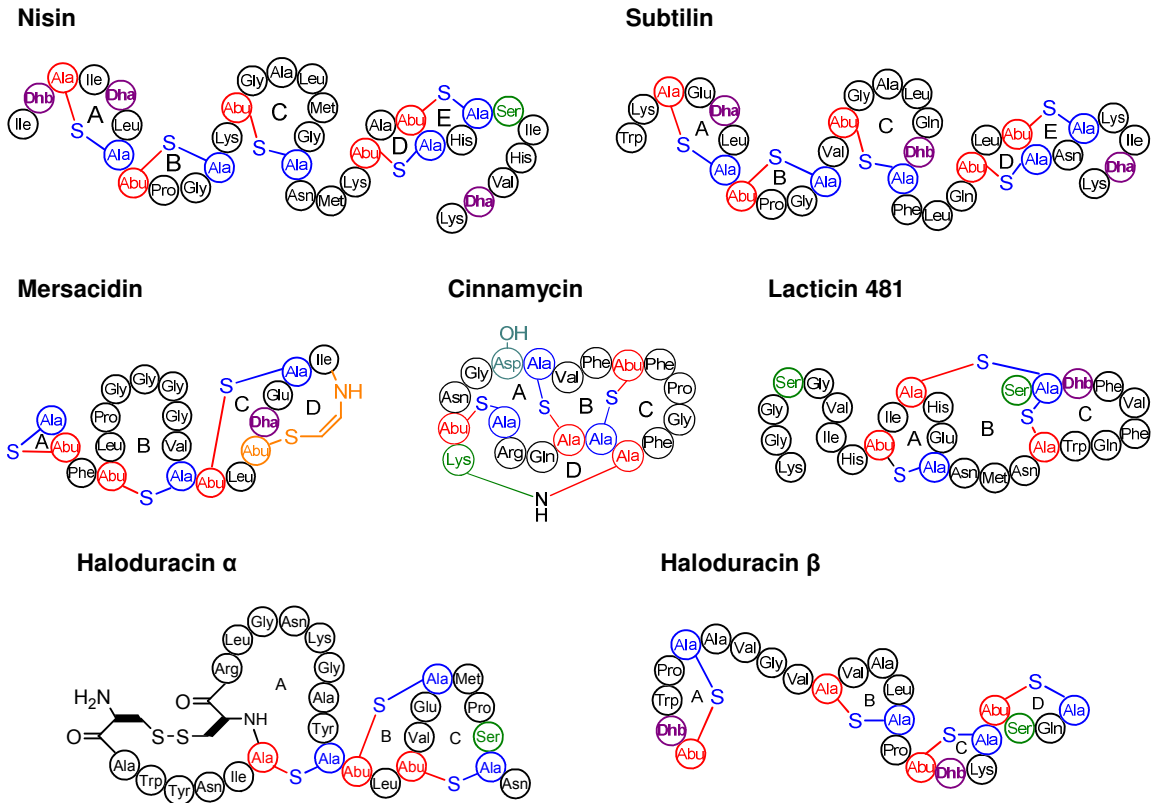


Figure 1.5. Representative lantibiotic structures. See Figure 1.4 for short hand notation of the structural motifs.

1.8 Nisin biosynthesis

Nisin is a 34 amino acid cationic peptide that becomes active after post translational modification and removal of a 23 amino acid leader peptide. Nisin, like all lantibiotics, is ribosomally translated and is post-translationally modified by membrane bound proteins. The dehydratase, NisB, eliminates the hydroxyl group from Ser and Thr residues, resulting in the formation of 2,3-didehydroalanine (Dha) and (Z)-2,3-didehydrobutyryne (Dhb), respectively. The cyclase, NisC, catalyzes the reaction of the dehydrated residues with Cys to make thioether rings called lanthionine (Lan) and methyllanthionine (MeLan),

respectively (Figures 1.6 & 1.7). The cyclization occurs in a regio- and stereospecific manner resulting in a D-configuration at the α -carbon originating from Ser/Thr. After NisT, an ATP binding (ABC) transporter, exports the modified peptide from *Lactococcus lactis* ATCC 11454, NisP proteolytically removes the leader peptide creating the active form of nisin (Figure 1.7). The two most studied natural variants of nisin, nisin A and Z, are identical except that Asn is present at position 27 in the latter instead of His (18). The tertiary structure of nisin and its amino acid composition creates an amphipathic peptide where all the side chains of the hydrophilic amino acids are positioned to one side of the molecule with the hydrophobic side chains positioned to the opposite side. This orientation is a characteristic of a pore forming antibiotic. The five thioether rings of nisin are separated into three N-terminal rings (1 Lan and 2 MeLan) and two C-terminal rings (2 MeLan) by a flexible linker at positions 20, 21, and 22 of the peptide. This flexible linker is essential for the formation of pores (141). The Lan and MeLan rings present in nisin provide structure and resistance to proteolytic cleavage and are essential for target recognition and binding (60, 103). Furthermore, nisin is resistant to trypsin cleavage despite possessing three Lys residues, which are usually targets for trypsin cleavage (17).

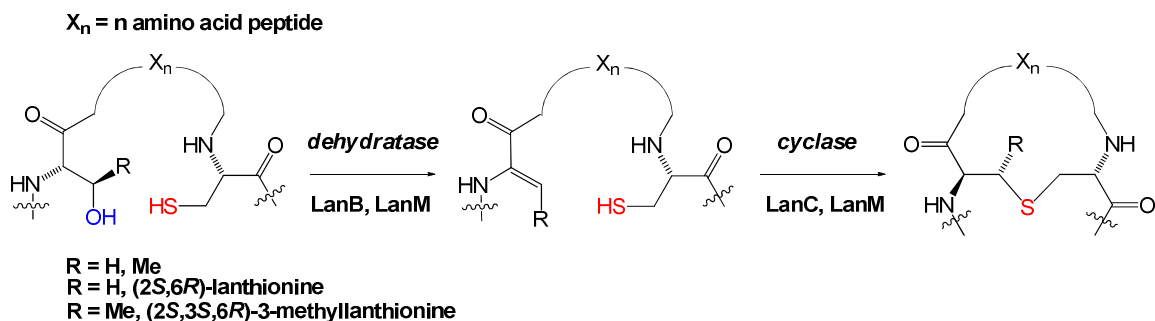


Figure 1.6. Formation of (methyl)lanthionine rings. Water is eliminated from Ser/Thr by the catalytic activity of the dehydratase. Ring formation is completed by a Michael-like addition via Cys thiol attack on the unsaturated amino acid.

Figure 1.7

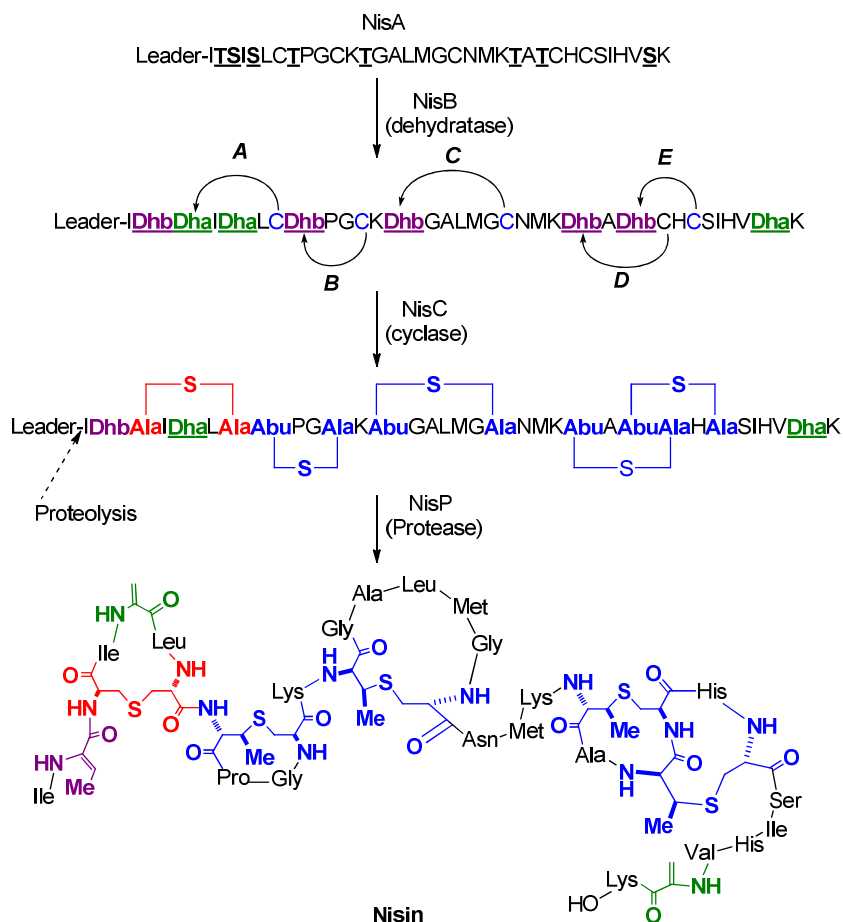


Figure 1.7. Biosynthesis of nisin (18). The colored Ser and Thr within the core peptide of the NisA precursor peptide are targets for NisB-catalyzed dehydration forming Dha (green) and Dhb (purple), respectively. The attack of the Cys thiols onto the unsaturated amino acids to form

Figure 1.7 (continued)

the lanthionine (red) and methyllanthionine (blue) rings, respectively, is catalyzed by NisC. After secretion from the cell, the unmodified leader peptide is proteolytically removed by NisP to form mature nisin.

1.9 Nisin target and mode of action

Nisin has the potential to function as a relevant treatment option for spore infections (19). Nisin has been used as a food preservative worldwide since the 1970s, and it is recognized by the World Health Organization and the United States Food and Drug Administration as a safe food additive that prevents spoilage in products such as milk, cheese, meats, and beer (18). Nisin is most effective against Gram-positive bacteria, and few strains have developed resistance in spite of unregulated worldwide use in the food industry, probably as a consequence of its three distinct modes of action (29). Nisin exerts its bactericidal effects through pore formation (105) and/or disruption of cell wall synthesis by functioning as a transglycosylase inhibitor that binds to lipid II (Figure 1.8A) (53, 145), a precursor for cell wall biogenesis. The third unique activity of nisin is the prevention of spore outgrowth (16, 51).

The target for nisin in vegetative cells is lipid II (12, 59). Through the use of fluorescein-labeled nisin, it has been demonstrated that nisin relocalizes lipid II such that it is no longer available for cell wall biosynthesis (53). Competitive assays performed with nisin and vancomycin, which also binds to lipid II, showed that vancomycin blocks the interaction between nisin and lipid II preventing pore formation. The inability of nisin to bind in the presence of vancomycin confirmed

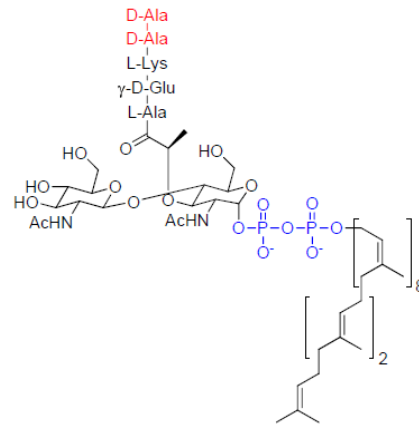
that lipid II is the target of nisin. In addition, nisin was able to kill vancomycin resistant *Enterococcus* via lipid II binding, which suggested different binding locations on lipid II for vancomycin and nisin (12). NMR studies subsequently demonstrated that the A and B rings of nisin interact with the pyrophosphate of lipid II via hydrogen bonding while the C-terminal portion inserts into the membrane for pore formation (10, 60). Vancomycin binds to the D-Ala-D-Ala region of lipid II (Figure 1.8A). Utilizing fluorescently labeled lipid II, the stoichiometry of pore formation by nisin was determined to be 4 lipid II molecules and 8 nisin molecules. In the case of cell wall biogenesis inhibition, radio-labeled lipid II substrates were used to monitor *in vitro* peptidoglycan formation, and in the presence of nisin, production of peptidoglycan was not detected (145). Using fluorescent microscopy, fluorescein-labeled nisin induced the re-localization of lipid II away from the septum of dividing bacteria where it is essential for cell wall formation, thus providing a mechanism for cell wall biosynthesis inhibition. This mechanism was confirmed as a distinct nisin activity with the use of non-pore forming variants of nisin (53).

The third activity of nisin, inhibition of spore outgrowth, was demonstrated first for *B. cereus* endospores utilizing phase contrast microscopy, which exhibited the presence of phase-dark germinated endospores instead of elongated vegetative cells in 5 µg/mL nisin after 180 min incubation (16). Clues into the possible mechanism underlying nisin-mediated outgrowth inhibition came from observations of iodoacetate and nitrosothiol treatment against endospores, which modified sulfhydryl groups associated with the plasma membrane also

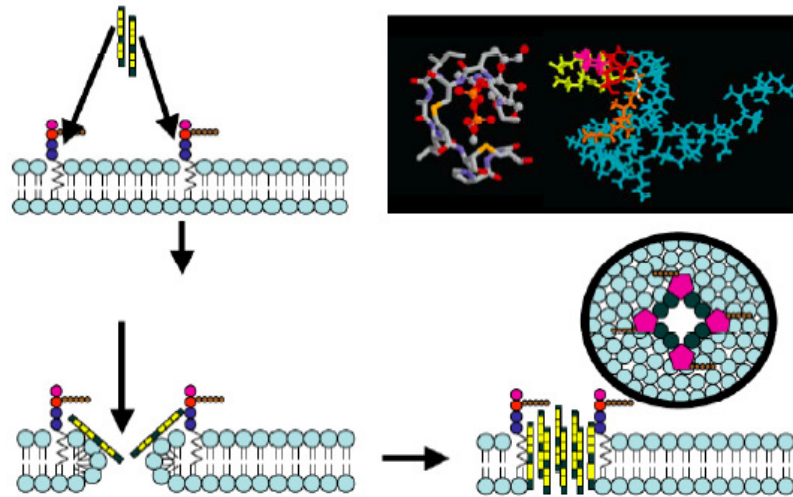
resulting in endospore outgrowth inhibition (88). Notably, pre-incubation with nisin resulted in a dramatic reduction in the incorporation of the radioactive iodoacetate in the endospores along with outgrowth inhibition, suggesting that nisin also interacts with sulfhydryl groups to inhibit endospore outgrowth (89). Additional experiments demonstrated that the presence of Dha5 (one of the three uncyclized dehydro amino acids) in nisin is essential for inhibiting endospore outgrowth. A Dha5Ala mutation resulted in the loss of outgrowth inhibition (16). The sulfhydryl-containing target was not identified. However, a recent report demonstrated that Dha5 was not essential for outgrowth inhibition when the same mutation was made and the inhibitory activity was tested against *B. subtilis*. Rather, it was reported that the A and B rings of nisin were both necessary for outgrowth inhibition, which suggests lipid II as the target for inhibiting outgrowth (103). With the accurate identification of the target and the required motifs for outgrowth inhibition, an antibiotic and/or a mechanism may be identified that would allow *B. anthracis* germination but inhibit outgrowth prior to or during the endospore-macrophage interaction, which would potentially allow the host an opportunity to efficiently control and eliminate the infection.

Figure 1.8

A



B



C

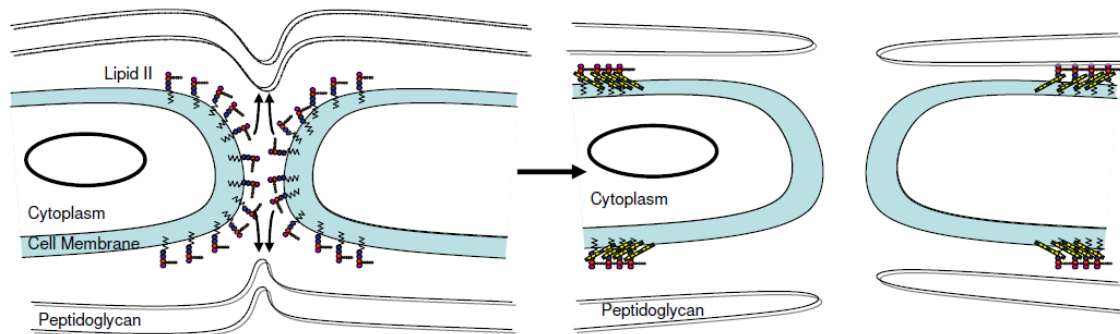


Figure 1.8. Modes of action for nisin. A. Lipid II is the penultimate precursor for cell wall biogenesis. Lipid II consists of an undecaprenyl membrane anchor attached to a disaccharide of N-acetylglucosamine- β -1,4-N-acetylmuramic acid. A pentapeptide is linked to the muramic acid,

Figure 1.8 (continued)

and in *B. anthracis* L-Lys is replaced by a diaminopimelic acid (DAP). The nisin binding site is highlighted in blue with the vancomycin binding site in red. B. Nisin pore formation. Hydrogen bonding interactions between the pyrophosphates of lipid II and nisin facilitates nisin-mediated pore formation. The N-terminus of nisin interacts with lipid II with the C-terminus of nisin inserting into the membrane of the bacterial cell. The pores that are formed are comprised of eight nisin and 4 lipid II molecules. The actual orientation of the lipid II and nisin molecules is unknown. The NMR structures illustrate that the binding of the A and B rings of nisin (cyan) interact with the pyrophosphate of lipid II (prenyl chain, orange; muramic acid, red; N-acetylglucosamine, magenta; pentapeptide, yellow; pyrophosphates, white). Cartoon of lipid II (phosphate, blue; muramic acid, red; N-acetylglucosamine, magenta; pentapeptide, brown). C. Nisin inhibits cell wall biogenesis by binding lipid II, which resides at the septum of dividing bacilli, and re-localizing lipid II away from the septum. This nisin-mediated relocalization sequesters lipid II to prevent its utilization as substrate for cell wall synthesis. As a consequence of nisin-lipid II interaction, nisin directly functions as a transglycosylation inhibitor preventing substrate interaction with cell wall synthetic enzymes, which reside at the septum. B and C. Nisin is represented in cartoon form as a dark green back bone with yellow squares indicating the 5 rings.

1.10 Nisin and subtilin immunity and regulation of biosynthesis

Immunity to nisin by the native producer is derived from a two-pronged approach, which includes the use of NisI and an ATP- dependent transporter complex, NisFEG. These two systems work together in a synergistic fashion to provide immunity (Figure 1.9). NisI is a constitutively expressed 25.9 kDa protein in its fully modified form. Native NisI contains a twin Arg consensus sequence allowing for export via the Sec system. Upon export, NisI undergoes a 19-amino acid N-terminal cleavage followed by lipidation of the new N-terminal Cys for

membrane anchoring (75). NisI has been shown to bind nisin specifically with a reported K_D of 0.6 – 2 μM based on surface plasmon resonance experiments (67), and this complex has been shown to be unstable in solution and to become insoluble (75). In terms of immunity, NisI reduces the concentration or amount of soluble nisin that is allowed to interact with the membrane thus preventing pore formation (18). Furthermore, NisI that is not lipidated is secreted into the environment to bind nisin and reduce the concentration of free nisin in solution (32, 75). Deletion studies have demonstrated that NisI provides the majority of the immunity towards nisin mediated cell death (75). In addition to NisI, *L. lactis* 11454 also utilizes an ATP-dependent complex to remove or pump nisin from the membrane, and this complex is organized with two NisF proteins, which contain the ATP binding motifs, interacting with the cytosolic portions of the trans-membrane proteins NisEG. The expression of these proteins is controlled by the two-component regulatory system *nisRK* (Figure 1.9) (18). Through the use of these two systems *L. lactis* acquires the essential immunity for the production of its deadly secondary metabolite.

Subtilin, like nisin, is a linear lantibiotic that contains 5 rings derived from the cyclization of Dha or Dhb with Cys. Nisin and subtilin display 63% sequence identity with the first set of rings in the exact same locations. Similarities between nisin and subtilin continue in the fact that both producer strains utilize an ATP dependent pump (SpaFEG for subtilin) as well as a stoichiometric binding protein (SpaI for subtilin) to reduce the concentration of the secondary metabolite in close association with the producing cell (18). However, this is where the

similarities end, since the subtilin producer, *B. subtilis* 6633, also has a mechanism to succinylate subtilin, drastically reducing its activity to 10% of the unsuccinylated variant (57). Also, SpaI has very little sequence similarity to NisI, and comprises only 143 amino acids compared to 226 for NisI. The presence of SpaI does not afford immunity to nisin with the converse being true as well (133).

When considering the regulation of immunity gene expression in addition to the clusters as a whole, both nisin and subtilin synthetic and immunity genes are controlled by a two-component regulatory system, LanRK, which activates expression (Figure 1.9). In the case of subtilin, SpaR will bind to Spa boxes located in front of *spaS* (structural gene), *spaB* (synthetic gene), and *spaI* (immunity gene) to induce preferential expression in the listed order (130). SpaRK also induced the expression of their own two-gene operon, but their expression is also controlled by σ^H , which is the first σ factor involved in sporulation. As a consequence of σ^H controlled gene expression, subtilin is expressed at very late logarithmic and stationary phase of growth prior to spore formation while nisin is expressed in logarithmic phase with lactic acid production. The activity of σ^H is inhibited by AbrB, and AbrB is inhibited by Spo0A, which is the master sporulation regulator. Thus, Spo0A activates σ^H and in turn, subtilin expression (63). Deletion of AbrB increases the amount of subtilin, all succinylated, with expression starting in logarithmic growth (57).

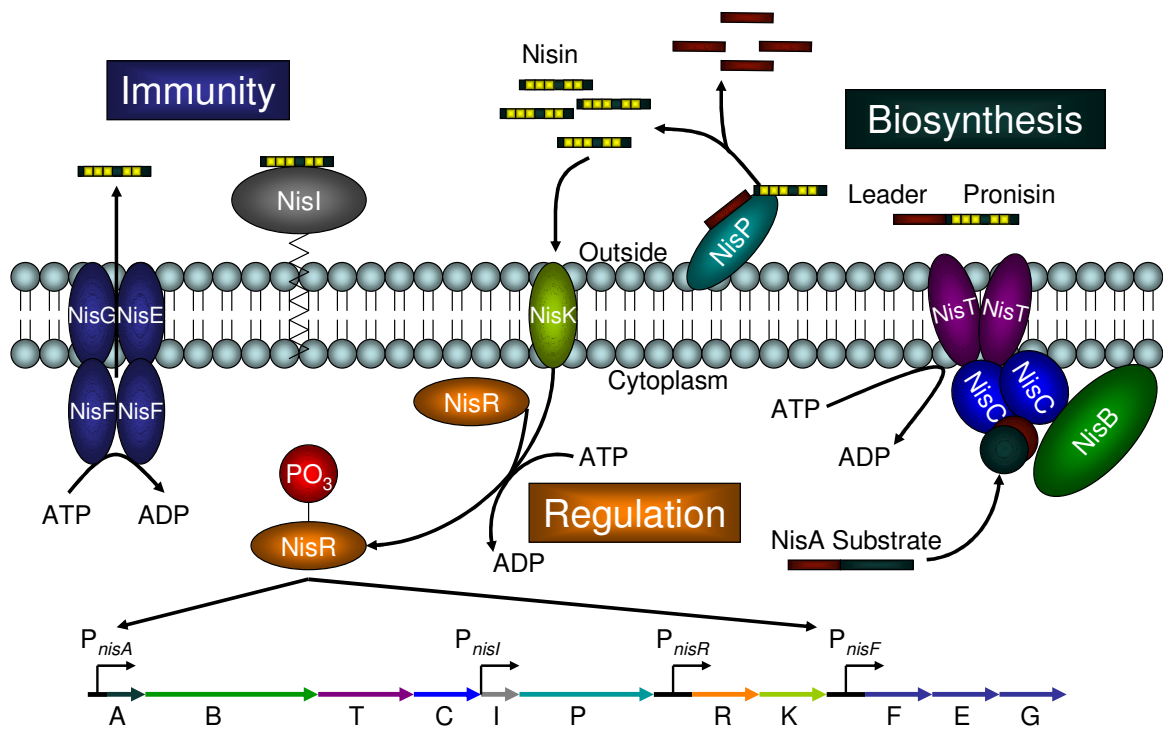


Figure 1.9. Schematic representation illustrating nisin biosynthesis, regulation, and immunity within a bacterial cell. Fully modified nisin functions as an activator for further nisin biosynthesis through the interaction with NisK inducing autophosphorylation. The phosphoryl group is transferred to an Asp residue of NisR, which activates the expression of the nisin biosynthetic operon (*nisABTCIP*) and the immunity operon (*nisFEG*). The expression of the regulatory genes and *nisl* are under the control of independent promoters. The gene product of *nisA* is dehydrated (NisB) and cyclized (NisC) installing 5 thioether rings. Inactive nisin is transported from the cell in an ATP dependent manner (NisT) where it is proteolytically activated (NisP). NisI provides immunity by binding nisin to lower the concentration around the membrane. NisFEG functions as an ATP dependent pump to remove nisin present within the membrane.

1.11 Antimicrobial resistance to nisin

In addition to the required natural resistance within the producing organism, a few studies of nisin resistance within other non-nisin producing bacteria have been reported. As a whole, Gram-negative bacteria generally demonstrate little growth inhibition in the presence of nisin because of the lipopolysaccharide outer membrane, which prevents nisin interaction with lipid II and the inner membrane (18, 75). Nisin has only demonstrated moderate efficacy against *E.coli* in high salt conditions (69). For Gram-positive bacteria, modifications of the cell membrane and cell wall or expression of proteases have provided resistance to nisin (18). For non-nisin producing *L. lactis*, a proteolytic enzyme, NSR, has been identified, and this enzyme cleaves nisin after the fifth ring removing the highly flexible C-terminal tail diminishing the pore forming activity of nisin (132). In *Clostridium botulinum* and *Listeria monocytogenes*, fatty acids have been modified to eliminate unsaturated and branched fatty acids within the cell membrane. This change allows for the tighter packing of the phospholipids within the membrane increasing membrane rigidity to prevent or decrease the efficiency of nisin membrane insertion for pore formation (25, 78-80). Furthermore, several *Bacillus* strains have used the association of divalent cations, Ca^{2+} , Co^{2+} , and Mg^{2+} in close proximity to the membrane and cell wall, to neutralize the overall negative charge of the cell membrane and cell wall and eliminate the attractive force towards cationic peptides, which prevents nisin interaction with the cell (25). Another method by which *Bacillus* and *Staphylococcus sp.* neutralize the net charge of the cell wall and membrane is

via cell wall modification with teichoic and teichuronic acids. Deletion of the *dltABCD* operon, which codes for the cell wall modifying proteins, rendered the resistant strain sensitive to nisin and cationic peptide inhibition (38, 94).

Recently, it has been reported that decreased production of glutamate as a consequence of a mutation in glutamate decarboxylase increased sensitivity to nisin in *L. monocytogenes*, however the exact mechanism of resistance associated with the presence of glutamate has not been elucidated (5).

Interestingly, many of the reported resistance mechanisms demonstrated by Gram-positive bacteria can easily be lost rendering the once resistant strain sensitive to nisin treatment after incubation in nisin free media. This observation demonstrates that these cell wall and membrane modifications are not permanent and are selectively disadvantageous in the absence of nisin.

1.12 Studies described in this thesis

As previously discussed, nisin has a unique third activity, which is the inhibition of spore outgrowth. At the start of my studies, the mechanism and target utilized for spore outgrowth inhibition had not been identified. Chapters 2 through 4 will present the identification of a mechanism as well as a target for outgrowth inhibition. As shown by these studies, outgrowth inhibition is not a unique activity but rather a phenotype of nisin-mediated pore formation. Chapter 5 will provide a brief discussion of the efforts to establish a representative *in vitro* *B. anthracis* infection model utilizing cultured mammalian immune cells that are a better reflection of non-germinating conditions during *in vivo* infections within the

lung than previous models. Utilizing this infection model, the investigation of how nisin alters the *B. anthracis* spore-immune cell interaction in the favor of the immune cell is presented in chapter 6. Chapter 7 will highlight initial studies into lantibiotic immunity gene localization and interaction with antimicrobial peptide. In chapter 8, a summary of the results in this thesis are presented with a discussion of the results as well as highlighting areas for potential future research.

1.13 References

1. **Abrami, L., M. Bischofberger, B. Kunz, R. Groux, and F. G. van der Goot.** 2010. Endocytosis of the anthrax toxin is mediated by clathrin, actin and unconventional adaptors. *PLoS Pathog* **6**:e1000792.
2. **Abrami, L., B. Kunz, and F. G. van der Goot.** 2010. Anthrax toxin triggers the activation of src-like kinases to mediate its own uptake. *Proc Natl Acad Sci U S A* **107**:1420-4.
3. **Abrami, L., N. Reig, and F. G. van der Goot.** 2005. Anthrax toxin: the long and winding road that leads to the kill. *Trends Microbiol* **13**:72-8.
4. **Banks, D. J., M. Barnajian, F. J. Maldonado-Arocho, A. M. Sanchez, and K. A. Bradley.** 2005. Anthrax toxin receptor 2 mediates *Bacillus anthracis* killing of macrophages following spore challenge. *Cell Microbiol* **7**:1173-85.
5. **Begley, M., P. D. Cotter, C. Hill, and R. P. Ross.** 2010. Glutamate decarboxylase-mediated nisin resistance in *Listeria monocytogenes*. *Appl Environ Microbiol*:6541-6.
6. **Beyer, W., and P. C. Turnbull.** 2009. Anthrax in animals. *Mol Aspects Med* **30**:481-9.
7. **Bierbaum, G., F. Gotz, A. Peschel, T. Kupke, M. van de Kamp, and H. G. Sahl.** 1996. The biosynthesis of the lantibiotics epidermin, gallidermin, Pep5 and epilancin K7. *Antonie Van Leeuwenhoek* **69**:119-127.

8. **Bierbaum, G., and H. G. Sahl.** 2009. Lantibiotics: mode of action, biosynthesis and bioengineering. *Curr Pharm Biotechnol* **10**:2-18.
9. **Blocher, J. C., and F. F. Busta.** 1985. Inhibition of germinant binding by bacterial spores in acidic environments. *Appl Environ Microbiol* **50**:274-9.
10. **Bonev, B. B., E. Breukink, E. Swiezewska, B. De Kruijff, and A. Watts.** 2004. Targeting extracellular pyrophosphates underpins the high selectivity of nisin. *Faseb J* **18**:1862-9.
11. **Bourgogne, A., M. Drysdale, S. G. Hilsenbeck, S. N. Peterson, and T. M. Koehler.** 2003. Global effects of virulence gene regulators in a *Bacillus anthracis* strain with both virulence plasmids. *Infect Immun* **71**:2736-43.
12. **Breukink, E., I. Wiedemann, C. van Kraaij, O. P. Kuipers, H. Sahl, and B. de Kruijff.** 1999. Use of the cell wall precursor lipid II by a pore-forming peptide antibiotic. *Science* **286**:2361-4.
13. **Brotz, H., M. Josten, I. Wiedemann, U. Schneider, F. Gotz, G. Bierbaum, and H. G. Sahl.** 1998. Role of lipid-bound peptidoglycan precursors in the formation of pores by nisin, epidermin and other lantibiotics. *Mol Microbiol* **30**:317-27.
14. **Brouillard, J. E., C. M. Terriff, A. Tofan, and M. W. Garrison.** 2006. Antibiotic selection and resistance issues with fluoroquinolones and doxycycline against bioterrorism agents. *Pharmacotherapy* **26**:3-14.
15. **CDC.** 2006. Fact Sheet: Anthrax Information for Health Care Providers, p. 178, 1 ed. Springer.
16. **Chan, W. C., H. M. Dodd, N. Horn, K. Maclean, L. Y. Lian, B. W. Bycroft, M. J. Gasson, and G. C. Roberts.** 1996. Structure-activity relationships in the peptide antibiotic nisin: role of dehydroalanine 5. *Appl Environ Microbiol* **62**:2966-9.
17. **Chan, W. C., M. Leyland, J. Clark, H. M. Dodd, L. Y. Lian, M. J. Gasson, B. W. Bycroft, and G. C. Roberts.** 1996. Structure-activity relationships in the peptide antibiotic nisin: antibacterial activity of fragments of nisin. *FEBS Lett* **390**:129-32.
18. **Chatterjee, C., Paul, M., Xie, L, van der Donk, W. A.** 2005. Biosynthesis and Mode of Action of Lantibiotics. *Chemical Reviews* **105**:633-683.
19. **Cheigh, C. I., and Y. R. Pyun.** 2005. Nisin biosynthesis and its properties. *Biotechnol Lett* **27**:1641-8.

20. **Chen, Y., S. Fukuoka, and S. Makino.** 2000. A novel spore peptidoglycan hydrolase of *Bacillus cereus*: biochemical characterization and nucleotide sequence of the corresponding gene, sleL. *J Bacteriol* **182**:1499-506.
21. **Chen, Y., F. C. Tenover, and T. M. Koehler.** 2004. β -lactamase gene expression in a penicillin-resistant *Bacillus anthracis* strain. *Antimicrob Agents Chemother* **48**:4873-7.
22. **Clatworthy, A. E., E. Pierson, and D. T. Hung.** 2007. Targeting virulence: a new paradigm for antimicrobial therapy. *Nat Chem Biol* **3**:541-8.
23. **Collier, R. J.** 2009. Membrane translocation by anthrax toxin. *Mol Aspects Med* **30**:413-22.
24. **Cowan, A. E., D. E. Koppel, B. Setlow, and P. Setlow.** 2003. A soluble protein is immobile in dormant spores of *Bacillus subtilis* but is mobile in germinated spores: implications for spore dormancy. *Proc Natl Acad Sci U S A* **100**:4209-14.
25. **Crandall, A. D., and T. J. Montville.** 1998. Nisin resistance in *Listeria monocytogenes* ATCC 700302 is a complex phenotype. *Appl Environ Microbiol* **64**:231-7.
26. **Cybulski, R. J., Jr., P. Sanz, F. Alem, S. Stibitz, R. L. Bull, and A. D. O'Brien.** 2009. Four superoxide dismutases contribute to *Bacillus anthracis* virulence and provide spores with redundant protection from oxidative stress. *Infect Immun* **77**:274-85.
27. **Dai, Z., and T. M. Koehler.** 1997. Regulation of anthrax toxin activator gene (*atxA*) expression in *Bacillus anthracis*: temperature, not CO₂/bicarbonate, affects AtxA synthesis. *Infect Immun* **65**:2576-82.
28. **Dang, J. L., K. Heroux, J. Kearney, A. Arasteh, M. Gostomski, and P. A. Emanuel.** 2001. *Bacillus* spore inactivation methods affect detection assays. *Appl Environ Microbiol* **67**:3665-70.
29. **Delves-Broughton, J., P. Blackburn, R. J. Evans, and J. Hugenholtz.** 1996. Applications of the bacteriocin, nisin. *Antonie Van Leeuwenhoek* **69**:193-202.
30. **Dixon, T. C., M. Meselson, J. Guillemin, and P. C. Hanna.** 1999. Anthrax. *N Engl J Med* **341**:815-26.

31. **Dowd, M. M., B. Orsburn, and D. L. Popham.** 2008. Cortex peptidoglycan lytic activity in germinating *Bacillus anthracis* spores. *J Bacteriol* **190**:4541-8.
32. **Draper, L. A., R. P. Ross, C. Hill, and P. D. Cotter.** 2008. Lantibiotic immunity. *Curr Protein Pept Sci* **9**:39-49.
33. **Drysdale, M., A. Bourgoigne, S. G. Hilsenbeck, and T. M. Koehler.** 2004. *atxA* controls *Bacillus anthracis* capsule synthesis via *acpA* and a newly discovered regulator, *acpB*. *J Bacteriol* **186**:307-15.
34. **Ekkelenkamp, M. B., M. Hanssen, S. T. Danny Hsu, A. de Jong, D. Milatovic, J. Verhoef, and N. A. van Nuland.** 2005. Isolation and structural characterization of epilancin 15X, a novel lantibiotic from a clinical strain of *Staphylococcus epidermidis*. *FEBS Lett* **579**:1917-22.
35. **Ezzell, J. W., Jr., and T. G. Abshire.** 1988. Immunological analysis of cell-associated antigens of *Bacillus anthracis*. *Infect Immun* **56**:349-56.
36. **Fey, G., G. W. Gould, and A. D. Hitchins.** 1964. Identification Of D-alanine as the auto-inhibitor of germination of *Bacillus globigii* spores. *J Gen Microbiol* **35**:229-36.
37. **Fischbach, M. A., and C. T. Walsh.** 2009. Antibiotics for emerging pathogens. *Science* **325**:1089-93.
38. **Fisher, N., L. Shetron-Rama, A. Herring-Palmer, B. Heffernan, N. Bergman, and P. Hanna.** 2006. The *dltABCD* operon of *Bacillus anthracis* Sterne is required for virulence and resistance to peptide, enzymatic, and cellular mediators of innate immunity. *J Bacteriol* **188**:1301-9.
39. **Genest, P. C., B. Setlow, E. Melly, and P. Setlow.** 2002. Killing of spores of *Bacillus subtilis* by peroxyntirite appears to be caused by membrane damage. *Microbiology* **148**:307-14.
40. **Gilmore, M. E., D. Bandyopadhyay, A. M. Dean, S. D. Linnstaedt, and D. L. Popham.** 2004. Production of muramic δ -lactam in *Bacillus subtilis* spore peptidoglycan. *J Bacteriol* **186**:80-9.
41. **Giorno, R., J. Bozue, C. Cote, T. Wenzel, K. S. Moody, M. Mallozzi, M. Ryan, R. Wang, R. Zielke, J. R. Maddock, A. Friedlander, S. Welkos, and A. Driks.** 2007. Morphogenesis of the *Bacillus anthracis* spore. *J Bacteriol* **189**:691-705.
42. **Goodman, J. W., and D. E. Nitecki.** 1967. Studies on the relation of a prior immune response to immunogenicity. *Immunology* **13**:577-83.

43. **Goto, Y., B. Li, J. Claesen, Y. Shi, M. J. Bibb, and W. A. van der Donk.** Discovery of unique lanthionine synthetases reveals new mechanistic and evolutionary insights. *PLoS Biol* **8**:e1000339.
44. **Gould, G. W., and A. J. Sale.** 1970. Initiation of germination of bacterial spores by hydrostatic pressure. *J Gen Microbiol* **60**:335-46.
45. **Guidi-Rontani, C.** 2002. The alveolar macrophage: the Trojan horse of *Bacillus anthracis*. *Trends Microbiol* **10**:405-9.
46. **Guidi-Rontani, C., M. Levy, H. Ohayon, and M. Mock.** 2001. Fate of germinated *Bacillus anthracis* spores in primary murine macrophages. *Mol Microbiol* **42**:931-8.
47. **Guidi-Rontani, C., and M. Mock.** 2002. Macrophage interactions. *Curr Top Microbiol Immunol* **271**:115-41.
48. **Guidi-Rontani, C., M. Weber-Levy, E. Labruyere, and M. Mock.** 1999. Germination of *Bacillus anthracis* spores within alveolar macrophages. *Mol Microbiol* **31**:9-17.
49. **Guignot, J., M. Mock, and A. Fouet.** 1997. AtxA activates the transcription of genes harbored by both *Bacillus anthracis* virulence plasmids. *FEMS Microbiol Lett* **147**:203-7.
50. **Gusarov, I., K. Shatalin, M. Starodubtseva, and E. Nudler.** 2009. Endogenous nitric oxide protects bacteria against a wide spectrum of antibiotics. *Science* **325**:1380-4.
51. **Gut, I. M., A. M. Prouty, J. D. Ballard, W. A. van der Donk, and S. R. Blanke.** 2008. Inhibition of *Bacillus anthracis* spore outgrowth by nisin. *Antimicrob Agents Chemother* **52**:4281-8.
52. **Hanna, P. C., B. A. Kruskal, R. A. Ezekowitz, B. R. Bloom, and R. J. Collier.** 1994. Role of macrophage oxidative burst in the action of anthrax lethal toxin. *Mol Med* **1**:7-18.
53. **Hasper, H. E., N. E. Kramer, J. L. Smith, J. D. Hillman, C. Zachariah, O. P. Kuipers, B. de Kruijff, and E. Breukink.** 2006. An alternative bactericidal mechanism of action for lantibiotic peptides that target lipid II. *Science* **313**:1636-7.
54. **Heffernan, B. J., B. Thomason, A. Herring-Palmer, and P. Hanna.** 2007. *Bacillus anthracis* anthrolysin O and three phospholipases C are functionally redundant in a murine model of inhalation anthrax. *FEMS Microbiol Lett* **271**:98-105.

55. **Heffernan, B. J., B. Thomason, A. Herring-Palmer, L. Shaughnessy, R. McDonald, N. Fisher, G. B. Huffnagle, and P. Hanna.** 2006. *Bacillus anthracis* phospholipases C facilitate macrophage-associated growth and contribute to virulence in a murine model of inhalation anthrax. *Infect Immun* **74**:3756-64.
56. **Heffron, J. D., B. Orsburn, and D. L. Popham.** 2009. Roles of germination-specific lytic enzymes CwlJ and SleB in *Bacillus anthracis*. *J Bacteriol* **191**:2237-47.
57. **Heinzmann, S., K. D. Entian, and T. Stein.** 2006. Engineering *Bacillus subtilis* ATCC 6633 for improved production of the lantibiotic subtilin. *Appl Microbiol Biotechnol* **69**:532-6.
58. **Hoffmaster, A. R., and T. M. Koehler.** 1997. The anthrax toxin activator gene *atxA* is associated with CO₂-enhanced non-toxin gene expression in *Bacillus anthracis*. *Infect Immun* **65**:3091-9.
59. **Hsu, S. T., E. Breukink, B. de Kruijff, R. Kaptein, A. M. Bonvin, and N. A. van Nuland.** 2002. Mapping the targeted membrane pore formation mechanism by solution NMR: the nisin Z and lipid II interaction in SDS micelles. *Biochemistry* **41**:7670-6.
60. **Hsu, S. T., E. Breukink, E. Tischenko, M. A. Lutters, B. de Kruijff, R. Kaptein, A. M. Bonvin, and N. A. van Nuland.** 2004. The nisin-lipid II complex reveals a pyrophosphate cage that provides a blueprint for novel antibiotics. *Nat Struct Mol Biol* **11**:963-7.
61. **Hu, H., Q. Sa, T. M. Koehler, A. I. Aronson, and D. Zhou.** 2006. Inactivation of *Bacillus anthracis* spores in murine primary macrophages. *Cell Microbiol* **8**:1634-42.
62. **Huang, S. S., D. Chen, P. L. Pelczar, V. R. Vepachedu, P. Setlow, and Y. Q. Li.** 2007. Levels of Ca²⁺-dipicolinic acid in individual *Bacillus* spores determined using microfluidic Raman tweezers. *J Bacteriol* **189**:4681-7.
63. **Kleerebezem, M.** 2004. Quorum sensing control of lantibiotic production; nisin and subtilin autoregulate their own biosynthesis. *Peptides* **25**:1405-14.
64. **Koehler, T. M.** 2002. *Anthrax*, 1 ed. Springer.
65. **Koehler, T. M.** 2009. *Bacillus anthracis* physiology and genetics. *Mol Aspects Med* **30**:386-96.

66. **Koehler, T. M., Z. Dai, and M. Kaufman-Yarbray.** 1994. Regulation of the *Bacillus anthracis* protective antigen gene: CO₂ and a trans-acting element activate transcription from one of two promoters. *J Bacteriol* **176**:586-95.
67. **Koponen, O., T. M. Takala, U. Saarela, M. Qiao, and P. E. Saris.** 2004. Distribution of the NisI immunity protein and enhancement of nisin activity by the lipid-free NisI. *FEMS Microbiol Lett* **231**:85-90.
68. **Kuipers, O. P., M. M. Beerthuyzen, P. G. de Ruyter, E. J. Luesink, and W. M. de Vos.** 1995. Autoregulation of nisin biosynthesis in *Lactococcus lactis* by signal transduction. *J Biol Chem* **270**:27299-304.
69. **Kuwano, K., N. Tanaka, T. Shimizu, K. Nagatoshi, S. Nou, and K. Sonomoto.** 2005. Dual antibacterial mechanisms of nisin Z against Gram-positive and Gram-negative bacteria. *Int J Antimicrob Agents* **26**:396-402.
70. **Lambert, E. A., and D. L. Popham.** 2008. The *Bacillus anthracis* SleL (YaaH) protein is an N-acetylglucosaminidase involved in spore cortex depolymerization. *J Bacteriol* **190**:7601-7.
71. **Li, B., D. Sher, L. Kelly, Y. Shi, K. Huang, P. J. Knerr, I. Joewono, D. Rusch, S. W. Chisholm, and W. A. van der Donk.** 2010. Catalytic promiscuity in the biosynthesis of cyclic peptide secondary metabolites in planktonic marine cyanobacteria. *Proc Natl Acad Sci U S A* **107**:10430-5.
72. **Lindeque, P. M., and P. C. Turnbull.** 1994. Ecology and epidemiology of anthrax in the Etosha National Park, Namibia. *Onderstepoort J Vet Res* **61**:71-83.
73. **Loshon, C. A., P. C. Genest, B. Setlow, and P. Setlow.** 1999. Formaldehyde kills spores of *Bacillus subtilis* by DNA damage and small, acid-soluble spore proteins of the α/β -type protect spores against this DNA damage. *J Appl Microbiol* **87**:8-14.
74. **Loshon, C. A., E. Melly, B. Setlow, and P. Setlow.** 2001. Analysis of the killing of spores of *Bacillus subtilis* by a new disinfectant, Sterilox. *J Appl Microbiol* **91**:1051-8.
75. **Lubelski, J., R. Rink, R. Khusainov, G. N. Moll, and O. P. Kuipers.** 2008. Biosynthesis, immunity, regulation, mode of action and engineering of the model lantibiotic nisin. *Cell Mol Life Sci* **65**:455-76.
76. **Makino, S., and R. Moriyama.** 2002. Hydrolysis of cortex peptidoglycan during bacterial spore germination. *Med Sci Monit* **8**:RA119-27.

77. **Martin, S. W., B. C. Tierney, A. Aranas, N. E. Rosenstein, L. H. Franzke, L. Apicella, N. Marano, and M. M. McNeil.** 2005. An overview of adverse events reported by participants in CDC's anthrax vaccine and antimicrobial availability program. *Pharmacoepidemiol Drug Saf* **14**:393-401.
78. **Mazzotta, A. S., A. D. Crandall, and T. J. Montville.** 1997. Nisin resistance in *Clostridium botulinum* spores and vegetative cells. *Appl Environ Microbiol* **63**:2654-2659.
79. **Mazzotta, A. S., and T. J. Montville.** 1999. Characterization of fatty acid composition, spore germination, and thermal resistance in a nisin-resistant mutant of *Clostridium botulinum* 169B and in the wild-type strain. *Appl Environ Microbiol* **65**:659-64.
80. **Mazzotta, A. S., and T. J. Montville.** 1997. Nisin induces changes in membrane fatty acid composition of *Listeria monocytogenes* nisin-resistant strains at 10 °C and 30 °C. *J Appl Microbiol* **82**:32-8.
81. **Melly, E., A. E. Cowan, and P. Setlow.** 2002. Studies on the mechanism of killing of *Bacillus subtilis* spores by hydrogen peroxide. *J Appl Microbiol* **93**:316-25.
82. **Mesnage, S., E. Tosi-Couture, P. Gounon, M. Mock, and A. Fouet.** 1998. The capsule and S-layer: two independent and yet compatible macromolecular structures in *Bacillus anthracis*. *J Bacteriol* **180**:52-8.
83. **Mock M, F. A.** 2001. Anthrax. *Annu Rev Microbiol.* **55**:647-71.
84. **Mogridge, J., K. Cunningham, and R. J. Collier.** 2002. Stoichiometry of anthrax toxin complexes. *Biochemistry* **41**:1079-82.
85. **Moir A.** 2006. How do spores germinate? *J Appl Microbiol* **101**:526-30.
86. **Moir, A., B. M. Corfe, and J. Behravan.** 2002. Spore germination. *Cell Mol Life Sci* **59**:403-9.
87. **Moir, A., and D. A. Smith.** 1990. The genetics of bacterial spore germination. *Annu Rev Microbiol* **44**:531-53.
88. **Morris, S. L., et al.** 1981. Inhibition of *Bacillus cereus* spore outgrowth by covalent modification of a sulfhydryl group by nitrosothiol and iodoacetate. *J Bacteriol* **148**:465-471.

89. **Morris, S. L., R. C. Walsh, and J. N. Hansen.** 1984. Identification and characterization of some bacterial membrane sulfhydryl groups which are targets of bacteriostatic and antibiotic action. *J Biol Chem* **259**:13590-4.
90. **Murayama, R., G. Akanuma, Y. Makino, H. Nanamiya, and F. Kawamura.** 2004. Spontaneous transformation and its use for genetic mapping in *Bacillus subtilis*. *Biosci Biotechnol Biochem* **68**:1672-80.
91. **Oman, T. J., and W. A. van der Donk.** 2010. Follow the leader: the use of leader peptides to guide natural product biosynthesis. *Nat Chem Biol* **6**:9-18.
92. **Passalacqua KD, B. N., Herring-Palmer A, Hanna P.** 2006. The superoxide dismutases of *Bacillus anthracis* do not cooperatively protect against endogenous superoxide stress. *J Bacteriol* **188**:3837-48.
93. **Patton, G. C., and W. A. van der Donk.** 2005. New developments in lantibiotic biosynthesis and mode of action. *Curr Opin Microbiol* **8**:543-51.
94. **Peschel, A., M. Otto, R. W. Jack, H. Kalbacher, G. Jung, and F. Gotz.** 1999. Inactivation of the *dlt* operon in *Staphylococcus aureus* confers sensitivity to defensins, protegrins, and other antimicrobial peptides. *J Biol Chem* **274**:8405-10.
95. **Piggot, P. J., and D. W. Hilbert.** 2004. Sporulation of *Bacillus subtilis*. *Curr Opin Microbiol* **7**:579-86.
96. **Piris-Gimenez, A., M. Paya, G. Lambeau, M. Chignard, M. Mock, L. Touqui, and P. L. Goossens.** 2005. *In vivo* protective role of human group IIa phospholipase A2 against experimental anthrax. *J Immunol* **175**:6786-91.
97. **Plomp, M., T. J. Leighton, K. E. Wheeler, H. D. Hill, and A. J. Malkin.** 2007. *In vitro* high-resolution structural dynamics of single germinating bacterial spores. *Proc Natl Acad Sci U S A* **104**:9644-9.
98. **Popham, D. L., J. Helin, C. E. Costello, and P. Setlow.** 1996. Muramic lactam in peptidoglycan of *Bacillus subtilis* spores is required for spore outgrowth but not for spore dehydration or heat resistance. *Proc Natl Acad Sci U S A* **93**:15405-10.
99. **Popham DL, S. S., Setlow P.** 1995. Heat, hydrogen peroxide, and UV resistance of *Bacillus subtilis* spores with increased core water content and with or without major DNA-binding proteins. *Appl Environ Microbiol* **61**:3633-8.

100. **Powell, J. F.** 1950. Factors affecting the germination of thick suspensions of *Bacillus subtilis* spores in L-alanine solution. *J Gen Microbiol* **4**:330-8.
101. **Raines, K. W., T. J. Kang, S. Hibbs, G. L. Cao, J. Weaver, P. Tsai, L. Baillie, A. S. Cross, and G. M. Rosen.** 2006. Importance of nitric oxide synthase in the control of infection by *Bacillus anthracis*. *Infect Immun* **74**:2268-76.
102. **Raymond, B., D. Leduc, L. Ravaux, R. Le Goffic, T. Candela, M. Raymondjean, P. L. Goossens, and L. Touqui.** 2007. Edema toxin impairs anthracidal phospholipase A2 expression by alveolar macrophages. *PLoS Pathog* **3**:e187.
103. **Rink, R., J. Wierenga, A. Kuipers, L. D. Kluskens, A. J. Driessen, O. P. Kuipers, and G. N. Moll.** 2007. Dissection and modulation of the four distinct activities of nisin by mutagenesis of rings A and B and by C-terminal truncation. *Appl Environ Microbiol* **73**:5809-16.
104. **Roelants, G. E., L. F. Whitten, A. Hobson, and J. W. Goodman.** 1969. Immunochemical studies on the poly-gamma-D-glutamyl capsule of *Bacillus anthracis*. VI. The *in vivo* fate and distribution to immunized rabbits of the polypeptide in immunogenic and nonimmunogenic forms. *J Immunol* **103**:937-43.
105. **Ruhr, E., and H. G. Sahl.** 1985. Mode of action of the peptide antibiotic nisin and influence on the membrane potential of whole cells and on cytoplasmic and artificial membrane vesicles. *Antimicrob Agents Chemother* **27**:841-5.
106. **Russell, B. H., R. Vasan, D. R. Keene, T. M. Koehler, and Y. Xu.** 2008. Potential dissemination of *Bacillus anthracis* utilizing human lung epithelial cells. *Cell Microbiol* **10**:945-57.
107. **Saile, E., and T. M. Koehler.** 2002. Control of anthrax toxin gene expression by the transition state regulator *abrB*. *J Bacteriol* **184**:370-80.
108. **Saile E, K. T.** 2006. *Bacillus anthracis* multiplication, persistence, and genetic exchange in the rhizosphere of grass plants. *Appl Environ Microbiol* **72**:3168-74.
109. **Schleifer, K. H. a. O. K.** 1972. Peptidoglycan types of bacterial cell walls and their taxonomic Implications. *Bacteriological Reviews* **36**:407-477.
110. **Schwartz, M.** 2009. Dr. Jekyll and Mr. Hyde: a short history of anthrax. *Mol Aspects Med* **30**:347-55.

111. **Scobie, H. M., and J. A. Young.** 2005. Interactions between anthrax toxin receptors and protective antigen. *Curr Opin Microbiol* **8**:106-12.
112. **Setlow B, A. S., Kitchel R, Koziol-Dube K, Setlow P.** 2006. Role of dipicolinic acid in resistance and stability of spores of *Bacillus subtilis* with or without DNA-protective α/β -type small acid-soluble proteins. *J Bacteriol* **188**:3740-7.
113. **Setlow, B., C. A. Loshon, P. C. Genest, A. E. Cowan, C. Setlow, and P. Setlow.** 2002. Mechanisms of killing spores of *Bacillus subtilis* by acid, alkali and ethanol. *J Appl Microbiol* **92**:362-75.
114. **Setlow, B., and P. Setlow.** 1996. Role of DNA repair in *Bacillus subtilis* spore resistance. *J Bacteriol* **178**:3486-95.
115. **Setlow, B., K. J. Tautvydas, and P. Setlow.** 1998. Small, acid-soluble spore proteins of the α/β type do not protect the DNA in *Bacillus subtilis* spores against base alkylation. *Appl Environ Microbiol* **64**:1958-62.
116. **Setlow, P. (ed.).** 1983. Germination and outgrowth, vol. II. London: Academic Press.
117. **Setlow, P.** 2007. I will survive: DNA protection in bacterial spores. *Trends Microbiol* **15**:172-80.
118. **Setlow, P.** 1992. I will survive: protecting and repairing spore DNA. *J Bacteriol* **174**:2737-41.
119. **Setlow, P.** 1995. Mechanisms for the prevention of damage to DNA in spores of *Bacillus* species. *Annu Rev Microbiol* **49**:29-54.
120. **Setlow, P.** 1994. Mechanisms which contribute to the long-term survival of spores of *Bacillus* species. *Soc Appl Bacteriol Symp Ser* **23**:49S-60S.
121. **Setlow, P.** 2003. Spore germination. *Curr Opin Microbiol* **6**:550-6.
122. **Setlow, P.** 2006. Spores of *Bacillus subtilis*: their resistance to and killing by radiation, heat and chemicals. *J Appl Microbiol* **101**:514-25.
123. **Shannon, J. G., C. L. Ross, T. M. Koehler, and R. F. Rest.** 2003. Characterization of anthrolysin O, the *Bacillus anthracis* cholesterol-dependent cytolysin. *Infect Immun* **71**:3183-9.
124. **Shapiro, M. P., B. Setlow, and P. Setlow.** 2004. Killing of *Bacillus subtilis* spores by a modified Fenton reagent containing CuCl_2 and ascorbic acid. *Appl Environ Microbiol* **70**:2535-9.

125. **Shatalin, K., I. Gusarov, E. Avetissova, Y. Shatalina, L. E. McQuade, S. J. Lippard, and E. Nudler.** 2008. *Bacillus anthracis*-derived nitric oxide is essential for pathogen virulence and survival in macrophages. *Proc Natl Acad Sci U S A* **105**:1009-13.
126. **Shepard, C. W., M. Soriano-Gabarro, E. R. Zell, J. Hayslett, S. Lukacs, S. Goldstein, S. Factor, J. Jones, R. Ridzon, I. Williams, and N. Rosenstein.** 2002. Antimicrobial postexposure prophylaxis for anthrax: adverse events and adherence. *Emerg Infect Dis* **8**:1124-32.
127. **Shin, S., Y. B. Kim, and G. H. Hur.** 1999. Involvement of phospholipase A2 activation in anthrax lethal toxin-induced cytotoxicity. *Cell Biol Toxicol* **15**:19-29.
128. **Sirard, J. C., C. Guidi-Rontani, A. Fouet, and M. Mock.** 2000. Characterization of a plasmid region involved in *Bacillus anthracis* toxin production and pathogenesis. *Int J Med Microbiol* **290**:313-6.
129. **Steichen, C. T., J. F. Kearney, and C. L. Turnbough, Jr.** 2007. Non-uniform assembly of the *Bacillus anthracis* exosporium and a bottle cap model for spore germination and outgrowth. *Mol Microbiol* **64**:359-67.
130. **Stein, T., S. Heinzmann, P. Kiesau, B. Himmel, and K. D. Entian.** 2003. The *spa*-box for transcriptional activation of subtilin biosynthesis and immunity in *Bacillus subtilis*. *Mol Microbiol* **47**:1627-36.
131. **Stojkovic, B., E. M. Torres, A. M. Prouty, H. K. Patel, L. Zhuang, T. M. Koehler, J. D. Ballard, and S. R. Blanke.** 2008. High-throughput, single-cell analysis of macrophage interactions with fluorescently labeled *Bacillus anthracis* spores. *Appl Environ Microbiol* **74**:5201-10.
132. **Sun, Z., J. Zhong, X. Liang, J. Liu, X. Chen, and L. Huan.** 2009. Novel mechanism for nisin resistance via proteolytic degradation of nisin by the nisin resistance protein NSR. *Antimicrob Agents Chemother* **53**:1964-73.
133. **Takala, T. M., and P. E. Saris.** 2006. C-terminus of Nisl provides specificity to nisin. *Microbiology* **152**:3543-9.
134. **Tennen, R., B. Setlow, K. L. Davis, C. A. Loshon, and P. Setlow.** 2000. Mechanisms of killing of spores of *Bacillus subtilis* by iodine, glutaraldehyde and nitrous acid. *J Appl Microbiol* **89**:330-8.
135. **Tournier, J. N., A. Quesnel-Hellmann, A. Cleret, and D. R. Vidal.** 2007. Contribution of toxins to the pathogenesis of inhalational anthrax. *Cell Microbiol* **9**:555-65.

136. **Tournier, J. N., S. Rossi Paccani, A. Quesnel-Hellmann, and C. T. Baldari.** 2009. Anthrax toxins: a weapon to systematically dismantle the host immune defenses. *Mol Aspects Med* **30**:456-66.
137. **Tournier, J. N., R. G. Ulrich, A. Quesnel-Hellmann, M. Mohamadzadeh, and B. G. Stiles.** 2009. Anthrax, toxins and vaccines: a 125-year journey targeting *Bacillus anthracis*. *Expert Rev Anti Infect Ther* **7**:219-36.
138. **Turnbull, P. C., N. M. Sirianni, C. I. LeBron, M. N. Samaan, F. N. Sutton, A. E. Reyes, and L. F. Peruski, Jr.** 2004. MICs of selected antibiotics for *Bacillus anthracis*, *Bacillus cereus*, *Bacillus thuringiensis*, and *Bacillus mycoides* from a range of clinical and environmental sources as determined by the Etest. *J Clin Microbiol* **42**:3626-34.
139. **van de Kamp, M., L. M. Horstink, H. W. van den Hooven, R. N. Konings, C. W. Hilbers, A. Frey, H. G. Sahl, J. W. Metzger, and F. J. van de Ven.** 1995. Sequence analysis by NMR spectroscopy of the peptide lantibiotic epilancin K7 from *Staphylococcus epidermidis* K7. *Eur J Biochem* **227**:757-71.
140. **van de Kamp, M., H. W. van den Hooven, R. N. Konings, G. Bierbaum, H. G. Sahl, O. P. Kuipers, R. J. Siezen, W. M. de Vos, C. W. Hilbers, and F. J. van de Ven.** 1995. Elucidation of the primary structure of the lantibiotic epilancin K7 from *Staphylococcus epidermidis* K7. Cloning and characterization of the epilancin-K7-encoding gene and NMR analysis of mature epilancin K7. *Eur J Biochem* **230**:587-600.
141. **Van de Ven, F. J., H. W. Van den Hooven, R. N. Konings, and C. W. Hilbers.** 1991. NMR studies of lantibiotics. The structure of nisin in aqueous solution. *Eur J Biochem* **202**:1181-8.
142. **van der Goot, G., and J. A. Young.** 2009. Receptors of anthrax toxin and cell entry. *Mol Aspects Med* **30**:406-12.
143. **Walsh, C.** 2003. *Antibiotics Actions, Origins, Resistance.* ASM PRes, Washington, D.C.
144. **Weaver, J., T. J. Kang, K. W. Raines, G. L. Cao, S. Hibbs, P. Tsai, L. Baillie, G. M. Rosen, and A. S. Cross.** 2007. The protective role of *Bacillus anthracis* exosporium in macrophage-mediated killing by nitric oxide. *Infect Immun* **75**:3894-901.

145. **Wiedemann, I., E. Breukink, C. van Kraaij, O. P. Kuipers, G. Bierbaum, B. de Kruijff, and H. G. Sahl.** 2001. Specific binding of nisin to the peptidoglycan precursor lipid II combines pore formation and inhibition of cell wall biosynthesis for potent antibiotic activity. *J Biol Chem* **276**:1772-9.
146. **Wilson, A. C., J. A. Hoch, and M. Perego.** 2009. Two small c-type cytochromes affect virulence gene expression in *Bacillus anthracis*. *Mol Microbiol* **72**:109-23.
147. **Young, J. A., and R. J. Collier.** 2007. Anthrax toxin: receptor binding, internalization, pore formation, and translocation. *Annu Rev Biochem* **76**:243-65.
148. **Young, S. B., and P. Setlow.** 2004. Mechanisms of *Bacillus subtilis* spore resistance to and killing by aqueous ozone. *J Appl Microbiol* **96**:1133-42.
149. **Young, S. B., and P. Setlow.** 2004. Mechanisms of killing of *Bacillus subtilis* spores by Decon and Oxone, two general decontaminants for biological agents. *J Appl Microbiol* **96**:289-301.
150. **Young, S. B., and P. Setlow.** 2003. Mechanisms of killing of *Bacillus subtilis* spores by hypochlorite and chlorine dioxide. *J Appl Microbiol* **95**:54-67.

CHAPTER 2: INHIBITION OF *BACILLUS ANTHRACIS* SPORE OUTGROWTH BY NISIN¹

2.1 Introduction

Nisin is a 34 amino acid peptide produced by *Lactococcus lactis* sbsp. *lactis* (ATCC 11454) (11), which has emerged as an important prototype for studying the novel antibacterial properties and structure-activity relationships characteristic of the lantibiotics (5, 34). Like all lantibiotics, nisin is ribosomally translated and then post-translationally modified to generate the 3 noncyclic, non-proteogenic amino acids, dehydroalanine and dehydrobutyrine, and 5 lanthionine or methyllanthionine thioether rings (11).

The utility of nisin derives from its capacity to act upon Gram-positive bacteria by two entirely different mechanisms (15, 48). Nisin forms pores in lipid membranes (48), but also functions as a transglycosylase inhibitor to disrupt cell wall biosynthesis via binding and mislocalization of lipid II (21, 57). By functioning as a “two-edged” sword, nisin has been relatively refractory to the emergence of microbial resistance, despite widespread and persistent use in the food industry as a preservative (15, 48).

An additional and poorly understood activity of nisin is the capacity to prevent the outgrowth of spores from several Gram-positive bacteria, including several *Bacillus* species (9, 10, 42, 44). To date, nisin inhibition of *Bacillus* spore outgrowth has been documented by various methods, including the spectrophotometric measurement of liquid culture turbidity (3), enumeration of

¹ Reproduced in part with permission from: " Inhibition of *Bacillus anthracis* spore outgrowth by nisin." *Antimicrob Agents Chemother.* **2008** Dec;52(12):4281-8. Copyright 2008 by the American Society for Microbiology.

colony forming units (CFU) (4, 14, 33, 36, 45), well-diffusion assays on solid agar (14, 41), and microscopic observations (43). Although useful, these approaches have provided few details about nisin's mode of action against *Bacillus* spores. At the onset of this work, it was not experimentally established whether nisin inhibits spore outgrowth by preventing germination initiation or, alternatively, at a step downstream of germination initiation. Additionally, the requirement for germination for nisin action had not been addressed. Finally, it was not clear whether or not nisin action requires actively growing organisms, analogous to many other antibiotics.

To address these issues, the effects of nisin on *Bacillus* spores and their development into replicating bacilli were evaluated using spores from *B. anthracis* Sterne 7702 as a model. The results from these studies indicate that nisin does not inhibit germination initiation; instead, germination is required for irreversible inhibition. Nisin acted rapidly upon germinating spores to prevent the establishment of oxidative metabolism or a membrane potential, possibly by a mechanism involving the disruption of membrane integrity. Nisin did not inhibit the removal of the outer spore structures (e.g. exosporium, cortex, and spore coat). Collectively, these data suggest that nisin acts upon spores immediately after the initiation of germination, and effectively blocks the capacity of *B. anthracis* to proliferate or produce virulence factors.

2.2 Results

2.2.1 Purification of nisin.

Nisin was purified from the food grade and commercial version of nisin known as Nisaplin®. Purification was performed via high performance liquid chromatography (HPLC) utilizing a Waters C4 column. A 0.1% trifluoroacetic acid and acetonitrile gradient from 0-100% over 45 min yielded a retention time of 27 min for nisin. Fortunately, the gradient was able to resolve wild-type (wt) nisin and a version of nisin missing a dehydration (Figure 2.1), and with purified nisin in hand, investigation into the mechanisms of nisin inhibition of spore outgrowth was made possible.

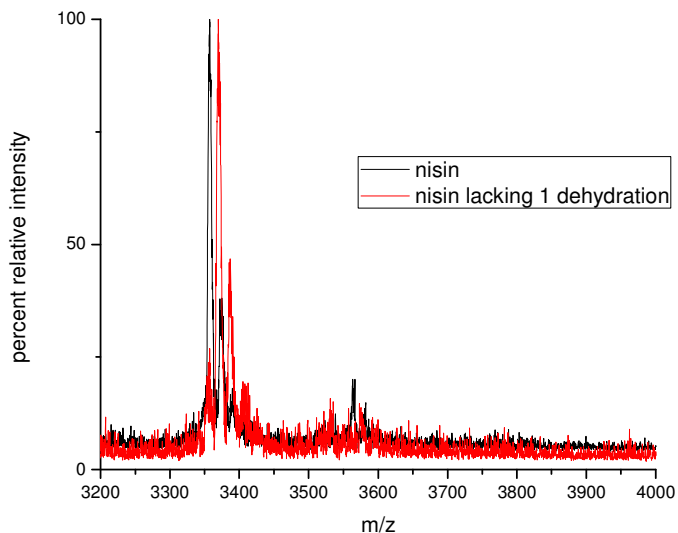


Figure 2.1. Nisin Purification. Nisin (wt, black) and nisin missing one dehydration (red) were purified from Nisaplin using high performance liquid chromatography with a C4 preparative column.

2.2.2 Growth inhibition by nisin.

Previous studies reported that nisin prevented the growth of *Bacillus* spores derived from several different species (4, 14, 33, 36, 45). To evaluate the action of nisin, spores were prepared from *B. anthracis* Sterne 7702, which is a strain commonly employed as a model for investigating the early stages of anthrax disease (24, 49). To validate earlier results, *B. anthracis* spores were incubated in BHI medium, which has been used to induce germination of *B. anthracis* spores (17), supplemented with either nisin (0.05 μ M to 100 μ M) or a buffer control (0.1 M MOPS pH 6.8). Pilot experiments confirmed that 0.1 M MOPS (pH 6.8) alone did not induce spore germination (data not shown). In BHI medium inoculated with 4.4×10^6 spores/mL, nisin inhibited *B. anthracis* growth, with IC₅₀ and IC₉₀ values of 0.57 μ M and 0.90 μ M, respectively (Table 2.1). The inhibitory activity of nisin against spores was not strictly dependent on BHI medium, as nisin inhibited *B. anthracis* spore outgrowth to the same degree in LB medium, or, MEM, DMEM, or RPMI cell culture media each supplemented with 10% FBS (data not shown). Relative to cultures at the initial time point, approximately 10,000-fold more colony forming units (CFUs) were recovered at 10 h from cultures supplemented with either 0.1 μ M nisin or 0.1 M MOPS pH 6.8. In contrast, no detectable CFUs were recovered from 10 h cultures that had been supplemented with 1, 10, or 100 μ M nisin (Figure 2.2A). Furthermore, no detectable CFUs were recovered from 3 or 8 h cultures when supplemented with 1 μ M nisin (Figure 2.2B). In addition, when bacilli were incubated in the

presence of 1 μM nisin, inhibition of bacterial growth was also observed with differential interference contrast microscopy (DIC) (Figure 2.3).

Based on the results of these experiments, subsequent studies were conducted using 4.0×10^6 spores/mL because this concentration of spores was sufficient to generate detectable readouts for each assay, and yielded similar IC_{50} and IC_{90} values to those calculated at a higher spore concentration (4.4×10^7 spores/mL; Table 2.1) while at the same time allowing for several full sets of experiments to be conducted from each spore preparation.

No. of spores/mL ^a	IC_{50} (μM) ^b	IC_{90} (μM) ^c
4.4×10^4	0.17 ± 0.01	0.41 ± 0.02
4.4×10^5	0.19 ± 0.01	0.44 ± 0.01
4.4×10^6	0.57 ± 0.03	0.90 ± 0.01
4.4×10^7	0.63 ± 0.06	0.98 ± 0.01

Table 2.1. IC_{50} and IC_{90} values of nisin against *B. anthracis* spores. Three independent experiments were performed in triplicate with different spore preparations and nisin purifications. The values are reported as the averages of three experiments. *a* Spores were freshly prepared from *B. anthracis* Sterne 7702. *b* Defined as the nisin concentration that inhibits the growth of cultures of *B. anthracis* spores by 50% at 16 h. *c* Defined as the nisin concentration that inhibits the growth of cultures of *B. anthracis* spores by 90% at 16 h.

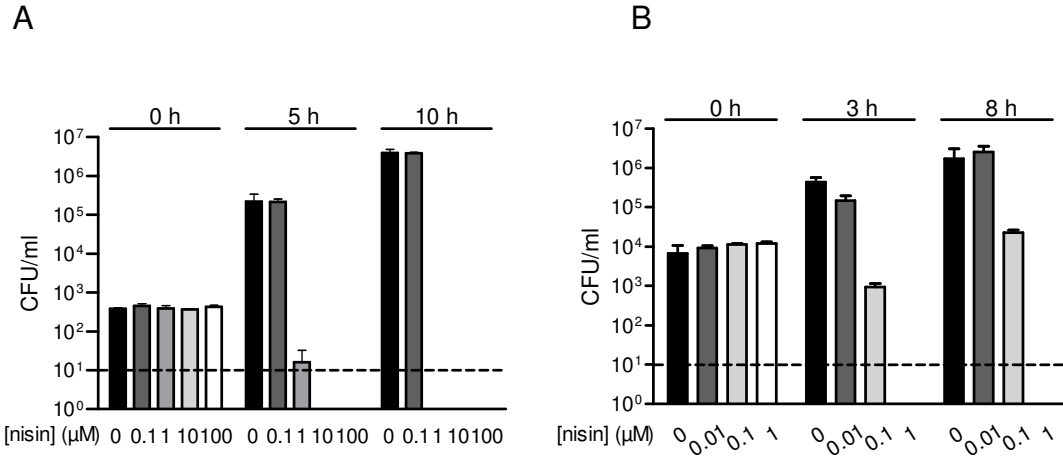


Figure 2.2. Nisin inhibition of *B. anthracis* growth. A. Spores. B. Bacilli. A & B. *B.*

anthracis was incubated in BHI at 37 °C with shaking in the absence and presence of nisin (0.01-100 μM, as indicated). At indicated time point, samples were taken and CFU plated to determine the number of viable cells. The dashed line indicates the threshold of sensitivity.

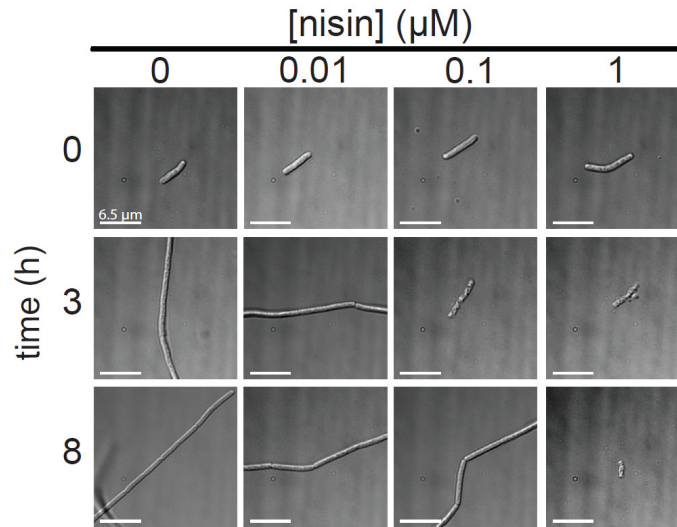


Figure 2.3. DIC microscopy of nisin inhibition of *B. anthracis* bacilli. Spores were incubated in BHI with indicated concentrations of nisin. The effects of nisin were monitored via DIC microscopy. White bar indicates 6.5 μm.

2.2.3 Nisin does not inhibit germination initiation.

The inability to recover CFUs from cultures of *B. anthracis* spores supplemented with nisin could be due to the irreversible inhibition of germination initiation. To evaluate this possibility, germination initiation was first monitored by measuring the characteristic loss of spore refractility that accompanies hydration of the spore structure, as indicated by a decrease in O.D._{600 nm} (31, 55). These experiments revealed a loss in refractility of >65% by 10 min in either the presence or absence of nisin (Figure 2.4A), indicating that nisin did not detectably alter hydration of the spores following germination initiation. Similarly, the loss of spore refractility was not altered in the presence of ciprofloxacin (0.01, 0.1, 1, and 10 μ M), an antibiotic commonly used to treat anthrax infections (data not shown). Incubation of spores with nisin alone (in the absence of known germinants) did not result in a loss of spore refractility (Figure 2.4B).

A second hallmark of germination initiation is the rapid loss of spore resistance to heat (31, 55). In both the presence and absence of nisin, spores demonstrated >80% loss in heat resistance by 5 min (Figure 2.5A), providing additional evidence that germination initiation was not altered in the presence of nisin. When spores were incubated in 0.1 M MOPS pH 6.8 supplemented with nisin, no loss in heat resistance was observed (Figure 2.5B), again confirming that nisin does not induce germination. Taken together, these results indicate that the loss of recoverable CFUs from cultures of spores supplemented with nisin was not due to the inhibition of germination initiation, thereby ruling out such a mechanism underlying the inhibitory action of nisin against spores. Instead,

these data seem to indicate that the loss of recoverable CFU from cultures of spores supplemented with nisin may be due to nisin-mediated killing of the germinated spores.

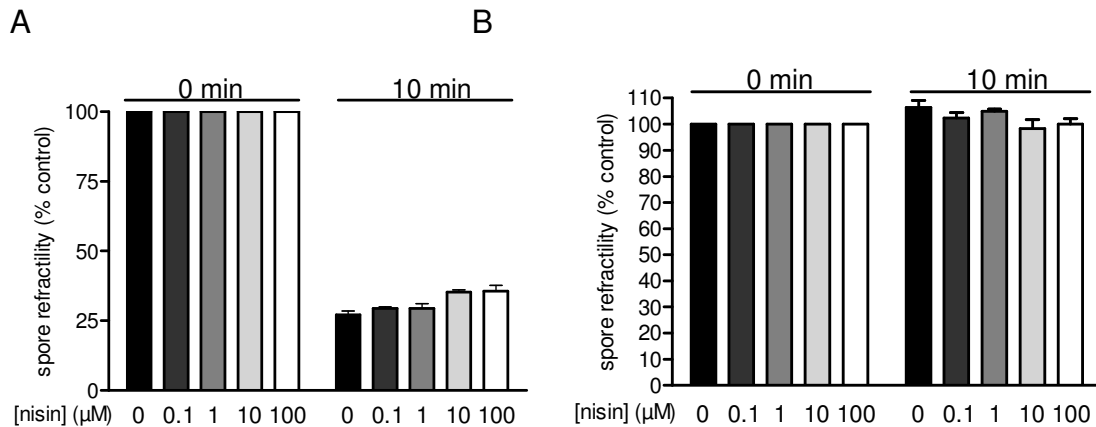


Figure 2.4. Effect of nisin on the loss of optical density. A. Effect of nisin in the presence of the germinant BHI. In all cases, the differences between spore refractility at 10 min relative to that at 0 min were statistically significant ($P < 0.05$). B. Effect of nisin in the absence of a germinant. A & B. The data are expressed as the percentage of the OD_{600} at time zero and 10 min relative to that of each culture at time zero. Shown is the mean of a single experiment conducted in triplicate as a representative of three independent experiments. Error bars indicate standard deviations.

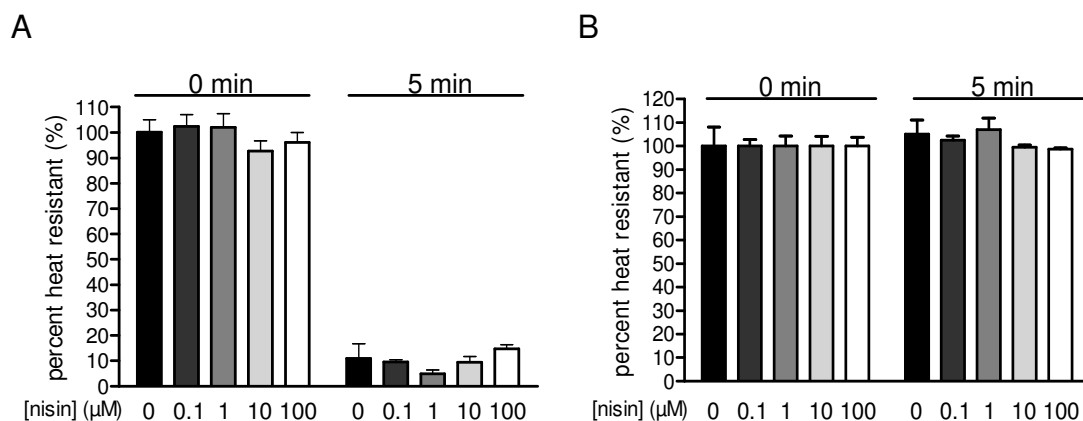


Figure 2.5. Effect of nisin on the loss of heat resistance. A. Effect of nisin in the presence of the germinant BHI. In all cases, the differences between the percentage of heat-resistant spores at 5 min relative to that at 0 min were statistically significant ($P < 0.05$). B. Effect of nisin in the absence of a germinant. A & B. At 0 and 5 min, samples were analyzed for heat resistance, as described under Materials and Methods. The data are expressed as the means of three experiments. Error bars indicate standard deviations.

2.2.4 Germination initiation is required for the inhibitory action of nisin.

Whether germination initiation is necessary for nisin to act against spores was investigated next. Spores were incubated in BHI medium, in BHI medium supplemented with 10 μM nisin, or in 0.1 M MOPS supplemented with 10 μM nisin. After 1 h, the spores were washed to lower the concentration of nisin in solution to approximately 1 nM, which is well below the IC_{50} . After washing, the spores were introduced into fresh BHI medium. As expected, spores that had been pre-incubated with nisin under germinating conditions did not grow when introduced into fresh BHI medium (Figure 2.6). In contrast, spores pre-incubated with nisin in the absence of germinant demonstrated robust growth in fresh BHI medium. These data indicate that germination initiation is a requisite for the inhibitory activity of nisin against spores.

To establish at which point during the germination process nisin-mediated inhibition becomes irreversible, spores were pre-incubated in BHI medium (to induce germination) supplemented with either nisin (10 μ M) or 0.1 M MOPS. At various times, samples from each culture were washed extensively to lower the concentration of nisin in the spore suspensions to levels well below the IC₉₀, and introduced into fresh BHI medium. These experiments revealed that exposure of *B. anthracis* spores to nisin for as little as 5 min under germinating conditions completely blocked growth of the germinated spores in fresh medium lacking nisin (Figure 2.7). These results suggest that the inhibitory action of nisin against spores becomes irreversible soon (<5 min) after germination is initiated.

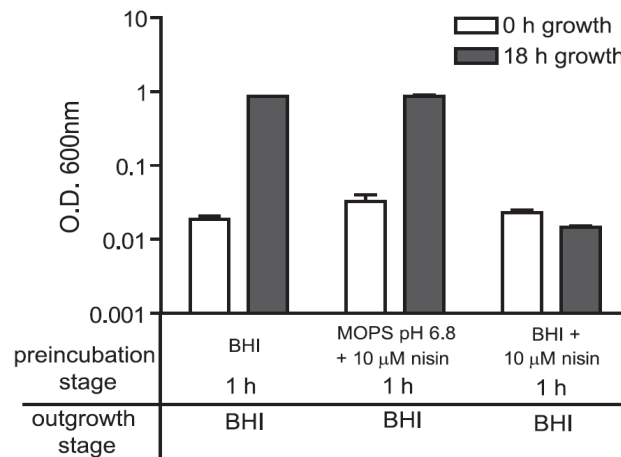


Figure 2.6. Germination is required for the inhibitory action of nisin. The data are expressed as the mean of a single experiment conducted in triplicate and are representative of those from two independent experiments. Error bars indicate standard deviations. In all cases, the differences between the OD₆₀₀ at 18 h relative to that at 0 h were statistically significant ($P < 0.05$).

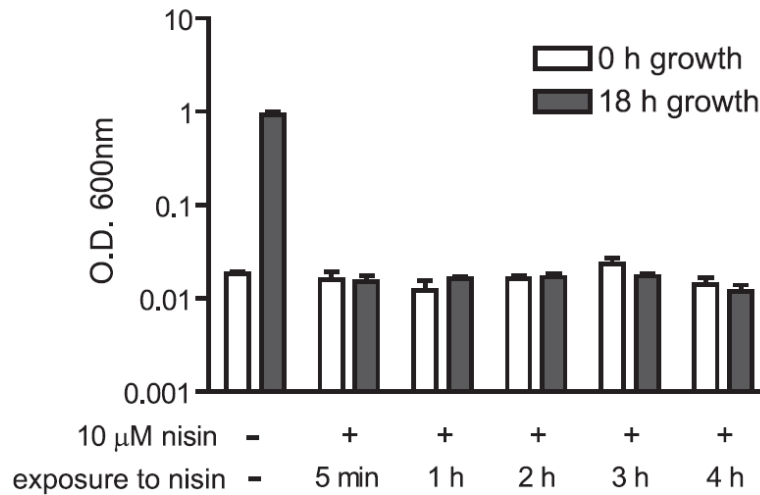


Figure 2.7. The inhibitory action of nisin is irreversible. The data are expressed as the mean of a single experiment conducted in triplicate and are representative of those from two independent experiments. Error bars indicate standard deviations. In each case in which the spores were exposed to nisin, the increase in the OD₆₀₀ at 18 h relative to that at 0 h was not statistically significant ($P < 0.05$).

2.2.5 Nisin prevents spore development into vegetative bacilli.

To obtain additional insights into the stage of germination during which nisin arrests the development of spores into replicating, vegetative bacilli, the extended growth of cultures were monitored in the presence or absence of nisin. As expected, the O.D.₆₀₀ of each of the samples decreased initially, reflecting the rapid hydration of spores that characteristically follows germination initiation (Fig. 4A). After approximately 50 min, cultures supplemented with 0.1 μ M nisin demonstrated clear bacterial growth, albeit at a slower rate than cultures lacking nisin (Figure 2.8A). In contrast, there was no evidence of growth in cultures supplemented with higher concentrations of nisin, neither at 180 min (Fig, 4A), nor at extended time points (12 h; data not shown). Examination of samples

removed from these cultures at 5 and 10 h by DIC microscopy revealed characteristic chains of vegetative bacilli from cultures supplemented with either 0.1 μM nisin or the buffer control (Figure 2.8B), whereas no bacilli were present within cultures supplemented with 1, 10, or 100 μM nisin (Figure 2.8B). These results indicated that at concentrations greater than IC_{90} , nisin prevents the development of germinated spores into vegetative bacilli. In contrast to the action of nisin, ciprofloxacin did not prevent the development of germinated spores into vegetative bacilli, even at concentrations (0.1 and 1 μM) that inhibit the growth of vegetative *B. anthracis* (Figure 2.8C). At 10 μM ciprofloxacin, a significant increase in both length and width was observed (Figure 2.8C, Table 2.2), which suggests that ciprofloxacin cannot directly inhibit outgrowth; however, due to the irreparable double stranded breaks in the DNA induced by ciprofloxacin, complete outgrowth into a vegetative cell was prevented as a consequence of improper protein expression.

Figure 2.8

A

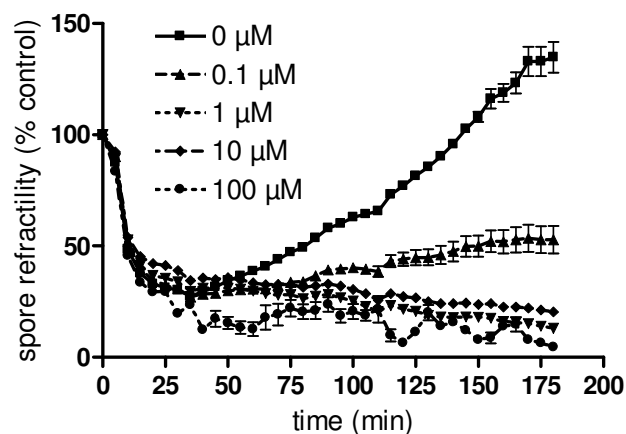


Figure 2.8 (Continued)

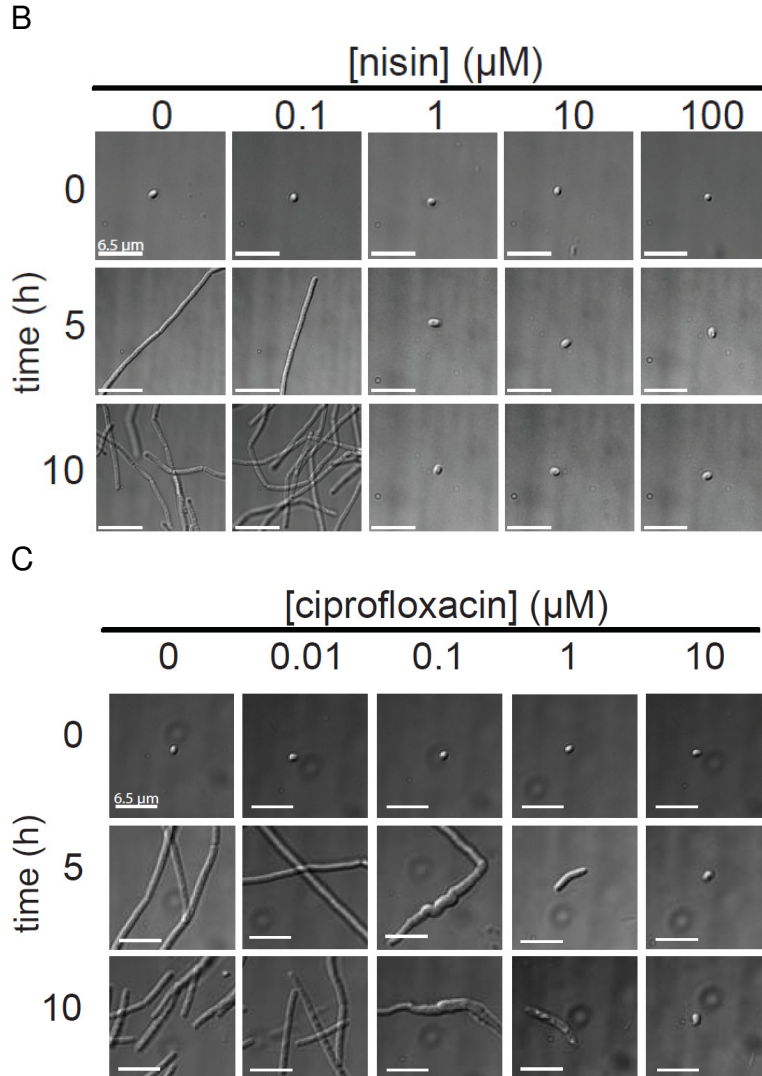


Figure 2.8. *B. anthracis* spores do not develop into vegetative bacilli in the presence of nisin. A. The data are expressed as the percentage of OD_{600} at each time point relative to the OD_{600} of each culture at time zero, which was the control in these experiments. The data are expressed as the means of a single experiment conducted in triplicate and are representative of those from three independent experiments. Error bars indicate standard deviations. B. Nisin effect on spore outgrowth. C. Ciprofloxacin effect on spore outgrowth. B & C. At time 0, 5, and 10 h, samples were removed and visualized by DIC microscopy. For each panel, a single spore is shown for clarity but is representative of all other *B. anthracis* spores within that sample. Bars, 6.5 μm . The data are representative of those from three independent experiments.

	10 μ M Nisin			10 μ M Ciprofloxacin		
	0 h	5 h	10 h	0 h	5 h	10 h
Length (μ m)	1.48 \pm 0.14	1.50 \pm 0.12	1.46 \pm 0.09	1.69 \pm 0.15	2.39 \pm 0.23*	2.21 \pm 0.26*
Width (μ m)	1.02 \pm 0.09	1.06 \pm 0.11	1.01 \pm 0.08	1.21 \pm 0.13	1.79 \pm 0.16*	1.59 \pm 0.14*

Table 2.2. Comparison of nisin and ciprofloxacin on the outgrowth of spores. The lengths and widths of the endospores and elongated endospores were measured using SoftWoRX Explorer Suite. (*) Using the Student t-test, a statistical difference was determined in size when 5 h and 10 h time points were compared to the 0 h time point for each inhibitor, $P < 0.0005$.

2.2.6 Spores incubated with nisin do not produce lethal toxin.

Although nisin prevents the development of spores into vegetative bacilli, it was not clear to what extent the action of nisin impairs additional events associated with spore germination. For *B. anthracis*, an important consideration is whether or not virulence factors, such as lethal toxin (LT) (53), are released prior to nisin-mediated killing of germinated spores. Spores were incubated under conditions that are known to induce LT production (23). In the absence of nisin, the two components of the bipartite LT, lethal factor (LF) and protective antigen (PA), were both readily detected by immunoblot analysis (Figure 2.9A). In contrast, neither LF nor PA was detected within culture supernatants prepared from *B. anthracis* cultures supplemented with 10 μ M nisin. By comparing the intensity of the cross-reacting material in 2-fold serially diluted cultured supernatants, the amounts of PA and LF were determined to be reduced at least 32- and 16-fold, respectively, in cultures supplemented with nisin compared to those supplemented with the buffer control (0.1 M MOPS pH 6.8; Figure 2.9B). Additional experiments showed that neither LF nor PA was detected within

homogenates of *B. anthracis* spores incubated for 1 h in BHI supplemented with nisin (Figure 2.10A), ruling out the possibility that LF or PA was present, but spore-associated. Finally, additional experiments indicated that nisin did not cause PA to precipitate out of solution (Figure 2.10B), ruling out another possible explanation for the absence of these proteins in *B. anthracis* cultures supplemented with nisin.

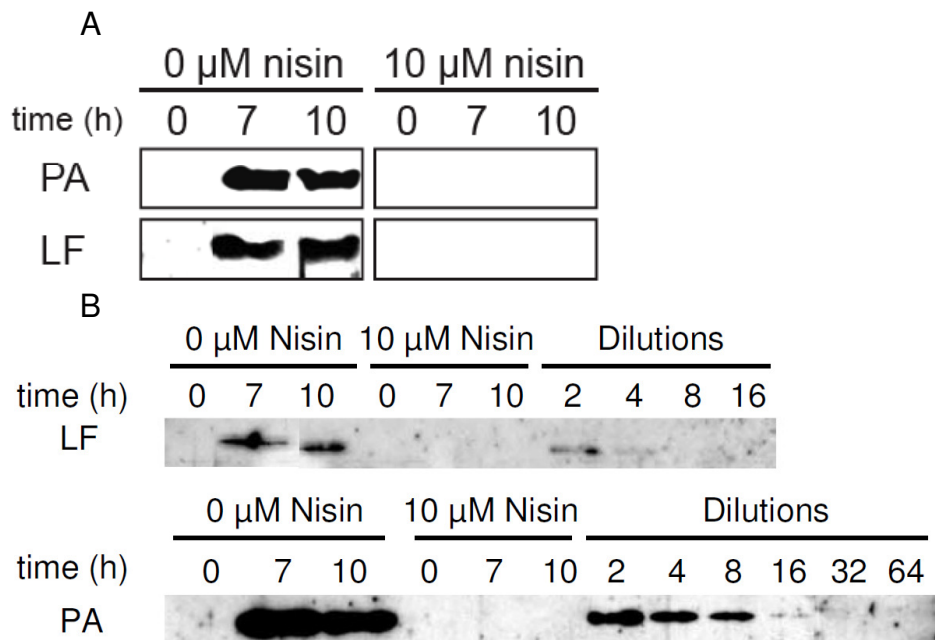


Figure 2.9. Effect of nisin on toxin expression. A. At 0, 7, and 10 h, culture supernatants were evaluated for the presence of LF and PA by immunoblot analysis. B. At 0, 7, and 10 h, culture supernatants were evaluated for the presence of LF and PA by immunoblot analysis. The 0 μM nisin 10 h culture supernatants were evaluated for the magnitude by which toxin expression was reduced via a series of 2-fold dilutions of culture supernatants. A & B. The samples in each lane were normalized for the volumes of the culture supernatants. The data are from a single experiment and are representative of data collected in three independent experiments.



Figure 2.10. Toxin association with organism and nisin induced precipitation of toxin. A. LF and PA were assayed within homogenates of *B. anthracis* bacilli or spores after incubation for 1 h in BHI supplemented with 10 μM nisin. B. Nisin induced precipitation of PA was assayed by immunoblot after incubation for 1 h in 0.1 M MOPS pH 6.8 supplemented with the indicated concentrations of nisin.

2.2.7 The action of nisin prevents spores from becoming metabolically active.

Dormant *B. anthracis* spores are metabolically inactive (50). One potential explanation for the lack of detectable LF or PA in *B. anthracis* cultures supplemented with nisin is the inability of germinating spores to establish an active metabolism. To evaluate this hypothesis, the cellular production of NAD(P)H was monitored as a measure of oxidative metabolism by determining the reduction of tetrazolium to formazan in a NAD(P)H-dependent manner (12). In the absence of nisin, a robust production of formazan was detected, beginning at 5-10 min after the initiation of germination, and the levels of formazan generated continued to increase during the course of the experiment (3 h) (Figure 2.11A). In the presence of 1, 10, or 100 μM nisin, small but detectable levels of formazan production were detected within 5-10 min after the initiation of germination, but formazan production did not continue to increase after this time.

Formazan production was detected in the presence of 0.1 μM nisin, albeit at a slower rate than in the absence of nisin. Formazan production was inhibited in the presence of 1 and 10 μM ciprofloxacin, but occurred in the presence of 0.01 and 0.1 μM ciprofloxacin, although to a lesser extent than in the absence of antibiotics (Figure 2.11B).

Because oxidative metabolism is linked to the establishment of an electrochemical gradient across the cytoplasmic membrane, the effects of nisin action on the establishment of a membrane potential within germinating spores were evaluated. In the presence of germinant, *B. anthracis* demonstrated significantly stronger staining with the membrane potential sensitive dye, 3,3'-diethyloxacarbocyanine iodide (DiOC_2) (30) than in the absence of germinant, indicating the establishment of membrane potential by 30 min subsequent to germination initiation (Figure 2.12A). In contrast, spores incubated in the presence of nisin demonstrated significantly less DiOC_2 staining at 30 min (Figure 2.12A), which indicated that at this early time point, nisin interfered with the establishment of membrane potential in germinating spores. By 5 and 10 h after germination initiation, spores incubated in the presence of 0.1 μM nisin demonstrated DiOC_2 staining similar to that of spores in the absence of nisin (94.9% MFI of spores in the absence of nisin; Figure 2.12C), indicating that these spores recovered and ultimately developed a membrane potential, although at a slower rate. Spores incubated in the presence of higher concentrations of nisin (1, 10, and 100 μM) did not demonstrate increased DiOC_2 staining at later time points (5 or 10 h; data not shown). Notably, in the presence of ciprofloxacin

(0.01, 0.1, 1, and 10 μM), germinating spores displayed DiOC₂ staining comparable to that measured in the absence of ciprofloxacin (approximately 80-100%; Figure 2.12B), indicating that, in contrast to nisin, ciprofloxacin did not prevent the establishment of membrane potential in germinating spores. Taken together, these studies suggest that nisin acts upon spores immediately after the initiation of germination, and that at concentrations non permissive for spore outgrowth (as demonstrated in Figure 2.8A & B), nisin prevents *B. anthracis* from becoming metabolically active.

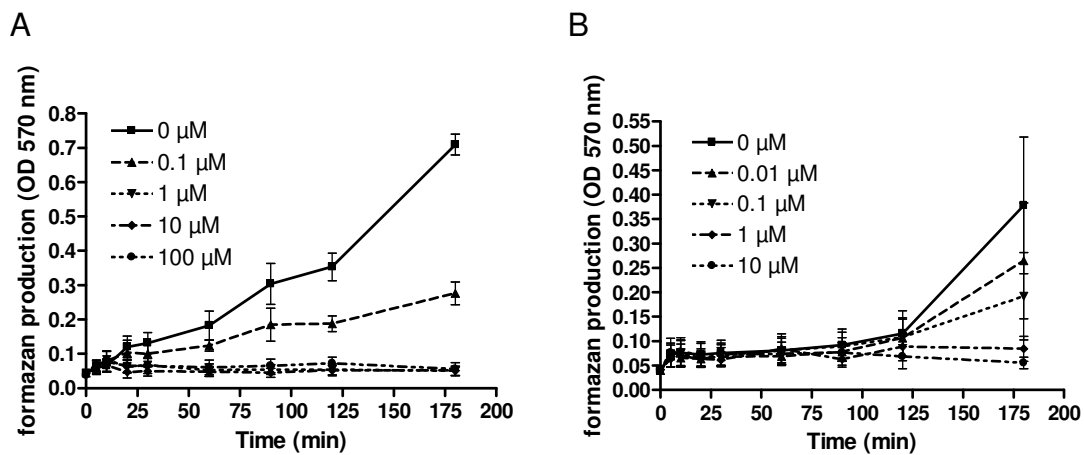


Figure 2.11. Effect of nisin and ciprofloxacin on oxidative metabolism establishment. A. Nisin. B. Ciprofloxacin. A & B. At the indicated times, aliquots were removed from the cultures and were evaluated for oxidative metabolism by measuring spectrophotometrically the production of formazan at 570 nm, as described under Materials and Methods.

Figure 2.12

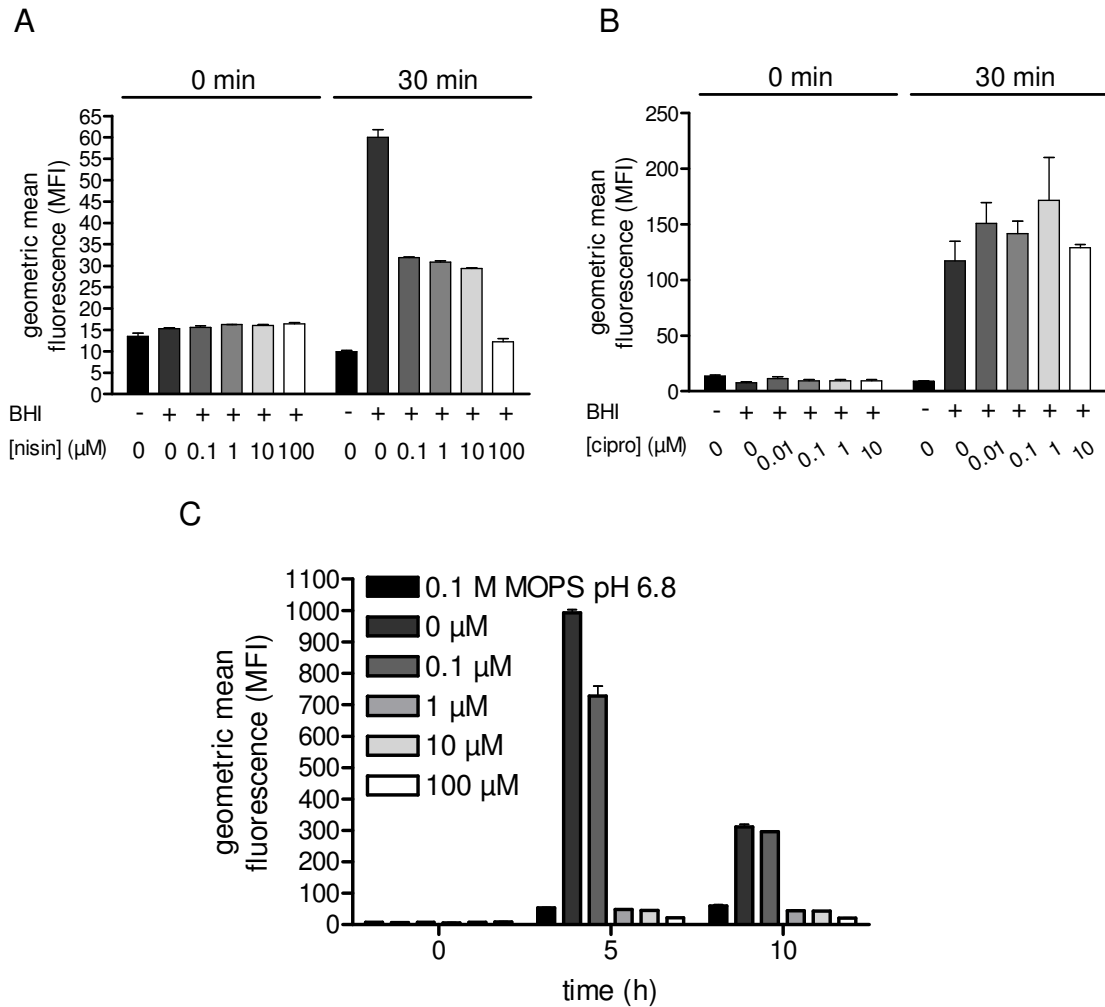


Figure 2.12. Effect of nisin and ciprofloxacin on membrane potential establishment. A. Nisin. The difference between the membrane potential at 30 min in the presence and the absence of nisin was statistically significant ($P < 0.05$). B. Ciprofloxacin. C. Nisin long term inhibition. At time zero (i.e., prior to the addition of nisin), 5 and 10 h, aliquots were removed from the cultures and evaluated for the membrane potential by measuring the DiOC₂-associated *B. anthracis* fluorescence by flow cytometry. The data are plotted as the MFI. The difference between the membrane potential at 5 and 10 h in the presence and the absence of nisin was statistically significant ($P < 0.05$) except for 0.1 μM at 10 h. A & B. At time zero (i.e., prior to the addition of nisin or ciprofloxacin) and 30 min, aliquots were removed from the cultures and evaluated for the membrane potential by measuring the DiOC₂-associated *B. anthracis*

Figure 2.12 (continued)

fluorescence by flow cytometry. The data are plotted as the MFI. A-C. Means of the data from a single experiment conducted in triplicate. The data are representative of those from three independent experiments. Error bars indicate standard deviations.

2.2.8 The effects of nisin action on membrane integrity.

The absence of oxidative metabolism in germinating spores in the presence of nisin could be due to a loss of membrane integrity (19, 52). To explore this possibility, germinating spores were evaluated for increases in membrane permeability by measuring the uptake of propidium iodide (PI) using flow cytometry. These experiments revealed that by 30 min, nisin induced 2-, 6-, 13-, or 56-fold increases in PI-uptake in spores incubated with 0.1, 1, 10, or 100 μM nisin, respectively, relative to spores incubated in the absence of nisin (Figure 2.13A). These experiments suggest that within germinating *B. anthracis* spores, nisin induces a dose-dependent disruption of membrane integrity. In contrast, in the presence of ciprofloxacin (0.01, 0.1, 1, or 10 μM) germinating spores exhibited only a modest (less than 2-fold) increase in PI-uptake (Figure 2.13B), further supporting the idea that nisin and ciprofloxacin affect the outgrowth of *B. anthracis* spores by fundamentally different mechanisms.

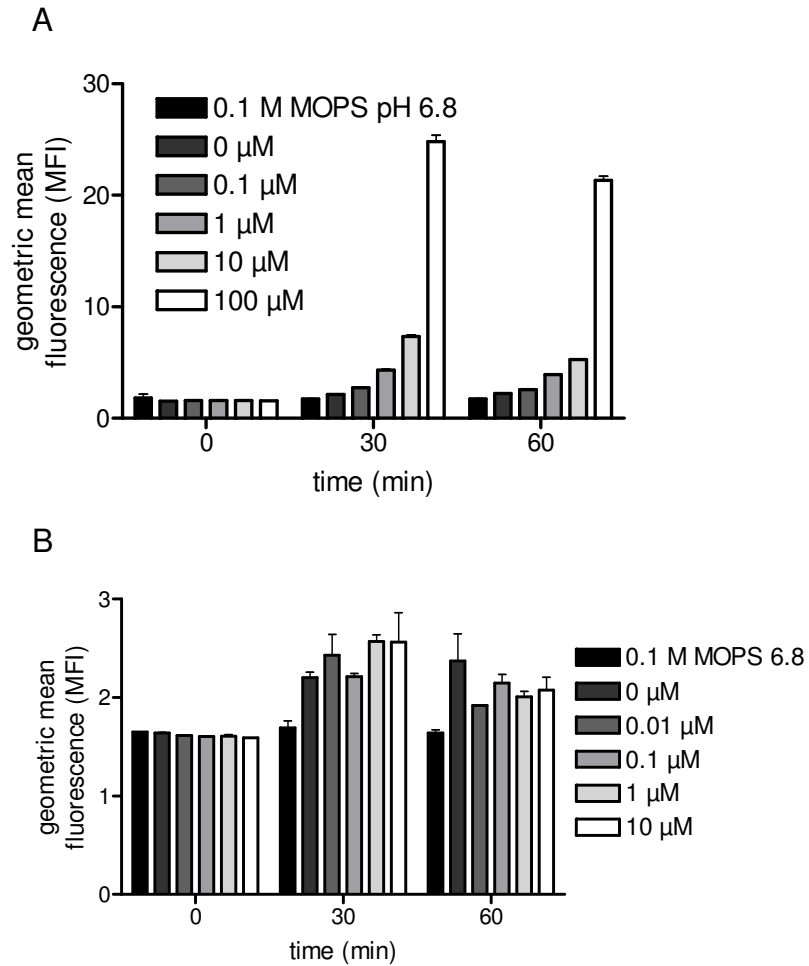


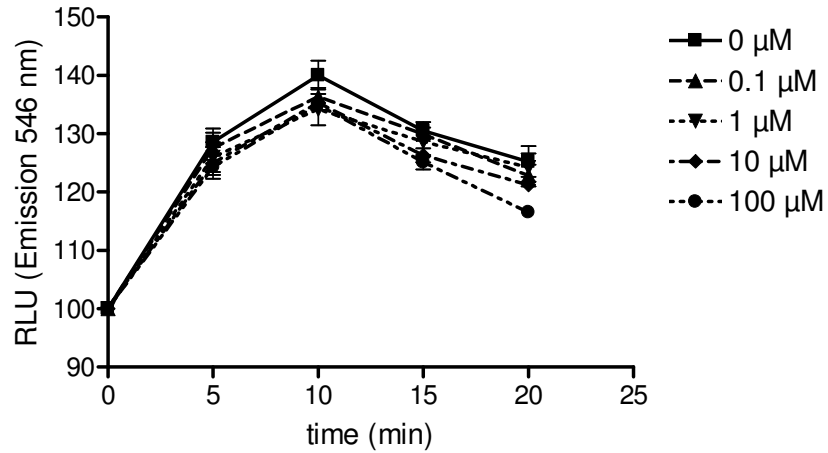
Figure 2.13. Effect of nisin and ciprofloxacin on membrane integrity. A. Nisin. In all cases, the differences in PI uptake in samples containing nisin at 30 and 60 min relative to that at 0 min were statistically significant ($P < 0.05$). B. Ciprofloxacin. A & B. At the indicated times, aliquots were removed from the cultures and evaluated for PI uptake, as described under Materials and Methods. The data were plotted as the geometric MFI. The means of the data from a single experiment conducted in triplicate are presented. The data are representative of those from three independent experiments. Error bars indicate standard deviations.

2.2.9 Nisin does not prevent spore remodeling during germination.

The inhibition of spore outgrowth could be due to disruption of the extensive remodeling of the spore structure that accompanies germination. To evaluate this possibility, the characteristic release of dipicolinic acid (DPA) from the spore structure, which occurs shortly after germination initiation (25, 56), was monitored. Both the magnitude and rate of DPA release were similar in the presence or absence of nisin (Figure 2.14A).

Nisin may inhibit “downstream” remodeling of the spore structure, which includes hydrolysis of the cortex and release from the spore coat and exosporium. In the absence of nisin, transmission electron microscopy (TEM) revealed that the core, cortex, spore coat and exosporium were readily evident in dormant spores (e.g. spores incubated in 0.1 M MOPS pH 6.8), but only the core remained in germinated spores (Figure 2.14B). Nisin did not inhibit the loss of cortex, spore coat, or exosporium in spores that had been incubated in BHI medium (Figure 2.14B). Taken together, these results indicate that nisin mediated action against spores does not involve the inhibition of the extensive remodeling of the spore structure.

A



B

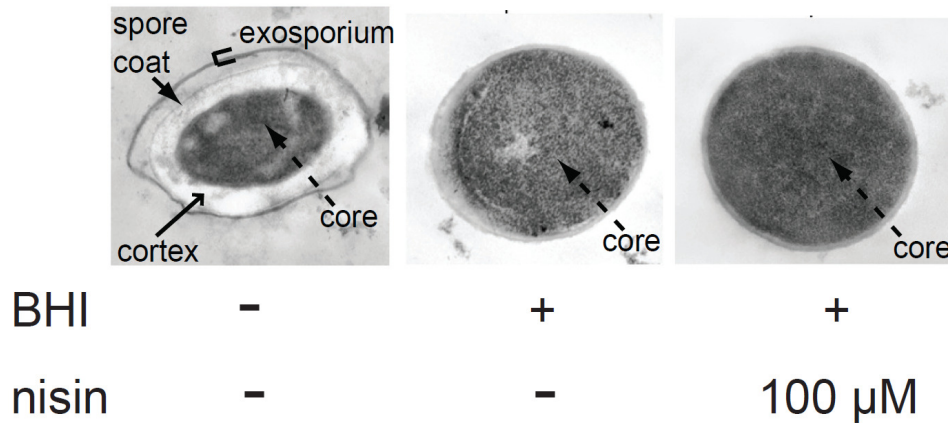


Figure 2.14. Effects of nisin on spore remodeling during germination. A. At the indicated times, cultures were evaluated for the release of DPA, as described under Materials and Methods. The means of the data from a single experiment conducted in triplicate are presented. The data are representative of those from three independent experiments. Error bars indicate standard deviations. B. After 90 min, the indicated samples were removed, fixed, and imaged by TEM, as described under Materials and Methods. RLU, relative light units.

2.2.10 Structural evaluation of nisin inhibition of bacilli and protoplasts.

In an effort to determine the overall structural effects nisin has on bacilli, nisin was incubated with bacilli and *B. anthracis* protoplasts, which were made by

incubating cells with 50 $\mu\text{g}/\text{mL}$ lysozyme. Cells and protoplasts were then fixed and processed for TEM and scanning electron microscopy (SEM) imaging. The SEM showed bacilli and protoplasts with a large pore-like structure that is located proximal to the pole or end of the rod shaped cell (Figure 2.15A). This pore-like structure could be an exceptionally large pore resulting from the disruption of the membrane by nisin. On the other hand and more likely, this structure may be an improperly formed septum due to early and asymmetrical cell division induced by the presence of nisin. This latter conclusion was previously drawn based on TEM data from the Benov laboratory (26). The authors concluded that nisin induced apremature and improper asymmetrical septum formation during cell division. The SEM images in Figure 2.15A support this conclusion monitoring the surface of the bacilli rather than a section in TEM. In addition, the location of the improper septum is also congruent with lipid II mis-localization that is induced by nisin (21). Furthermore, our TEM images of bacilli and protoplasts are congruent with the findings of Benov and coworkers (26). In the presence of nisin, ruffling of the membrane is observed in both protoplast and bacilli due to membrane disruption (Figure 2.15B). Moreover, the membrane separates from the cell wall in the TEM image of a cell (Figure 2.15B).

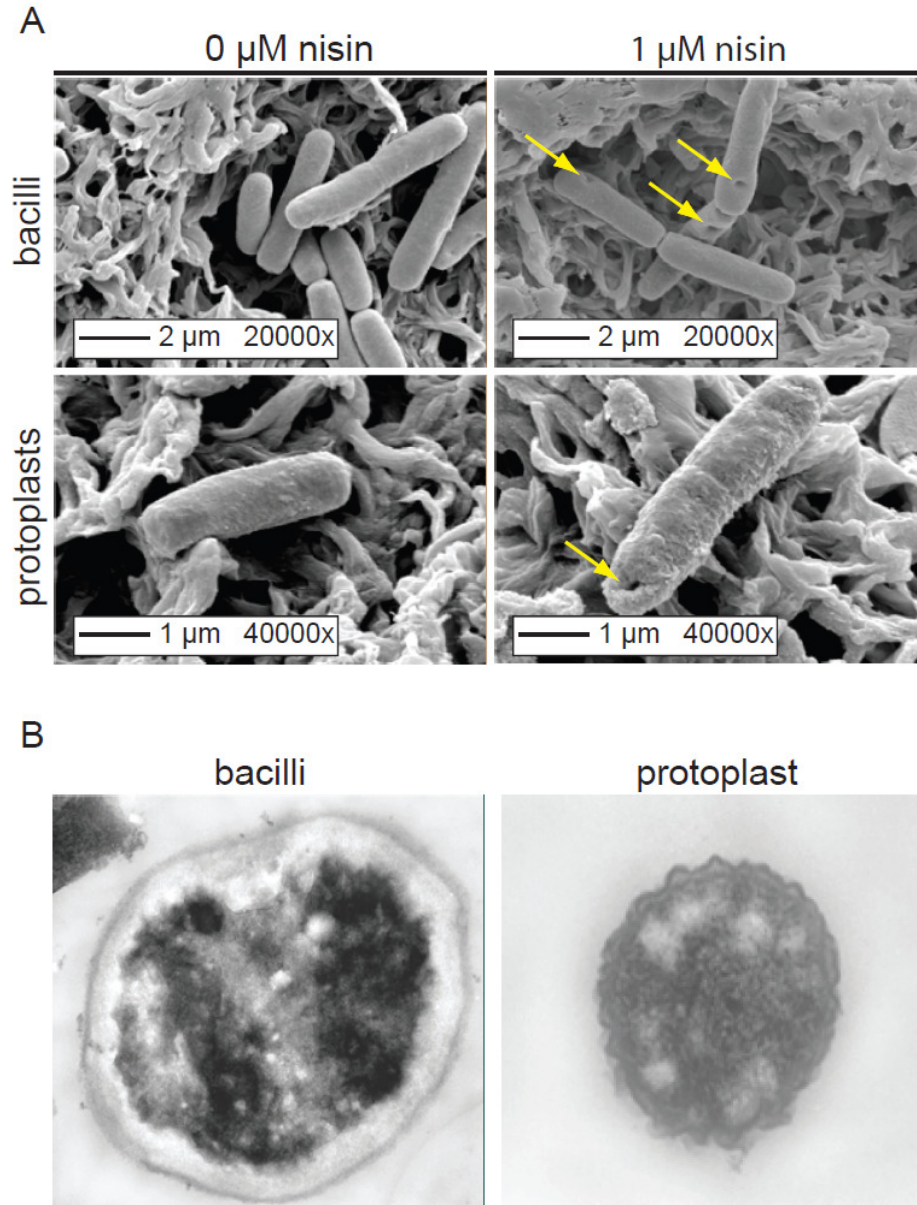


Figure 2.15. Structural evaluation of nisin inhibition of bacilli and protoplasts. A. SEM images of bacilli and protoplasts in the presence and absence of 1 μM nisin. B. TEM images of bacilli and protoplast in the presence of 1 μM nisin. A & B. Cells and protoplasts were incubated with nisin for 30 min, fixed, prepared for SEM and TEM imaging, and pictures were taken as described in "Materials and Methods".

2.2.11 Structural evaluation of nisin inhibition of spores.

In an effort to gain additional insights into the overall structural effect of nisin, SEM images were obtained of spores germinated in the presence of nisin. Dormant endospores, which were incubated in 0.1M MOPS at 37 °C as a control, displayed the typical ridge pattern of a dormant endospore (17). Previous research performed in the Driks laboratory using atomic force microscopy demonstrated that the observed ridges are typical for *Bacillus* endospores morphology (17). The endospores that were allowed to germinate had a smoothing of the ridges and increased in size presumably due to hydration of the endospore. The endospore that was incubated in BHI with nisin had a morphology distinct from the previous two conditions. The ridges of the dormant spore had disappeared, but the surface of the germinated endospore was very rough and had pockets or dimples present over the entire structure.

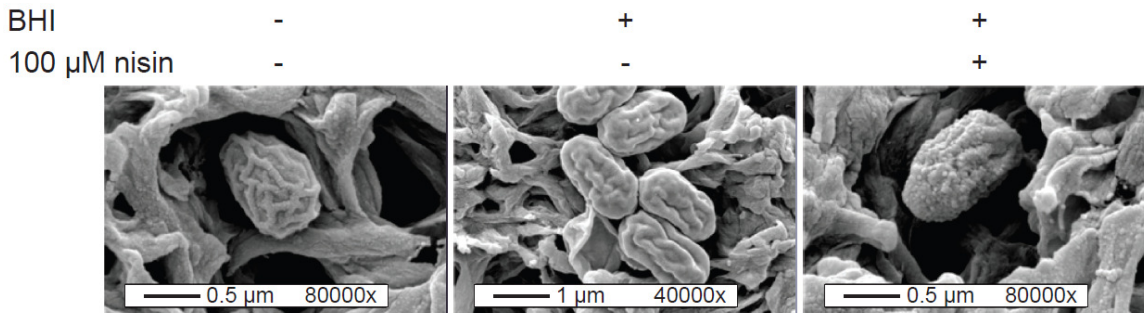


Figure 2.16. Structural evaluation of nisin inhibition of spores. Spores were incubated in the presence of 0.1 M MOPS pH 6.8 (non-germinating), BHI (germinating), and BHI with 100 μ M nisin for 1.5 h. Spores were fixed, underwent SEM sample preparation, and were imaged via SEM.

2.2.12 Effect of delayed addition of nisin on growth.

In an effort to identify a point within the growth cycle of *B. anthracis* where nisin is no longer effective, nisin was added to *B. anthracis* cultures at different points along a growth curve that started with dormant spores and culminated with stationary phase bacilli. *B. anthracis* endospores at an initial concentration of 8×10^7 spores/mL were incubated in BHI at 37 °C. At every hour from 0-12 h, nisin was added to a series of 12 cultures and the subsequent growth curves were monitored (final concentration 10 µM nisin). The effects of nisin were monitored by changes in optical density as a measure of growth at 600 nm throughout the 12 h. First, the results demonstrate that germination occurred in the presence of 10 µM nisin within 1 h indicated by the decrease in O.D. (Figure 2.17). While germination was not inhibited, nisin had the ability to inhibit the growth of *B. anthracis* through logarithmic growth, as shown by the large reduction in optical density post nisin addition due to cell lysis (Figure 2.17). Nisin also has an initial inhibitory effect on cells treated in late logarithmic and stationary phase, but if enough time is allotted for recovery, *B. anthracis* growth returns (Figure 2.17).

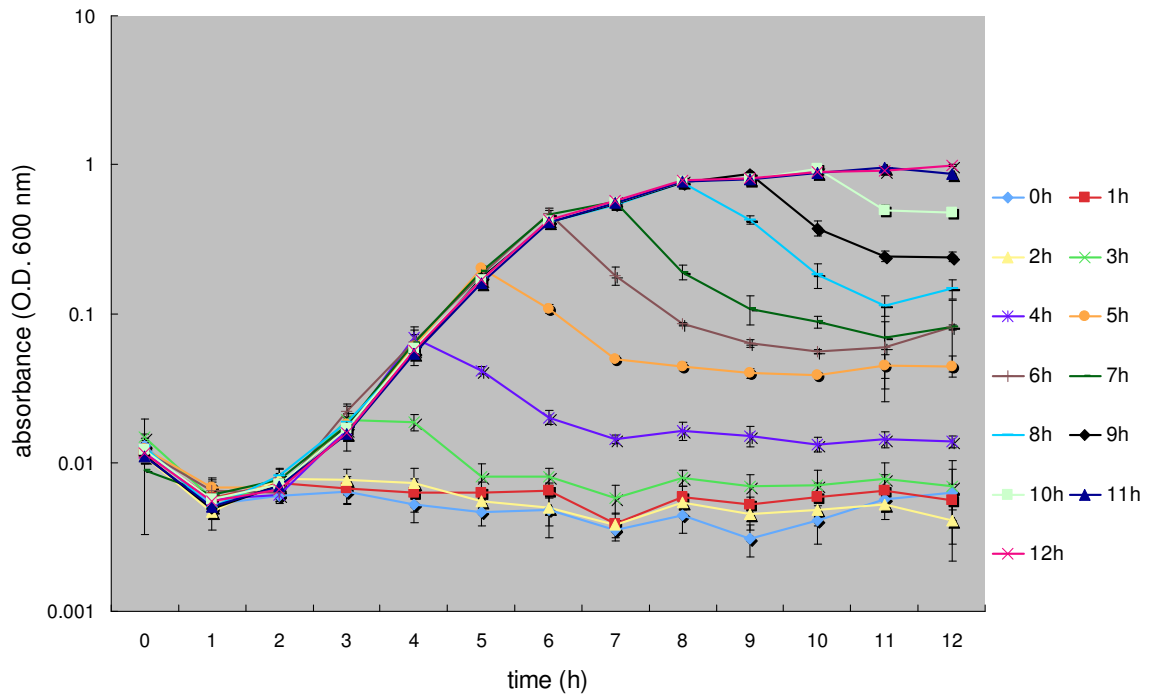


Figure 2.17. Effect of delayed addition of nisin on growth. At every hour from 0-12 h, nisin was added to a series of 12 parallel growth curves performed in triplicate. The effects of nisin were then monitored by the change in optical density at 600 nm as a measure of growth.

2.2.13 pH effects on *B. anthracis* spore germination.

A preliminary investigation was performed to determine the effect of pH on germination. Spores were germinated with BHI at pH 4 - 8, and reduction of optical density was monitored. As depicted in Figure 2.18, the change in pH had a dramatic effect on the ability of the endospore to germinate. At a pH ≤ 6 , endospores were not able to germinate. At a pH of 6, the rate of germination was reduced with very similar germination kinetics observed at pH 7 and 8. These data demonstrate that the pH of the cultures is an important parameter for assays that involve the germination of endospores.

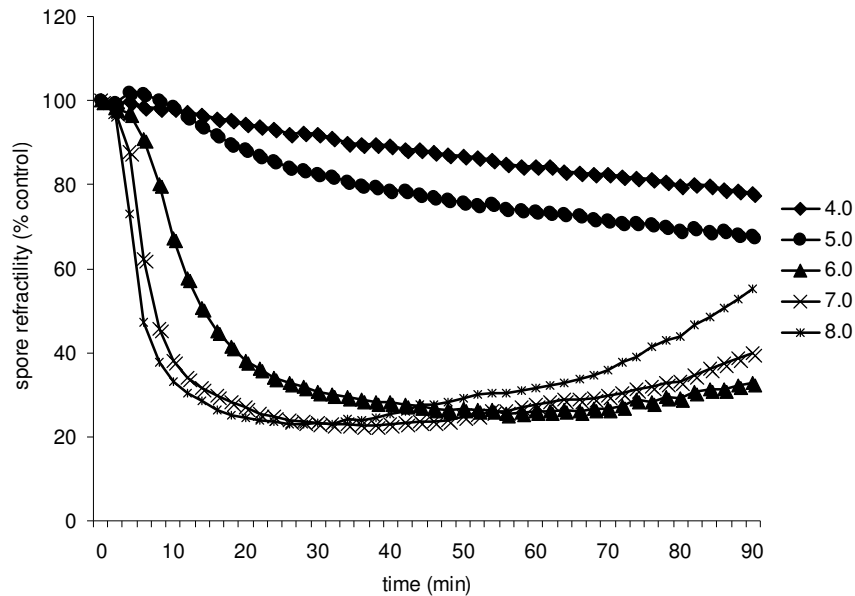


Figure 2.18. pH effects on *B. anthracis* spore germination. The data are expressed as the percentage of the OD₆₀₀ at time zero and 10 min relative to that of each culture at time zero. Shown is the mean of a single experiment conducted in triplicate as a representative of three independent experiments. No error bars are shown for clarity.

2.3 Discussion

The inhibitory action of nisin against spores of *Clostridium* and *Bacillus* pathogens has been recognized for well over 50 years (7, 39). However, the mode of action responsible for preventing spore outgrowth had not been characterized in detail previously. Using *B. anthracis* Sterne 7702 as a model, the data presented here demonstrate that spores lose heat resistance and become hydrated in the presence of nisin, thereby ruling out a possible mechanism of inhibition where nisin blocks germination initiation. Rather, germination initiation is a requisite for nisin action. These observations are consistent with a previous report on the lantibiotic subtilin, a close analog of nisin

that also inhibits spore outgrowth without disrupting spore hydration (32). The current study revealed for the first time that nisin rapidly and irreversibly inhibits growth by preventing the establishment of oxidative metabolism and membrane potential in germinating spores, possibly revealing an underlying explanation for the absence of *B. anthracis* proliferation. On the other hand, we observed no detectable effects of nisin on the typical changes associated with the dissolution of the outer spore structures (e.g. spore coats, cortex, and exosporium). Thus, the action of nisin reveals insights into germination by uncoupling two critical sequences of events necessary for the outgrowth of spores – establishment of metabolism and shedding of the external spore structures.

The capacity of nisin to prevent germinating *B. anthracis* spores from establishing a full membrane potential or oxidative metabolism is likely linked to the disruption of membrane integrity. Although nisin at 1 μM induced only a 6-fold increase in PI uptake above background as compared to a 56-fold increase at 100 μM nisin (Fig 8), spore outgrowth and metabolic activity were still inhibited, and spores were unable to establish a full membrane potential through 10 h. In contrast, ciprofloxacin, which is recommended for treatment of anthrax infections (8), did not prevent the establishment of a membrane potential in germinating spores, and had an almost negligible effect on membrane integrity, consistent with the notion that these two antibiotics inhibit the outgrowth of germinating spores by fundamentally different mechanisms.

Two distinct mechanisms, membrane pore formation and the prevention of cell wall biosynthesis, contribute to the bactericidal activity of nisin against

vegetative Gram-positive bacteria (6, 21, 48). The studies in this chapter do not directly reveal which, if either, of these two mechanisms is primarily responsible for preventing the outgrowth of *B. anthracis* spores. However, nisin's capacity to disrupt membrane integrity within germinating spores suggests that the membrane pore-forming activity may be important for inhibiting spore outgrowth. In black lipid systems, nisin pores allow the efflux of ATP (48), and it is conceivable that in germinating spores, the efflux of ATP through nisin pores could deprive *B. anthracis* of the energy required for macromolecular synthesis and oxidative metabolism. Moreover, formation of nisin pores (20) can counteract proton efflux required for membrane potential establishment and ATP formation (40, 50). Because nisin-mediated inhibition of outgrowth requires germination initiation, its target of action likely becomes accessible only subsequent to germination initiation. The data in this chapter cannot rule out that nisin inhibition of cell wall biogenesis, especially at lower nisin concentrations where disruption of membrane integrity is more modest, may also contribute to the prevention of spore outgrowth. Moreover, considering the structural differences between spores and vegetative bacilli, one also cannot dismiss the possibility that nisin may act upon germinating spores by a fundamentally different mechanism than those employed against bacilli. One study with *B. cereus* implicated accessible thiol groups within *B. cereus* spores as potential targets for nisin resulting in outgrowth inhibition (43), although a specific molecular target was not identified in that report. Prior structure-activity studies suggested that the dehydroalanine in position 5 of nisin is important for inhibition of *Bacillus* spore outgrowth (9, 43),

but this dehydrated residue is not essential for bioactivity in vegetative cells. In contrast, a more recent study reported that this dehydroalanine was not essential for nisin's inhibitory activity against *Bacillus subtilis* spores (46). Thus, structure-activity relationships to identify structural features important for the various consequences of nisin against spores remained an important focus and such studies are described in chapter 3.

Nisin is an FDA-approved natural product that has been used for 40 years in food-preservation, due in part to the selective toxicity of this lantibiotic towards Gram-positive bacteria (13, 15, 54). In this study, *B. anthracis* was used as a model, but previous work indicated that nisin was also inhibitory against spores from other *Bacillus* species (3, 7, 31), (33, 36, 45) as well as from *Clostridia* (37) species suggesting that the new information from this study regarding the inhibitory activity of nisin will be applicable to the action of nisin against spores from these other organisms as well. Here, nisin was demonstrated to act upon and kill germinated spores of *B. anthracis* prior to development into elongated and dividing bacilli and before lethal toxin was generated. Notably, this mode of activity is in contrast to several other widely used classes of antibiotics including ciprofloxacin, whose mechanism of action require ongoing cell activity and/or proliferation (2, 16, 18, 22), and are thus not as likely to be effective against germinating spores. Collectively, these properties potentially make nisin an attractive chemotherapeutic agent for prophylaxis or post-exposure treatment of spore-forming *Bacillus* or *Clostridia* pathogens.

2.4 Materials and Methods

2.4.1 Spore preparations.

An aliquot (100 µl) of an overnight culture of *B. anthracis* Sterne 7702 grown in brain heart infusion broth (3.7% Bacto Brain Heart Infusion [BD Diagnostics, Franklin Lakes, NJ], Millipore deionized water, 0.5% glycerol) at 37 °C was plated onto Difco sporulation medium agar plates (8 g/liter Difco nutrient broth (BD Diagnostics), 1 g/liter KCl, 250 mg/liter MgSO₄·7H₂O, 15 g/liter agar) and incubated at 30 °C under ambient CO₂. After 3 days, each plate was washed with deionized water (10 ml), and the washes were pooled and filtered sequentially through 3.1- and 1.2-µm glass filters from National Scientific Company (through VWR, Rochester, NY) to remove vegetative cells and clumped spores (38). The spore suspensions were incubated at 65 °C for 30 min to inactivate any remaining heat-sensitive organisms. The spores were washed three times with deionized water (centrifugation at 3,270 x *g* for 30 min), and stored in deionized water (10 ml) at 4 °C. Spores were prepared on a weekly basis and used within 7 days. (51). Enumeration of spores or bacilli was performed using a Petroff-Hauser hemocytometer under a light microscope at 400x magnification (Nikon Alphaphot YS, Melville, NY). A typical spore preparation yielded 10 mL of spores at a concentration of 2.0 x 10⁹ spores/mL.

2.4.2 Nisin purification.

A sample of 500 mg Nisaplin (50% denatured milk proteins, 2.5% nisin, and 47.5% sodium chloride; Danisco, Copenhagen, Denmark) was suspended in

30% acetonitrile (Sigma, St. Louis, MO) with 0.1% trifluoroacetic acid (TFA, 10 mL; Sigma). The suspension was sonicated for 20 min followed by centrifugation at 1500 xg for 10 min to remove all insoluble material. Reverse Phase-High Performance Liquid Chromatography (RP-HPLC, Waters, Milford, MS) was performed with a PrePack C4 semi-preparative column (Waters, Milford, MS, diameter 25 mm, length 100 mm) with a gradient of 0-100% acetonitrile at 8 mL/min. Under these conditions, nisin had a retention time of 28 min. Acetonitrile and TFA were removed from fractions containing nisin by rotary evaporation followed by lyophilization to remove water. Prior to use, lyophilized nisin was weighed on an analytical balance and dissolved in 0.1 M MOPS pH 6.8 to yield the desired concentration. The identity of purified nisin was confirmed by Matrix Assisted Laser Desorption/Ionization – Time Of Flight (MALDI-TOF) mass spectrometry (General Electric, NY). As an additional quality control measure, purified nisin was evaluated for inhibitory activity against *Lactococcus lactis* 117 (ATTC 15577) cells grown in GM17 broth (3.7% M17 Media, 0.5% dextrose; BD Biosciences) at 30 °C. Purified nisin inhibited *L. lactis* 117 with an IC₅₀ value of 0.0021 μM, in excellent agreement with previous studies (6, 28, 29), indicating that the purification protocol yielded nisin with the expected biological activity.

2.4.3 Culturing *B. anthracis* spores.

B. anthracis Sterne 7702 spores at a concentration of 4.0×10^6 spores/mL, unless otherwise indicated, were incubated in BHI medium supplemented with nisin (0.1, 1, 10, and 100 μM), ciprofloxacin (0.01, 0.1, 1 and

10 μM), or with 0.1 M 3-(N-morpholino)propanesulfonic acid (MOPS; Sigma) pH 6.8 as a mock control. In these studies, changes in germinating spores caused by nisin were compared to those induced by ciprofloxacin, which is an antibiotic recommended for the treatment of anthrax. The published MIC of ciprofloxacin against *B. anthracis* is 0.193 μM (35), which provided the basis for the concentrations of ciprofloxacin used in these studies. For non-germinating conditions, 0.1 M MOPS pH 6.8 was substituted for BHI medium. All incubations were performed at 37 °C under aeration (180 rpm on a rotary shaker; Thermo Fisher Scientific Inc., Waltham, MA, or otherwise indicated) and ambient CO₂ (e.g. 0.03% CO₂). In pilot experiments, spores were incubated in alternative media, which were Luria-Bertani (LB; B10 g/L Lacto Tryptone, 5 g/L NaCl, 5 g/L Bacto Yeast Extract; BD Diagnostics), RPMI-1640 medium (ATCC) containing FBS (10%; JRH Biosciences, Lenexa, KA), MEM JRH Biosciences) containing FBS (10%), or DMEM (JRH Biosciences) containing FBS (10%). *B. anthracis* protoplasts were made by incubating cells with 50 $\mu\text{g}/\text{mL}$ lysozyme in 1x PBS pH 7.2 for 30 min at 37 °C and washed 2x to remove lysozyme with 1x PBS pH 7.2.

2.4.4 Determination of IC₅₀ and IC₉₀ values of nisin against endospores.

B. anthracis endospores at a final concentration of 4.4×10^4 , 4.4×10^5 , 4.4×10^6 , or 4.4×10^7 spores/mL were incubated in BHI medium supplemented with varying concentrations of nisin (0.05 μM to 100 μM) or with 0.1 M MOPS pH 6.8 (as a negative control). The IC₅₀ and IC₉₀ values were derived from plots of

O.D._{600 nm} at 16 h versus nisin concentration and are the concentrations of nisin that inhibited *B. anthracis* growth in BHI medium by 50% or 90%, respectively.

2.4.5 CFU quantification.

Spores were serially diluted and plated on Luria-Bertani (LB; B10 g/L Bacto Tryptone, 5 g/L NaCl, 5 g/L Bacto Yeast Extract, 15 g/L Bacto Agar; BD Biosciences) agar plates. After 12-18 h at 37 °C *B. anthracis* colonies were counted, from which CFU/mL were calculated.

2.4.6 Spore hydration.

The hydration of spores was determined by measuring the loss of spore refractility at 600 nm, using a Synergy 2 plate reader (BioTek Instruments, Inc Winooski, VT). *B. anthracis* spores were incubated, as described under “Culturing *B. anthracis* spores,” except that a 96-well plate was used shaking for 15 s prior to each read. Data is represented as a percentage of O.D._{600 nm} at each time point relative to the O.D._{600 nm} of the spore suspensions at the beginning of the experiment (t=0 min).

2.4.7 Heat resistance.

Spores were diluted into 0.1 M MOPS pH 6.8 containing D-alanine and D-histidine (both at 10 mM; Sigma), to prevent further germination initiation of dormant spores, and identical aliquots were incubated at either 65 °C or on ice for 30 min. Viable *B. anthracis* were quantified by plating serial dilutions and

enumerating CFU. The percentage of heat resistant spores was calculated by dividing CFU recovered from samples heated at 65 °C by CFU recovered from samples incubated on ice.

2.4.8. Differential interference contrast microscopy.

At indicated times, samples were removed from *B. anthracis* cultures and fixed during incubation in 3% formaldehyde (Sigma) for 30 min at 37 °C followed by mounting on glass slides in 20% glycerol (Sigma). DIC microscopy images were collected using an Applied Precision assembled DeltaVision EpiFluorescence microscope containing an Olympus Plan Apo 100x oil objective with NA 1.42 and a working distance of 0.15 mm, and images were processed using SoftWoRX Explorer Suite (Issaquah, WA).

2.4.9 Immunoblot analysis.

At the indicated times, samples removed from *B. anthracis* cultures grown in the presence of 0.2 % bicarbonate (w/v), at 37 °C under 5 % CO₂, were centrifuged for 10 min at 21,000 *xg*. Culture supernatants were denatured by the addition of an equal volume of 2x SDS sample buffer (4% SDS, 100 mM TRIS, 0.4 mg bromophenol blue/mL, 0.2 M DTT, 20% glycerol). The samples were boiled for 5 min, and resolved by SDS-PAGE (10% acrylamide). The contents of the gels were electrotransferred to nitrocellulose membranes (Pierce, Rockford, IL). The PA and LF were probed utilizing anti-PA (QED Bioscience Inc, San Diego, CA) and anti-LF (QED Bioscience Inc, San Diego, CA) mouse monoclonal

antibodies, respectively. Goat HRP-conjugated anti-mouse IgG (Abcam Inc.; Cambridge, MA) were used as secondary antibodies, and cross-reacting material was visualized after exposing the blots to X-ray film (Denville Scientific Inc.; Metuchen, NJ) in the presence of the Enhanced Chemiluminescence Immunoblotting reagent (Pierce, Rockford, IL). For experiments to investigate PA or LF association with spores, spore homogenates were prepared by vortexing spore suspensions 10 times with 0.1 mm glass beads for 30 s.

2.4.10 Oxidative metabolism.

Samples from each culture were diluted into 0.1 M MOPS pH 6.8 containing D-alanine and D-histidine (both at 10 mM; Sigma), to prevent further germination initiation of dormant spores. Each sample was then incubated with 3-(4,5-di-methylthiazol-2-yl) 2,5-diphenyltetrazolium bromide (tetrazolium; 5 mg/mL) for 30 min at 37 °C. The conversion of tetrazolium to formazan was measured at 570 nm using a Synergy 2 plate reader (12).

2.4.11 Membrane potential.

B. anthracis spores were incubated, as described under “Culturing *B. anthracis* spores,” except for the presence of a fluorescent membrane potential-sensitive dye, 3-3'-diethyloxycarbocyanine iodide (DiOC₂; Invitrogen, Carlsbad, CA; 300 nM) (30). At the indicated times, membrane potential was assessed by measuring an increase in *B. anthracis*-associated DiOC₂ fluorescence using flow cytometry (Beckman Coulter EPICS XL-MCL™ flow cytometer, Fullerton, CA),

exciting at 488 nm with an argon laser and measuring the fluorescence emission through a bandpass filter at 525/20 nm. At least 10,000 events were detected for each sample, and the data were analyzed using FCS Express 3.00.0311 V Lite Standalone. The data were plotted as the geometric mean of the fluorescence intensity (MFI).

2.4.12 Membrane integrity.

Membrane integrity was evaluated by measuring the uptake of propidium iodide (PI) (19, 52). Samples from each culture were incubated with PI (60 μ M; Molecular Probes Inc., Leiden, NL) in an ice bath for 10 min (1). *B. anthracis*-associated fluorescence was measured using flow cytometry as described above under “Membrane Integrity,” except that fluorescence emission was measured using a bandpass filter at 675/20 nm.

2.4.13 Quantification of dipicolinic acid (DPA; 2,6-pyridinedicarboxylic acid).

DPA release was monitored by measuring fluorescence resonance energy transfer between DPA and terbium (25, 47). *B. anthracis* spores were incubated, similar to that described above under “Culturing *B. anthracis* spore,” except for in the presence of TbCl₃ (200 μ M; Sigma, St. Louis, MO). The DPA-terbium complex was excited at 280 nm, and emission was monitored at 546 nm, using a Synergy 2 plate reader.

2.4.14 Transmission electron microscopy (TEM).

B. anthracis spores from each culture were concentrated by centrifugation (21,000 xg for 30 min), the pellets were resuspended in Karnovsky's Fixative (27), and samples were prepared for TEM analysis, as previously described (58). Images were collected using a CMI Hitachi H600 TEM (Tokyo, Japan) in the University of Illinois College of Veterinary Medicine Microscopy Facility.

2.4.15 Scanning electron microscopy (SEM).

Bacilli were incubated in absence or in the presence of 1 μM nisin with growth media for 1.5 h. Cells were fixed with paraformaldehyde and gluteraldehyde. Cells were then removed from the fixative by 0.2 μm filtration, dehydrated, and gold sputtered. All the processing of the samples was done in the University of Illinois Veterinary Medicine Microscopy Facility. Pictures were taken using the ESEM (Philips XL30 ESEM-FEG, FEI Company; Hillsboro, OR) at Beckman Institute.

2.4.16 Statistics.

Error bars represent standard deviations. *P*-values were calculated with the Student's *t*-test using paired, one-tailed distribution. *P* < 0.05 indicates statistical significance.

2.5 References

1. **Ananta, E., and D. Knorr.** 2004. Evidence on the role of protein biosynthesis in the induction of heat tolerance of *Lactobacillus rhamnosus* GG by pressure pre-treatment. *Int J Food Microbiol* **96**:307-13.
2. **Anderl, J. N., J. Zahler, F. Roe, and P. S. Stewart.** 2003. Role of nutrient limitation and stationary-phase existence in *Klebsiella pneumoniae* biofilm resistance to ampicillin and ciprofloxacin. *Antimicrob Agents Chemother* **47**:1251-6.
3. **Badaoui Najjar, M., D. Kashtanov, and M. L. Chikindas.** 2007. Epsilon-poly-L-lysine and nisin A act synergistically against Gram-positive food-borne pathogens *Bacillus cereus* and *Listeria monocytogenes*. *Lett Appl Microbiol* **45**:13-8.
4. **Black, E. P., M. Linton, R. D. McCall, W. Curran, G. F. Fitzgerald, A. L. Kelly, and M. F. Patterson.** 2008. The combined effects of high pressure and nisin on germination and inactivation of *Bacillus* spores in milk. *J Appl Microbiol*.
5. **Breukink, E., and B. de Kruijff.** 2006. Lipid II as a target for antibiotics. *Nat Rev Drug Discov* **5**:321-32.
6. **Breukink, E., I. Wiedemann, C. van Kraaij, O. P. Kuipers, H. Sahl, and B. de Kruijff.** 1999. Use of the cell wall precursor lipid II by a pore-forming peptide antibiotic. *Science* **286**:2361-4.
7. **Campbell, L. L., Jr., and E. E. Sniff.** 1959. Effect of subtilin and nisin on the spores of *Bacillus coagulans*. *J Bacteriol* **77**:766-70.
8. **CDC.** 2001. Update: Interim recommendations for antimicrobial prophylaxis for children and breastfeeding mothers and treatment of children with anthrax. *MMWR Morb Mortal Wkly Rep* **50**:1014-6.
9. **Chan, W. C., H. M. Dodd, N. Horn, K. Maclean, L. Y. Lian, B. W. Bycroft, M. J. Gasson, and G. C. Roberts.** 1996. Structure-activity relationships in the peptide antibiotic nisin: role of dehydroalanine 5. *Appl Environ Microbiol* **62**:2966-9.
10. **Chan, W. C., M. Leyland, J. Clark, H. M. Dodd, L. Y. Lian, M. J. Gasson, B. W. Bycroft, and G. C. Roberts.** 1996. Structure-activity relationships in the peptide antibiotic nisin: antibacterial activity of fragments of nisin. *FEBS Lett* **390**:129-32.
11. **Chatterjee, C., Paul, M., Xie, L, van der Donk, W. A.** 2005. Biosynthesis and Mode of Action of Lantibiotics. *Chem Rev* **105**:633-683.

12. **Coligan, J. E.** 1991. Current Protocols in Immunology. Wiley.
13. **Cotter, P. D., C. Hill, and R. P. Ross.** 2005. Bacteriocins: developing innate immunity for food. *Nat Rev Microbiol* **3**:777-88.
14. **Cruz, J., and T. J. Montville.** 2008. Influence of nisin on the resistance of *Bacillus anthracis* Sterne spores to heat and hydrostatic pressure. *J Food Prot* **71**:196-9.
15. **Delves-Broughton, J., P. Blackburn, R. J. Evans, and J. Hugenholtz.** 1996. Applications of the bacteriocin, nisin. *Antonie Van Leeuwenhoek* **69**:193-202.
16. **Fux, C. A., S. Wilson, and P. Stoodley.** 2004. Detachment characteristics and oxacillin resistance of *Staphylococcus aureus* biofilm emboli in an in vitro catheter infection model. *J Bacteriol* **186**:4486-91.
17. **Giorno, R., J. Bozue, C. Cote, T. Wenzel, K. S. Moody, M. Mallozzi, M. Ryan, R. Wang, R. Zielke, J. R. Maddock, A. Friedlander, S. Welkos, and A. Driks.** 2007. Morphogenesis of the *Bacillus anthracis* spore. *J Bacteriol* **189**:691-705.
18. **Gradelski, E., B. Kolek, D. Bonner, and J. Fung-Tomc.** 2002. Bactericidal mechanism of gatifloxacin compared with other quinolones. *J Antimicrob Chemother* **49**:185-8.
19. **Gunther, S., W. Geyer, H. Harms, and S. Muller.** 2007. Fluorogenic surrogate substrates for toluene-degrading bacteria--are they useful for activity analysis? *J Microbiol Methods* **70**:272-83.
20. **Hasper, H. E., B. de Kruijff, and E. Breukink.** 2004. Assembly and stability of nisin-lipid II pores. *Biochemistry* **43**:11567-75.
21. **Hasper, H. E., N. E. Kramer, J. L. Smith, J. D. Hillman, C. Zachariah, O. P. Kuipers, B. de Kruijff, and E. Breukink.** 2006. An alternative bactericidal mechanism of action for lantibiotic peptides that target lipid II. *Science* **313**:1636-7.
22. **Herbert, D., C. N. Paramasivan, P. Venkatesan, G. Kubendiran, R. Prabhakar, and D. A. Mitchison.** 1996. Bactericidal action of ofloxacin, sulbactam-ampicillin, rifampin, and isoniazid on logarithmic- and stationary-phase cultures of *Mycobacterium tuberculosis*. *Antimicrob Agents Chemother* **40**:2296-9.
23. **Hoffmaster, A. R., and T. M. Koehler.** 1997. The anthrax toxin activator gene *atxA* is associated with CO₂-enhanced non-toxin gene expression in *Bacillus anthracis*. *Infect Immun* **65**:3091-9.

24. **Hu, H., Q. Sa, T. M. Koehler, A. I. Aronson, and D. Zhou.** 2006. Inactivation of *Bacillus anthracis* spores in murine primary macrophages. *Cell Microbiol* **8**:1634-42.
25. **Huang SS, C. D., Pelczar PL, Vepachedu VR, Setlow P, Li YQ.** 2007. Levels of Ca²⁺-dipicolinic acid in individual *Bacillus* spores determined using microfluidic Raman tweezers. *J Bacteriol* **Epub ahead of print**.
26. **Hyde, A. J., J. Parisot, A. McNichol, and B. B. Bonev.** 2006. Nisin-induced changes in *Bacillus* morphology suggest a paradigm of antibiotic action. *Proc Natl Acad Sci U S A* **103**:19896-901.
27. **Karnovsky, M. L.** 1965. A formaldehyde-glutaraldehyde fixative of high osmolarity for use in electron microscopy. *J Cell Biol* **27**:137A-138A.
28. **Kramer, N. E., E. J. Smid, J. Kok, B. de Kruijff, O. P. Kuipers, and E. Breukink.** 2004. Resistance of Gram-positive bacteria to nisin is not determined by lipid II levels. *FEMS Microbiol Lett* **239**:157-61.
29. **Kuwano, K., N. Tanaka, T. Shimizu, K. Nagatoshi, S. Nou, and K. Sonomoto.** 2005. Dual antibacterial mechanisms of nisin Z against Gram-positive and Gram-negative bacteria. *Int J Antimicrob Agents* **26**:396-402.
30. **Laflamme, C., J. Ho, M. Veillette, M. C. de Latremaille, D. Verreault, A. Meriaux, and C. Duchaine.** 2005. Flow cytometry analysis of germinating *Bacillus* spores, using membrane potential dye. *Arch Microbiol* **183**:107-12.
31. **Levinson, H. S., and M. T. Hyatt.** 1966. Sequence of events during *Bacillus megaterim* spore germination. *J Bacteriol* **91**:1811-8.
32. **Liu, W., and J. N. Hansen.** 1993. The antimicrobial effect of a structural variant of subtilin against outgrowing *Bacillus cereus* T spores and vegetative cells occurs by different mechanisms. *Appl Environ Microbiol* **59**:648-51.
33. **Lopez-Pedemonte, T. J., A. X. Roig-Sagues, A. J. Trujillo, M. Capellas, and B. Guamis.** 2003. Inactivation of spores of *Bacillus cereus* in cheese by high hydrostatic pressure with the addition of nisin or lysozyme. *J Dairy Sci* **86**:3075-81.
34. **Lubelski, J., R. Rink, R. Khusainov, G. N. Moll, and O. P. Kuipers.** 2008. Biosynthesis, immunity, regulation, mode of action and engineering of the model lantibiotic nisin. *Cell Mol Life Sci* **65**:455-76.

35. **Luna, V. A., D. S. King, J. Gulledge, A. C. Cannons, P. T. Amuso, and J. Cattani.** 2007. Susceptibility of *Bacillus anthracis*, *Bacillus cereus*, *Bacillus mycooides*, *Bacillus pseudomycooides* and *Bacillus thuringiensis* to 24 antimicrobials using Sensititre automated microbroth dilution and Etest agar gradient diffusion methods. *J Antimicrob Chemother* **60**:555-67.
36. **Mansour, M., D. Amri, A. Bouttefroy, M. Linder, and J. B. Milliere.** 1999. Inhibition of *Bacillus licheniformis* spore growth in milk by nisin, monolaurin, and pH combinations. *J Appl Microbiol* **86**:311-24.
37. **Mazzotta, A. S., A. D. Crandall, and T. J. Montville.** 1997. Nisin Resistance in *Clostridium botulinum* spores and vegetative cells. *Appl Environ Microbiol* **63**:2654-2659.
38. **McKevitt, M. T., K. M. Bryant, S. M. Shakir, J. L. Larabee, S. R. Blanke, J. Lovchik, C. R. Lyons, and J. D. Ballard.** 2007. Effects of endogenous D-alanine synthesis and autoinhibition of *Bacillus anthracis* germination on in vitro and in vivo infections. *Infect Immun* **75**:5726-34.
39. **Mikolajcik, E. M., C. B. Reeves, and W. J. Harper.** 1965. Efficacy of nisin as a sporicidal agent in the presence of L-alanine. *J Dairy Sci* **48**:1522-4.
40. **Moir A.** 2006. How do spores germinate? *J Appl Microbiol* **101**:526-30.
41. **Montville, T. J., T. De Siano, A. Nock, S. Padhi, and D. Wade.** 2006. Inhibition of *Bacillus anthracis* and potential surrogate bacilli growth from spore inocula by nisin and other antimicrobial peptides. *J Food Prot* **69**:2529-33.
42. **Morris, S. L., and J. N. Hansen.** 1981. Inhibition of *Bacillus cereus* spore outgrowth by covalent modification of a sulfhydryl group by nitrosothiol and iodoacetate. *J Bacteriol* **148**:465-471.
43. **Morris, S. L., R. C. Walsh, and J. N. Hansen.** 1984. Identification and characterization of some bacterial membrane sulfhydryl groups which are targets of bacteriostatic and antibiotic action. *J Biol Chem* **259**:13590-4.
44. **Paik, S. H., A. Chakicherla, and J. N. Hansen.** 1998. Identification and characterization of the structural and transporter genes for, and the chemical and biological properties of, sublancin 168, a novel lantibiotic produced by *Bacillus subtilis* 168. *J Biol Chem* **273**:23134-42.
45. **Pol, I. E., W. G. van Arendonk, H. C. Mastwijk, J. Krommer, E. J. Smid, and R. Moezelaar.** 2001. Sensitivities of germinating spores and carvacrol-adapted vegetative cells and spores of *Bacillus cereus* to nisin and pulsed-electric-field treatment. *Appl Environ Microbiol* **67**:1693-9.

46. **Rink, R., J. Wierenga, A. Kuipers, L. D. Kluskens, A. J. Driessen, O. P. Kuipers, and G. N. Moll.** 2007. Dissection and modulation of the four distinct activities of nisin by mutagenesis of rings A and B and by C-terminal truncation. *Appl Environ Microbiol* **73**:5809-16.
47. **Rosen, D. L.** 1997. Bacterial spore detection and determination by use of terbium dipicolinate photoluminescence. *Analytical Chemistry* **69**:1082-1085.
48. **Ruhr, E., and H. G. Sahl.** 1985. Mode of action of the peptide antibiotic nisin and influence on the membrane potential of whole cells and on cytoplasmic and artificial membrane vesicles. *Antimicrob Agents Chemother* **27**:841-5.
49. **Russell, B. H., R. Vasan, D. R. Keene, T. M. Koehler, and Y. Xu.** 2008. Potential dissemination of *Bacillus anthracis* utilizing human lung epithelial cells. *Cell Microbiol* **10**:945-57.
50. **Setlow, P.** 2003. Spore germination. *Curr Opin Microbiol* **6**:550-6.
51. **Stojkovic, B., E. M. Torres, A. M. Prouty, H. K. Patel, L. Zhuang, T. M. Koehler, J. D. Ballard, and S. R. Blanke.** 2008. High-throughput, single-cell analysis of macrophage interactions with fluorescently labeled *Bacillus anthracis* spores. *Appl Environ Microbiol* **74**:5201-10.
52. **Sunny-Roberts, E. O., and D. Knorr.** 2008. Evaluation of the response of *Lactobacillus rhamnosus* VTT E-97800 to sucrose-induced osmotic stress. *Food Microbiol* **25**:183-9.
53. **Tournier, J. N., A. Quesnel-Hellmann, A. Cleret, and D. R. Vidal.** 2007. Contribution of toxins to the pathogenesis of inhalational anthrax. *Cell Microbiol* **9**:555-65.
54. **van Kraaij, C., W. M. de Vos, R. J. Siezen, and O. P. Kuipers.** 1999. Lantibiotics: biosynthesis, mode of action and applications. *Nat Prod Rep* **16**:575-87.
55. **Vary, J. C., and H. O. Halvorson.** 1965. Kinetics of germination of *Bacillus* spores. *J Bacteriol* **89**:1340-7.
56. **Vepachedu, V. R., K. Hirneisen, D. G. Hoover, and P. Setlow.** 2007. Studies of the release of small molecules during pressure germination of spores of *Bacillus subtilis*. *Lett Appl Microbiol* **45**:342-8.

57. **Wiedemann, I., E. Breukink, C. van Kraaij, O. P. Kuipers, G. Bierbaum, B. de Kruijff, and H. G. Sahl.** 2001. Specific binding of nisin to the peptidoglycan precursor lipid II combines pore formation and inhibition of cell wall biosynthesis for potent antibiotic activity. *J Biol Chem* **276**:1772-9.
58. **Zhang, J., N. Dalal, M. A. Matthews, L. N. Waller, C. Saunders, K. F. Fox, and A. Fox.** 2007. Supercritical carbon dioxide and hydrogen peroxide cause mild changes in spore structures associated with high killing rate of *Bacillus anthracis*. *J Microbiol Methods* **70**:442-51.

CHAPTER 3: MECHANISM OF NISIN INHIBITION OF *BACILLUS ANTHRACIS* SPORE OUTGROWTH

3.1 Introduction

Nisin A is a 34-amino acid polycyclic peptide produced by *Lactococcus lactis* sbsp. *lactis* ATCC 11454 (Figure 3.1A). As described in chapter 1, nisin acts upon Gram-positive bacteria by two distinct mechanisms (3). The compound forms pores in cell membranes (24), and inhibits cell wall biosynthesis by disruption of transglycosylation via lipid II binding and mislocalization (13, 31). With two mechanisms of action, nisin has been relatively unaffected by the emergence of microbial resistance, despite widespread and persistent use as a food preservative (9, 17).

Nisin also inhibits the outgrowth of germinated bacterial spores (6, 12, 19, 20, 25). The studies in chapter 2 suggested that membrane disruption prevents the establishment of a membrane potential and oxidative metabolism (12). Whether these processes are mediated by nisin binding to lipid II was not evaluated. Indeed, it is not clear whether or not lipid II is accessible on the surface of spores. Moreover, several studies have suggested that a protein target mediates nisin's inhibitory action on spore outgrowth (6, 15, 20), potentially ruling out a role for lipid II binding in nisin-dependent inhibition of spore outgrowth.

To better understand the mechanism of inhibition of spore outgrowth, the effects of nisin, vancomycin, and truncated nisin analogs (Figure 3.1A & B) on germination and outgrowth of *Bacillus anthracis* Sterne 7702 spores were compared in this study. The studies presented in this chapter suggest that nisin

does bind lipid II on spores, and that lipid II binding is essential, but not sufficient for outgrowth inhibition, whereas membrane disruption is essential.

Figure 3.1

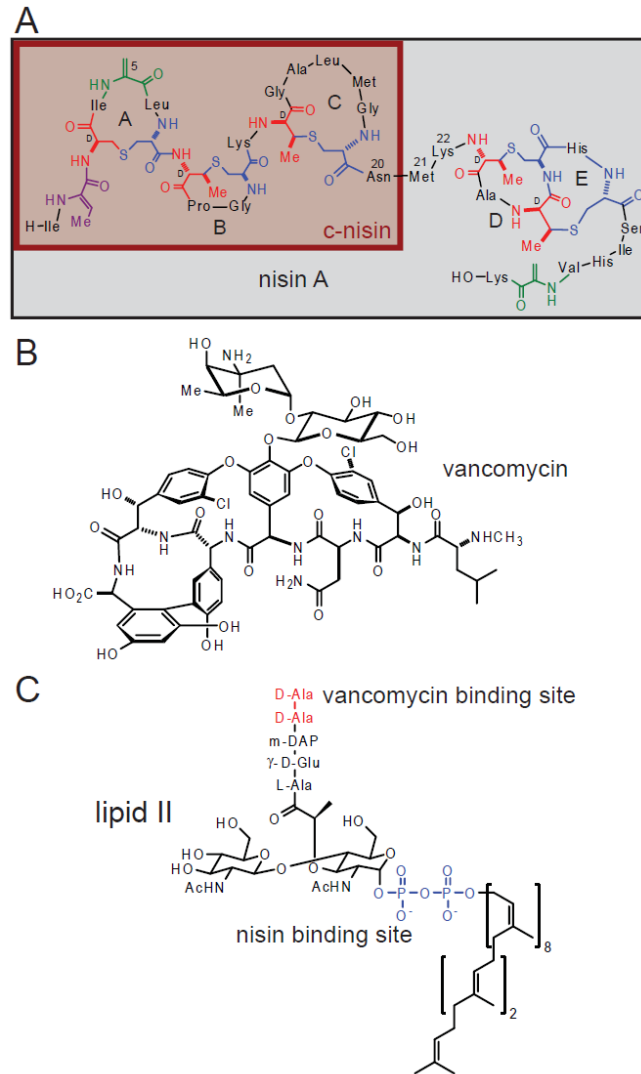


Figure 3.1. Structures of nisin, vancomycin, and lipid II. A. The structure of nisin A. Dehydrated amino acids dehydroalanine (Dha) and dehydrobutyrine (Dhb) are indicated in green and magenta, respectively. Amino acids involved in the formation of lanthionine and methyl-lanthionine rings are indicated in red and blue, respectively. The numbers indicated the locations of the amino acids that were mutated in the following nisin variants: S5A (Dha5A), N20P/M21P, and M21P/K22P. The N-terminal fragment resulting from chymotrypsin cleavage (c-nisin) is

Figure 3.1 (continued)

highlighted in maroon. B. The structure of vancomycin. C. The structure of lipid II in *B. anthracis*. The vancomycin binding site is indicated in red and the nisin binding site is indicated in blue.

3.2 Results

3.2.1 Fluorescently-labeled nisin analogs bind to lipid II and have similar properties as wild type nisin.

To further evaluate the mechanism by which nisin inhibits the outgrowth of germinated *B. anthracis* spores, it was first determined whether or not nisin binds to spore-associated lipid II. For this purpose, bodipy-633-labeled nisin (b-nisin) and fluorescein-labeled nisin (f-nisin) were synthesized to probe their localization on spores using fluorescence microscopy. The fluorescein label, which is located predominantly at the C-terminal lysine residue of nisin, or the bodipy label, which is located predominantly at the N-terminus, did not have major deleterious effects on nisin activity, as fluorescently-labeled nisin inhibited *B. anthracis* growth with IC₉₀ values of 5.4 μM and 6.5 μM for b-nisin and f-nisin, respectively, which correspond to a 6- and 7-fold loss in activity, respectively, compared to unmodified nisin (12). These findings are consistent with observations in previous reports using nisin labeled with 5-(aminoacetamido)fluorescein at the C-terminal carboxylate, which also resulted in an active analog (13). Additional experiments that confirm very similar activities of fluorescently labeled nisin analogs and wild type nisin are presented in later sections in this chapter. Importantly, control studies revealed that these labeled nisin analogs neither induced nor inhibited germination initiation, as monitored by the loss of optical density associated with

spore hydration during germination (not shown), analogous to findings unmodified nisin reported in chapter 2 (6, 12).

The localization of b-nisin was compared with a known lipid II binding probe, fluorescein-vancomycin, (f-vancomycin) (29). Vancomycin interacts with the D-Ala-D-Ala part of lipid II (3, 18, 26), which is distinct from the binding site of nisin that features the pyrophosphate group (Figure 3.1C) (14). Fluorescently labeled vancomycin has been used previously to investigate lipid II localization on vegetative bacilli (8, 29). Like nisin, vancomycin (at concentrations up to 100 μM) neither induced (not shown) nor inhibited spore germination (Figure 3.2). To verify that fluorescently labeled nisin can be used to detect the localization of lipid II, vegetative *B. anthracis* cells were incubated with f-nisin or b-nisin (Figure 3.3). Previous studies have demonstrated that nisin relocates lipid II to patches in bacilli (13). In our experiments, f-nisin and b-nisin also localized in patches on *B. anthracis* (Figure 3.3). Collectively, these experiments provide support that the fluorescently labeled nisin analogs bind to lipid II.

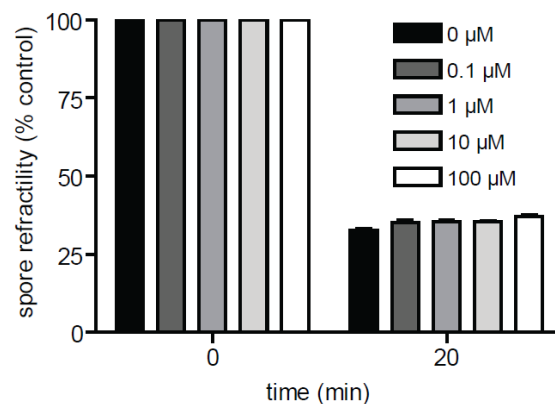


Figure 3.2. Effect of vancomycin on germination. The data are expressed as the percentage of the OD_{600} relative to that of each culture at time zero. Error bars indicate standard deviation.

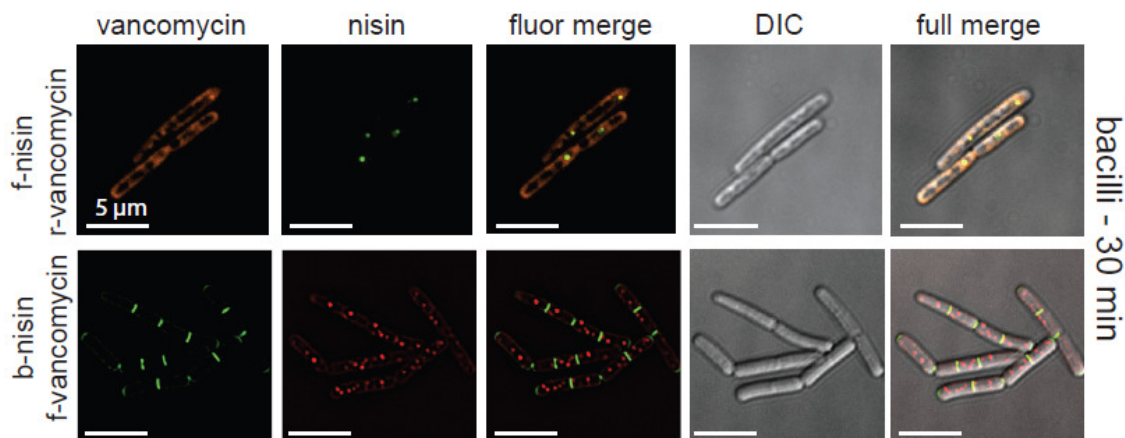


Figure 3.3. Localization of labeled nisin and vancomycin on *B. anthracis* vegetative cells.

Vegetative cells were incubated in BHI with 0.1 μM fluorescein-nisin (f-nisin) and rhodamine-vancomycin (r-vancomycin) or 0.1 μM b-nisin and f-vancomycin. At time 30 min, samples were removed and visualized by epi-fluorescence microscopy. For each panel, a single vegetative cell is shown for clarity but is representative of all other *B. anthracis* vegetative cells within that sample.

3.2.2 Nisin binds to lipid II of germinated spores.

In the presence of both b-nisin and f-vancomycin (both at 1 μM), the outgrowth of germinated spores was inhibited, and b-nisin and f-vancomycin were associated with spores (Figure 3.4A), although with distinct binding patterns. Vancomycin bound diffusely over the entire surface of germinated spores, whereas nisin was localized in a more punctate fashion, and predominantly near the poles of the germinated spores, where co-localization with vancomycin was observed (Figure 3.4 B, C, Figure 3.5). It is possible that the clustering of b-nisin near the poles reflects the localization of lipid II that is required for the biosynthesis of new cell wall during the outgrowth process. However, when spores were germinated in the presence of non-inhibiting concentrations of b-nisin (0.4 μM), the localization of nisin occurred both at the

pole and along the long axis of the germinating (30 and 60 min) as well as outgrowing (120 min) spore (Figure 3.6). Therefore, although we do not consider it likely, it cannot be ruled out that the observed strong localization at the poles at concentrations of b-nisin that inhibit spore outgrowth may be the result of nisin-induced re-localization of lipid II to the pole.

In an effort to determine whether cortex and cell wall degradation and processing alter lipid II localization as well as the co-localization of nisin and vancomycin, a series of cortex hydrolase mutants evaluated for their ability to alter nisin-vancomycin co-localization. These *B. anthracis* constructs were graciously provided by Dr. David Popham, and his laboratory has demonstrated that single knockouts of either $\Delta selB$ or $\Delta cwJ1$ slowed the rate of cortex hydrolysis while the double mutant, $\Delta selB\Delta cwJ1$, eliminated cortex hydrolysis in a *B. anthracis* 34F2 background (17, 18). In the presence of both b-nisin and f-vancomycin (both at 1 μ M), the outgrowth of variants of germinated spores were inhibited, and b-nisin and f-vancomycin were associated with spores (Supplementary Figure S6A), with a similar binding among all the 34F2 spore variants as well as *B. anthracis* 7702 (Figure 2). As previously demonstrated Pearson's coefficient confirmed that nisin and vancomycin were highly co-localized at all time points for all hydrolase variants (n=30; Supplementary Figure S6B). Furthermore, hydrolase knockout spores incubated with f-vancomycin (1 μ M) in the absence of nisin showed relatively uniform labeling at 30 min, with more punctuate labeling at 60 min (Supplementary Figure S6C). Outgrowth of spores into bacilli altered the localization of vancomycin to bands that cross the long axis

of the bacilli at 120 min at a site congruent with cell division (Supplementary Figure S6C) (27). Direct disruption of lipid II co-localization by nisin-vancomycin was not possible since *B. anthracis* is highly resistant to bacitracin and fosfomycin, which would deplete the spore of lipid II (28-30). Also, genetically altering lipid II or cell wall synthesis prevents the formation of a viable and heat resistant spore (31-33).

Figure 3.4

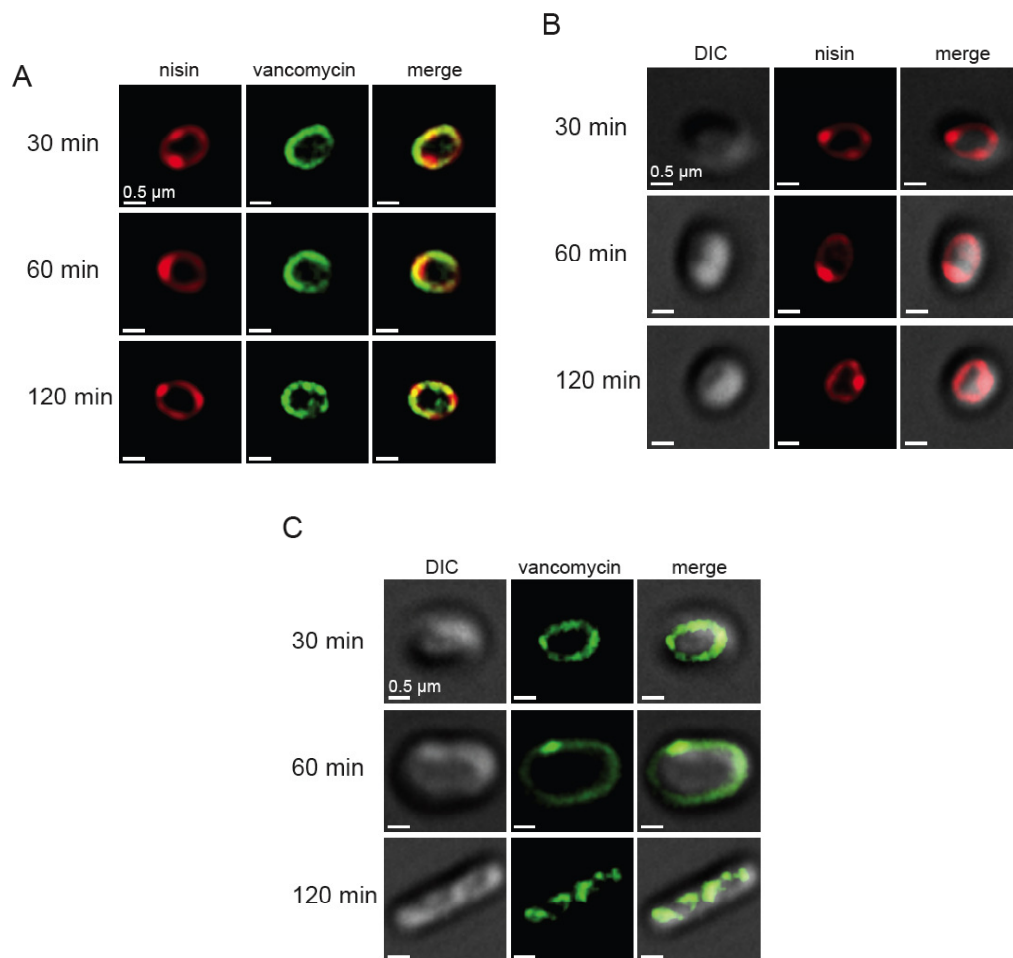


Figure 3.4. Nisin and vancomycin localization on spores. At time 30, 60, and 120 min, samples were removed and visualized by epi-fluorescence microscopy. A. Dual antibiotic incubations of germinated spores were performed with bodipy-nisin (b-nisin, red) and fluorescein-

Figure 3.4 (continued)

vancomycin (f-vancomycin, green) at 1 μ M. Co-localization is indicated by yellow in merged images B. Single antibiotic incubation of germinated spores with b-nisin (red) at 1 μ M. C. Single antibiotic incubation of germinated spores with f-vancomycin (green) at 1 μ M. A-C. For each panel, a single spore is shown for clarity, but the image is representative of all other *B. anthracis* spores within that sample.

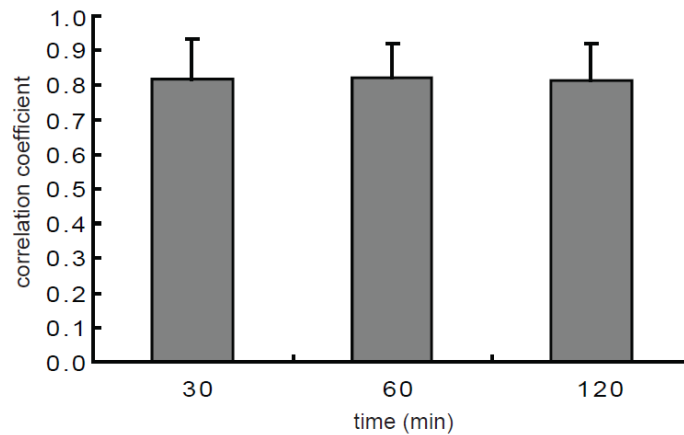


Figure 3.5. Quantification of nisin and vancomycin co-localization by Pearson's coefficient. At time 30, 60, and 120 min, samples were removed and visualized by epifluorescence microscopy. Images were processed and Pearson's coefficient co-localization analysis of 50 spores per condition was performed using SoftWoRX Explorer Suite. Analysis of the co-localization with Pearson's coefficient identified that nisin and vancomycin were highly co-localized throughout the spore in addition to the punctate formations with a coefficient of 0.81 for all time points.

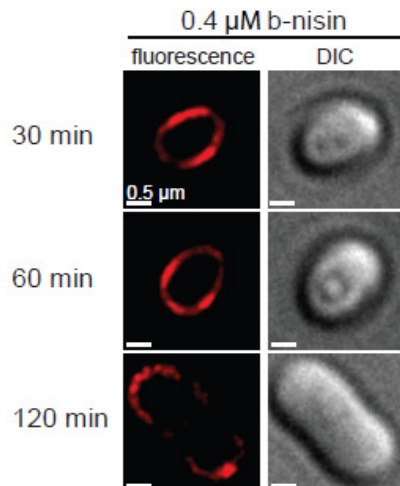


Figure 3.6 Localization of Lipid II in sub-inhibitory concentration of nisin. At time 30, 60, and 120 min, samples were removed and visualized by epi-fluorescence microscopy. Single antibiotic incubation of germinated spores with b-nisin (red) at 0.4 μ M. For each panel, a single spore is shown for clarity, but the image is representative of all other *B. anthracis* spores within that sample.

The distinct binding patterns of b-nisin and f-vancomycin were not caused by intrinsic differences between bodipy and fluorescein, because switching the labels (e.g. using fluorescein-labeled nisin and rhodamine-labeled vancomycin) resulted in very similar binding patterns (Figure 3.7A-C). Furthermore, the patterns of nisin and vancomycin binding were independent of the order that the compounds were introduced (Figure 3.8A). Finally, in the absence of vancomycin, the incubation of spores with b-nisin under germinating conditions also resulted in punctate localization at the pole of the spore with some diffuse fluorescence associated with the spore membrane (Figure 3.4B). Taken together, these results validate the notion that the distinct binding pattern of nisin on the surface of germinated spores is neither dependent on nor affected by either the conjugated fluor or vancomycin.

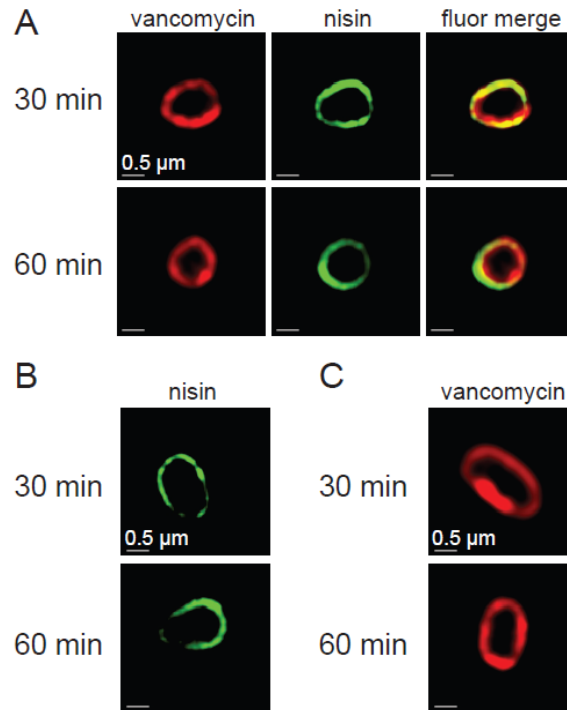


Figure 3.7. Effect of fluorescent label on antibiotic localization. A and B. At time 30, 60, and 120 min, samples were removed and visualized by epi-fluorescence microscopy. A. Incubation of germinated spores with f-nisin (green) and b-vancomycin (red) at 1 μM. Co-localization is indicated by yellow in merged images B. Single antibiotic incubation of germinated spores with f-nisin (green) or b-vancomycin (red) at 1 μM. A and B. For each panel, a single spore is shown for clarity but is representative of all other *B. anthracis* spores within that sample.

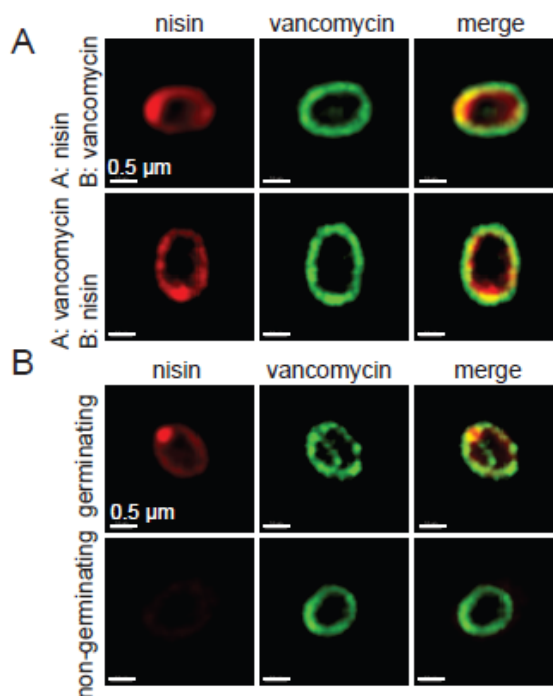


Figure 3.8. Conditional effects on antibiotic localization. Spores were germinated for 30 min followed by the addition of labeled antibiotic A at 1 μ M for 5 min and then subsequent addition of labeled antibiotic B for 5 min at 1 μ M. Samples were removed and visualized by epi-fluorescence microscopy. Dual antibiotic incubations of germinated spores were performed with b-nisin (red) and f-vancomycin (green). B. Spores were incubated with a germinant (BHI) or without a germinant (0.1 M MOPS pH 6.8) in the presence of both labeled antibiotics. At 30 min, samples were removed and visualized by epi-fluorescence microscopy. A and B. For each panel, a single spore is shown for clarity but is representative of all other *B. anthracis* spores within that sample.

Complete co-localization of nisin and vancomycin was not expected since vancomycin binds the D-Ala-D-Ala structure present in both the pentapeptide of the non-crosslinked cell wall and cortex in addition to the pentapeptide of lipid II (4), whereas nisin will bind to the pyrophosphate that is only present in lipid II (Figure 3.1C) (14). Reflective of these differences in binding specificities, nisin did not detectably associate with dormant spores (Figure 3.8B), indicating that

lipid II was not accessible prior to germination initiation. In contrast, vancomycin was visibly associated with dormant spores (Figure 3.8B), which we speculate is due to the accessibility of non-crosslinked peptidoglycan within the spore cortex.

Incubation of spores with f-vancomycin (1 μM) in the absence of nisin showed relatively uniform labeling at 30 min, with more punctuate labeling at 60 min (Figure 3.4C). Outgrowth of spores into bacilli altered the localization of vancomycin to bands that cross the long axis of the bacilli at 120 min (Figure 3.4C). This localization of vancomycin in outgrown spores is similar to lipid II localization observed previously in vegetative bacilli of *Bacillus subtilis* and illustrates the helical localization of lipid II along the long axis of the rod-shaped cell (8, 29).

To further confirm that b-nisin binds to lipid II associated with germinated spores, competition-binding experiments were performed. These studies revealed that a 100-fold molar excess of unlabeled vancomycin significantly reduced binding of b-nisin to the surface of germinated spores (Figure 3.9A). Likewise, a 100-fold molar excess of unmodified nisin significantly inhibited the binding of f-vancomycin to the surface of spores under germinating conditions (Figure 3.9B). As mentioned above, complete competition is not expected since these two compounds, in addition to sharing lipid II as target, also have non-overlapping binding sites (non-crosslinked cell wall for vancomycin and the membrane for nisin). Importantly, 100-fold molar excess of unmodified nisin also significantly reduced the binding of b-nisin to germinated spores (Figure 3.9C),

providing additional evidence that b-nisin and wild type nisin bind to the same targeted.

In an effort to determine whether cortex and cell wall degradation and processing alter lipid II localization as well as the co-localization of nisin and vancomycin, a series of cortex hydrolase mutants evaluated for their ability to alter nisin-vancomycin co-localization. These *B. anthracis* constructs were graciously provided by Dr. David Popham, and his laboratory has demonstrated that single knockouts of either $\Delta seIB$ or $\Delta cwIJ1$ slowed the rate of cortex hydrolysis while the double mutant, $\Delta seIB\Delta cwIJ1$, eliminated cortex hydrolysis in a *B. anthracis* 34F2 background (17, 18). In the presence of both b-nisin and f-vancomycin (both at 1 μ M), the outgrowth of variants of germinated spores were inhibited, and b-nisin and f-vancomycin were associated with spores (Supplementary Figure S6A), with a similar binding among all the 34F2 spore variants as well as *B. anthracis* 7702 (Figure 2). As previously demonstrated Pearson's coefficient confirmed that nisin and vancomycin were highly co-localized at all time points for all hydrolase variants (n=30; Supplementary Figure S6B). Furthermore, hydrolase knockout spores incubated with f-vancomycin (1 μ M) in the absence of nisin showed relatively uniform labeling at 30 min, with more punctuate labeling at 60 min (Supplementary Figure S6C). Outgrowth of spores into bacilli altered the localization of vancomycin to bands that cross the long axis of the bacilli at 120 min at a site congruent with cell division (Supplementary Figure S6C) (27). Direct disruption of lipid II co-localization by nisin-vancomycin was not possible since *B. anthracis* is highly resistant to bacitracin and

fosfomycin, which would deplete the spore of lipid II (28-30). Also, genetically altering lipid II or cell wall synthesis prevents the formation of a viable and heat resistant spore (31-33).

Although these results indicate that nisin binds to lipid II, the microscopy data do not reveal whether lipid II is the only nisin target in germinated spores. Previous studies suggested that nisin may bind covalently to a protein target during outgrowth inhibition through a Michael-like addition of a Cys of a spore protein to Dha5 of nisin (6, 15, 20). However, extensive efforts did not identify a cognate protein receptor when using fluorescent or biotin labeled nisin as a probe since a nisin-mediated band shift or the appearance of a nisin-labeled protein band did not occur (Figure 3.10), which is consistent with earlier results emerging from mutagenesis of Dha5 (23).

Figure 3.9

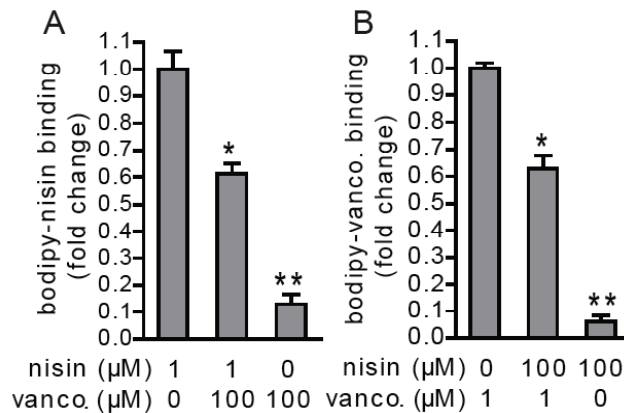


Figure 3.9 (continued)

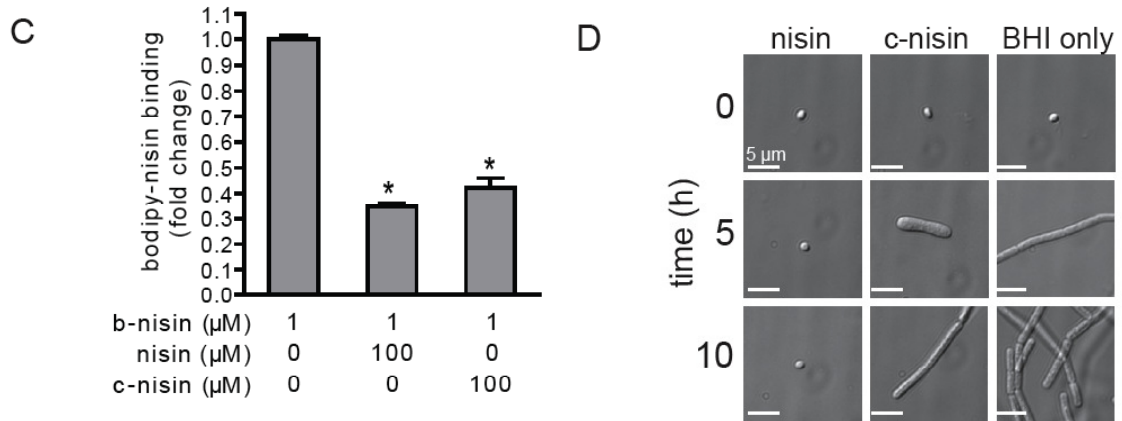


Figure 3.9. Competition assays with nisin and vancomycin. A. Competition assay of spore binding of unlabeled vancomycin and b-nisin. * indicates a $P < 0.05$ between b-nisin (1 μM) only treated spores and spores pretreated with unlabeled vancomycin (100 μM) prior to b-nisin addition (1 μM). ** indicates a $P < 0.05$ between b-nisin-treated (1 μM) spores and spores treated with unlabeled vancomycin (100 μM). B. Binding competition assay of unlabeled nisin in competition with b-vancomycin. * indicates a $P < 0.05$ between b-vancomycin (1 μM) only treated spores and spores pretreated with unlabeled nisin (100 μM) prior to b-vancomycin addition (1 μM). ** indicates a $P < 0.05$ between b-vancomycin (1 μM) only treated spores and spores treated with unlabeled nisin (100 μM) only. C. Competition assay of unlabeled chymotrypsin cleaved nisin (c-nisin) in competition with b-nisin. * indicates a $P < 0.05$ between b-nisin (1 μM) only treated spores and spores pretreated with unlabeled c-nisin (100 μM) prior to b-nisin addition (1 μM). * indicates a $P < 0.05$ between control (0 μM nisin) spores and spores pretreated with unlabeled nisin or unlabeled c-nisin (100 μM) prior to b-vancomycin addition (1 μM). In A-C the data are plotted as the mean fluorescent intensity (MFI) associated with the binding of the labeled antibiotic. D. At time 0, 5, and 10 h, samples were removed and visualized by DIC microscopy. For each panel, a single spore is shown for clarity, but the image is representative of all other *B. anthracis* spores within that sample. Bars, 5 μm . The data are representative of those from three independent experiments.

Figure 3.10

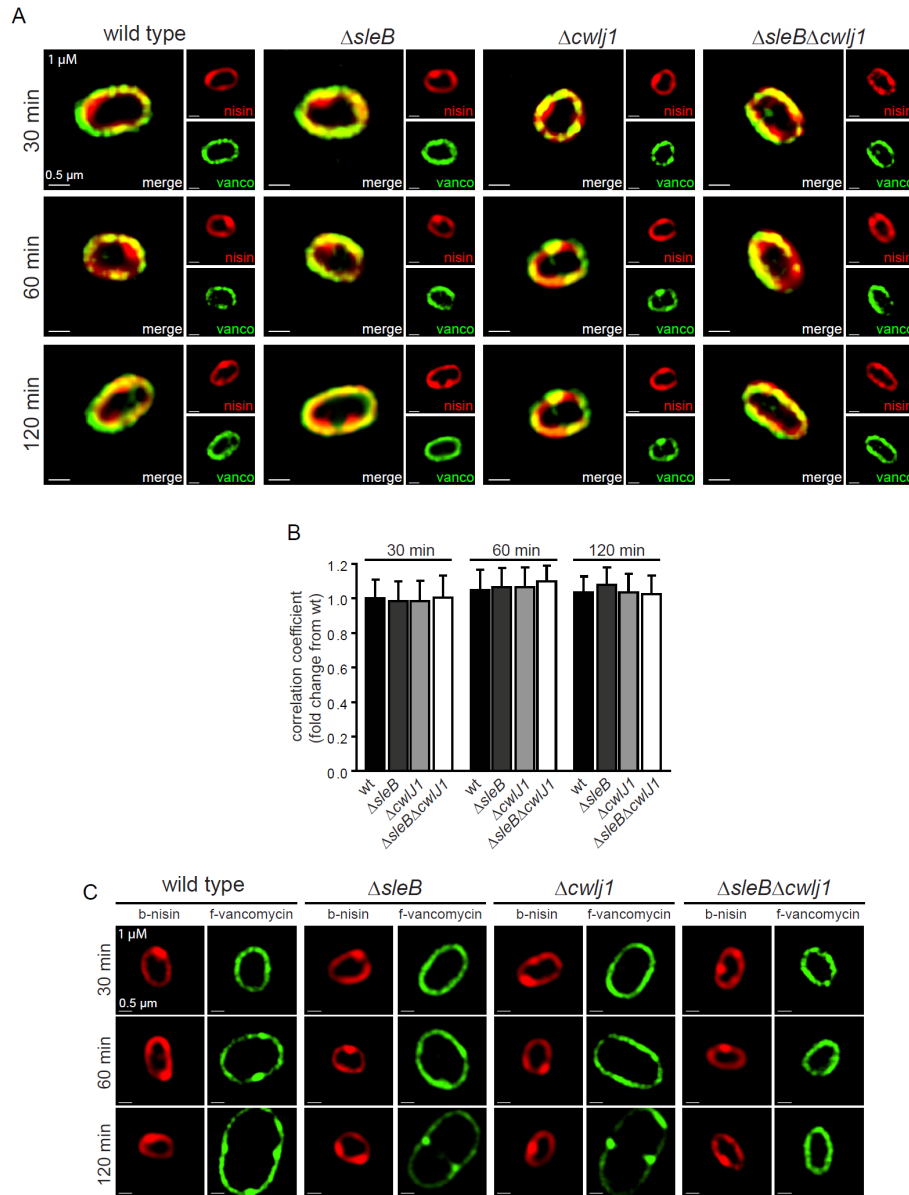


Figure 3.10. Cortex hydrolase mutants do not alter nisin and vancomycin co-localization at lipid II. At time 30, 60, and 120 min, samples were removed and visualized by epifluorescence microscopy. A. Dual antibiotic incubation of germinated spores were performed with bodipy-nisin (b-nisin, red) and fluorescein-vancomycin (f-vancomycin, green) at 1 μ M. Co-localization is indicated by yellow in merged images. B. Images were processed and Pearson's coefficient co-localization analysis of 30 spores per condition was performed using SoftWoRX Explorer Suite. Analysis of the co-localization with Pearson's coefficient, identified that nisin and

Figure 3.10 (continued)

vancomycin where highly co-localized throughout the spore. C. Single antibiotic incubation of germinated spores with b-nisin (red) or f-vancomycin (green) at 1 μ M. A,C. For each panel, a single spore is shown for clarity but is the image is representative of all other *B. anthracis* spores within that sample.

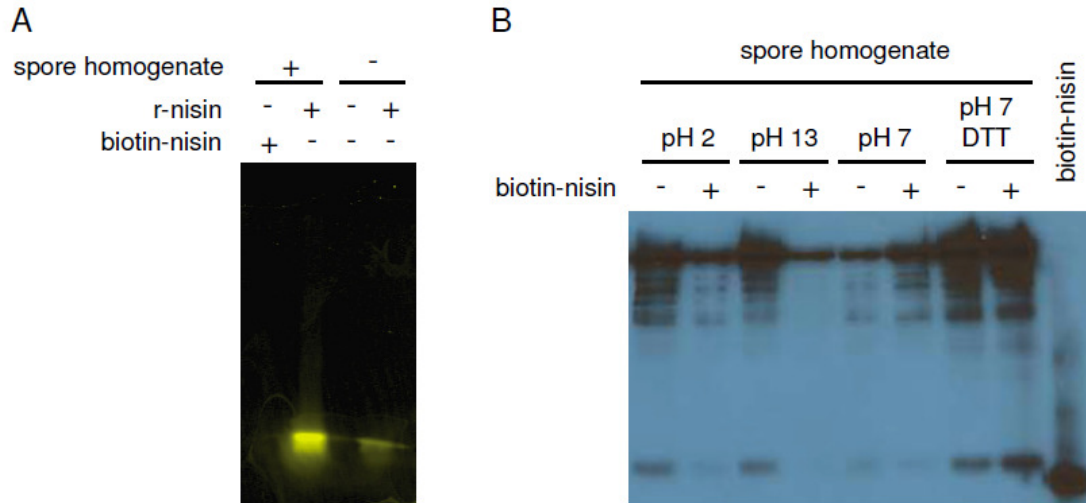


Figure 3.11. Utilizing biotin or fluorescently labeled nisin to identify or isolate a covalent protein target. A. Fluorescence gel analysis for rhodamine-nisin (r-nisin) conjugates to a spore protein utilizing SDS page separation of proteins and imaging with a GE Typhoon fluorescence gel scanner. Only a r-nisin band is observed. B. Immunoblot analysis of biotin-nisin conjugates to a spore protein probing with streptavidin conjugated to horseradish peroxidase. A,B. Spores were germinated for 30 min in BHI in the presence or absence of labeled nisin, boiled for 20 min in the presence of 1 mM tris(2-carboxyethyl)phosphine (TCEP), 4.8 M urea, 3% sodium dodecyl sulfate (SDS), homogenated by vortexing with glass beads (30 sec x 10).

3.2.3 Lipid II binding is not sufficient to inhibit outgrowth.

Nisin binds spore-associated lipid II and inhibits spore outgrowth, but whether lipid II binding alone is sufficient for nisin-dependent outgrowth inhibition was not evident from the studies described thus far. To evaluate this possibility,

we studied the action of a purified amino-terminal chymotryptic fragment of nisin (c-nisin) that retained the A, B, and C rings of the full-length parent compound. C-nisin contains the necessary N-terminal portion of nisin required for lipid II binding (14) but is unable to form pores (11). Competition assays between c-nisin and b-nisin revealed that the binding of b-nisin to germinated spores was significantly reduced in the presence of 100-fold molar excess of c-nisin (Figure 3.9C), once more providing evidence that b-nisin recognizes and binds lipid II. When incubated with germinated spores, c-nisin did not demonstrate significant inhibition of spore outgrowth (Figure 3.9D, Table 3.1), although a slight delay in the elongation of vegetative bacilli was observed. These data indicate that while the chymotrypsin-derived amino terminal nisin fragment binds lipid II, this fragment alone does not inhibit the outgrowth of germinated spores. Interestingly, truncated nisin A mutants lacking rings D and E were unable to permeabilize the membranes or cause a disruption of membrane potential within *L. lactis*, but these mutants retained the capacity to inhibit the outgrowth of *B. subtilis* spores (46), which is contradictory to the results presented here. However, the previously reported outgrowth results were obtained by measuring optical density at 600 nm to indicate outgrowth, which is an indirect measurement of outgrowth, while results reported here utilized microscopy to provide direct visual observations of the lack of outgrowth inhibition. Furthermore, the spore and cell wall structural differences between *B. subtilis* and *B. anthracis* could potentially afford the differing results. Consistent with above result, vancomycin, which also binds lipid II, albeit at a different recognition site, was also incapable of inhibiting

the outgrowth of germinated spores (Figure 3.4, Figure 3.11, Figure 3.12, Table 3.2). Together, these results support the model that lipid II binding alone is not sufficient to inhibit the outgrowth of germinated spores.

Comparison of nisin and c-nisin outgrowth inhibition			
Antibiotic ^a	Length of <i>B. anthracis</i> ^b		
	0 h	5 h	10 h
nisin	1.59 ± 0.07	1.50 ± 0.06	1.59 ± 0.06
c-nisin	1.56 ± 0.07	8.72 ± 2.88*	7.95 ± 1.18*

Table 3.1. Comparison of nisin and c-nisin outgrowth inhibition. ^a Spores were incubated in BHI with 10 μM of the indicated antibiotic. ^b At indicated time points samples were taken and visualized utilizing DIC microscopy. Size analysis, reported in μm, was performed with SoftWoRX Explorer Suite. n = 30. *Indicates significantly longer spores in the listed condition than spores at 0 h and spores at the identical time incubated in the presence of nisin, P < 0.001.

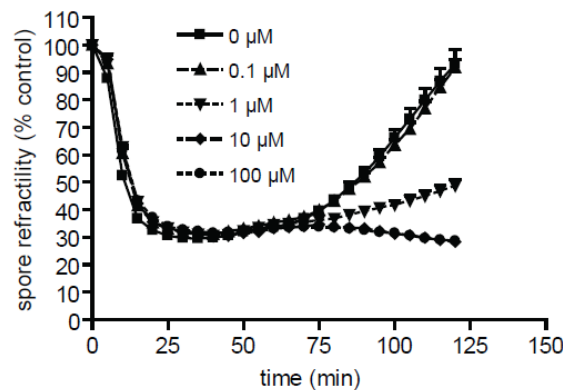


Figure 3.12. Lipid II binding is not sufficient for outgrowth inhibition - growth curves. The data are expressed as the percentage of OD₆₀₀ at each time point relative to the OD₆₀₀ of each culture at time zero, which was the control in these experiments. Error bars indicate standard deviations. The concentrations of vancomycin (μM) for each condition are indicated within the graph.

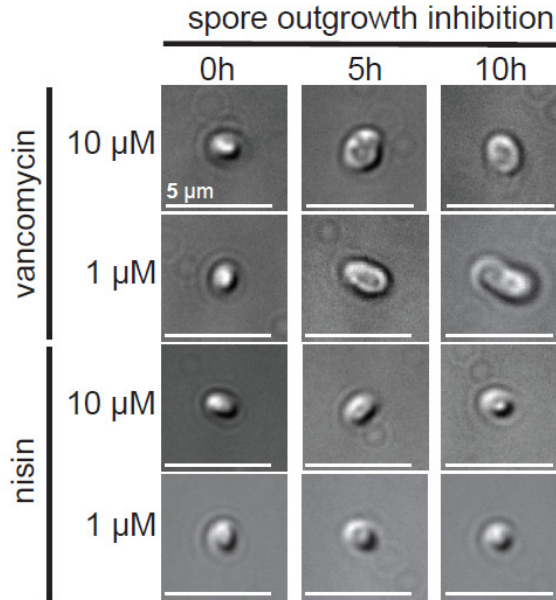


Figure 3.13. Lipid II binding is not sufficient for outgrowth inhibition - microscopy. At time 0, 5, and 10 h, samples were removed and visualized by DIC microscopy. For each panel, a single spore is shown for clarity but is representative of all other *B. anthracis* spores within that sample.

Comparison of outgrowth inhibition by nisin and vancomycin			
Antibiotic ^a	Length of <i>B. anthracis</i> ^b		
	0 h	5 h	10 h
nisin	1.48 ± 0.14	1.50 ± 0.12	1.46 ± 0.09
vancomycin	1.56 ± 0.18	2.46 ± 0.18*	2.47 ± 0.33*

Table 3.2. Comparison of outgrowth inhibition by nisin and vancomycin. ^aSpores were incubated in BHI with 10 μM of the indicated antibiotic. ^b At indicated time points samples were taken and visualized utilizing DIC microscopy. Size analysis, reported in μm, was performed with SoftWoRX Explorer Suite. n = 30. *Indicates significantly longer spores in the listed condition than spores at 0 h and spores at the identical time incubated in the presence of nisin, P < 0.001.

3.2.4 Lipid II binding is associated with nisin-dependent loss of membrane potential.

As described in chapter 2, nisin prevents the establishment of the membrane potential in germinated spores (12). Although the results presented in this chapter support the binding of nisin to lipid II, they do not establish whether nisin binding to lipid II is important for nisin-dependent membrane potential dissipation. To evaluate this possibility, the membrane potential was first measured in germinated spores in the presence of vancomycin. Importantly, vancomycin alone did not cause a decrease in membrane potential (Figure 3.13A, B). However, nisin was able to prevent the establishment of a membrane potential (Figure 3.13A-C). Furthermore, a significant decrease of nisin-dependent reduction of the trans-membrane potential of spores was observed in the presence of a 100-fold molar excess of vancomycin (Figure 3.13A). Moreover, germination of spores in the presence of c-nisin resulted in significantly less reduction of spore trans-membrane potential (Figure 3.13C). Because these studies were carried out under conditions where vancomycin or c-nisin reduced the binding of b-nisin to spores (Figures 3.9C and 3.13A), these results suggest that nisin-dependent reduction of the trans-membrane potential requires binding to lipid II in newly germinated spores.

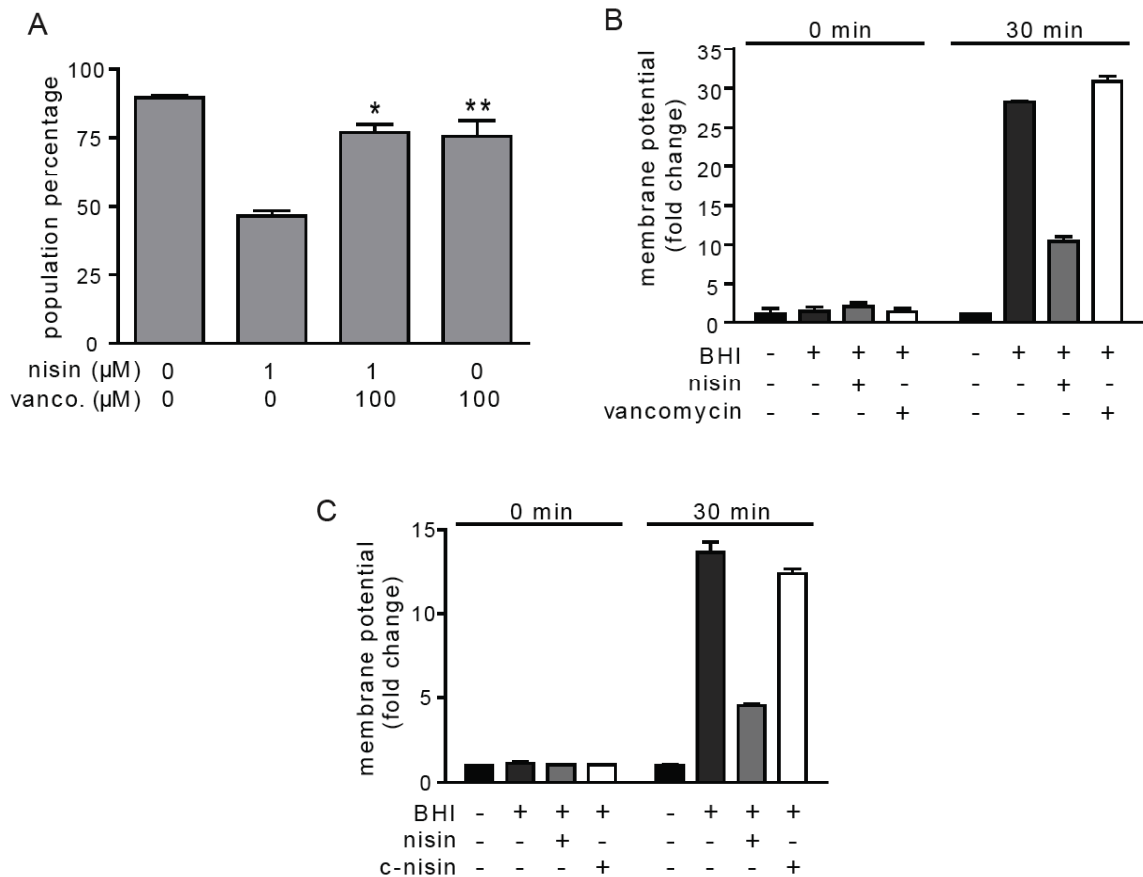


Figure 3.14. Lipid II binding is not sufficient to inhibit membrane potential establishment via membrane disruption. A. Functional competition assay using nisin-induced dissipation of the membrane potential as a read-out. The data is plotted as the population of spores exhibiting a native membrane potential per 10,000 spores as observed by flow cytometry. Pre-incubation with vancomycin blocks nisin-mediated membrane potential dissipation. * indicates a p-value < 0.05 between nisin (1 μM) only treated spores and spores pretreated with vancomycin (100 μM) prior to nisin addition (1 μM). ** indicates a p-value < 0.05 between non-treated spores and spores treated with vancomycin (100 μM) only. B, C. At time 0 (prior to the addition of nisin) and 30 min aliquots were removed from the cultures and evaluated for membrane potential by measuring the DiOC₂-associated *B. anthracis* fluorescence by flow cytometry. Data are rendered as the fold change in membrane potential relative to spores in the presence of 0.1 M MOPS pH 6.8 at the indicated time point. +: presence of BHI (germinant), 10 μM nisin, 10 μM c-nisin, or 10 μM vancomycin. -: absence of BHI (germinant), nisin, c-nisin, or vancomycin.

3.2.5 Lipid II binding is associated with nisin-dependent alterations in membrane integrity.

As described in chapter 2, nisin disrupts the membrane integrity of germinated spores (12), but the data thus far do not determine whether nisin-lipid II interactions are required for this activity. Therefore, experiments were conducted to examine the effect on membrane integrity. Nisin induced significantly more PI uptake than c-nisin in over 92% of the population of spores (Figure 3.14A and B). Vancomycin was not able to induce an increase in PI uptake (Figure 3.14B). In addition, only nisin was able to render the germinated spore metabolically inactive prior to outgrowth (Figure 3.15). Collectively, these results suggest that an association between nisin and lipid II is important for the disruption of membrane integrity.

Figure 3.15

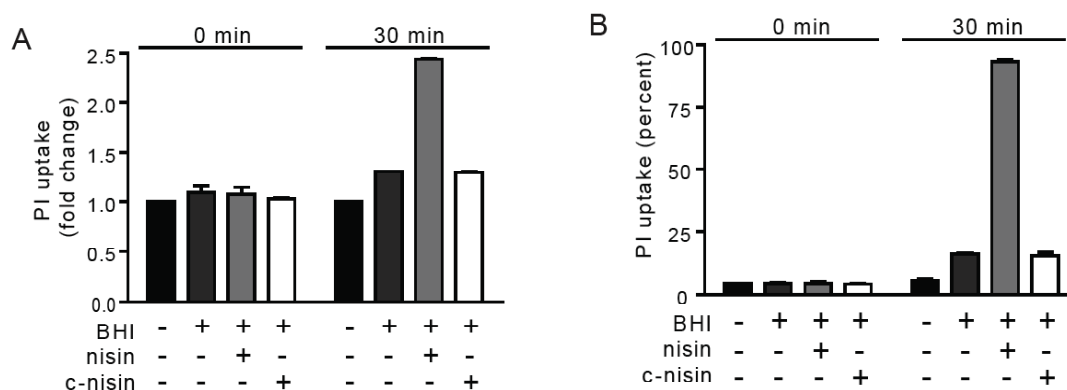


Figure 3.15 (continued)

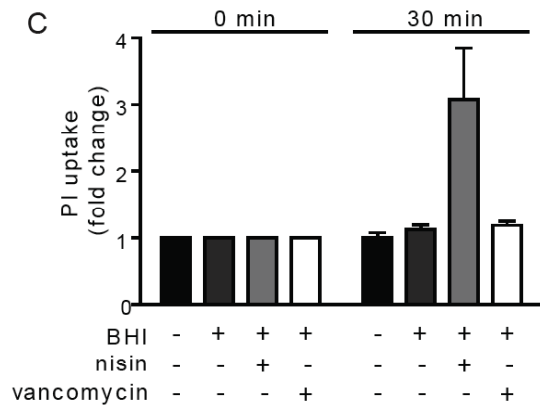


Figure 3.15. C-terminal region of nisin is essential for preventing a membrane potential, spore outgrowth, and membrane disruption. At time 0 (prior to the addition of nisin) and 30 min, aliquots were removed from the cultures and evaluated for the following: A, C. Membrane disruption by measuring PI uptake by *B. anthracis* using flow cytometry, B. Population of spores exhibiting an increase in fluorescence associated with PI uptake. The data are plotted as the percent of PI positive spores. A, C. Data are rendered as the fold change PI uptake relative to spores in the presence of 0.1 M MOPS pH 6.8 at the indicated time point. A-C. +: presence of BHI (germinant), 10 μ M nisin, 10 μ M c-nisin, or 10 μ M vancomycin. -: absence of BHI (germinant), nisin, c-nisin, or vancomycin.

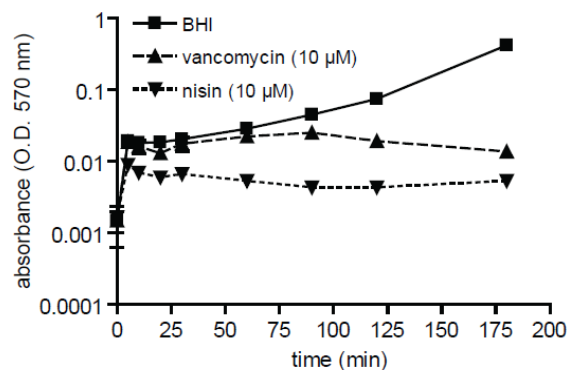


Figure 3.16. Lipid II binding is not sufficient to disrupt metabolic function during germination. At the indicated times, aliquots were removed from the cultures and were evaluated for oxidative metabolism by spectrophotometrically measuring the production of formazan at 570 nm.

3.2.6 Modification of the nisin hinge region, but not Dha5, results in the loss of outgrowth inhibition.

Previous studies have reported conflicting results as to whether Dha5 is essential for outgrowth inhibition (6, 15, 20, 23). Therefore, experiments were conducted to determine the necessity of Dha5 for membrane disruption resulting in outgrowth inhibition. Nisin and nisin-Dha5-Ala were heterologously produced in *E. coli* (h-nisin and h-nisin S5A) (27), purified, and assessed for their ability to disrupt the membrane, inhibit establishment of a membrane potential, and prevent outgrowth of germinated spores. Both lantibiotics inhibited membrane potential establishment and spore outgrowth and increased PI uptake (Figure 3.16, Table 3.3) to the same extent. These results show that Dha5 is not essential for spore outgrowth inhibition, as also reported previously by Moll and coworkers (23), and that the mutation does not change the mechanism of inhibition.

A second region of interest for mutation is the hinge region between the three N-terminal rings and the two C-terminal rings. The double mutants N20P/M21P and M21P/K22P have been shown previously to retain lipid II binding affinity but not pore-forming activity (10, 13, 31). These mutants were prepared in this study by heterologous expression in *E. coli* and were analyzed for their ability to disrupt the spore membrane and inhibit membrane potential establishment and spore outgrowth. The inhibitory activity of the nisin variants tested against *Micrococcus flavus*, which is a highly sensitive indicator strain. The data demonstrated high antimicrobial activity for the hinge mutants were

consistent with previously published results as shown in Table 3.3 (10, 13, 31). However, as depicted in Figure 3.16, both mutants lost the ability to inhibit spore outgrowth, disrupt the membrane, and inhibit establishment of a membrane potential (see also Table 3.4). These data corroborate the findings with the truncated analog c-nisin and demonstrate that the ability to disrupt the spore membrane is essential for outgrowth inhibition.

nisin variant	IC ₅₀ and IC ₉₉ of nisin variants against <i>Micrococcus flavus</i> ^a	
	IC ₅₀ ^b	IC ₉₉ ^c
nisin	1.74 ± 0.05	3.20 ± 0.31
h-nisin	1.79 ± 0.09	3.74 ± 0.50
h-nisin S5A	1.76 ± 0.07	3.21 ± 0.42
h-nisin N20PM21P	2.03 ± 0.01	5.56 ± 0.01
h-nisin M21PK22P	1.90 ± 0.03	4.58 ± 0.18

Table 3.3. IC₅₀ and IC₉₉ of nisin variants against *Micrococcus flavus*. Three independent experiments were performed in triplicate. The values are reported as the averages of three experiments. ^bDefined as the nisin concentration that inhibits the growth of cultures of *Micrococcus flavus* by 50% at 8 h. ^cDefined as the nisin concentration that inhibits the growth of cultures of *Micrococcus flavus* by 99% at 8 h.

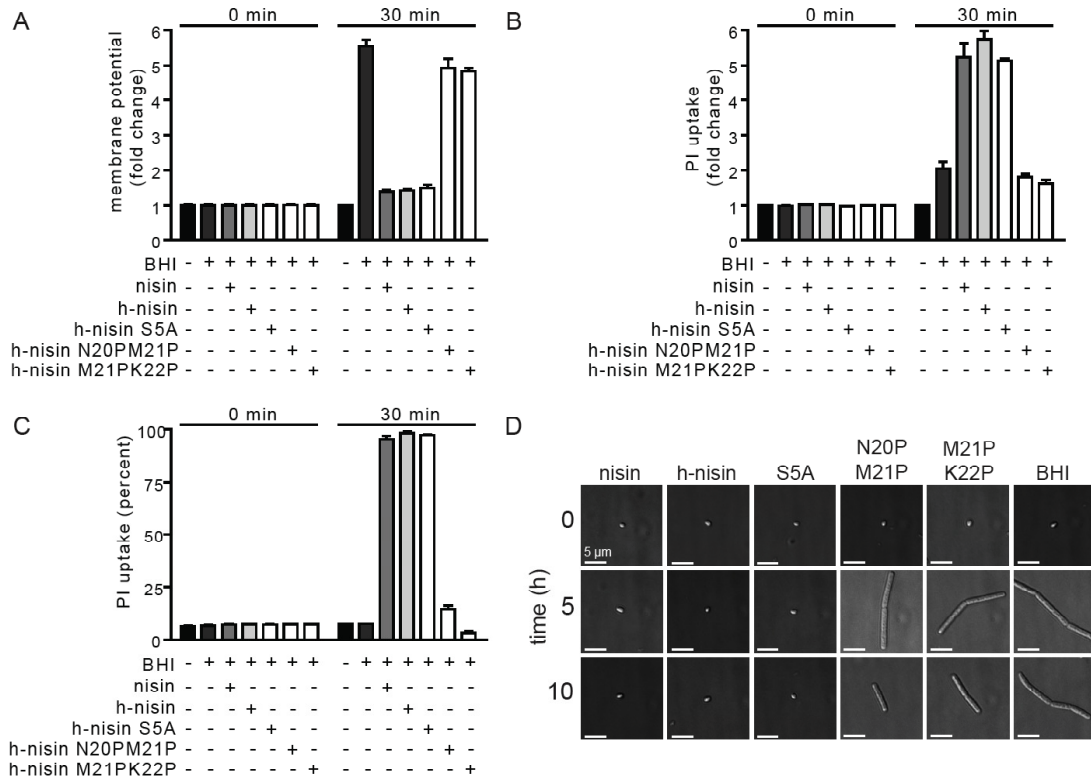


Figure 3.17. A flexible hinge region, not Dha5, is essential for preventing a membrane potential, spore outgrowth, and membrane disruption. At time 0 (prior to the addition of nisin) and 30 min, aliquots were removed from the cultures and evaluated for the following: A. Membrane potential by measuring the fluorescence of DiOC₂-associated *B. anthracis* using flow cytometry. B. Membrane disruption by measuring PI uptake by *B. anthracis* using flow cytometry. C. Population of spores exhibiting an increase in fluorescence associated with PI uptake. The data are plotted as the percent of PI positive spores. A, B. Data are rendered as the fold change in membrane potential (A) or PI uptake (B) relative to spores in the presence of 0.1 M MOPS pH 6.8 at the indicated time point. A-C. +: presence of BHI (germinant) or nisin variant (10 μ M). -: absence of BHI (germinant) or nisin variant. D. At time 0, 5, and 10 h, samples were removed from cultures containing 10 μ M of the indicated nisin variant and visualized by DIC microscopy. For each panel, a single spore is shown for clarity, but the image is representative of all other *B. anthracis* spores within that sample. Bars, 5 μ m. The data are representative of those from three independent experiments.

Comparison of outgrowth inhibition by nisin variants			
Antibiotic ^a	Length of <i>B. anthracis</i> ^b		
	0 h	5 h	10 h
nisin	1.65 ± 0.12	1.68 ± 0.10	1.67 ± 0.13
h-nisin	1.67 ± 0.12	1.67 ± 0.14	1.70 ± 0.13
h-nisin S5A	1.68 ± 0.12	1.69 ± 0.12	1.70 ± 0.12
h-nisin N20P/M21P	1.67 ± 0.12	7.04 ± 1.12*	5.91 ± 1.67*
h-nisin M21P/K22P	1.65 ± 0.15	7.76 ± 1.60*	5.45 ± 1.68*

Table 3.4. Comparison of outgrowth inhibition by nisin variants. ^aSpores were incubated in BHI with 10 μM of the indicated antibiotic. ^bAt indicated time points samples were taken and visualized utilizing DIC microscopy. Size analysis, reported in μm, was performed with SoftWoRX Explorer Suite. n = 30. *Indicates significantly longer spores in the listed condition than spores at 0 h and spores at the identical time incubated in the presence of nisin, P < 0.001.

3.2.7 Membrane depolarization inhibits spore outgrowth.

Previous studies have identified that the nisin pores allow the efflux of ions, Rb⁺ and Cl⁻, as well as small molecules such as Glu and Pro (24). To determine whether membrane depolarization alone is sufficient for outgrowth inhibition, the activity of nisin was compared to a non-specific membrane depolarizer, carbonyl cyanide 4-(trifluoromethoxy)phenylhydrazone (FCCP). As compared to the outgrowth inhibition of 1 μM nisin, 10 μM FCCP was required to inhibit outgrowth through 10 h (Figure 3.17, Table 3.5). Additionally, 1 μM FCCP was able to visually slow the kinetics of outgrowth when compared to BHI only conditions (Figure 3.17, Supplemental Table 3.5). These findings suggest that dissipation of membrane potential alone, at sufficient concentration of a depolarizer, will inhibit outgrowth. However, nisin's interaction with a specific target to prevent membrane potential establishment as well as the potential flow

of additional ions and small molecules aids in nisin-mediated outgrowth inhibition and killing of germinated spore.

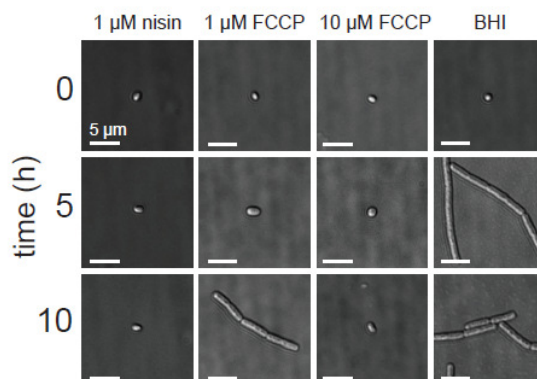


Figure 3.18. Outgrowth inhibition results from membrane depolarization. At time 0, 5, and 10 h, samples were removed and visualized by DIC microscopy. For each panel, a single spore is shown for clarity, but the image is representative of all other *B. anthracis* spores within that sample. Bars, 5 μm . The data are representative of those from three independent experiments.

Comparison of nisin and FCCP outgrowth inhibition			
Antibiotic ^a	Length of <i>B. anthracis</i> ^b		
	0 h	5 h	10 h
nisin (1 μM)	1.65 \pm 0.12	1.68 \pm 0.10	1.67 \pm 0.13
FCCP (1 μM)	1.68 \pm 0.12	2.27 \pm 0.58*	5.80 \pm 0.93*
FCCP (10 μM)	1.69 \pm 0.11	1.80 \pm 0.26	1.93 \pm 0.43

Table 3.5. Comparison of nisin and FCCP outgrowth inhibition. ^aSpores were incubated in BHI with 10 μM of the indicated antibiotic. ^bAt indicated time points samples were taken and visualized utilizing DIC microscopy. Size analysis, reported in μm , was performed with SoftWoRX Explorer Suite. $n = 30$. *Indicates significantly longer spores in the listed condition than spores at 0 h and spores at the identical time incubated in the presence of nisin, $P < 0.001$.

3.3 Discussion

The studies presented in chapter 2 and elsewhere (4, 6, 12, 20) implicated nisin-mediated alterations in the membrane integrity and prevention of the establishment of a membrane potential as the mechanism by which nisin inhibits spore outgrowth. Whether or not interactions with lipid II were important for these activities was not determined. Utilizing fluorescently labeled nisin and vancomycin, competition experiments, and nisin analogs, lipid II was identified in this study as the target for nisin binding to induce inhibition of spore outgrowth. Lipid II binding alone is not sufficient for outgrowth inhibition, however, which requires membrane disruption. Modification of Dha5 to Ala does not result in the loss of outgrowth inhibition and membrane disruption. We anticipate that lantibiotics such as subtilin (16, 22), epidermin (5), and haloduracin (21) also inhibit spore outgrowth via membran disruption and that lipid II binding may also be involved in nisin inhibition of other spore-forming bacteria from the genera *Bacillus* and *Clostridium*, including those of medical relevance such as *C. botulinum* and *C. difficile*.

3.4 Materials and Methods

3.4.1 Spore preparations.

Spores were prepared from *B. anthracis* Sterne 7702, as described previously (28). Enumeration of spores was performed using a Petroff-Hauser hemacytometer under a light microscope at 400x magnification (Nikon Alphaphot

YS, Mellville, NY). A typical spore preparation yielded 10 mL of spores at a concentration of 2.0×10^9 spores/mL.

3.4.2 Nisin purification.

Nisin was purified and characterized as described previously (12).

3.4.3 Labeling of nisin and vancomycin.

Nisin was reacted with NHS-fluorescein (Pierce, Rockford, IL), NHS-rhodamine (Pierce), or with NHS-BODIPY-633 (Invitrogen, Carlsbad, CA) to generate an analog with a single fluorescein group (f-nisin), a single rhodamine group (r-nisin), or a single BODIPY group (b-nisin) after purification. The reactions were carried out according to the manufacturer's protocols except that a 0.75:1 molar ratio of NHS-fluorophore and nisin was used. Proteolytic digest of the fluorescently labeled compounds and subsequent analysis by LC-MS showed that the label was located at the N-terminal portion of nisin for BODIPY 633 and the C-terminal portion of nisin for fluorescein. Labeling reactions were stopped with the addition of 100-fold molar excess of Tris (Sigma, St. Louis, MO) after a 3 h reaction time at room temperature (25 °C). Reactions were analyzed via matrix assisted laser desorption ionization - time of flight (MALDI-TOF) and electrospray ionization (ESI) mass spectrometry (MS) (Applied Biosystems, Carlsbad, CA). Vancomycin was labeled with NHS-rhodamine to obtain r-vancomycin, with NHS-fluorescein to generate f-vancomycin, or with NHS-BODIPY-633 to produce b-vancomycin as previously described (29) and MALDI-TOF mass spectrometry.

Vancomycin labeling occurs on the amino group of the vancosamine sugar (Figure 3.1B) (29). All labeled compounds were purified by reverse phase-high performance liquid chromatography (RP-HPLC, Waters, Milford, MS) utilizing a C4 semi-preparative column (Waters, Milford, MS) with a linear gradient of 0-100% acetonitrile (Fisher Chemical, Fairlawn, NJ) with 0.1% trifluoroacetic acid (Sigma) over 40 min. Acetonitrile, TFA, and water were removed from fractions containing nisin or vancomycin by rotary evaporation followed by lyophilization. The identity of purified nisin (Figure 3.18 A-C) and vancomycin (Figure 3.18 D-F) was confirmed by MALDI-TOF and ESI MS. Prior to use, lyophilized nisin and vancomycin were weighed on a micro-analytical balance and dissolved in 0.1 M MOPS pH 6.8 to yield the desired concentration.

Figure 3.19

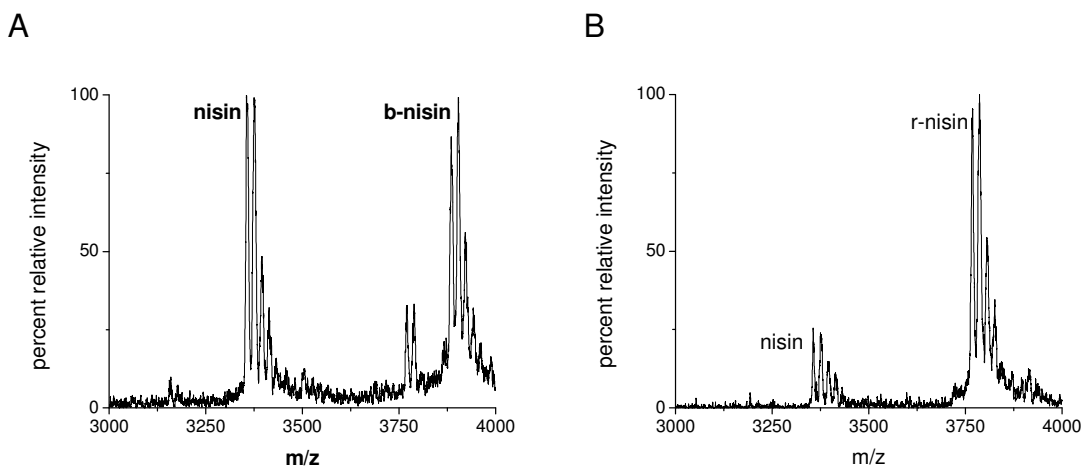


Figure 3.19 (continued)

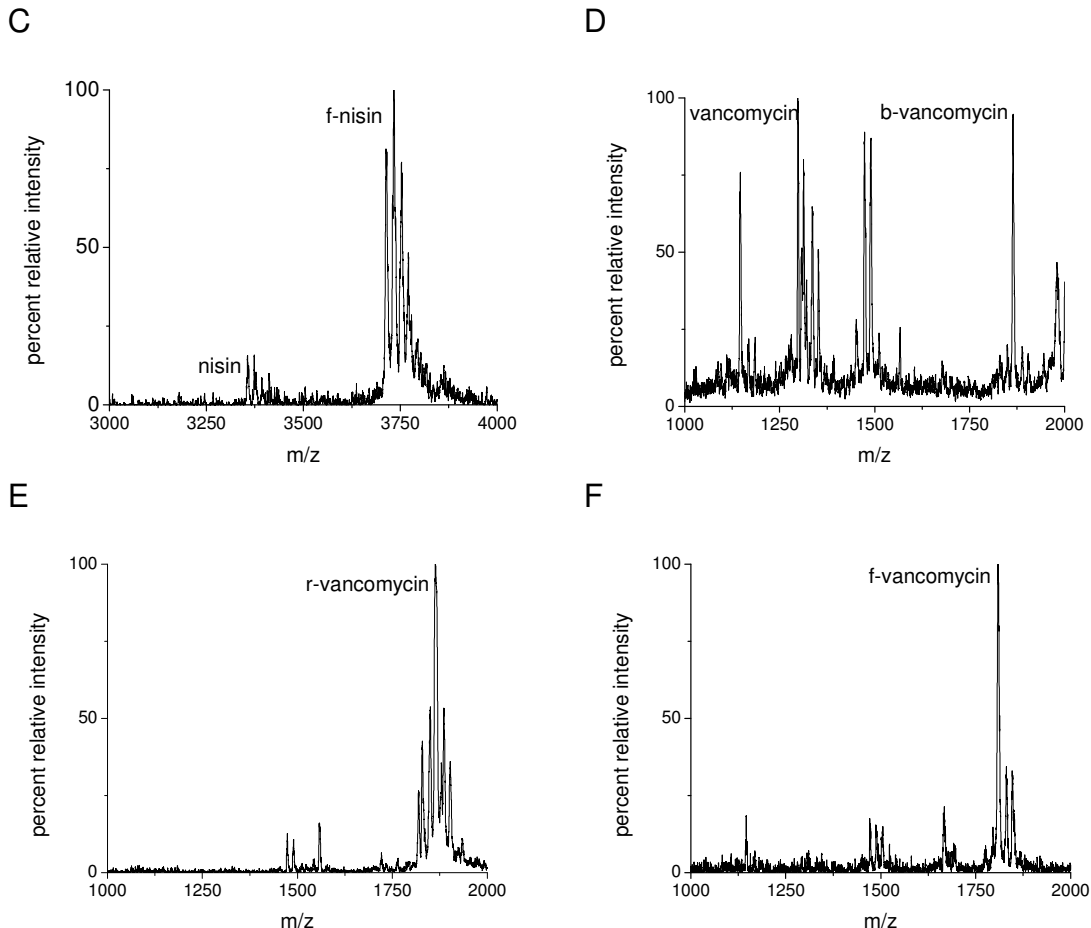


Figure 3.19. Fluorescent labeling of nisin and vancomycin. Both nisin (A-C) and vancomycin (D-F) were independently labeled with NHS-fluorescein, rhodamine, and BODIPY-633. Reactions were purified by HPLC and analyzed via MALDI-TOF mass spectrometry.

3.4.4 Truncation of nisin with chymotrypsin.

Proteolysis of nisin with chymotrypsin was performed as previously described (7). Reactions were analyzed by MALDI-TOF MS. The N-terminal chymotryptic segment (c-nisin, Figure 1A) was purified from full length nisin and the C-terminal fragment by RP-HPLC utilizing a C4 semi-preparative column (Waters, Milford, MA) with a linear gradient of 0-100% acetonitrile over 40 min.

Acetonitrile, TFA, and water were removed from fractions containing c-nisin by rotary evaporation followed by lyophilization. The identity of purified c-nisin was confirmed by MALDI-TOF and ESI mass spectrometry. Prior to use, lyophilized c-nisin was weighed on an analytical balance and dissolved in 0.1 M MOPS pH 6.8 to yield the desired concentration.

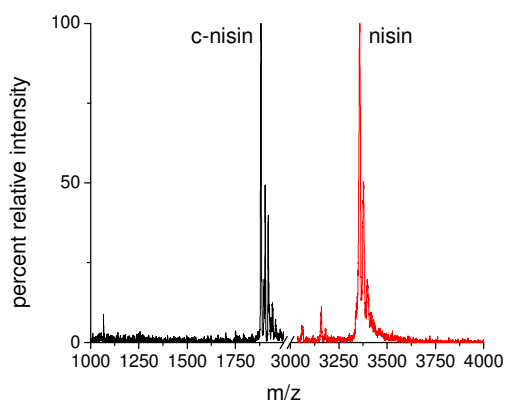


Figure 3.20. Chymotrypsin cleavage nisin and purification of c-nisin. Purified nisin (red) was cleaved after Asn20 with chymotrypsin rendering an N-terminal fragment containing the first 3 rings of nisin (Figure 3.1). The c-nisin (black) was purified by HPLC and analyzed via MALDI-TOF mass spectrometry.

3.4.5 Culturing *B. anthracis* spores.

B. anthracis Sterne 7702 spores at a concentration of 4.0×10^6 spores/mL were incubated in brain heart infusion medium (BHI; BD Bioscience San Jose, CA) supplemented with nisin (at 1 or 10 μ M), c-nisin (10 μ M), nisin variants (S5A, N20PM21P, or M21PK22P at 10 μ M) vancomycin (at 0.1, 1, 10 or 100 μ M), carbonyl cyanide 4-(trifluoromethoxy)phenylhydrazone (FCCP at 1 or 10 μ M), or with 0.1 M 3-(N-morpholino)propanesulfonic acid (MOPS; Sigma) at pH 6.8 as a control. For non-germinating conditions, 0.1 M MOPS (pH 6.8) was substituted

for BHI medium. All incubations were performed at 37 °C under aeration at 180 rpm on a rotary shaker (Thermo Fisher Scientific Inc., Waltham, MA) and under ambient CO₂.

3.4.6 Characterization of antibiotic effects on germination and outgrowth.

Experiments investigating spore hydration, oxidative metabolism, membrane potential, and membrane integrity were performed as previously described (12).

3.4.7 Differential interference contrast (DIC) and epi-fluorescence microscopy.

At indicated times, samples were removed from *B. anthracis* cultures and fixed by incubation in 4% formaldehyde (Sigma) for 30 min at 37 °C followed by mounting on glass slides in 20% glycerol (Sigma) or Slow-Fade[®] antifade reagent (Invitrogen) under glass cover slips for epi-fluorescence microscopy. Live epi-fluorescence microscopy was also performed by mounting samples on glass slides in 0.5% agarose under cover slips. Images were collected using an Applied Precision assembled DeltaVision EpiFluorescence microscope containing an Olympus Plan Apo 100x oil objective with NA 1.42 and a working distance of 0.15 mm. Images were processed and Pearson's coefficient co-localization analysis of 50 spores per condition was performed using SoftWoRX Explorer Suite (Issaquah, WA). Acquisition of epi-fluorescence images utilized FITC (Ex: 490/20 Em: 528/28), rhodamine (Ex: 555/28 Em: 617/73), and Cy5

(Ex: 640/20 Em: 685/40) to visualize fluorescein, rhodamine, and BODIPY-633 fluorescence, respectively.

3.4.8 Functional competition assay.

Competitive binding of nisin and vancomycin was evaluated utilizing a functional assay in which vancomycin prevented nisin-mediated loss of membrane potential via lipid II binding (4). Spores were incubated in BHI medium (germinating conditions), in the presence of 10 mM L-Ala and inosine (germinating conditions), or in 0.1 M MOPS pH 6.8 (non-germinating conditions) with DIOC₂ for 60 min at 37 °C followed by incubation with 0 or 100 µM vancomycin for 2 min. Nisin was added to cultures at a final concentration of 1.0 µM, and the effect on membrane potential disruption was immediately assayed with flow cytometry through 10,000 counts to observe the population of spores that exhibited reduced membrane potential in the presence of nisin. The MIC of vancomycin against *B. anthracis* is 0.5-3.5 µM (1, 2, 30), but the antimicrobial effects of vancomycin under the conditions used here are not manifested until spores have been germinated and incubated in the presence of vancomycin for 90 min, which is well after the timeframe of interest in this investigation.

3.4.9 Competition binding assay.

Competitive binding of nisin and vancomycin was evaluated by determining the interaction of the fluorescently labeled antibiotic (nisin or vancomycin) with lipid II in the presence of the other unlabeled antibiotic (in 100-

fold molar excess) as a competitor. Spores were incubated in either BHI (germinating) or 0.1 M MOPS pH 6.8 (non-germinating) for 60 min at 37 °C followed by incubation with 0 or 100 µM of the unlabeled antibiotic for 5 min at 37 °C. The labeled antibiotic was then added to cultures at a final concentration of 1.0 µM. The binding of the labeled antibiotic to the spores was assayed by flow cytometry to observe the reduction in antibiotic-associated increase in fluorescence in the presence of the competing unlabeled antibiotic. Analytical flow cytometry-based assays were carried out using a Beckman Coulter Epics XL-MCL flow cytometer equipped with a 70-µm nozzle, a 633-nm HeNe laser, and a 17-mV output. The band pass filter used for detecting labeled antibiotic binding was 660/20. Spore analysis was standardized for side/forward scatter and fluorescence by using a suspension of fluorescent beads (Beckman Coulter Inc., Fullerton, CA). At least 10,000 events were detected for each experiment (>2,000 events per min). Events were recorded on a log fluorescence scale. Density plots and fluorescence intensity histograms were generated using FCS Express 3.00.0311 V Lite Standalone. Sample debris (as indicated by lower forward and side scatter and a lack of PI staining) represented a small fraction (1 to 2%) of the detected events and was excluded from analysis.

3.4.10 Site-directed mutagenesis.

Mutagenesis of *nisA* was performed using the QuikChange mutagenesis kit from Stratagene (La Jolla, CA). First, complementary mutagenic primers (Table 3.6) were designed containing the desired mutation(s) in the center of the

primer and 20 to 25 bases of a perfectly complementary sequence on either side. Reaction mixtures were prepared as described in the QuikChange protocol with pRSFDuet-1nisAB as the plasmid template (27) for the generation of NisA S5A and M21P mutants. After cycling of the reaction mixture 18 times in a thermal cycler (MJ Research, Waltham, MA), the resulting mixture was digested with DpnI (New England Biolabs, Ipswich, MA), and the resulting DNA was transformed into supercompetent *E. coli* DH5 α cells. The resulting mutant plasmids were isolated, and the entire gene was sequenced to ensure that only the appropriate mutations were introduced. For double mutations, a second round of site directed mutagenesis was performed utilizing pRSFDuet-1nisAB-M21P as the plasmid template for the generation of NisA N20PM21P and M21PK22P mutants.

Primer sequences used for mutagenesis			
Gene	Desired Mutation	Primer ^a	Primer Sequence (5'→3') ^b
<i>nisA</i>	S5A	nisA-S5AFor	5'-GGTGCATCACCACGCATTACAAGTATT <u>CGC</u> CTATG TACACCCGGTTGTAACAACAG-3'
		nisA-S5ARev	5'-CCACGTTAGTGGTGCCTAATGTTTCATAA <u>CGC</u> GATACA TGTGGCCCAACATTTTGTTC-3'
<i>nisA</i>	M21P	nisA-M21PFor	5'-ACAGGAGCTCTGATGGGTTGTAAC <u>CCCC</u> AAAACAGC AACTTGTCTATTGTAGT-3'
		nisA-M21PRev	5'-TGTCTCGAGACTACCCAACATT <u>GGGG</u> TTTTGTCTG TTGAACAGTAACATCA-3'
<i>nisA</i>	N20PM21P	nisA-N20PM21PFor	5'-AAAACAGGAGCTCTGATGGGTTG <u>CCCCC</u> AAAAC AGCAACTTGTCTATTGTAGT-3'
		nisA-N20PM21PRev	5'-TTTTGTCCTCGAGACTACCCAAC <u>AGGGGG</u> TTTTG TCGTTGAACAGTAACATCA-3'
<i>nisA</i>	M21PK22P	nisA-M21PK22PFor	5'-GGAGCTCTGATGGGTTGTAAC <u>CCCCC</u> CACAGCAACT TGTCATTGTAGTAATCAC-3'
		nisA-M21PK22PRev	5'-CCTCGAGACTACCCAACATT <u>GGGGGG</u> GTGTCGTTGA ACAGTAACATCATTAGTG-3'

Table 3.6. Primer sequences used for mutagenesis. ^a Primers were designed in accordance with the QuikChange site-directed mutagenesis protocol by Stratagene (La Jolla, CA) and were synthesized by Integrated DNA Technologies (Coralville, IA). ^b Underlined sequences indicate engineered codon mutations.

3.4.11 Over expression of *nisA* and mutants with *in vivo* posttranslational modifications.

Electro-competent *E. coli* BL21(DE3) cells were co-transformed with pRSFDuet-1 containing *nisA* variants and *nisB* genes and pACYCDuet-1 containing the *nisC* gene (27) (Table 3.7). Overnight culture grown from a single colony transformant was used as inoculum to grow 2 L of terrific broth medium (0.12 % Pancreatic Digest of Casein, BD Biosciences, San Jose, CA; 0.24 % Yeast Extract, BD Biosciences; 0.094 % K₂HPO₄, Fisher Chemical; 0.022 % KH₂PO₄, Fisher Chemical) containing 50 µg/L kanamycin (Sigma) and 25 µg/L chloramphenicol (Sigma) at 37 °C until the OD_{600nm} reached about 0.6. The incubation temperature was then changed to 18 °C and the culture was induced with 0.5 mM IPTG (Sigma). The induced cells were shaken continually at 18 °C for an additional 18 h. The cells were harvested by centrifugation (10,000×g for 10 min, Beckman JA-10 rotor, Brea, CA). The cell pellet was resuspended in 45 mL of start buffer (20 mM Tris, pH 8.0; 500 mM NaCl, Fisher Chemical), 10% glycerol (Fisher Chemical), and lysed by sonication (35 % amplitude, 4.4 s pulse, 9.9 s pause for total 25 min; Sonics & Materials, Inc., Newtown, CT). The sample was centrifuged at 23,700×g for 30 min at 4 °C. The supernatant was loaded onto Talon® cobalt affinity resin (Clontech, Mountain View, CA) pre-equilibrated with start buffer. After 1 hour of gentle agitation at 4 °C, the resin was washed twice with 10 mL of start buffer and once with 10 mL of wash buffer (start buffer + 30 mM imidazole, Sigma). The peptide was eluted from the resin with 8 mL of elution buffer (start buffer + 1 M imidazole).

The pellet from the first sonication and centrifugation was homogenized via sonication (35 % amplitude, 4.4 s pulse, 9.9 s pause for total 25 min) in start buffer. The cell homogenates were centrifuged at 23,700 g for 30 min at 4 °C. The supernatant was loaded onto Talon® cobalt affinity resin for a second round of affinity protein purification as previously described. The pellet was resuspended in 30 mL of denaturing buffer (6 M guanidine hydrochloride, Sigma; 20 mM NaH₂PO₄, Sigma; 500 mM NaCl, pH 7.5) utilizing sonication (35 % amplitude, 4.4 s pulse, 9.9 s pause for total 25 min). The insoluble portion was removed by centrifugation at 23,700 g for 30 min at 4 °C, and the supernatant was loaded onto Talon® cobalt affinity resin. The resin was washed with denaturing buffer containing 30 mM imidazole and eluted with 8 mL of denaturing buffer containing 1 M imidazole. The eluents from all three cobalt affinity purifications were desalted via RP-HPLC utilizing a C4 semi-preparative column with a linear gradient of 0-100% acetonitrile with 0.1% TFA over 40 min. The fractions containing modified prenisin were lyophilized and analyzed by MALDI-TOF MS.

<i>E. coli</i> BL21 (DE3) expression plasmids		
Plasmid	Relevant Characteristics ^a	Reference
pRSFDuet-1nisAB	MCS1 contains polyHis- <i>nisA</i> , MCS2 contains <i>nisB</i> , Kan ^r	Shi, X., <i>et al.</i> (29)
pACYCDuet-1nisC	<i>nisC</i> , Cam ^r	Shi, X., <i>et al.</i> (29)
pRSFDuet-1nisAB-S5A	polyHis- <i>nisAS5A</i>	This study
pRSFDuet-1nisAB-M21P	polyHis- <i>nisAM21P</i>	This study
pRSFDuet-1nisAB-N20PM21P	polyHis- <i>nisAN20PM21P</i>	This study
pRSFDuet-1nisAB-M21PK22P	polyHis- <i>nisAM21PK22P</i>	This study

Table 3.7. *E. coli* BL21 (DE3) expression plasmids. ^aAll plasmids contain two multiple cloning sites (MCS) with gene expression under the control of an IPTG T7 inducible promoter. MCS1 pRSF-Duet-1nisAB installs an N-terminal poly-His₆-tag on the product of *nisA* expression. Neither *nisB* nor *nisC* are tagged allowing for cobalt affinity purification of the modified prenisin. The amino acid changes of the nisin variants are indicated.

3.4.12 Cleavage of modified prenisin with trypsin and purification of nisin variants.

Modified prenisin (500 μM) and trypsin (30 μM, Worthington Biochemicals, Lakewood, NJ) were incubated in a 100:3 ratio at room temperature for 3 h with 150 rpm mixing on a platform shaker (New Brunswick Scientific, Edison NJ). The resulting mixture was checked by MALDI-TOF MS and the desired proteolytic fragment corresponding to mature nisin or its variants were observed - calculated: 3352.5152 m/z – M+H (heterologously expressed nisin, h-nisin), 3354.5608 m/z - M+H (h-nisin S5A), 3301.5673 m/z - M+H (h-nisin N20PM21P), and 3287.9826 m/z - M+H (h-nisin M21PK22P) - observed: 3352.5005 m/z – M+H (heterologously expressed nisin, h-nisin), 3354.4946 m/z - M+H (h-nisin S5A), 3301.7642 m/z - M+H (h-nisin N20PM21P), and 3287.8738 m/z - M+H (h-nisin M21PK22P). Nisin and variants were purified from the cleavage reaction

via RP-HPLC utilizing a C4 semi-preparative column with a linear gradient of 0-100% acetonitrile with 0.1% TFA over 40 min. The fractions containing nisin variants were lyophilized and analyzed by spectrometry MALDI-TOF and ESI MS.

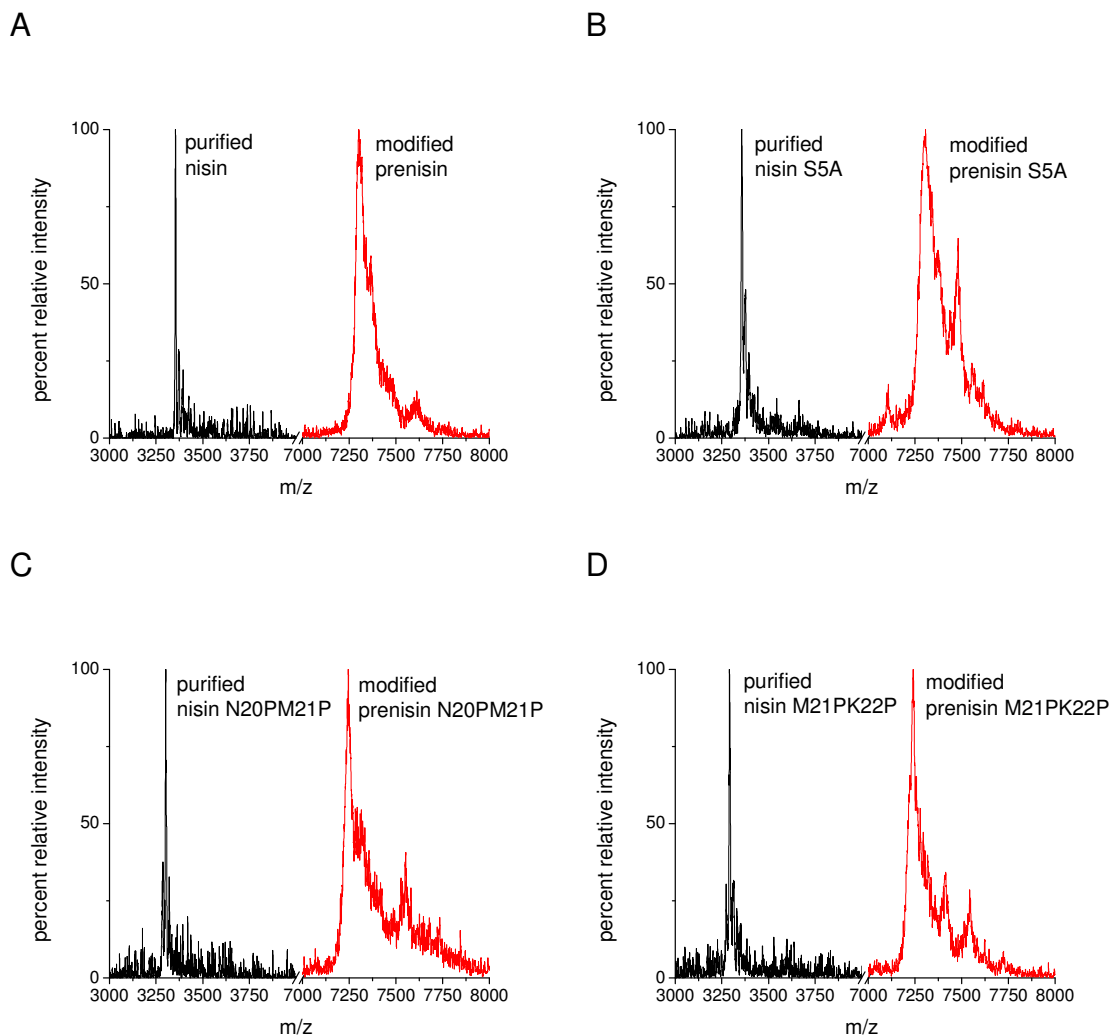


Figure 3.21. Cleavage of modified nisin and purification of h-nisin variants. The leader of heterologously expressed and purified modified prenisin variants (red) was removed by proteolytic cleavage with trypsin rendering fully modified nisin containing all posttranslational (Figure 3.1). The h-nisin variants (black) were purified by HPLC and analyzed via MALDI-TOF mass spectrometry.

3.5 References

1. **Athamna, A., M. Athamna, N. Abu-Rashed, B. Medlej, D. J. Bast, and E. Rubinstein.** 2004. Selection of *Bacillus anthracis* isolates resistant to antibiotics. *J Antimicrob Chemother* **54**:424-8.
2. **Athamna, A., M. Massalha, M. Athamna, A. Nura, B. Medlej, I. Ofek, D. Bast, and E. Rubinstein.** 2004. *In vitro* susceptibility of *Bacillus anthracis* to various antibacterial agents and their time-kill activity. *J Antimicrob Chemother* **53**:247-51.
3. **Breukink, E., and B. de Kruijff.** 2006. Lipid II as a target for antibiotics. *Nat Rev Drug Discov* **5**:321-32.
4. **Breukink, E., I. Wiedemann, C. van Kraaij, O. P. Kuipers, H. Sahl, and B. de Kruijff.** 1999. Use of the cell wall precursor lipid II by a pore-forming peptide antibiotic. *Science* **286**:2361-4.
5. **Brotz, H., M. Josten, I. Wiedemann, U. Schneider, F. Gotz, G. Bierbaum, and H. G. Sahl.** 1998. Role of lipid-bound peptidoglycan precursors in the formation of pores by nisin, epidermin and other lantibiotics. *Mol Microbiol* **30**:317-27.
6. **Chan, W. C., H. M. Dodd, N. Horn, K. Maclean, L. Y. Lian, B. W. Bycroft, M. J. Gasson, and G. C. Roberts.** 1996. Structure-activity relationships in the peptide antibiotic nisin: role of dehydroalanine 5. *Appl Environ Microbiol* **62**:2966-9.
7. **Chan, W. C., M. Leyland, J. Clark, H. M. Dodd, L. Y. Lian, M. J. Gasson, B. W. Bycroft, and G. C. Roberts.** 1996. Structure-activity relationships in the peptide antibiotic nisin: antibacterial activity of fragments of nisin. *FEBS Lett* **390**:129-32.
8. **Daniel, R. A., and J. Errington.** 2003. Control of cell morphogenesis in bacteria: two distinct ways to make a rod-shaped cell. *Cell* **113**:767-76.
9. **Delves-Broughton, J., P. Blackburn, R. J. Evans, and J. Hugenholtz.** 1996. Applications of the bacteriocin, nisin. *Antonie Van Leeuwenhoek* **69**:193-202.
10. **Field, D., P. M. Connor, P. D. Cotter, C. Hill, and R. P. Ross.** 2008. The generation of nisin variants with enhanced activity against specific Gram-positive pathogens. *Mol Microbiol* **69**:218-30.
11. **Giffard, C. J., H. M. Dodd, N. Horn, S. Ladha, A. R. Mackie, A. Parr, M. J. Gasson, and D. Sanders.** 1997. Structure-function relations of variant and fragment nisins studied with model membrane systems. *Biochemistry* **36**:3802-10.

12. **Gut, I. M., A. M. Prouty, J. D. Ballard, W. A. van der Donk, and S. R. Blanke.** 2008. Inhibition of *Bacillus anthracis* spore outgrowth by nisin. *Antimicrob Agents Chemother* **52**:4281-8.
13. **Hasper, H. E., N. E. Kramer, J. L. Smith, J. D. Hillman, C. Zachariah, O. P. Kuipers, B. de Kruijff, and E. Breukink.** 2006. An alternative bactericidal mechanism of action for lantibiotic peptides that target lipid II. *Science* **313**:1636-7.
14. **Hsu, S. T., E. Breukink, E. Tischenko, M. A. Lutters, B. de Kruijff, R. Kaptein, A. M. Bonvin, and N. A. van Nuland.** 2004. The nisin-lipid II complex reveals a pyrophosphate cage that provides a blueprint for novel antibiotics. *Nat Struct Mol Biol* **11**:963-7.
15. **Liu, W., and J. N. Hansen.** 1993. The antimicrobial effect of a structural variant of subtilin against outgrowing *Bacillus cereus* T spores and vegetative cells occurs by different mechanisms. *Appl Environ Microbiol* **59**:648-51.
16. **Liu, W., and J. N. Hansen.** 1992. Enhancement of the chemical and antimicrobial properties of subtilin by site-directed mutagenesis. *J Biol Chem* **267**:25078-85.
17. **Lubelski, J., R. Rink, R. Khusainov, G. N. Moll, and O. P. Kuipers.** 2008. Biosynthesis, immunity, regulation, mode of action and engineering of the model lantibiotic nisin. *Cell Mol Life Sci* **65**:455-76.
18. **Molinari, H., A. Pastore, L. Y. Lian, G. E. Hawkes, and K. Sales.** 1990. Structure of vancomycin and a vancomycin/D-Ala-D-Ala complex in solution. *Biochemistry* **29**:2271-7.
19. **Montville, T. J., T. De Siano, A. Nock, S. Padhi, and D. Wade.** 2006. Inhibition of *Bacillus anthracis* and potential surrogate bacilli growth from spore inocula by nisin and other antimicrobial peptides. *J Food Prot* **69**:2529-33.
20. **Morris, S. L., R. C. Walsh, and J. N. Hansen.** 1984. Identification and characterization of some bacterial membrane sulfhydryl groups which are targets of bacteriostatic and antibiotic action. *J Biol Chem* **259**:13590-4.
21. **Oman, T. J., and W. A. van der Donk.** 2009. Insights into the mode of action of the two-peptide lantibiotic haloduracin. *ACS Chem Biol* **4**:865-74.
22. **Parisot, J., S. Carey, E. Breukink, W. C. Chan, A. Narbad, and B. Bonev.** 2008. Molecular mechanism of target recognition by subtilin, a class I lanthionine antibiotic. *Antimicrob Agents Chemother* **52**:612-8.

23. **Rink, R., J. Wierenga, A. Kuipers, L. D. Kluskens, A. J. Driessen, O. P. Kuipers, and G. N. Moll.** 2007. Dissection and modulation of the four distinct activities of nisin by mutagenesis of rings A and B and by C-terminal truncation. *Appl Environ Microbiol* **73**:5809-16.
24. **Ruhr, E., and H. G. Sahl.** 1985. Mode of action of the peptide antibiotic nisin and influence on the membrane potential of whole cells and on cytoplasmic and artificial membrane vesicles. *Antimicrob Agents Chemother* **27**:841-5.
25. **Scott, V. N., and S. L. Taylor.** 1981. Effect of nisin on the outgrowth of *Clostridium botulinum* Spores. *J Food Sci* **46**:117-120.
26. **Sheldrick, G. M., P. G. Jones, O. Kennard, D. H. Williams, and G. A. Smith.** 1978. Structure of vancomycin and its complex with acetyl-D-alanyl-D-alanine. *Nature* **271**:223-5.
27. **Shi, Y., X. Yang, N. Garg, and W. A. van der Donk.** 2010. Production of Lantipeptides in *Escherichia coli*. *J Am Chem Soc*:10.1021/ja109044r.
28. **Stojkovic, B., E. M. Torres, A. M. Prouty, H. K. Patel, L. Zhuang, T. M. Koehler, J. D. Ballard, and S. R. Blanke.** 2008. High-throughput, single-cell analysis of macrophage interactions with fluorescently labeled *Bacillus anthracis* spores. *Appl Environ Microbiol* **74**:5201-10.
29. **Tiyanont, K., T. Doan, M. B. Lazarus, X. Fang, D. Z. Rudner, and S. Walker.** 2006. Imaging peptidoglycan biosynthesis in *Bacillus subtilis* with fluorescent antibiotics. *Proc Natl Acad Sci U S A* **103**:11033-8.
30. **Turnbull, P. C., N. M. Sirianni, C. I. LeBron, M. N. Samaan, F. N. Sutton, A. E. Reyes, and L. F. Peruski, Jr.** 2004. MICs of selected antibiotics for *Bacillus anthracis*, *Bacillus cereus*, *Bacillus thuringiensis*, and *Bacillus mycoides* from a range of clinical and environmental sources as determined by the Etest. *J Clin Microbiol* **42**:3626-34.
31. **Wiedemann, I., E. Breukink, C. van Kraaij, O. P. Kuipers, G. Bierbaum, B. de Kruijff, and H. G. Sahl.** 2001. Specific binding of nisin to the peptidoglycan precursor lipid II combines pore formation and inhibition of cell wall biosynthesis for potent antibiotic activity. *J Biol Chem* **276**:1772-9.

CHAPTER 4: CHARACTERIZATION OF NISIN-MEDIATED MEMBRANE DISRUPTION UTILIZING *BACILLUS ANTHRACIS* SPORES

4.1 Introduction

The ability of nisin to kill both bacterial spores and vegetative cells via membrane disruption or inhibition of cell wall biogenesis mediated through the interaction with lipid II (4, 7, 8) (chapters 2, 3) encouraged further mechanistic studies to characterize the interaction of nisin with the membrane of living organisms, specifically the membrane of germinated *Bacillus anthracis* spores. Previous studies utilizing *Bacillus* vegetative cells and artificial black lipids have identified that a nisin-mediated pore is generated measuring approximately 2 nm in diameter (18), that is slightly anion specific (9, 11), allows the flow of amino acids as well as ions through the pore (11), and eventually leads to lysis of the vegetative cell (2). However, similar studies have not been undertaken with bacterial spores, which structurally are quite different than vegetative cells with regards to membrane and extracellular structures such as the cell wall and the presence of a spore coat (5).

The data presented in this chapter demonstrates that nisin induced the flow of both ions and small molecules across the spore membrane. This flow can be blocked with either a blocker (DIDS) of protein channels or polyethylene glycol (PEG) units of appropriate size (3350 Da). These data indicate that within nisin-treated spores, known blockers of membrane channels of approximately 2 nm in diameter inhibit the movement of small molecules from the intracellular to extracellular environment. Furthermore, nisin-treated spores do not exhibit detectable membrane lysis. The lack of nisin induced lysis of spores would be

beneficial in the treatment of spore-mediated bacterial infections since the release of bacterial immuno-modulators such as peptidoglycan would not occur. Overall, these results support a model where, in contrast to previous reports of nisin-mediated cell lysis of vegetative bacilli, nisin kills germinated *B. anthracis* spores by membrane disruption, resulting in depolarization of the membrane and thereby preventing the establishment of productive metabolism that normally occurs during spore outgrowth. Ian Gut was primarily responsible for the design of these studies, data analysis and rendering, and writing this chapter. Paul E. Dilfer and Stephanie Czeschin, two undergraduate research associates supervised by Ian Gut, performed the experiments.

4.2 Results

4.2.1 Nisin induces the flow of ions across the spore membrane.

Previous studies have demonstrated that nisin treatment of spores resulted in the efflux of protons preventing the establishment of a membrane potential during spore germination (5, chapter 2). In studies utilizing *B. subtilis* bacilli, nisin induced the efflux of Rb^+ and Cl^- from vegetative bacteria (11). However, it was not clear whether larger molecular weight ions were also released from nisin-treated spores. To evaluate this possibility, *B. anthracis* Sterne 7702 spores were germinated in the presence of nisin. The release of K^+ or Cl^- were measured using the membrane impermeable dye indicators potassium binding fluorescent indicator tetraammonium salt, (PBFI), or 6-methoxy-*N*-(3-sulfopropyl)quinolinium (SPQ), respectively. Preliminary studies

confirmed that neither PBF1 nor SPQ inhibited spore germination, or reduced *B. anthracis* viability (Table 4.1). In addition, nisin did not alter the fluorescent properties of PBF1 or SPQ (Table 4.2). A significant increase in PBF1 fluorescence was detected when spores were incubated with 10 μ M nisin suggesting that nisin induced a detectable efflux of K^+ (Figure 4.1A). Likewise, a significant decrease in SPQ fluorescence was detected when spores were incubated with 10 μ M nisin, suggesting that nisin induced a detectable efflux of Cl^- (Figure 4.1B). As a positive control, 1% Triton X-100 induced efflux of both K^+ and Cl^- (data not shown). These data demonstrate that nisin-induced spore membrane disruption mediated the efflux of both cations and anions, which suggests the absence of ion selectivity.

Effect of indicator dyes on <i>B. anthracis</i> spore germination and viability		
	Spore germination ^a	Organism viability ^a
DiSBAC ₂ (3)	+	+
PBF1 ^b	+	+
PicoGreen ^{TM,b}	+	+
PrestoBlue ^{TM,b}	+	+
SPQ ^b	+	+
Vybrant TM Cytotoxicity Assay Kit ^b	+	+

Table 4.1. Effect of indicator dyes on *B. anthracis* spore germination and viability.

^a Spores (4.0×10^6) were cultured with brain heart infusion broth in the absence and presence of the phenotypic indicator. Germination initiation was scored as (+) if a significant loss in optical density at 600 nm was observed. Organism viability was scored as (+) if there was not a significant loss of recoverable CFU, quantified by dilution spot plating. +: germination occurred or organisms remained viable. -: germination was inhibited or organisms were no longer viable. ^b Concentration of the phenotypic indicators are listed in "Materials and Methods.

	Effects of channel blockers, polyethylene glycols, and nisin on phenotypic indicator fluorescence ^a			
	PBFI	PicoGreen TM	PrestoBlue TM	SPQ
DIDS ^b	-	-	-	↓
DPC ^b	-	-	-	-
TEA ^b	-	-	-	-
PEG-92 ^b	-	↑	-	-
PEG-600 ^b	-	-	-	-
PEG-3350 ^b	-	-	-	-
PEG-6000 ^b	-	-	-	-
PEG-20000 ^b	-	↑	-	-
nisin ^b	-	-	-	-

Table 4.2. Effects of channel blockers, polyethylene glycols, and nisin on phenotypic indicator fluorescence. ^a Phenotypic indicators were used at the concentration listed in "Materials and Methods" and were incubated with the channel blockers, polyethylene glycols, and nisin in the absence of spores for 30 min, and the fluorescence intensity was monitored spectrofluorometrically using a Biotek Synergy 2 fluorescence plate reader utilizing the appropriate excitation and emission filter sets. ^b Channel blockers, polyethylene glycols, and nisin at concentrations as described in "Culturing *B. anthracis* spores" were evaluated for their ability to alter phenotypic indicator fluorescence. ↑: increased fluorescence. -: did not alter fluorescence. ↓: decreased fluorescence.

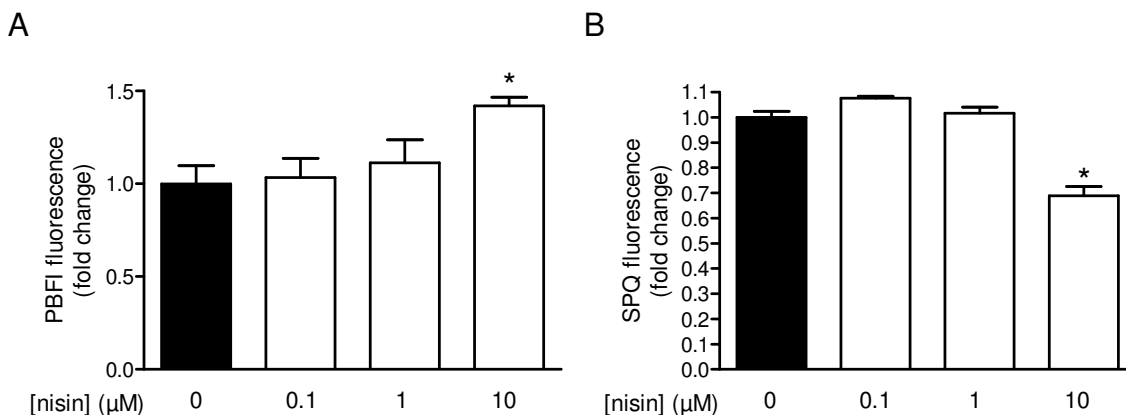


Figure 4.1. Nisin induced ion efflux from germinating spores. K^+ efflux (A) or Cl^- efflux (B) from spores in the absence or presence of nisin monitored as described in "Materials and Methods". The data are expressed as the fold fluorescence change at 20 min after the addition of nisin (0.1-10 μ M) relative to spores germinated in the absence of nisin. * indicates a $P < 0.05$ between control (0 μ M nisin, black) and experimental condition (0.1 - 10 μ M nisin, white). Error bars indicate standard deviations.

4.2.2 Nisin mediates small molecule movement across the spore membrane.

Previous studies with germinating spores or vegetative cells of *Bacillus* species have identified the influx of propidium iodide or efflux of amino acids (Lys, Glu, and Pro) upon the addition of nisin (5, 11). To further evaluate the movement of small molecules, PicoGreenTM influx was monitored. As a result of the absence of high-energy small molecules, ATP and NAD(P)H, and free amino acids within a dormant spore, the fluorescent DNA binding agent PicoGreenTM was used as a surrogate for small molecule movement. Initial experiments determined that PicoGreenTM did not inhibit spore germination or reduce viability (Table 4.1), and nisin did not alter the fluorescent properties of PicoGreenTM

(Table 4.2). When spores were germinated in the presence of nisin, a dose dependent PicoGreen™ staining of the spore DNA was observed with increasing concentrations of nisin (Figure 4.2). As a positive control, 1% Triton X-100 induced robust staining of spore DNA (data not shown). These data further supported the model that small molecules pass freely through the nisin perturbed spore membranes.

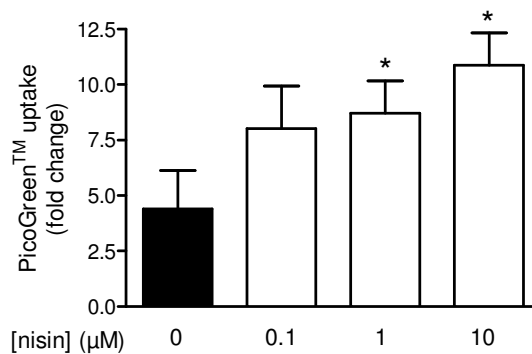


Figure 4.2. Nisin induced PicoGreen™ uptake. PicoGreen™ uptake as a function of nisin concentration was monitored as described under "Materials and Methods". The data are expressed as the fold fluorescence change at 20 min after the addition of nisin (0.1-10 μM) relative to dormant spores in the absence of nisin. * indicates a $P < 0.05$ between control (0 μM nisin, black) and experimental condition (0.1 - 10 μM nisin, white). Error bars indicate standard deviations.

4.2.3 Nisin does not induce spore lysis.

Previous studies reported that vegetative *B. subtilis* were lysed in the presence of nisin (2), resulting in the loss of optical density of actively replicating cultured bacteria with nisin treatment. However, our studies to evaluate whether nisin induces membrane lysis of germinated *B. anthracis* spores revealed that

nisin-dependent membrane perturbation did not result in the release of glucose-6-phosphate dehydrogenase (G6PD) (Figure 4.3) or DNA (Figure 4.4). In contrast, extracellular G6PD was detected in samples incubated with Triton X-100 (Figure 4.3). Preliminary experiments indicated that the reagents in the Vybrant™ cytotoxicity assay kit (i.e. G6PD release) did not inhibit germination, or reduce *B. anthracis* viability (Table 4.1). Likewise, extracellular DNA from *B. anthracis* spores was detected in the presence of TritonX-100, but not nisin (Figure 4.4). These data support a model that spores undergo membrane perturbation resulting in the release of small molecular compounds, but not high molecular weight macromolecules, consistent with the formation of a pore.

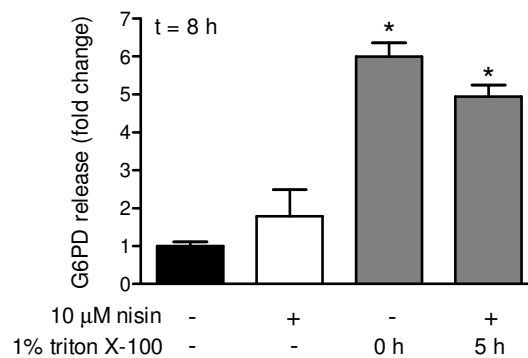


Figure 4.3. Nisin does not induce G6PD release. The effect of nisin on G6PD release as a function of membrane disruption was monitored as described in "Materials and Methods". The data are expressed as the fold fluorescence change at 8 h after the addition of nisin (10 μM, white) or 1% Triton X-100 at indicated time points relative to spore germinated in the absence of nisin. * indicates a $P < 0.05$ between control (0 μM nisin and 0% Triton X-100, black) and experimental condition (1% Triton X-100, gray). Error bars indicate standard deviations.

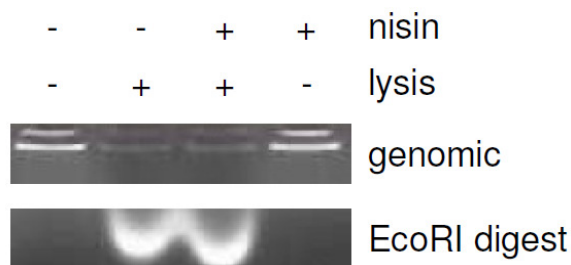


Figure 4.4. Nisin does not induce DNA release. Agarose gel of spores germinated in the absence and presence of 10 μ M nisin and processed as described in "Materials and Methods". Only those samples that were treated with the lysis cocktail (see Materials and Methods) and boiled produced an EcoRI banding pattern indicating DNA release. The presence of a genomic band indicates the lack of DNA release from the spore. +: 10 μ M nisin or lysed samples. -: 0 μ M nisin or non-lysed samples.

4.2.4 Nisin renders the germinating spore metabolically inactive.

Results presented in chapter 2 indicated that the development of oxidative metabolism in germinated spores is inhibited in the presence of nisin. However, monitoring the conversion of a tetrazolium substrate to formazan is explicitly an endpoint assay that possesses limited sensitivity while being highly hazardous as a result of formazan production. The use of PrestoBlueTM as a fluorescence indicator of oxidative metabolism facilitates both endpoint and kinetic assays that are highly sensitive without the production of a toxic product. *B. anthracis* spores were germinated in the presence of PrestoBlueTM with increasing concentrations of nisin (0-10 μ M), and a dose-dependent reduction of oxidative metabolism was observed (Figure 4.5). This result confirmed previous results (chapter 2) and provided an additional highly sensitive assay to evaluate the effectiveness of channel blockers to alleviate nisin inhibition of oxidative metabolism establishment.

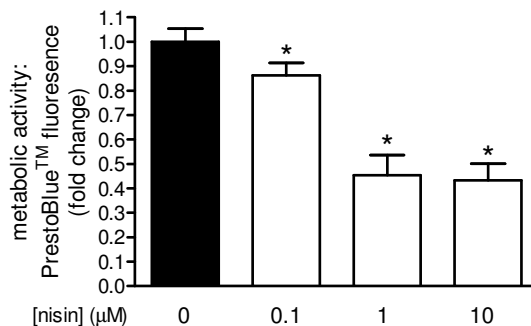


Figure 4.5. Nisin prevents the establishment of an oxidative metabolism. The effect of nisin on metabolism establishment as a function of membrane disruption was monitored as described in "Materials and Methods". The data are expressed as the fold fluorescence change at 90 min after the addition of nisin (0.1-10 μM) relative to spores germinated in the absence of nisin. * indicates a p-value < 0.05 between control (0 μM nisin, black) and experimental condition (0.1 - 10 μM nisin, white). Error bars indicate standard deviations.

4.2.5 Blocking nisin-mediated membrane disruption with ionic channel inhibitors.

The finding that, in the presence of nisin, small molecules, but not macromolecules, are released from spores into the extracellular environment suggests that nisin alters the membrane barrier in a limited fashion. Notably, nisin was previously reported to form ion-conducting channels (approximately 2 nm diameter) in artificial membranes (18), but it is not clear whether or not nisin forms similar channels within the membrane of spores.

To evaluate the requirements for nisin-dependent efflux of ions from germinated spores, it was investigated whether known protein ion channel blockers might alter nisin-mediated ion movement out of germinated spores. The cationic blocker, tetraethylammonium (TEA), and, the anionic blockers,

isothiocyanatostilbene-2,2'-disulfonate (DIDS), and diphenylamine-2-carboxylic acid (DPC), were evaluated for their ability to alter the movement of ions and small molecules in the presence of nisin. In eukaryotic cell biology, these channel blockers have been demonstrated to block transmembrane ion channels. Specifically, TEA is used to block K⁺ channels (6) while DIDS and DPC have been used as nonspecific and voltage gated Cl⁻ channel blockers (3, 14, 15). These blockers were chosen to determine ion selectivity as well as size (Table 4.3). It must be pointed out that these blockers are not validated channel inhibitors for a nisin-induced pore, and there was no expectation that any of these compounds would cause a complete block of nisin-mediated ion efflux. In initial experiments, it was determined that none of the channel blockers inhibited germination or reduced *B. anthracis* viability (Table 4.3). DIDS displayed a quenching effect of SPQ; however, this effect did not affect accurate interpretation of results (Table 4.2). When evaluating the blocker effects on K⁺ release upon nisin addition, both TEA and DIDS exhibited a significant reduction in K⁺ release (Figure 4.6A, Table 4.3). However, only DIDS blocked Cl⁻ release (Figure 4.6C, Table 4.3) and PicoGreenTM influx (Figure 4.6E, Table 4.3) and a very small but statistically significant increase in oxidative metabolism (Figure 4.7A). Utilizing a concentration of DIDS just below its cytotoxic level (1000 μM) increased the inhibition of small molecule and ion movement across the membrane (Figure 4.6 B, D, F) while further enhancing the establishment of oxidative metabolism (Figure 4.7B). With an assumed stoichiometry of 1:1 of DIDS per nisin-induced membrane disruption, these data suggest that nisin

perturbation of the spore created a potential pore that was greater than 1 nm in diameter and was slightly anion selective since only DIDS, with a linear length of 1.3 nm, was able to alter the transmembrane flow of K⁺, Cl⁻, and PicoGreen™.

	Ion selectivity	Linear length (nm) ^b	Spore germination ^c	Organism viability ^c	Channel blocker inhibition of the phenotypic event as a function of nisin pore formation ^a					
					Metabolism establishment ^d	Cl ⁻ efflux ^d	K ⁺ efflux ^d	Pico-Green influx ^d	Out-growth ^d	Spore killing ^d
DIDS	anion	1.3	+	+	+	+	+	+	-	-
DPC	anion	1.0	+	+	-	-	-	-	-	-
TEA	cation	0.7	+	+	-	-	+	-	-	-

Table 4.3. Channel blocker inhibition of the listed phenotypic event as a function of nisin pore formation. ^a Nisin inhibits spore outgrowth and survival through pore formation that mediates the efflux and influx of small molecules and ions. These phenotypic events of spore germination were monitored in the presence of channel blockers (concentration indicated in "Culturing *B. anthracis* spores"). ^b An energy minimized structure was created and maximal lengths were determined utilizing ChemDraw Ultra (CambridgeSoft, Chambridge, MA). ^c Spores were cultured with brain heart infusion broth in the absence and presence of the channel blockers. Germination initiation was observed as a loss in optical density at 600 nm as a result of spore hydration. Effects on *B. anthracis* were determined by monitoring viable organisms quantified by dilution spot plating. +: germination occurred or organisms remained viable. -: germination was inhibited or organisms were no longer viable. ^d Nisin prevented membrane potential and metabolism establishment and growth while facilitating the flow of small molecules and ions across the membrane. Channel blockers were evaluated for their ability to prevent the events associated with nisin inhibition. +: blocked nisin associated phenotype. -: retained nisin associated phenotype.

Figure 4.6

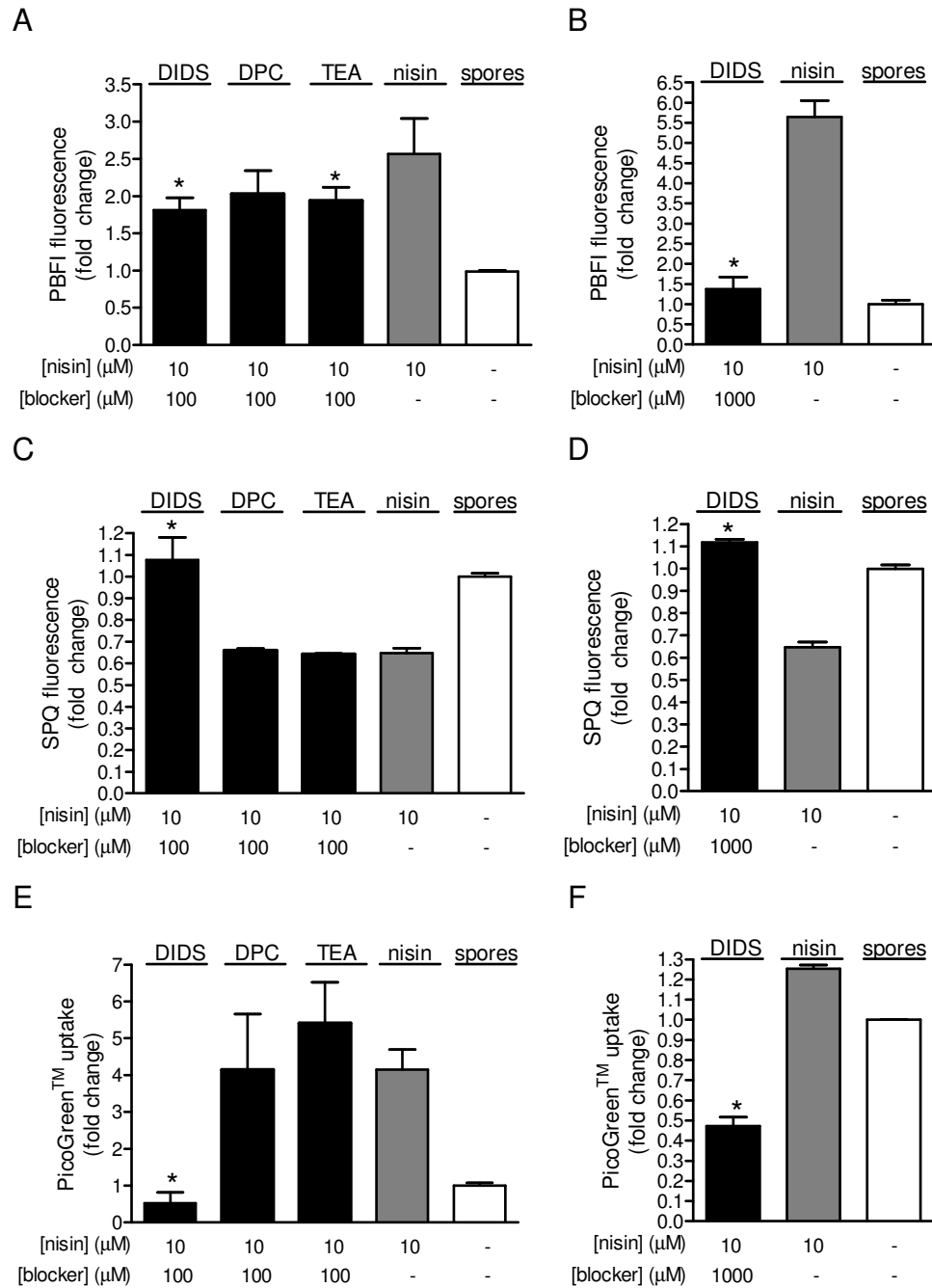


Figure 4.6. DIDS blocks nisin-mediated ion and small molecule movement across the spore membrane. The effect of ionic channel blockers on nisin induced K^+ efflux (A, B), Cl^- efflux (C, D), and PicoGreen™ influx (E) was monitored as described in "Materials and Methods". The data are expressed as the fold fluorescence change at 20 min after the addition of nisin (10 μM) relative to spores germinated in the absence of nisin and with the indicated ionic blocker. *

Figure 4.6 (continued)

indicates a $P < 0.05$ between nisin treated (10 μM nisin, gray) and experimental condition (100 μM ionic blocker and 10 μM nisin, black). Error bars indicate standard deviations.

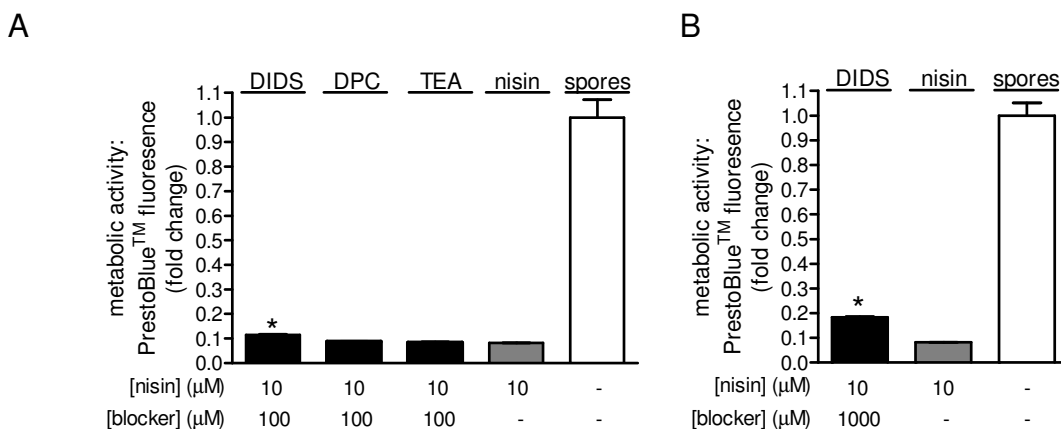


Figure 4.7. DIDS reduced nisin inhibition of oxidative metabolism. The effect of ionic

channel blockers on nisin inhibition of metabolism establishment was monitored as described in "Materials and Methods". A. Comparison of channel blockers at 100 μM . B. DIDS activity against nisin at highest non-cytotoxic concentration, 1000 μM . The data are expressed as the fold fluorescence change at 90 min after the addition of nisin (10 μM) relative to spore germinated in the absence of both nisin and with the indicated ionic blocker. * indicates a $P < 0.05$ between nisin treated (10 μM nisin, gray) and experimental condition (100 μM ionic blocker and 10 μM nisin, black). Error bars indicate standard deviations.

4.2.6 Blocking nisin-mediated membrane disruption with PEGs.

The above results provide insight into ion selectivity for nisin-induced membrane disruption. Experiments were then conducted to determine a more accurate measure of a presumed nisin-induced pore within the spore membrane utilizing polyethylene glycol chains (PEGs) of increasing size to measure the diameter of the pore. Previous studies have identified the intrinsic hydrodynamic radii for PEG-92, 600, 3350, 6000, and 20000 m.w (Table 4.4), and PEGs have

been used in biophysics to measure the diameter of transmembrane protein ion channels (1). PEGs that are either too large or too small will not appropriately fill the nisin pore allowing the flow of ions or small molecules while PEGs of the approximate size of the disruption will fill the membrane perturbation and block ion and small molecule movement. It must be pointed out that PEGs are not validated channel inhibitors for nisin-induced pores and are general pore sizing agents (1), which may result in incomplete or partial blocking of nisin activity. However, they will provide insights into the characteristics of nisin-mediated membrane disruption. PEG-600, 3350, and 6000 displayed the most significant reduction of K^+ efflux (Figure 4.8A, Table 4.4) while only PEG-3350 reduced the efflux of Cl^- (Figure 4.8B, Table 4.4). Additionally, PEG-3350 and 6000 were able to prevent the uptake of PicoGreenTM (Figure 4.8C, Table 4.4). PEG-92 and 20000 could not be used with the PicoGreenTM uptake assay because these PEGs altered PicoGreenTM fluorescence preventing accurate results (Table 2.2). It is presumed that the inability of PEG-600 and 6000 to block nisin-induced Cl^- efflux is a function of inappropriate size. However, charge potentially aided PEG-600 and 6000 in the blocking of K^+ efflux through the interaction of K^+ with oxygen's lone pairs of electrons present in the repeating glycol unit of PEGs. This would potentially create an artificial blocking of K^+ efflux. PEG-6000 can effectively prevent PicoGreenTM uptake despite an improper size of PEG-6000 for appropriate disruption blockage. The substantially increased size of the small molecule PicoGreenTM as compared to an ion facilitates a disruption blocking phenotype. None of the PEGs were able to enhance oxidative metabolism

establishment, which may be a function of their lack of specificity or ion selectivity (Figure 4.9). These results with the ion channel blocker suggest that the nisin-induced membrane disruption has a diameter of 1.0 - 2.5 nm, which is congruent with previous electrophysiology results of nisin-mediated interactions with black lipids (18).

Table 4.4

	Hydrodynamic radius (nm) ^b	Spore germination ^c	Organism viability ^c	PEG inhibition of the phenotypic event as a function of nisin pore formation ^a					
				Metabolism establishment ^d	Cl ⁻ efflux ^d	K ⁺ efflux ^d	Pico-Green influx ^{d,e}	Out-growth ^d	Spore killing ^d
PEG-92	0.31	+	+	-	-	-	N/A	-	-
PEG-600	0.78	+	+	-	-	+	-	-	-
PEG-3350	1.63	+	+	-	+	+	+	-	-
PEG-6000	2.50	+	+	-	-	+	+	-	-
PEG-20000	3.21	+	+	-	-	-	N/A	-	-

Table 4.4. PEG inhibition of the several phenotypic events as a function of nisin membrane disruption. ^a Nisin inhibits spore outgrowth and survival through membrane disruption that mediates the efflux and influx of small molecules and ions. These phenotypic events were monitored in the presence of 1% PEGs with increasing lengths. ^b Hydrodynamic radius of PEGs were previously reported by V.F. Antonov, et al. (1). ^c Spores were cultured with brain heart infusion broth in the absence and presence of the PEGs. Germination initiation was observed as a loss in optical density at 600 nm as a result of spore hydration. Effects on *B. anthracis* were determined by monitoring viable organisms quantified by dilution spot plating. +: germination occurred or organisms remained viable. -: germination was inhibited or organisms were no longer viable. ^d Nisin prevented membrane potential and metabolism establishment and growth while facilitating the flow of small molecules and ions across the membrane. PEGs were evaluated for their ability to prevent the events associated with nisin inhibition. +: blocked nisin associated phenotype. -: retained nisin associated phenotype. ^e PicoGreenTM fluorescence was affected by

Table 4.4 (continued)

the addition of PEG-92 and 20000 to the extent that the date was no longer accurate. PEG effects on PicoGreen™ have been documented previously, <http://probes.invitrogen.com/media/pis/mp07581.pdf>.

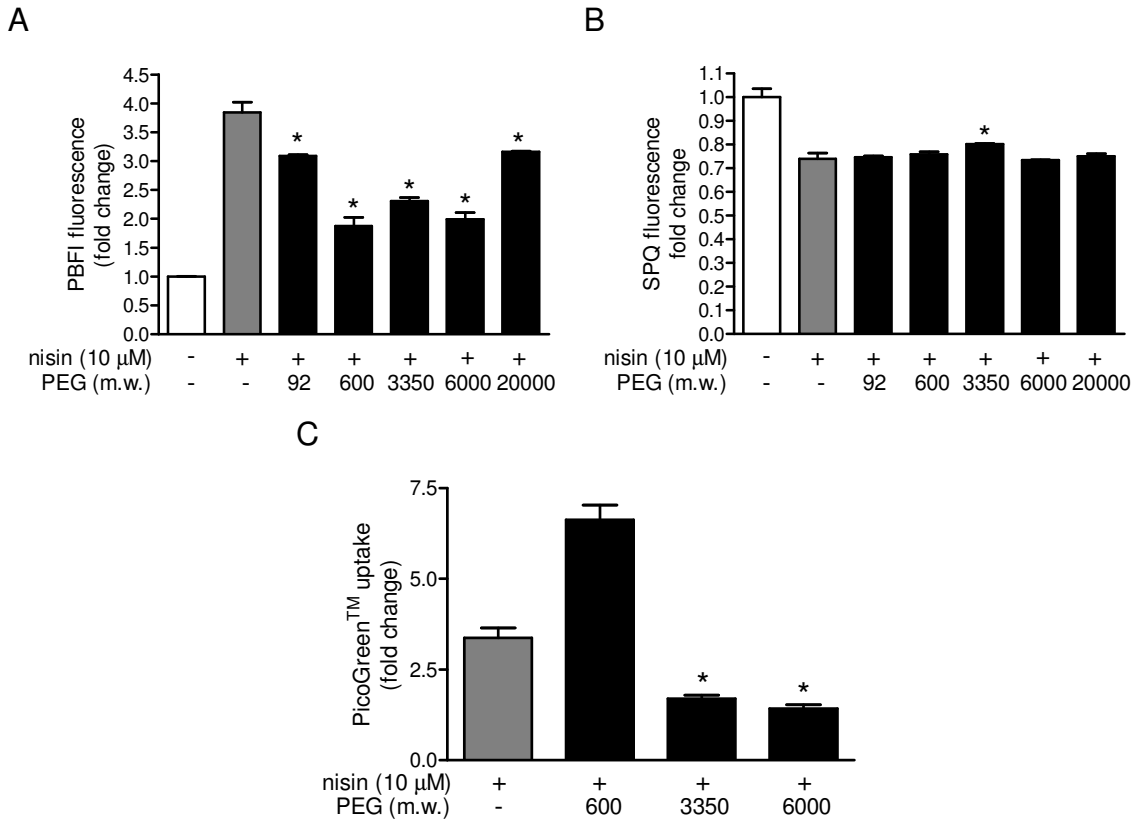


Figure 4.8. PEGs block nisin-mediated ion and small molecule movement across the spore membrane. The effect of PEGs on nisin induced K^+ efflux (A), Cl^- efflux (B), and PicoGreen™ influx was monitored as described in "Materials and Methods". A,B. The data are expressed as the fold fluorescence change at 20 min after the addition of nisin (10 μM) relative to spore germinated in the absence of nisin and with the indicated PEG. C. The data are expressed as the fold fluorescent change at 20 min after the addition of nisin (10 μM) relative to dormant spores in the absence of nisin and with the indicated PEG. * indicates a $P < 0.05$ between nisin treated (10 μM nisin, gray) and experimental condition (1% μM PEG and 10 μM nisin, black). Error bars indicate standard deviations.

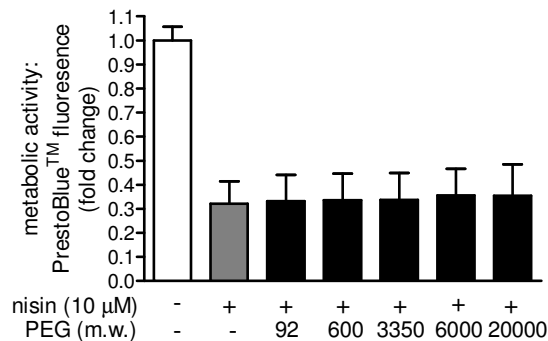


Figure 4.9. PEGs did not reduce nisin inhibition of oxidative metabolism. The effect PEGs on nisin inhibition of metabolism establishment was monitored as described in "Materials and Methods". The data are expressed as the fold fluorescence change at 90 min after the addition of nisin (10 μM) relative to spore germinated in the absence of nisin and with the indicated PEG. * indicates a $P < 0.05$ between nisin treated (10 μM nisin, gray) and experimental condition (1% μM PEG and 10 μM nisin, black). Error bars indicate standard deviations.

4.2.7 Blocking the nisin pore does not alter spore viability or outgrowth.

As result of the minimal increase in metabolic activity afforded to germinating spores by charged channel blockers and PEGs in the presence of nisin (Figure 4.7, 4.9), these molecules were evaluated for their ability to promote spore outgrowth and viability. The addition of ionic channel blockers and PEGs to spores germinated in the presence of nisin neither promoted spore outgrowth (Table 4.3, 4.4) nor increased spore viability (Figure 4.10, Table 4.3, 4.4). The blocking effects of either molecule type were not sufficient to aid *B. anthracis* spores against the membrane disrupting effects of nisin that result in outgrowth inhibition.

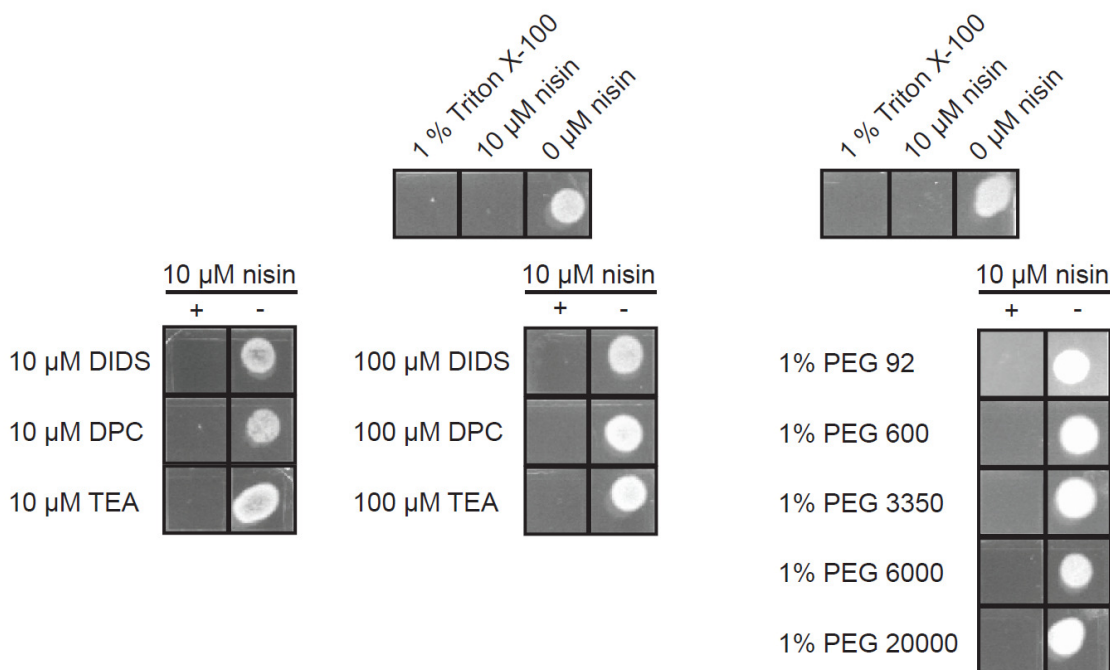


Figure 4.10. Channel blockers and PEGs do not increase *B. anthracis* viability in the presence of nisin. The effect PEGs and ionic blockers on nisin inhibition *B. anthracis* viability was monitored as described in "CFU quantification". Spores were germinated for 30 min in the presence of nisin, PEGs, ionic blockers, and Triton X-100 (control) at indicated concentrations followed by spot blot quantification of viable *B. anthracis*. +: indicates the presence of 10 μM nisin within cultures. -: indicates the absence of 10 μM nisin within cultures.

4.3. Discussion

The studies described in previous chapters identified membrane disruption and lipid II binding as the mechanism and target, respectively, for the inhibition of *B. anthracis* spore outgrowth. However, few insights into the characteristics of membrane disruption were determined. Previous research identified that the nisin-induced pore in vegetative cells was slightly anion selective and allowed the efflux of amino acid and ions across the membrane of *B. subtilis* vegetative cells (9, 11). Moreover, electrophysiology measurements of nisin pores in artificial

membranes demonstrated a 2 nm nisin-induced pore (18). The research present in this chapter builds on these studies by suggesting that nisin membrane disruption induces pore formation that is slightly anion selective and approximately 1.0 - 2.5 nm diameter within a spore membrane, which is congruent with previous studies (9, 11, 18).

Of particular interest is that nisin inhibition does not mediate spore lysis (Figure 4.3, 4.4), which is different from the lysis observed with nisin treatment of vegetative cells (2). This phenotype is beneficial when treating *B. anthracis* spore infections preventing the release of spore derived immuno-modulatory agents such as microbial membrane components, toxins, and peptidoglycan. This phenotype would limit the chances of septicemia or toxemia as well as a potential detrimental inflammatory response (5, 16, 17).

Spores are devoid of high energy compounds such as ATP and NAD(P)H (12). However, spores contain significant ADP stores in addition to free amino acids in the later stages of germination as a result of protein degradation (10). Unfortunately, spores are highly intractable particles, which necessitate the use of surrogate indicators to characterize what molecules flow across the spore membrane upon nisin treatment. Several assays were developed utilizing tools from eukaryotic cell biology to monitor ion and small molecule flux as well as metabolism establishment that are both sensitive and non-hazardous. These assays helped to identify that nisin mediates the efflux of anions and cations as well as small molecules across the membrane to collapse ion gradients across the microbial membrane. The uptake of propidium iodide (chapter 2) and

PicoGreen™ in the presence of nisin strongly suggests small molecules such as ADP and amino acids will freely flow from the germinating spore further preventing spore viability. The use of channel blockers and PEGs, which was borrowed from membrane channel cell biology, provided an approach to characterize the selectivity and diameter of the nisin membrane and suggest pore formation within a spore membrane. Despite the increase in metabolic activity in addition to reducing the flow of small molecules and ions particularly afforded by DIDS, none these blockers were able to increase viability and outgrowth of the spore. These results speak to the robust microbial killing properties of nisin and provide impetus for studying how nisin alters spore infections both *in vitro* and *in vivo* as well as investigating the properties of other pore-forming antimicrobials similar to nisin, particularly linear and two component lantibiotics.

4.4 Materials and Methods

4.4.1 Spore preparations.

Spores were prepared from *B. anthracis* Sterne 7702, as described previously (13). Enumeration of spores was performed using a Petroff-Hauser hemocytometer under a light microscope at 400x magnification (Nikon Alphaphot YS, Mellville, NY). A typical spore preparation yielded 10 mL of spores at a concentration of 2.0×10^9 spores/mL.

4.4.2 Nisin purification.

Nisin was purified and characterized as described previously (5).

4.4.3 Culturing *B. anthracis* spores.

B. anthracis Sterne 7702 spores at a concentration of 4.0×10^6 spores/mL were incubated in brain heart infusion medium (BHI; BD Bioscience San Jose, CA) or 10 mM L-Alanine (Sigma) and L-Inosine (Sigma) supplemented with nisin (1 or 10 μ M), 4,4'-di-isothiocyanatostilbene-2,2'-disulfonate (DIDS; 1, 10, 100, or 1000 μ M; Sigma), diphenylamine-2-carboxylic acid (DPC; 1, 10, or 100 μ M; Sigma), tetraethylammonium (TEA; 1, 10, or 100 μ M; Sigma), polyethylene glycol (PEG; 1 % 600, 3350, 6000, or 20000 MW, Sigma), 1 % Triton X-100 (Lysis buffer; Fisher Chemical, Fairlawn, NJ), or with 0.1 M 3-(N-morpholino)propanesulfonic acid (MOPS; Sigma) at pH 6.8 as a control. For non-germinating conditions, 0.1 M MOPS (pH 6.8) was substituted for BHI medium. All incubations were performed at 37 °C under aeration at 180 rpm on a rotary shaker (Thermo Fisher Scientific Inc., Waltham, MA) and under ambient CO₂.

4.4.4 CFU quantification.

Spores were serially diluted and spread plated or spot blotted on Luria-Bertani (LB; B10 g/L Bacto Tryptone, 5 g/L NaCl, 5 g/L Bacto Yeast Extract, 15 g/L Bacto Agar; BD Biosciences) agar plates. After 12-18 h at 37 °C *B. anthracis* colonies were counted, from which CFU/mL were calculated.

4.4.5 Spore hydration.

The hydration of spores was determined by measuring the loss of spore refractility at 600 nm by using a Synergy 2 plate reader (BioTek Instruments, Inc., Winooski, VT). *B. anthracis* spores were incubated, as described under "Culture of *B. anthracis* spores," except that a 96-well plate was used and the plate was shaken for 15 s prior to each read. The data are presented as a percentage of the OD₆₀₀ at each time point relative to the OD₆₀₀ of the spore suspensions at the beginning of the experiment (time zero).

4.4.6 Heat resistance.

Spores were diluted into 0.1 M MOPS pH 6.8 containing D-alanine and D-histidine (both at 10 mM; Sigma, St. Louis, MO), to prevent further germination initiation of dormant spores, and identical aliquots were incubated at either 65 °C or on ice for 30 min. Viable *B. anthracis* were quantified by plating serial dilutions and enumerating CFU. The percentage of heat resistant spores was calculated by dividing CFU recovered from samples heated at 65 °C by CFU recovered from samples incubated on ice.

4.4.7 Oxidative metabolism.

B. anthracis spores were incubated, as described under "Culturing *B. anthracis* spores," except for the presence of a oxidative metabolism indicator, PrestoBlue™ (PB; 1 x; Invitrogen). PB fluorescence occurs upon the establishment of an oxidative metabolism, specifically an active TCA cycle.

Spore suspension fluorescence was monitored spectrofluorometrically using a Biotek Synergy 2 fluorescence plate reader exciting via a Tungsten Halogen SQ Xenon Flashbulb utilizing a bandpass filter at 540/25 nm and measuring the fluorescence emission through a bandpass filter at 590/20 nm.

4.4.8 Membrane integrity.

B. anthracis spores were incubated, as described under “Culturing *B. anthracis* spores,” except for the presence of a fluorescent membrane impermeable dye PicoGreen® (PG; 1 x; Invitrogen). PG fluorescence occurs upon DNA binding resulting from membrane disruption. *B. anthracis*-associated fluorescence was monitored spectrofluorometrically using a Biotek Synergy 2 fluorescence plate reader (Winooski, VT) exciting via a Tungsten Halogen SQ Xenon Flashbulb utilizing a bandpass filter at 485/20 nm and measuring the fluorescence emission through a bandpass filter at 528/20 nm.

4.4.9 Potassium release.

B. anthracis spores were incubated, as described under “Culturing *B. anthracis* spores,” except for the presence of a membrane impermeable potassium binding fluorescent indicator tetraammonium salt (PBFI; 1 µM; Invitrogen). PBFI fluorescence occurs upon K⁺ binding within the extracellular medium resulting from membrane disruption. Medium fluorescence was monitored spectrofluorometrically using a Biotek Synergy 2 fluorescence plate reader exciting via a Tungsten Halogen SQ Xenon Flashbulb utilizing a bandpass

filter at 360/40 nm and measuring the fluorescence emission through a bandpass filter at 508/20 nm.

4.4.10 Chloride release.

B. anthracis spores were incubated, as described under “Culturing *B. anthracis* spores,” except for the presence of a membrane impermeable fluorescent Cl⁻ indicator, 6-methoxy-*N*-(3-sulfopropyl)quinolinium (SPQ; 0.5 μM; Invitrogen). SPQ fluorescence is quenched upon Cl⁻ binding within the extracellular medium resulting from membrane disruption. Medium fluorescence was monitored spectrofluorometrically using a Biotek Synergy 2 fluorescence plate reader exciting via a Tungsten Halogen SQ Xenon Flashbulb utilizing a bandpass filter at 360/40 nm and measuring the fluorescence emission through a bandpass filter at 460/40 nm.

4.4.11 Cell lysis - glucose-6-phosphate dehydrogenase (G6PD) release.

B. anthracis spores were incubated, as described under “Culturing *B. anthracis* spores,” except for the presence of the membrane impermeable reagents of the Vybrant™ Cytotoxicity Assay Kit (2.0 mM resazurin, 1 x reaction mixture - diaphorase, glucose-6-phosphate, and NADP⁺; Invitrogen) to monitor G6PD release via an enzyme coupled assay according to manufacturers protocols. Fluorescence occurs upon G6PD release into the extracellular medium resulting from membrane disruption. Medium fluorescence was monitored spectrofluorometrically using a Biotek Synergy 2 fluorescence plate

reader exciting via a Tungsten Halogen SQ Xenon Flashbulb utilizing a bandpass filter at 540/25 nm and measuring the fluorescence emission through a bandpass filter at 590/20 nm.

4.4.12 Cell lysis - DNA release.

B. anthracis spores were incubated, as described under “Culturing *B. anthracis* spores.” Germinated spore suspensions were split into equal volumes and washed twice with 1 x PBS. One set of spores, 0 and 10 μ M nisin present during germination, were resuspended in with 1 x PBS and kept on ice. The second set of spores, 0 and 10 μ M nisin present during germination, were resuspended in 4% sodium dodecyl sulfate (SDS, Fisher Chemical), 0.04% Triton X-100, and 0.01 M dithiothreitol (DTT, Fisher Chemical), and boiled for 30 min. All samples were cooled to 4 $^{\circ}$ C on ice for 15 min, and EcoRI buffer (New England Biolabs, Ipswich, MA) was added at a ratio of 5 μ L per 255 μ L total volume and mixed. EcoRI was added at a ratio of 1 μ L per 256 μ L total volume, mixed, and incubated at 37 $^{\circ}$ C for 1 h. DNA digestion was visualized utilizing 1 % agarose gel electrophoresis and staining with ethidium bromide (Fisher Chemical).

4.4.13 Statistics.

All data are representative of those from three or more independent experiments. Error bars represent standard deviations. *P* values were calculated with Student's *t* test using paired, one tailed distribution. *P* values of <0.05

indicate statistical significance. All statistics, including means, standard deviations, and Student's *t* tests, were calculated using Microsoft Excel (version 11.0).

4.5 References

1. **Antonov, V. F., E. Y. Smirnova, A. A. Anosov, V. P. Norik, and O. Y. Nemchenko.** 2008. PEG Blocking of Single Pores Arising on Phase Transitions in Unmodified Lipid Bilayers. *Biophysics* **53**:390-395.
2. **Bauer, R., and L. M. Dicks.** 2005. Mode of action of lipid II-targeting lantibiotics. *Int J Food Microbiol* **101**:201-16.
3. **Breuer, W.** 1990. Reconstitution of a kidney chloride channel and its identification by covalent labeling. *Biochim Biophys Acta* **1022**:229-36.
4. **Breukink, E., I. Wiedemann, C. van Kraaij, O. P. Kuipers, H. Sahl, and B. de Kruijff.** 1999. Use of the cell wall precursor lipid II by a pore-forming peptide antibiotic. *Science* **286**:2361-4.
5. **Gut, I. M., A. M. Prouty, J. D. Ballard, W. A. van der Donk, and S. R. Blanke.** 2008. Inhibition of *Bacillus anthracis* spore outgrowth by nisin. *Antimicrob Agents Chemother* **52**:4281-8.
6. **Hallows, K. R., J. E. McCane, B. E. Kemp, L. A. Witters, and J. K. Foskett.** 2003. Regulation of channel gating by AMP-activated protein kinase modulates cystic fibrosis transmembrane conductance regulator activity in lung submucosal cells. *J Biol Chem* **278**:998-1004.
7. **Hasper, H. E., N. E. Kramer, J. L. Smith, J. D. Hillman, C. Zachariah, O. P. Kuipers, B. de Kruijff, and E. Breukink.** 2006. An alternative bactericidal mechanism of action for lantibiotic peptides that target lipid II. *Science* **313**:1636-7.
8. **Hsu, S. T., E. Breukink, E. Tischenko, M. A. Lutters, B. de Kruijff, R. Kaptein, A. M. Bonvin, and N. A. van Nuland.** 2004. The nisin-lipid II complex reveals a pyrophosphate cage that provides a blueprint for novel antibiotics. *Nat Struct Mol Biol* **11**:963-7.
9. **Moll, G. N., G. C. Roberts, W. N. Konings, and A. J. Driessen.** 1996. Mechanism of lantibiotic-induced pore-formation. *Antonie Van Leeuwenhoek* **69**:185-91.

10. **Paidhungat, M., and P. Setlow.** 2002. Spore Germination and Outgrowth, p. 537-548. *In* A. L. Sonenshein, J. A. Hoch, and R. Losick (ed.), *Bacillus subtilis* and Its Closest Relatives from Genes to Cells. American Society for Microbiology, Washington, D.C.
11. **Ruhr, E., and H. G. Sahl.** 1985. Mode of action of the peptide antibiotic nisin and influence on the membrane potential of whole cells and on cytoplasmic and artificial membrane vesicles. *Antimicrob Agents Chemother* **27**:841-5.
12. **Setlow, P.** 2006. Spores of *Bacillus subtilis*: their resistance to and killing by radiation, heat and chemicals. *J Appl Microbiol* **101**:514-25.
13. **Stojkovic, B., E. M. Torres, A. M. Prouty, H. K. Patel, L. Zhuang, T. M. Koehler, J. D. Ballard, and S. R. Blanke.** 2008. High-throughput, single-cell analysis of macrophage interactions with fluorescently labeled *Bacillus anthracis* spores. *Appl Environ Microbiol* **74**:5201-10.
14. **Sunose, H., K. Ikeda, Y. Saito, A. Nishiyama, and T. Takasaka.** 1993. Nonselective cation and Cl channels in luminal membrane of the marginal cell. *Am J Physiol* **265**:C72-8.
15. **Thinnes, F. P., A. Schmid, R. Benz, and N. Hilschmann.** 1990. Studies on human porin. III. Does the voltage-dependent anion channel "Porin 31HL" form part of the chloride channel complex, which is observed in different cells and thought to be affected in cystic fibrosis? *Biol Chem Hoppe Seyler* **371**:1047-50.
16. **Tournier, J. N., A. Quesnel-Hellmann, A. Cleret, and D. R. Vidal.** 2007. Contribution of toxins to the pathogenesis of inhalational anthrax. *Cell Microbiol* **9**:555-65.
17. **Tournier, J. N., R. G. Ulrich, A. Quesnel-Hellmann, M. Mohamadzadeh, and B. G. Stiles.** 2009. Anthrax, toxins and vaccines: a 125-year journey targeting *Bacillus anthracis*. *Expert Rev Anti Infect Ther* **7**:219-36.
18. **Wiedemann, I., R. Benz, and H. G. Sahl.** 2004. Lipid II-mediated pore formation by the peptide antibiotic nisin: a black lipid membrane study. *J Bacteriol* **186**:3259-61.

CHAPTER 5: *BACILLUS ANTHRACIS* SPORE INTERACTIONS WITH MAMMALIAN CELLS: EFFECTS OF MEDIUM COMPOSITION ON THE OUTCOME OF AN *IN VITRO* INFECTION²

5.1 Introduction

Inhalational anthrax commences with the deposition of *Bacillus anthracis* spores into the bronchioalveolar spaces of the lungs, and culminates with the systemic dissemination of vegetative bacilli within the host (10, 15, 49). Within the lungs, internalization of dormant spores, possibly by several different types of host cells, is believed to be a key step for initiating the transition from the localized to disseminated stages of infection. Alveolar macrophages are reported to transport spores out of the lungs to regional lymph nodes (7, 8, 24, 44). Dendritic cells have also been implicated in the rapid carriage of spores to the draining lymph nodes (5, 47). Finally, alveolar epithelial cells have recently been demonstrated to internalize spores both *in vitro* and *in vivo* (39-41), and have been proposed to facilitate the transcytosis of *B. anthracis* across the epithelial barrier. Taken together, these findings suggest that *B. anthracis* may escape the lungs by several distinct mechanisms.

To characterize the interaction of *B. anthracis* spores with host cells during the early stages of inhalational anthrax, *in vitro* models of infection have been widely implemented (5, 9, 18-20, 26, 28, 36, 37, 42, 51). The tractability of *in vitro* models has facilitated new insights into the molecular and cellular basis of spore binding and uptake, as well as host cell responses. Nonetheless, the use of *in vitro* models has resulted in a striking lack of consensus as to the responses and

² Reproduced in part with permission from: " *Bacillus anthracis* spore interactions with mammalian cells: Relationship between germination state and the outcome of *in vitro* infections." *BMC Microbiol.* **2011** Feb;11(46). Copyright 2011 by BioMed Central.

fates of both intracellular *B. anthracis* and infected cells. Although there are multiple reports of germinated spores within host cells (9, 18, 19, 21, 51), several studies have indicated that germinated spores ultimately kill macrophages (9, 42, 51), while others have reported that macrophages readily kill intracellular *B. anthracis* (26, 28). The lack of consensus may be due, in part, to fundamental differences between the infection models used by research groups, which includes variability in bacterial strains, mammalian cells, and experimental conditions employed.

An important issue that is likely to directly influence the outcome of *in vitro* models of infection is the germination state of spores as they are internalized into host cells. Several *in vivo* lines of evidence support the idea that spores remain dormant in the alveolar spaces of the lungs prior to uptake. First, dormant spores have been recovered from the lungs of animals several months after initial infection (16, 24). Second, all spores collected from the bronchial alveolar fluids of spore-infected Balb/c mice were found to be dormant (8, 21). In contrast, a substantial percentage of intracellular spores recovered from alveolar macrophages were germinated (21). Third, real time *in vivo* imaging failed to detect germinated spores within lungs, despite the effective delivery of dormant spores to these organs (13, 17, 53). One of these studies [25] reported that vegetative bacteria detected in the lungs during disseminated *B. anthracis* infection arrived at the lungs via the bloodstream, rather than originating from *in situ* spore growth. Finally, using spores that had been engineered to emit a bioluminescent signal immediately after germination initiation, a recent study

reported that germination was commenced in a mouse model of infection only after spore uptake into alveolar macrophages (44). However, despite considerable evidence that the lung environment is not intrinsically germinating for *B. anthracis* spores, most *in vitro* infection models have been conducted using culture media containing fetal bovin serum (FBS) and/or specific L-amino acids or nucleotides at concentrations previously demonstrated to promote germination of spores *in vitro* (4, 12, 25, 33, 34, 43, 51, 52). Under such conditions, it is likely that, in these previous studies, host cells were infected with heterogeneous populations of germinated and dormant spores.

This chapter presents studies that were performed to directly evaluate the manner in which the germination state of *B. anthracis* spores under *in vitro* culture conditions influences the infection of mammalian cells. Germinating and non-germinating culture conditions were used to compare the interaction of spores prepared from *B. anthracis* Sterne 7702 with RAW264.7 macrophage-like cells, as well as several other cell lines. These studies revealed that the uptake of *B. anthracis* into cells was largely unaffected by the germination state of spores. In contrast, the number of viable, intracellular *B. anthracis* recovered from infected cells, as well as the viability of the infected cells, was dependent on the germination state of spores during uptake. These results support the idea that the germination state of spores is an important consideration when interpreting results from *in vitro* infections with *B. anthracis* spores.

5.2 Results

5.2.1 The composition of cell culture medium influences the germination and outgrowth of *B. anthracis* spores.

Several commonly used mammalian cell culture media, in the presence or absence of fetal bovine serum (FBS), were first evaluated for the capacity to induce germination when incubated with dormant spores prepared from *B. anthracis* Sterne 7702 (1.0×10^8 spores/mL) at 37 °C and under 5% CO₂. Loss of optical density and heat resistance were used as classical indicators for the initiation of spore germination and loss of dormancy (31, 32, 45). These studies revealed that regardless of the medium tested, *B. anthracis* spores underwent germination initiation and outgrowth when incubated in the presence of FBS (Table 5.1, Figure 5.1A, B), as indicated by increased sensitivity of the spores to heat treatment (29), as well as a time-dependent decrease in spore refractility, which indicates rehydration of the spore core following germination initiation (22). When spores were exposed to Dulbecco's modified Eagle's medium (DMEM) or Roswell Park Memorial Institute (RPMI) 1640 medium plus 10% FBS, 86.0% and 83.4% of the spore population, respectively, converted from heat-resistant to heat sensitive forms within 10 min, and 97.6% and 96.6% of the spore population, respectively, converted to heat sensitive forms within 60 min (data not shown), indicating that germination initiation occurred under these medium conditions. These results are consistent with a previous study reporting that approximately 98% of the Sterne spores germinated within an hour when incubated in DMEM plus 10% FBS (51). Dose response studies revealed that

germination initiation was induced in DMEM containing 1% FBS, but not 0.5% FBS (Table 5.2). Spore germination or outgrowth was not dependent on the commercial source of FBS, as similar results were obtained with FBS purchased from 3 different vendors (data not shown, experiments were performed by Bojana Stojkovic and Dr. Angela M. Prouty). The capacity of spore preparations to germinate and outgrow were confirmed by incubating dormant spores in the presence of the known germinants, L-alanine and L-inosine (each at 10 mM, in phosphate buffered saline, PBS, pH 7.2) or Luria-Bertani broth (LB) (Figure 5.2), as previously reported (2, 14, 27). The time dependent increase in culture density (Figure 5.1A) and morphological conversion of spores into elongated bacilli (Figure 5.1C) indicated that in medium containing FBS, there was outgrowth of spores into vegetative bacilli.

In the absence of FBS, several media were discovered to induce germination initiation and outgrowth of *B. anthracis* spores (Table 5.1). Germination initiation (30-60 min) and outgrowth were detected when spores were incubated in brain heart infusion (BHI) broth (Table 5.1, Figure 5.3), modified minimum essential medium alpha modification (MEM α) (Table 5.1, Figure 5.3), CO₂-independent media (CIM) (Table 5.1), or McCoy's 5A (M5A) (Table 5.1). Each of these cell culture formulations contains all 20 amino acids, is enriched particularly in the known germinant L-alanine (15-20 mg/L), and also contains non-specified nucleotides. Notably, some nucleotides function as germinants (35, 45, 50). In contrast, spores incubated in minimum essential medium (MEM), Dulbecco's modified eagle medium (DMEM), Roswell Park

Memorial Institute (RPMI) 1640 medium, advanced MEM (AMEM), eagle MEM (EMEM), basal medium eagle (BME), or Ham's F-12 (F-12) did not germinate, even after 4 h (Figure 5.3, Table 5.3). Each of these media possesses lower concentrations of L-alanine (<10 mg/L) than those media that induced germination, and generally lacked nucleotides. These results emphasize that care must be exercised when selecting a culture medium for conducting *in vitro* infections under non-germinating conditions.

Figure 5.1

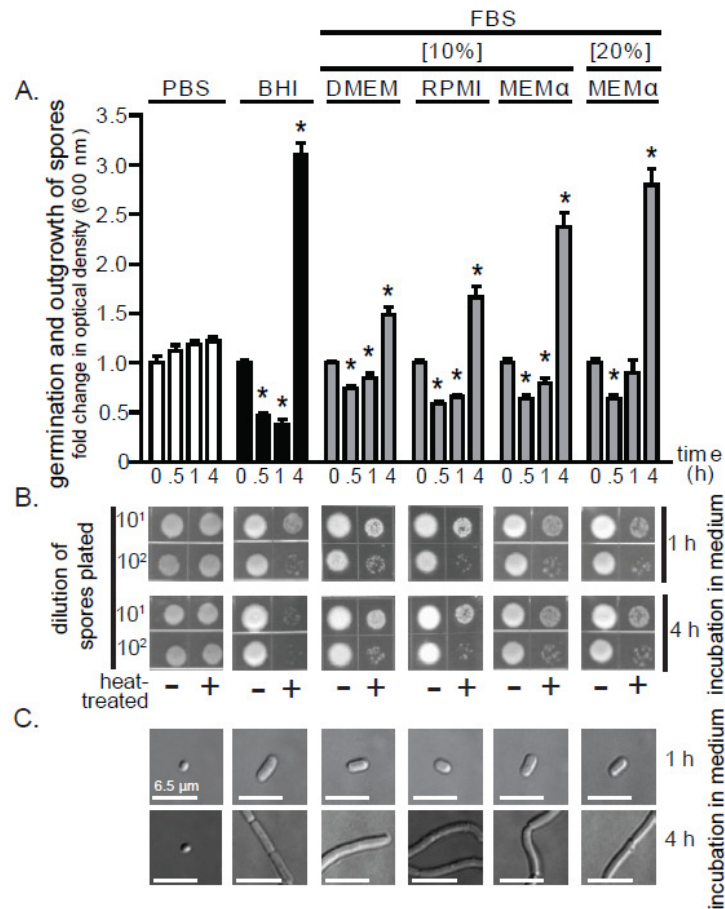


Figure 5.1. FBS in cell culture media promotes germination and outgrowth of *B. anthracis* spores. Spores (1.0×10^8 spore/mL) prepared from *B. anthracis* Sterne 7702 were incubated in 96-well plates at 37 °C and with rotary agitation within the indicated medium.

Figure 5.1 (continued)

Germination and outgrowth of spores were monitored at the indicated times. Medium conditions are listed at the top of the figure, and applicable to A, B, and C. A. Optical determination of germination and outgrowth. The data are rendered as the O.D. (600 nm) of the spore suspension at the indicated time (0.5, 1, or 4 h) relative to the original O.D. (600 nm) of the spore suspension at the start of the 37 °C incubation (e.g. time=0). For BHI, DMEM, RPMI, and MEM α , initial decreases in O.D. (600 nm) reflect the loss of spore refractility that occurs subsequent to germination initiation, while the increases in O.D. (600 nm) measured at later time points (1 and 4 h) reflects replication of vegetative bacteria. For PBS, the modest increases in O.D. (600 nm) are due to time-dependent evaporation of the medium. Error bars indicate standard deviations. For each medium tested, the *P*-values were calculated to evaluate the statistical significance of the differences between O.D. (600 nm) values at the indicated times and O.D. (600 nm) values at the initial time point. B. Sensitivity of spores to heat as a function of medium conditions. Aliquots from the spore cultures were removed at 1 or 4 h, as indicated, incubated for 30 min at either at 65 °C or on ice, diluted 10¹- or 10²-fold (PBS pH 7.2), as indicated, spotted (10 μ L) on LB plates, and incubated at 25 °C. After 18 h, the plates were photographed. T: total. HT: heat-treated. C. Visual determination of *B. anthracis* spore outgrowth as a function of cell culture medium. Aliquots from the spore cultures were removed at 1 or 4 h, as indicated, and analyzed for outgrowth using DIC microscopy. The data are rendered as images in which the bars indicate a length of 6.5 μ m. The data in A are combined from 3 independent experiments. The data in B and C are from a single experiment, and are representative of those obtained in 3 independent experiments.

Figure 5.2

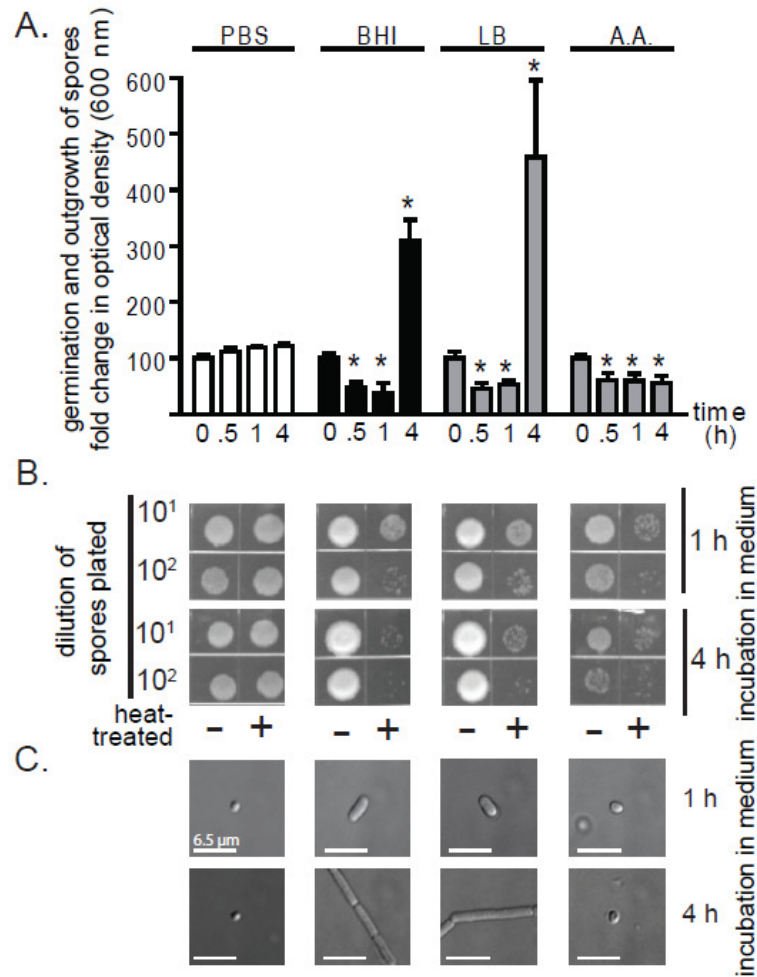


Figure 5.2. Rich media and amino acids promote germination and outgrowth of *B. anthracis* spores. Spores (1.0×10^8 spore/mL) prepared from *B. anthracis* Sterne 7702 were incubated in 96-well plates at 37 °C and with rotary agitation within the indicated medium. Germination and outgrowth of spores were monitored at the indicated times. Medium conditions are listed at the top of the figure, and applicable to A, B, and C. A. Optical determination of germination and outgrowth. The data are rendered as the O.D. (600 nm) of the spore suspension at the indicated time (0.5, 1, or 4 h) relative to the original O.D. (600 nm) of the spore suspension at the start of the 37 °C incubation (e.g. time=0). For BHI, LB, and Amino acids (A.A.), initial decreases in O.D. (600 nm) reflect the loss of spore refractility that occurs subsequent to germination initiation, while the increases in O.D. (600 nm) measured at later time points (1 and 4

Figure 5.2 (continued)

h) reflects replication of vegetative bacteria. For PBS, the modest increases in O.D. (600 nm) are due to time-dependent evaporation of the medium. Error bars indicate standard deviations. For each medium tested, the *P*-values were calculated to evaluate the statistical significance of the differences between O.D. (600 nm) values at the indicated times and O.D. (600 nm) values at the initial time point. B. Sensitivity of spores to heat as a function of medium conditions. Aliquots from the spore cultures were removed at 1 or 4 h, as indicated, incubated for 30 min at either at 65 °C or on ice, diluted 10¹- or 10²-fold (PBS pH 7.2), as indicated, spotted (10 µL) on LB plates, and incubated at 25 °C. After 18 h, the plates were photographed. T: total. HT: heat-treated. C. Visual determination of *B. anthracis* spore outgrowth as a function of cell culture medium. Aliquots from the spore cultures were removed at 1 or 4 h, as indicated, and analyzed for outgrowth using DIC microscopy. The data are rendered as images in which the bars indicate a length of 6.5 µm. The data in A are combined from 3 independent experiments. The data in B and C are from a single experiment, and are representative of those obtained in 3 independent experiments.

Figure 5.3

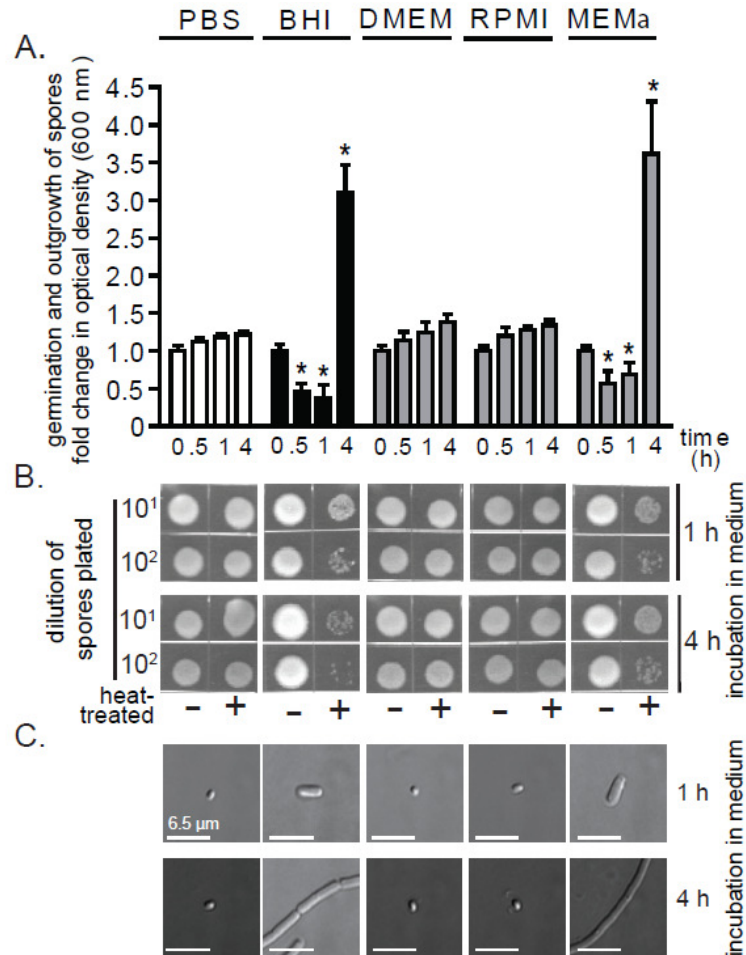


Figure 5.3. *B. anthracis* spore germination and outgrowth in FBS-free cell culture media. Spores (1.0×10^8 spore/mL) prepared from *B. anthracis* Sterne 7702 were incubated in 96-well plates at 37 °C and with rotary agitation within the indicated medium. Germination and outgrowth of spores were monitored at the indicated times. Medium conditions are listed at the top of the figure, and are applicable to A, B, and C. A. Optical determination of germination and outgrowth. The data are rendered as the O.D. (600 nm) of the spore suspension at the indicated time (0.5, 1, or 4 h) relative to the original O.D. (600 nm) of the spore suspension at the start of the 37 °C incubation (e.g. time=0). Error bars indicate standard deviations. For each medium tested, the *P*-values were calculated to evaluate the statistical significance of the differences between O.D. (600 nm) values at the indicated times and O.D. (600 nm) values at the initial time point.

Figure 5.3 (continued)

B. Sensitivity of spores to heat as a function of medium conditions. Aliquots from the spore cultures were removed at 1 or 4 h, as indicated, incubated for 30 min at either at 65 °C or on ice, diluted 10¹- or 10²-fold (PBS pH 7.2), as indicated, spotted (10 µL) on LB plates, and incubated at 25 °C. After 18 h, the plates were photographed. T: total. HT: heat-treated. C. Visual determination of *B. anthracis* spore outgrowth as a function of cell culture medium. Aliquots from the spore cultures were removed at 1 or 4 h, as indicated, and analyzed for outgrowth using DIC microscopy. The data are rendered as images in which the bars indicate a length of 6.5 µm. The data in A are combined from 3 independent experiments. The data in B and C are from a single experiment and are representative of those obtained in 3 independent experiments.

medium ^a	FBS ^b	germination ^c	outgrowth ^d	
			1 h	4 h
DMEM	-	-	-	-
	+	+	+	+
RPMI	-	-	-	-
	+	+	+	+
MEM α	-	+	+	+
	+	+	+	+
MEM	-	-	-	-
	+	+	+	+
AMEM	-	-	-	-
	+	+	+	+
EMEM	-	-	-	-
	+	+	+	+
BME	-	-	-	-
	+	+	+	+
CIM	-	+	+	+
	+	+	+	+
F-12	-	-	-	-
	+	+	+	+
M5A	-	+	+	+
	+	+	+	+
BHI	-	+	+	+
LB	-	+	+	+
AA	-	+	-	-

Table 5.1. FBS and cell culture media effects on germination and outgrowth of *B. anthracis* spores. ^a Three independent experiments were performed with three different spore preparations, each conducted in triplicate. ^b Spores prepared from *B. anthracis* Sterne 7702 were incubated in the indicated medium. ^c Indicates the presence (+) or absence (-) of 10% FBS in the indicated medium. ^d Spores were scored positive (+) for germination if the OD_{600 nm} of the suspended spores decreased by more than 10% after 30 min incubation in the indicated medium. ^e Using DIC microscopy, spores were scored positive (+) for outgrowth if the spores bodies were visibly larger at 1 h, and had developed into vegetative bacteria by 4 h. ^f AA refers to L-alanine and L-inosine (each at 10 mM, in PBS pH 7.2).

medium ^a	FBS (%) ^b	germination ^c	outgrowth ^e	
			1 h	4 h
DMEM	0.0	-	-	-
	0.1	-	-	-
	0.5	-	-	-
	1.0	+	-	+
	5.0	+	+	+
	10.0	+	+	+

Table 5.2. Concentration dependence of FBS induced germination. ^a Three independent experiments were performed with three different spore preparations, each conducted in triplicate. ^b Spores prepared from *B. anthracis* Sterne 7702 were incubated in the indicated medium. ^c Indicates the presence (+) or absence (-) of 10% FBS in the indicated medium. ^d Spores were scored positive (+) for germination if the OD_{600 nm} of the suspended spores decreased by more than 10% after 30 min incubation in the indicated medium. ^e Using DIC microscopy, spores were scored positive (+) for outgrowth if the spores bodies were visibly larger at 1 h, and had developed into vegetative bacteria by 4 h.

5.2.2 Effects of pre-conditioned culture medium on the germination state of *B. anthracis* spores.

We next considered the possibility that cell culture media that normally do not promote spore germination may be converted to germinating media when incubated in the presence of mammalian cells. To evaluate this possibility, *B. anthracis* spores were incubated in DMEM or RPMI that had been “pre-conditioned” in the presence of RAW264.7 cells or MH-S cells, respectively. These studies revealed that neither DMEM nor RPMI, following a pre-conditioning period of 4 h, induced germination of *B. anthracis* spores (Figure 5.4A). Likewise, medium withdrawn from RAW264.7 cells infected for 1 or 4 h

with dormant spores at a multiplicity of infection of 10 (MOI 10) also remained non-germinating (Figure 5.4B). Finally, medium withdrawn from RAW264.7 cells infected with dormant spores (MOI 10) contained only heat resistant *B. anthracis*, and no heat sensitive spores (Figure 5.4), indicating that the extracellular spores remained dormant through the first 4 hours of infection. When the pre-conditioning period was extended to 24 h, both DMEM and RPMI induced germination, but negligible outgrowth at 4 h, of spores (Figure 5.4A). Spore germination was eliminated by dialyzing (12-14 kDa molecular mass cutoff) the 24 h preconditioned DMEM or RPMI, but not by heat treatment (95 °C for 10 min, or, 65 °C for 30 min; data not shown), suggesting that the germinating factors were relatively small molecular weight, heat-resistant factors. Nonetheless, these studies confirm that *in vitro* models can be established that maintain a non-germinating environment for at least the first 4 h of infection.

Figure 5.4

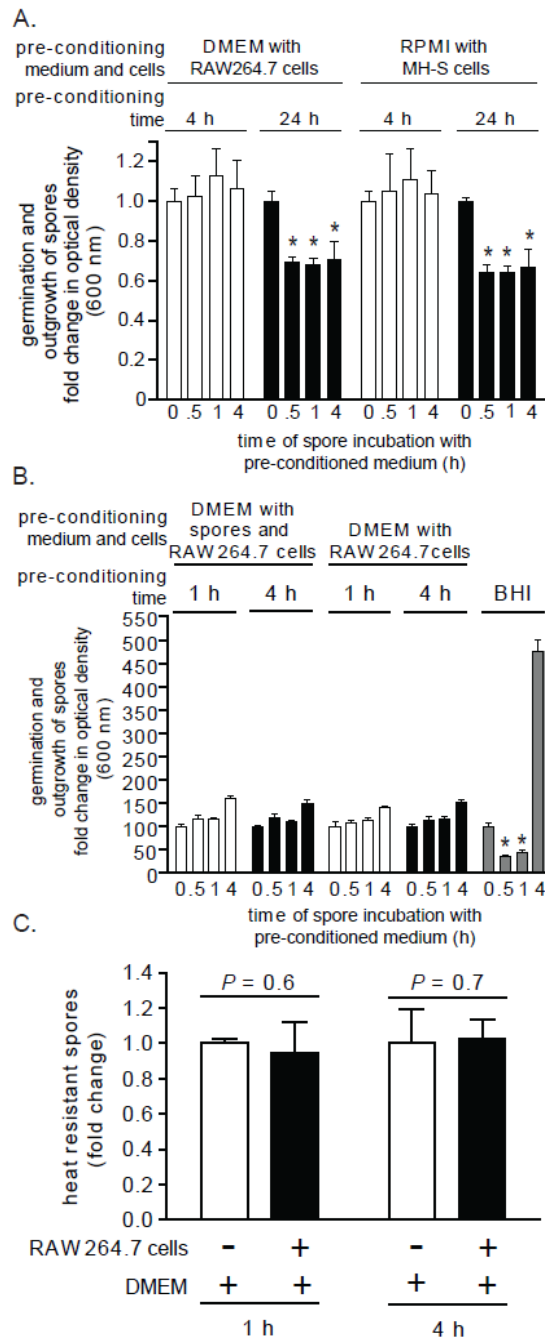


Figure 5.4. The effects of pre-conditioned culture medium on the germination state of *B. anthracis* spores. DMEM (A, B) or RPMI (B) was pre-conditioned by incubating with monolayers of RAW264.7 (A, B) or MH-S cells (B), respectively, at 37 °C and under 5% CO₂, in the absence (A) or presence (MOI 10) of (B) of spores prepared from *B. anthracis* Sterne 7702.

Figure 5.4 (continued)

(A, B). After 4 h (white bars) or 24 h (black bars) (A), or after 1 (white bars) and 4 h (black bars) (B), as indicated, the medium was removed from the monolayers, filter sterilized, and then incubated with spores (1.0×10^8 spore/mL) prepared from *B. anthracis* Sterne 7702 in 96-well plates at 37 °C and with rotary agitation. Germination and outgrowth of spores were monitored at 0, 0.5, 1, or 4 h, as indicated, by measuring O.D. (600 nm). The results are rendered as the O.D. (600 nm) of the spore suspension at the indicated time relative to the original O.D. (600 nm) of the spore suspension at the start of the 37 °C incubation (e.g. time=0). *P*-values were calculated to evaluate the statistical significance of the differences between O.D. (600 nm) values at the initial time point and O.D. (600 nm) values at the indicated times. For B, BHI (gray bars) was used as a positive control to monitor germination and outgrowth. C. An equal number of spores prepared from *B. anthracis* Sterne 7702 were incubated at 37 °C and under 5% CO₂ in DMEM (no FBS) in the absence (white bars) or presence (black bars) of RAW264.7 cells (MOI 10). At 1 or 4 h, as indicated, aliquots of culture medium were removed and spores were evaluated for heat resistance. The results are rendered as the number of heat resistant spores relative to spores incubated in DMEM alone, which were normalized to 1.0. *P*-values were calculated to evaluate the statistical significance of the differences in heat resistant spores between those incubated in the presence or absence of RAW264.7 cells. For A-C, the results were obtained by combining the data collected from three independent experiments, each conducted in triplicate, and the error bars indicate standard deviations.

5.2.3 Mammalian cells remain viable and functional for at least 4 h in FBS-free culture medium.

Although a non-germinating environment was maintained for at least 4 h in FBS-free media (Figure 5.4), it was unclear whether viable and functional cells could be maintained in FBS-free medium over this same time period. Studies to evaluate this issue revealed that over a 4 h period, RAW264.7 cells in DMEM

demonstrated essentially identical viability (Figure 5.5A), cell cycle progression (Figure 5.5B), and metabolic activity (Figure 5.5C) in the absence or presence of FBS (10%). Even after 24 h, the viability (Figure 5.5A) and cell cycle profiles (Figure 5.5B) were not significantly different for RAW264.7 cells cultured in the absence or presence of FBS. The metabolic activity of RAW264.7 cells increased after 24 h, but significantly more so in the presence than absence of FBS (Figure 5.5C), which we speculate was due to greater overall proliferation and number of cells in FBS-enriched medium. These results confirmed that, for at least 4 h, *in vitro* models of infection can be conducted under entirely non-germinating culture conditions without loss of host cell viability, cell cycle progression, or metabolic function.

Figure 5.5

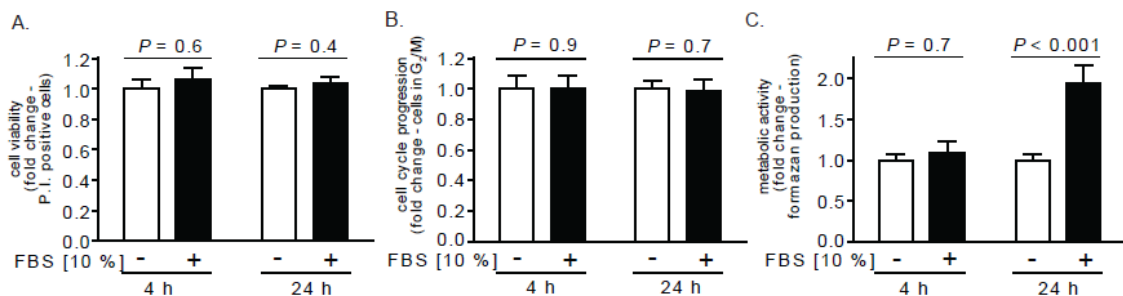


Figure 5.5. Viability, cell cycle progression, and metabolic activity of RAW264.7 cells cultured under germinating or non-germinating conditions. RAW264.7 cells were incubated at 37 °C in DMEM in the presence (+, black bars) or absence (-, white bars) of FBS, and then evaluated at 4 or 24 h, as indicated, for viability (A), cell cycle progression (B), and metabolic activity (C). A. The cells were assayed for PI uptake, as described under Materials and Methods. The data are rendered as the relative PI uptake normalized at both 4 and 24 h to cells incubated in the absence of FBS. B. The cells were analyzed for their cell cycle profiles, as described under

Figure 5.5 (continued)

Materials and Methods. The data are rendered as the relative numbers of cells in G₂/M normalized at both 4 and 24 h to cells incubated in the absence of FBS. C. The cells were analyzed for conversion of MTT to formazan. The data are rendered as the fold change of formazan production normalized at both 4 and 24 h to cells incubated in the absence of FBS. To generate the bar graphs, data were combined from three independent experiments, each conducted in triplicate. Error bars indicate standard deviations. The *P* values were calculated to evaluate the statistical significance of the differences in viability (A), cell cycle progression (B), and metabolism (C) between cells cultured in the absence or presence of FBS.

5.2.4 Germination state of spores does not alter the uptake by mammalian cells.

The demonstration that cultured RAW264.7 cells remained viable and functional in FBS-free cell culture medium did not directly address the possibility that spore uptake by mammalian cells might be substantially different under germinating and non-germinating cell culture conditions. To evaluate this issue, Alexa Fluor 488-labeled spores were incubated with RAW264.7, MH-S, or JAWSII cells (MOI 10) in the absence or presence of FBS (10%). After 5 or 60 min, intracellular spores were monitored using flow cytometry to measure cell associated fluorescence that was not sensitive to the membrane-impermeable, Alexa Fluor 488 quenching agent, trypan blue (48). These studies revealed that for each cell line tested, neither the percentage of infected cells within the population (Figure 5.6A-C), nor the overall increase in intracellular spores (Figure 5.6D-F), was significantly different in the presence or the absence of FBS. Collectively, these results revealed that the uptake of *B. anthracis* spores by

mammalian cells is essentially the same within germinating and non-germinating *in vitro* environments.

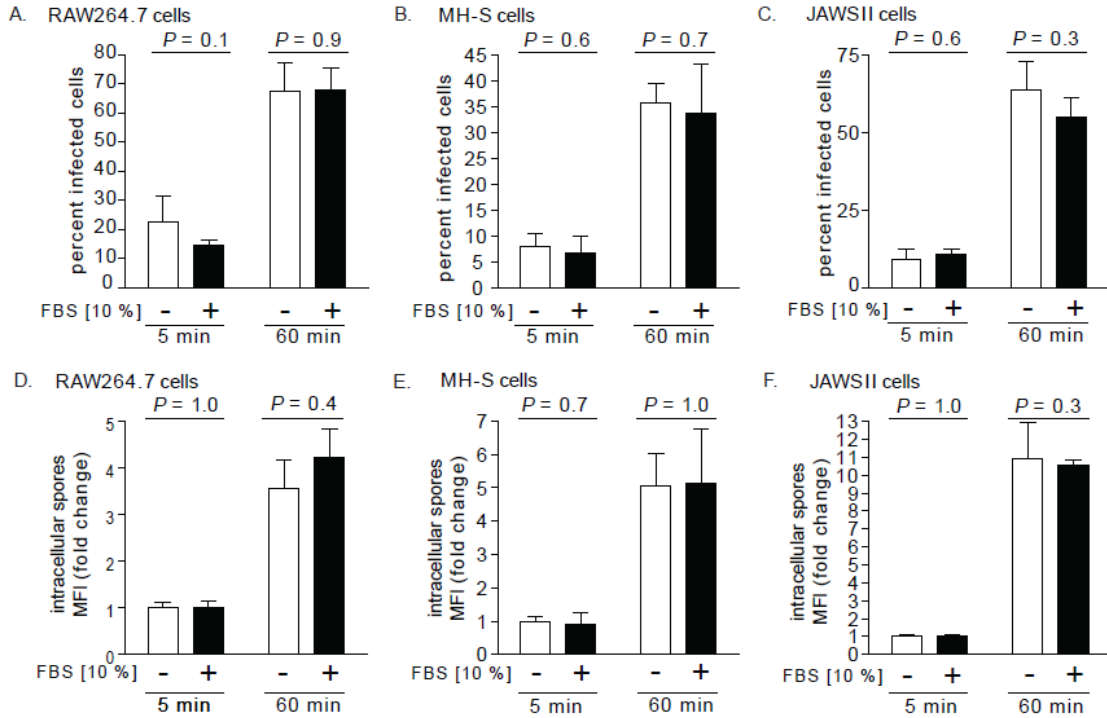


Figure 5.6. Uptake of *B. anthracis* spores into mammalian cells cultured under germinating or non-germinating conditions. RAW264.7 cells (A, D), MH-S cells (B, E), or JAWSII cells (C, F) were incubated with *B. anthracis* spores (MOI 10) in DMEM, RPMI, or DMEM, respectively, in the presence (+, black bars) or absence (-, white bars) of FBS (10%), and then evaluated at 5 or 60 min by flow cytometry and in the presence of trypan blue (0.5%) for the percentage of cells with intracellular spores (A-C), and, for total cell associated spore fluorescence (D-F), as described under Materials and Methods. In A-C, the data are rendered as the percentage of infected cells with the entire population that has internalized spores. In D-F, the data are expressed as the change in MFI, normalized to cells at 5 min post infection in FBS-free medium. To generate the bar graphs, data were combined from three independent experiments, each conducted in triplicate. Error bars indicate standard deviations. The *P* values were calculated to evaluate the statistical significance of the differences in percent infected cells (A) or total intracellular spores (B) between cells incubated in the absence or presence of FBS.

5.2.5 Germination state of spores influences the number of viable, intracellular *B. anthracis*.

Although the uptake of *B. anthracis* spores into mammalian cells was independent of the presence or absence of FBS in the culture medium, it was not clear whether the outcome of infection would also be similar under germinating and non-germinating conditions. To evaluate this issue, the recovery of viable, intracellular *B. anthracis* was compared subsequent to uptake by RAW264.7 cells in the absence or presence of FBS (10%), using the gentamicin protection assay (1, 28, 41, 48). These studies indicated that there were not significant differences in intracellular CFU after 5 min post-infection (Figure 5.7). However, after 60 or 240 min post infection, significantly greater CFU were recovered from cells in DMEM lacking FBS relative to cells incubated in the presence of FBS (Figure 5.7). Similar results were obtained when studies were conducted with MH-S cells and JAWSII cells (not shown). In addition, spores that were pre-germinated and washed to remove the germinants were also evaluated for their intracellular survival in the absence of FBS to determine whether a loss of recoverable CFU was a function of the spore germination state or opsonization as a result of FBS addition. Again, these studies indicated that there were not significant differences in intracellular CFU after 5 min post-infection (Figure 5.7). However, after 60 or 240 min post infection, significantly greater CFU were recovered from cells that were infected with dormant spores during a non-germinating infection (Figure 5.7). Although the exact mechanisms underlying the greater recovery of spores from infections conducted under non-germinating

conditions are not clear, we demonstrate that germinated spores are more susceptible than dormant spores to killing after uptake from the cell surface. This potential explanation is consistent with earlier reports that spores that had been intentionally pre-germinated prior to exposure to mammalian cells were more readily killed than dormant spores upon uptake into mammalian cells (26, 51). These results support the idea that the germination state of *B. anthracis* spores is a critical determinant of the fate of the intracellular bacteria.

Figure 5.7

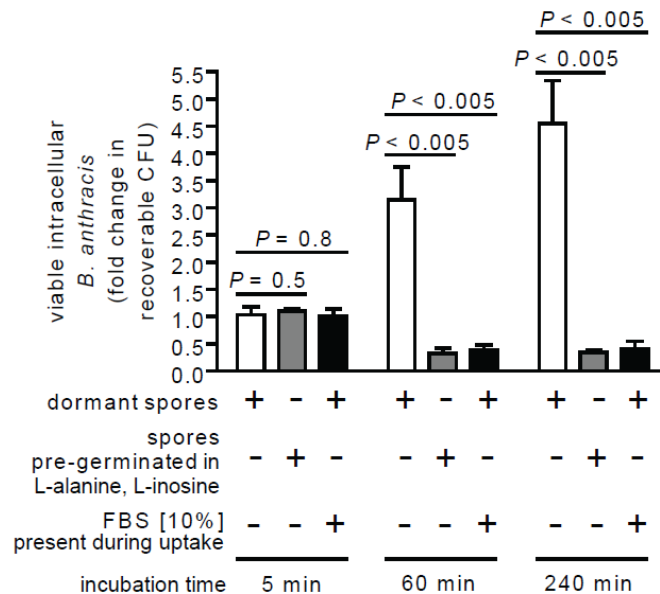


Figure 5.7. The germination state of spores influences the viability of intracellular *B. anthracis*. RAW264.7 cells were incubated for 30 min with dormant *B. anthracis* spores (MOI 10) in DMEM in the presence (+, black bars) or absence (-, white bars) of FBS (10%) or pre-germinated *B. anthracis* spores (MOI 10) in DMEM in the absence of FBS (grey bars). After 30 min, the cells were washed to remove extracellular *B. anthracis*, and then further incubated with FBS (10%) and, as described under “Methods,” with gentamicin to germinate and kill any remaining spores that had not been germinated. After 15 min, the cells were washed and then further incubated in the absence of gentamicin. At 5, 60, or 240 min after removal of gentamicin,

Figure 5.7 (continued)

as indicated, the RAW264.7 cells were lysed, and the lysates were evaluated for viable *B. anthracis*, as described under Materials and Methods. For pre-germinated spores, *B. anthracis* spore were germinated with 10 mM L-alanine and L-inosine in 1x PBS pH 7.2 for 30 min and washed twice with 1x PBS pH 7.2 to remove germinants. The data were rendered as the fold-change in recoverable CFU in the absence or presence of FBS, relative to cells at 5 min post infection in the absence of FBS. The rendered data were combined from three independent experiments, each conducted in triplicate. Error bars indicate standard deviations. The *P* values were calculated to evaluate the statistical significance of the differences in recoverable CFU between cells infected in the absence or presence of FBS.

5.2.6 Germination state of B. anthracis spores influences the viability of RAW264.7 cells during in vitro infection.

The greater number of viable, intracellular *B. anthracis* recovered from cells infected under non-germinating conditions (Figure 5.7) prompted us to examine whether the viability of infected host cells might also be influenced by the germination state of spores during uptake. To evaluate this issue, RAW264.7 cells were incubated with *B. anthracis* spores (MOI 10) in the presence or absence of FBS (10%). Subsequent to employing the same gentamicin-protection procedure used for monitoring intracellular *B. anthracis* (Figure 5.7), PI uptake by RAW264.7 cells was measured at 5 min, 1 h, and 4 h, post-infection. These studies revealed that at 4 h post-infection, there was approximately 2-fold greater PI uptake, indicating a significantly greater loss in viability of RAW264.7 cells that had been incubated with spores in FBS-deficient medium, as compared to FBS-enriched medium (Figure 5.8). When evaluated at 8 h post-infection, PI

uptake was nearly 5-fold greater in RAW264.7 cells that had been incubated with *B. anthracis* spores in FBS-deficient medium (data not shown). Understanding the reasons underlying these significant differences in the viability of infected cells will require future studies, but we speculate that the greater intracellular load of *B. anthracis* in cells infected under non-germinating conditions (Figure 5.7) may directly contribute to the higher degree of cell death.

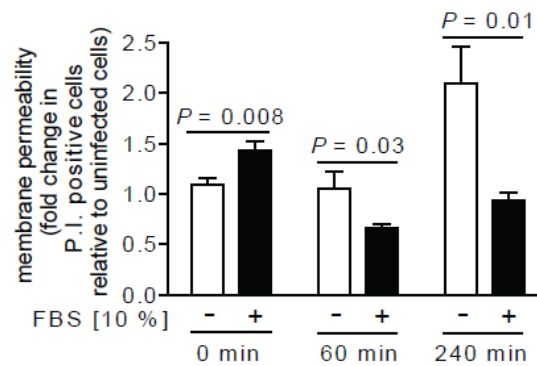


Figure 5.8. The germination state of spores influences the viability of *B. anthracis*-infected cells. RAW264.7 cells were incubated for 30 min with *B. anthracis* spores (MOI 10) in DMEM in the presence (+, black bars) or absence (-, white bars) of FBS (10%). After 30 min, the cells were washed to remove extracellular *B. anthracis*, and then further incubated with FBS (10%) and, as described under “Methods,” with gentamicin to germinate and kill any remaining spores that had not been germinated. After 15 min, the cells were washed and then further incubated in the absence of gentamicin. At 0 (immediately after gentamicin removal), 60, or 240 min after removal of gentamicin, as indicated, the cells were evaluated for mammalian cell death via PI uptake, as described under Materials and Methods. The data are rendered as the fold-increase of PI uptake relative to non-infected cells in the absence or presence of FBS at 5, 60, or 240 min, as indicated. The rendered data have been combined from three independent experiments, each conducted in triplicate. Error bars indicate standard deviations. The *P* values were calculated to evaluate the statistical significance of the differences between the fold-increase of PI uptake between cells incubated with spores in the absence or presence of FBS.

5.3 Discussion

Despite compelling evidence that during *in vivo* infection, the alveolar spaces of the lungs are intrinsically non-germinating, and dormant spores are taken up by mammalian cells prior to germination (8, 13, 16, 17, 21, 24, 44, 53), many studies involving *in vitro* models of infection have been conducted under germinating medium conditions (4, 12, 25, 33, 34, 43, 51, 52). Most studies have been conducted in cell culture medium containing 2-10% FBS, including those using RAW264.7 cells (38, 46), and the germination state of spores have not generally been monitored or controlled for during *in vitro* infections.

Several *in vitro* models have employed additives to the culture medium in an attempt to modulate germination. Several studies used D-alanine and/or D-histidine (25, 26, 30), known inhibitors of germination initiation. However, interpretation of these studies may be complicated by the finding that D-alanine/D-histidine, when added subsequent to spore uptake into macrophages, alter the extent to which spores germinate (25), suggesting that these D-amino acid germination inhibitors diffuse into host cells and affect spore germination within intracellular vesicles. Horse serum has been used by several groups to limit spore outgrowth during infection (3, 4, 25, 51). However, 10% horse serum in DMEM only slows, but does not eliminate the germination initiation of spores (51). The finding that RAW264.7 cells maintain viability, cell cycle progression, and mitochondrial metabolic activity for at least 4 h when maintained in serum-free medium (Figure 5.5), indicates that *in vitro* infections, at least with

RAW264.7 cells, can be conducted under non-germinating conditions using FBS-free medium.

Both spore (Figure 5.7) and host cell (Figure 5.8) viability were influenced by the germination state of spores at the time of uptake. Because several cell lines internalized the same number of spores under both germinating and non-germinating conditions (Figure 5.6), it is unlikely that differences in the outcome of infection are due solely to initial differences in spore load. Rather, we speculate that, in contrast to dormant spores, germinated spores might be more vulnerable to growth inhibition and/or killing during phagocytosis. These results are consistent with previous reports in which infections were conducted with spores in medium containing FBS or fetal calf serum (i.e. germinating conditions). Generally, within the first 4-5 h post-infection, losses were observed in intracellular CFU recovered from primary human dendritic cells (37), primary mouse alveolar macrophages (37), J774.A1 murine macrophage-like cells (36), bone marrow derived macrophages from A/J mice (43), or RAW 264.7 cells (9).

This study demonstrates that the infection of RAW 264.7 cells by *B. anthracis* spores is influenced by the germination state of spores, as dictated by the *in vitro* culture medium. The extent to which the germination state of *B. anthracis* spores ultimately affects the outcome of infections using cells other than RAW264.7 cells may ultimately depend on the properties idiosyncratic to that particular cell type or cell line. However, our results indicate the importance of rigorously considering the germinating properties of the culture medium when

establishing *in vitro* models to study the infection of host cells with *B. anthracis* spores.

5.4 Materials and Methods

5.4.1 Spore preparations and fluorescent labeling.

Spores were prepared from *B. anthracis* Sterne 7702 and enumerated using a hemacytometer (Thermo Fisher Scientific, Waltham, MA), as described previously (48). As quality control, spore preparations were tested for both heat resistance and the capacity to germinate, as described (48).

5.4.2 Mammalian cell culture.

Abelson murine leukemia virus-transformed murine macrophages derived from ascites of BALB/c mice (RAW 264.7 macrophage-like cells; CRL-2278; ATCC, Manassas, VA) were maintained within a humidified environment at 37 °C and under 5% CO₂ in complete DMEM, (Thermo Scientific, Waltham, MA) containing penicillin (100 U; Gibco BRL, Grand Island, NY), streptomycin (0.1 mg/ml; Gibco BRL), L-glutamine (2 mM; Sigma, St. Louis, MO), and FBS (10%; JRH Biosciences, Lenexa, KS). MH-S cells (CRL-2019; ATCC) were maintained within a humidified environment at 37 °C and under 5% CO₂ in complete RPMI medium (Thermo Scientific) containing penicillin-streptomycin (100 U, Gibco BRL), L-glutamine (4 mM), and FBS (10%). JAWSII (CRL-11904; ATCC) were maintained within a humidified environment at 37 °C and under 5% CO₂ in complete MEM α (Thermo Scientific) containing penicillin-

streptomycin (100 U), L-glutamine (4 mM), and FBS (20%). All tissue culture plasticware was purchased from Corning Incorporated (Corning, NY).

5.4.3 Evaluation of *B. anthracis* spore germination in cell culture media.

Using 96 well plates, spores prepared from *B. anthracis* 7702 (10^8 spores/mL) were incubated at 37 °C and under 5% CO₂ in BHI (BD Biosciences, San Jose, CA), LB (0.1 % tryptone, BD Biosciences; 0.05 % yeast extract, BD Biosciences; 0.05 % NaCl, Fisher Chemical, Fairlawn, NJ), PBS pH 7.2 (Mediatech, Manassas, VA), or germinating amino acids (10 mM L-alanine, 1 mM L-inosine, both from Sigma) in PBS pH 7.2. In other studies, spores were incubated in 96 well plates (10^8 spores/mL) and at 37 °C and under 5% CO₂ in the following cell culture media without or with FBS (10%, unless otherwise indicated; Mediatech): DMEM (0.1, 0.5, 1, 5 or 10% FBS), RPMI-1640, MEM α modification (10 or 20% FBS), MEM (Mediatech), AMEM (Gibco), EMEM (Mediatech), BME (Sigma), CIM (Gibco), Ham's F-12 (Mediatech), McCoy's 5A (M5A, ATCC), or DMEM with 10% FBS and 10 mM D-alanine (Sigma) and D-histidine (Sigma). In some assays, FBS obtained from Mediatech was substituted with FBS purchased from Invitrogen or Sigma. As described previously (22), spore germination was evaluated by measuring loss in spore refractility or loss of heat resistance, while outgrowth was monitored by monitoring the elongation of bacilli using a Delta Vision RT microscope (Applied Precision; Issaquah, WA), outfitted with an Olympus Plan Apo 100x oil objective. DIC images were collected

using a Photometrics CoolSnap HQ camera; (Photometrics, Tucson; AZ), and processed using SoftWoRX Explorer Suite (version 3.5.1, Applied Precision Inc).

5.4.4 Pre-conditioning of cell culture media.

To pre-condition cell culture medium, monolayers of RAW264.7 or MH-S cells in 24-well plates (80 to 95% confluency) were washed three times with Hanks' balanced salt solution (HBSS) and then incubated in DMEM (for RAW264.7 cells) or RPMI-1640 (for MH-S cells) without FBS and penicillin-streptomycin in a humidified environment at 37 °C and under 5% CO₂. After 4 or 24 h, the medium was withdrawn, centrifuged (600 x *g* for 5 min), and the supernatant was filter sterilized using a 0.22 µm filter (Corning). To evaluate heat sensitivity, some of the filter-sterilized pre-conditioned medium was incubated at 95 °C for 10 min or, alternatively, 65 °C for 30 min. Alternatively, some of the filter-sterilized pre-conditioned medium (3 mL) was dialyzed four times against PBS pH 7.2 (500 mL), using dialysis tubing with 12,000-14,000 molecular mass cutoff (Spectrum Laboratories, Inc., Rancho Dominguez, CA), each time for 6 h.

5.4.5 Mammalian cell viability.

To evaluate the viability of RAW264.7, MH-S, or JAWSII cells, alterations in membrane permeability, as indicated by relative PI (1 µg/mL; Invitrogen Molecular Probes, Eugene, OR) uptake, were measured using flow cytometry, as previously described (48).

5.4.6 Flow cytometry.

Analytical flow cytometry was carried out using a Beckman Coulter EPICS XL-MCL™ flow cytometer equipped with a 70-µm nozzle, 488 nm line of an air-cooled argon-ion laser, and 400 mV output. The band pass filter used for detection of Alexa Fluor 488 spores was 525/10 nm. The long pass filter used for cell cycle phase determination assays and mammalian cell viability assays was 655 nm/LP. Cell analysis was standardized for side/forward scatter and fluorescence by using a suspension of fluorescent beads (Beckman Coulter Inc., Fullerton, CA). At least 10,000 events were detected for each experiment (>2000 events per min). Events were recorded on a log fluorescence scale and evaluated using FCS Express 3.00.0311 V Lite Standalone. Sample debris (as indicated by lower forward and side scatter and a lack of PI staining) represented a small fraction (1 to 2%) of the detected events and was excluded from analysis.

5.4.7 Cell cycle assay.

To compare the cell-cycle profiles of RAW264.7 cells cultured in FBS-containing medium or FBS-free medium, relative PI uptake was measured using flow cytometry. At 4 or 24 h, as indicated, cells were incubated at room temperature with Cellstripper™ (Mediatech). After 15 min, the cells were further diluted with PBS pH 7.2 containing 10% FBS (800 mL). The cell suspensions were centrifuged for 5 min at 500 xg at room temperature. The pellets were resuspended in 300 µL of PBS pH 7.2 at room temperature, fixed by adding anhydrous ethanol (100%, 700 µL prechilled to -20 °C, Fisher Scientific) with

continuous vortexing, and then further incubated for at least 2 h at -20 °C. The cells were centrifuged for 5 min at 500 xg at room temperature, and the pellets were resuspended in 1 mL of PBS pH 7.2, and then incubated at room temperature for 30 min. The cells were centrifuged 5 min at 500 xg at room temperature. The cell pellets were resuspended in 300 µL PBS pH 7.2, 0.1% Triton X-100 (MP Biomedicals, Solon, OH), DNase-free RNase A (100 mg/mL; Sigma), and PI (10 µg/mL), and further incubated at room temperature for 60 min. The stained cells were analyzed by flow cytometry.

5.4.8 Mammalian cell metabolism assay.

To compare the metabolic activities of RAW264.7 cells cultured in FBS-containing medium or FBS-free medium, the relative conversion of tetrazolium 3-(4,5-di-methylthiazol-2-yl)-2,5-diphenyltetrazolium bromide (tetrazolium; 5 mg/mL, Sigma) to formazan over 30 min and at 37 °C was measured at 570 nm with a Synergy 2 plate reader (BioTek Instruments, Inc., Winooski, VT), as described (6, 22).

5.4.9 In vitro infection of mammalian cells with B. anthracis.

Mammalian cells (5.0×10^5 total cells/well) were incubated in the appropriate complete medium, as indicated above under “Mammalian cell culture,” for two days in a humidified environment at 37 °C and under 5% CO₂, resulting in 80-95% confluency. To calculate the number of spores needed to achieve MOI 10, cells from several wells were detached using Cellstripper™ and

enumerated using a hemacytometer. The cells were used only if greater than 90% of the cells excluded trypan blue; generally, greater than 95% of the cells within the monolayer excluded trypan blue. Prior to the addition of labeled spores, cells were washed three times with HBSS and then incubated in DMEM (RAW264.7 and JAWSII) or RPMI-1640 (MH-S), without or with FBS, as indicated. To synchronize the exposure of cells to spores, spores were immediately and gently centrifuged (600 x *g* for 5 min) onto the surfaces of cells. The plates were incubated within a humidified environment at 37 °C and under 5% CO₂ for the indicated times prior to analysis.

5.4.10 Quantification of *B. anthracis* uptake by mammalian cells.

Internalization of *B. anthracis* spores by mammalian cells was quantified using a previously described flow cytometry based assay (48). Briefly, the indicated mammalian cell lines were seeded into 48-well plates (Corning) in order to achieve 80-95% confluency after two days of incubation. As previously described (48), *B. anthracis* spores were labeled using an amine reactive Alexa Fluor® 488 carboxylic acid, succinimidyl ester (Molecular Probes–Invitrogen). Alexa Fluor 488-labeled *B. anthracis* spores were quantified using a hemacytometer, added to cells at the desired MOI, and immediately but gently centrifuged (300 *xg* for 5 min) onto the surface of cells. The plates were incubated within a humidified environment at 37 °C and under 5% CO₂ for the indicated times prior to analysis using flow cytometry, as previously described (48)

To discriminate intracellular spores from those which remain surface-associated during infection, cells were analyzed in the presence of trypan blue, a membrane-impermeable, Alexa Fluor 488® fluorescence quenching agent (23). Previously, 0.5% trypan blue was demonstrated to completely quench the fluorescence emission of Alexa Fluor 488-labeled spores bound to the surface of mammalian cells, while having no effect on the fluorescence emission of internalized spores (48). From these data, the percentage of cells with internalized *B. anthracis* was calculated by dividing the number of viable cells with greater than background auto-fluorescence by the total number of viable cells. For spore internalization experiments, viable mammalian cells (typically 90-98% of the total events) were readily identified by their high forward scatter and lack of propidium iodide (PI) staining. A second distinct population, (2-10%) of dead cells was routinely detected with relatively lower forward scatter (which indicates a smaller size) and positive PI staining (indicating non-viable cells; data not shown). Over the course of 60 min, we observed no detectable increase in cell death in the presence of labeled spores, as indicated by PI uptake (data not shown). Finally, sample debris (as indicated by relatively lower forward and side scatter and a lack of PI staining) represented a small fraction (1-2%) of the detected events. Based on these data, the data from subsequent experiments were gated to include only viable cells, while excluding non-viable cells, cellular debris, and spores not associated with cells. Alternatively, the time dependent total uptake of spores was determined by plotting the geometric mean of the fluorescence intensity (MFI).

5.4.11 Quantification of viable, intracellular *B. anthracis*.

Cells were incubated with dormant *B. anthracis* spores, as indicated above. For germinated *B. anthracis* spore infections, *B. anthracis* spore were germinated with 10 mM L-alanine and L-inosine in 1x PBS pH 7.2 for 30 min and washed twice with 1x PBS pH 7.2 to remove germinants and enumerated as described above. After 30 min, cells were washed three times with HBSS, and further incubated in the indicated medium with FBS (10%) and gentamicin (100 µg/ml) to kill all external germinated spores. After 15 min, the cells were washed three times with HBSS, and further incubated in the indicated appropriate medium supplemented with FBS (10%). At the indicated times, the cells were lysed by incubating with sterile tissue culture grade water (Mediatech) for 5 min at 25 °C. Serial dilutions of the lysates were plated on LB agar plates and incubated overnight at 37 °C. CFU were enumerated by direct counting of visible colonies and correcting for the appropriate dilution.

5.4.12 Statistics.

All data are representative of those from three or more independent experiments. The *Q*-test was performed to eliminate data that were statistical outliers (11). Error bars represent standard deviations. *P* values were calculated with Student's *t* test using paired, one-tailed distribution. *P* < 0.05 indicates statistical significance. Statistical analyses to calculate means, standard deviations, and Student's *t* tests, were calculated using Microsoft Excel (version 11.0).

5.5 References

1. **Banks, D. J., M. Barnajian, F. J. Maldonado-Arocho, A. M. Sanchez, and K. A. Bradley.** 2005. Anthrax toxin receptor 2 mediates *Bacillus anthracis* killing of macrophages following spore challenge. *Cell Microbiol* **7**:1173-85.
2. **Barlass, P. J., C. W. Houston, M. O. Clements, and A. Moir.** 2002. Germination of *Bacillus cereus* spores in response to L-alanine and to inosine: the roles of *gerL* and *gerQ* operons. *Microbiology* **148**:2089-95.
3. **Bergman, N. H., E. C. Anderson, E. E. Swenson, B. K. Janes, N. Fisher, M. M. Niemeyer, A. D. Miyoshi, and P. C. Hanna.** 2007. Transcriptional profiling of *Bacillus anthracis* during infection of host macrophages. *Infect Immun* **75**:3434-44.
4. **Bergman, N. H., K. D. Passalacqua, R. Gaspard, L. M. Shetron-Rama, J. Quackenbush, and P. C. Hanna.** 2005. Murine macrophage transcriptional responses to *Bacillus anthracis* infection and intoxication. *Infect Immun* **73**:1069-80.
5. **Cleret, A., A. Quesnel-Hellmann, A. Vallon-Eberhard, B. Verrier, S. Jung, D. Vidal, J. Mathieu, and J. N. Tournier.** 2007. Lung dendritic cells rapidly mediate anthrax spore entry through the pulmonary route. *J Immunol* **178**:7994-8001.
6. **Coligan, J. E.** 1991. *Current Protocols in Immunology*. Wiley.
7. **Cote, C. K., K. M. Rea, S. L. Norris, N. van Rooijen, and S. L. Welkos.** 2004. The use of a model of *in vivo* macrophage depletion to study the role of macrophages during infection with *Bacillus anthracis* spores. *Microb Pathog* **37**:169-75.
8. **Cote, C. K., N. Van Rooijen, and S. L. Welkos.** 2006. Roles of macrophages and neutrophils in the early host response to *Bacillus anthracis* spores in a mouse model of infection. *Infect Immun* **74**:469-80.
9. **Dixon, T. C., A. A. Fadl, T. M. Koehler, J. A. Swanson, and P. C. Hanna.** 2000. Early *Bacillus anthracis*-macrophage interactions: intracellular survival survival and escape. *Cell Microbiol* **2**:453-63.
10. **Dixon, T. C., M. Meselson, J. Guillemin, and P. C. Hanna.** 1999. Anthrax. *N Engl J Med* **341**:815-26.
11. **Dixon, W.** 1950. Analysis of extreme values. *Ann Math Stat* **21**:488-506.

12. **Dozmorov, M., W. Wu, K. Chakrabarty, J. L. Booth, R. E. Hurst, K. M. Coggeshall, and J. P. Metcalf.** 2009. Gene expression profiling of human alveolar macrophages infected by *B. anthracis* spores demonstrates TNF- α and NF- κ B are key components of the innate immune response to the pathogen. *BMC Infect Dis* **9**:152.
13. **Drysdale, M., S. Heninger, J. Hutt, Y. Chen, C. R. Lyons, and T. M. Koehler.** 2005. Capsule synthesis by *Bacillus anthracis* is required for dissemination in murine inhalation anthrax. *Embo J* **24**:221-7.
14. **Fisher, N., and P. Hanna.** 2005. Characterization of *Bacillus anthracis* germinant receptors *in vitro*. *J Bacteriol* **187**:8055-62.
15. **Frankel, A. E., S. R. Kuo, D. Dostal, L. Watson, N. S. Duesbery, C. P. Cheng, H. J. Cheng, and S. H. Leppla.** 2009. Pathophysiology of anthrax. *Front Biosci* **14**:4516-24.
16. **Friedlander, A. M., S. L. Welkos, M. L. Pitt, J. W. Ezzell, P. L. Worsham, K. J. Rose, B. E. Ivins, J. R. Lowe, G. B. Howe, P. Mikesell, and et al.** 1993. Postexposure prophylaxis against experimental inhalation anthrax. *J Infect Dis* **167**:1239-43.
17. **Glomski, I. J., A. Piris-Gimenez, M. Huerre, M. Mock, and P. L. Goossens.** 2007. Primary involvement of pharynx and peyer's patch in inhalational and intestinal anthrax. *PLoS Pathog* **3**:e76.
18. **Guidi-Rontani, C.** 2002. The alveolar macrophage: the Trojan horse of *Bacillus anthracis*. *Trends Microbiol* **10**:405-9.
19. **Guidi-Rontani, C., M. Levy, H. Ohayon, and M. Mock.** 2001. Fate of germinated *Bacillus anthracis* spores in primary murine macrophages. *Mol Microbiol* **42**:931-8.
20. **Guidi-Rontani, C., and M. Mock.** 2002. Macrophage interactions. *Curr Top Microbiol Immunol* **271**:115-41.
21. **Guidi-Rontani, C., M. Weber-Levy, E. Labruyere, and M. Mock.** 1999. Germination of *Bacillus anthracis* spores within alveolar macrophages. *Mol Microbiol* **31**:9-17.
22. **Gut, I. M., A. M. Prouty, J. D. Ballard, W. A. van der Donk, and S. R. Blanke.** 2008. Inhibition of *Bacillus anthracis* spore outgrowth by nisin. *Antimicrob Agents Chemother* **52**:4281-8.
23. **Hed, J., G. Hallden, S. G. Johansson, and P. Larsson.** 1987. The use of fluorescence quenching in flow cytometry to measure the attachment and ingestion phases in phagocytosis in peripheral blood without prior cell separation. *J Immunol Methods* **101**:119-25.

24. **Henderson, D. W., S. Peacock, and F. C. Belton.** 1956. Observations on the prophylaxis of experimental pulmonary anthrax in the monkey. *J Hyg (Lond)* **54**:28-36.
25. **Hu, H., J. Emerson, and A. I. Aronson.** 2007. Factors involved in the germination and inactivation of *Bacillus anthracis* spores in murine primary macrophages. *FEMS Microbiol Lett* **272**:245-50.
26. **Hu, H., Q. Sa, T. M. Koehler, A. I. Aronson, and D. Zhou.** 2006. Inactivation of *Bacillus anthracis* spores in murine primary macrophages. *Cell Microbiol* **8**:1634-42.
27. **Ireland, J. A., and P. C. Hanna.** 2002. Amino acid- and purine ribonucleoside-induced germination of *Bacillus anthracis* Δ Sterne endospores: *gerS* mediates responses to aromatic ring structures. *J Bacteriol* **184**:1296-303.
28. **Kang, T. J., M. J. Fenton, M. A. Weiner, S. Hibbs, S. Basu, L. Baillie, and A. S. Cross.** 2005. Murine macrophages kill the vegetative form of *Bacillus anthracis*. *Infect Immun* **73**:7495-501.
29. **Levinson, H. S., and M. T. Hyatt.** 1966. Sequence of events during *Bacillus megaterim* spore germination. *J Bacteriol* **91**:1811-8.
30. **McKevitt, M. T., K. M. Bryant, S. M. Shakir, J. L. Larabee, S. R. Blanke, J. Lovchik, C. R. Lyons, and J. D. Ballard.** 2007. Effects of endogenous D-alanine synthesis and autoinhibition of *Bacillus anthracis* germination on in vitro and in vivo infections. *Infect Immun* **75**:5726-34.
31. **Moir, A.** 2006. How do spores germinate? *J Appl Microbiol* **101**:526-30.
32. **Moir, A., B. M. Corfe, and J. Behravan.** 2002. Spore germination. *Cell Mol Life Sci* **59**:403-9.
33. **Oliva, C., C. L. Turnbough, Jr., and J. F. Kearney.** 2009. CD14-Mac-1 interactions in *Bacillus anthracis* spore internalization by macrophages. *Proc Natl Acad Sci U S A* **106**:13957-62.
34. **Oliva, C. R., M. K. Swiecki, C. E. Griguer, M. W. Lisanby, D. C. Bullard, C. L. Turnbough, Jr., and J. F. Kearney.** 2008. The integrin Mac-1 (CR3) mediates internalization and directs *Bacillus anthracis* spores into professional phagocytes. *Proc Natl Acad Sci U S A* **105**:1261-6.
35. **Paidhungat, M., and P. Setlow.** 2000. Role of *ger* proteins in nutrient and nonnutrient triggering of spore germination in *Bacillus subtilis*. *J Bacteriol* **182**:2513-9.

36. **Pickering, A. K., and T. J. Merkel.** 2004. Macrophages release tumor necrosis factor alpha and interleukin-12 in response to intracellular *Bacillus anthracis* spores. *Infect Immun* **72**:3069-72.
37. **Pickering, A. K., M. Osorio, G. M. Lee, V. K. Grippe, M. Bray, and T. J. Merkel.** 2004. Cytokine response to infection with *Bacillus anthracis* spores. *Infect Immun* **72**:6382-9.
38. **Porasuphatana, S., G. L. Cao, P. Tsai, F. Tavakkoli, T. Huwar, L. Baillie, A. S. Cross, P. Shapiro, and G. M. Rosen.** 2010. *Bacillus anthracis* endospores regulate ornithine decarboxylase and inducible nitric oxide synthase through ERK1/2 and p38 mitogen-activated protein kinases. *Curr Microbiol.*
39. **Russell, B. H., Q. Liu, S. A. Jenkins, M. J. Tuvim, B. F. Dickey, and Y. Xu.** 2008. *In vivo* demonstration and quantification of intracellular *Bacillus anthracis* in lung epithelial cells. *Infect Immun* **76**:3975-83.
40. **Russell, B. H., R. Vasan, D. R. Keene, T. M. Koehler, and Y. Xu.** 2008. Potential dissemination of *Bacillus anthracis* utilizing human lung epithelial cells. *Cell Microbiol* **10**:945-57.
41. **Russell, B. H., R. Vasan, D. R. Keene, and Y. Xu.** 2007. *Bacillus anthracis* internalization by human fibroblasts and epithelial cells. *Cell Microbiol* **9**:1262-74.
42. **Ruthel, G., W. J. Ribot, S. Bavari, and T. A. Hoover.** 2004. Time-lapse confocal imaging of development of *Bacillus anthracis* in macrophages. *J Infect Dis* **189**:1313-6.
43. **Sabet, M., H. B. Cottam, and D. G. Guiney.** 2006. Modulation of cytokine production and enhancement of cell viability by TLR7 and TLR9 ligands during anthrax infection of macrophages. *FEMS Immunol Med Microbiol* **47**:369-79.
44. **Sanz, P., L. D. Teel, F. Alem, H. M. Carvalho, S. C. Darnell, and A. D. O'Brien.** 2008. Detection of *Bacillus anthracis* spore germination *in vivo* by bioluminescence imaging. *Infect Immun* **76**:1036-47.
45. **Setlow, P.** 2003. Spore germination. *Curr Opin Microbiol* **6**:550-6.
46. **Shakir, S. M., K. M. Bryant, J. L. Larabee, E. E. Hamm, J. Lovchik, C. R. Lyons, and J. D. Ballard.** 2010. Regulatory interactions of a virulence-associated serine/threonine phosphatase-kinase pair in *Bacillus anthracis*. *J Bacteriol* **192**:400-9.

47. **Shetron-Rama, L. M., A. C. Herring-Palmer, G. B. Huffnagle, and P. Hanna.** 2010. Transport of *Bacillus anthracis* from the lungs to the draining lymph nodes is a rapid process facilitated by CD11c+ cells. *Microb Pathog* **49**:38-46.
48. **Stojkovic, B., E. M. Torres, A. M. Prouty, H. K. Patel, L. Zhuang, T. M. Koehler, J. D. Ballard, and S. R. Blanke.** 2008. High-throughput, single-cell analysis of macrophage interactions with fluorescently labeled *Bacillus anthracis* spores. *Appl Environ Microbiol* **74**:5201-10.
49. **Tournier, J. N., A. Quesnel-Hellmann, A. Cleret, and D. R. Vidal.** 2007. Contribution of toxins to the pathogenesis of inhalational anthrax. *Cell Microbiol* **9**:555-65.
50. **Weiner, M. A., T. D. Read, and P. C. Hanna.** 2003. Identification and characterization of the *gerH* operon of *Bacillus anthracis* endospores: a differential role for purine nucleosides in germination. *J Bacteriol* **185**:1462-4.
51. **Welkos, S., A. Friedlander, S. Weeks, S. Little, and I. Mendelson.** 2002. *In-vitro* characterisation of the phagocytosis and fate of anthrax spores in macrophages and the effects of anti-PA antibody. *J Med Microbiol* **51**:821-31.
52. **Xue, Q., S. A. Jenkins, C. Gu, E. Smeds, Q. Liu, R. Vasan, B. H. Russell, and Y. Xu.** 2010. *Bacillus anthracis* spore entry into epithelial cells is an actin-dependent process requiring c-Src and PI3K. *PLoS One* **5**:e11665.
53. **Zaucha, G. M., L. M. Pitt, J. Estep, B. E. Ivins, and A. M. Friedlander.** 1998. The pathology of experimental anthrax in rabbits exposed by inhalation and subcutaneous inoculation. *Arch Pathol Lab Med* **122**:982-92.

CHAPTER 6: NISIN MODULATION OF *BACILLUS ANTHRACIS* SPORE AND IMMUNE CELL INTERACTIONS AND SURVIVAL

6.1 Introduction

Spores enter the mammalian host via broken skin, the gastrointestinal tract when ingested orally, and the lungs through inhalation of spores, which is the most deadly route of infection (11, 14, 23-25). Interaction between immune cells and *B. anthracis* spores is essential for infection and dissemination of disease within a host especially within an inhalation infection, which is contingent upon spore-immune cell interaction that results in phagocytosis of inhaled spores by alveolar macrophages or dendritic cells sampling the alveolar space.

Dissemination of infection into the spleen and liver begins with trafficking of spore-containing immune cells to regional lymph nodes followed by the release of *B. anthracis* spores or bacilli into the bloodstream (24, 26, 39). The establishment of a systemic infection without medical intervention will result in bacteremia, toxemia, and ultimately death of the host (15, 39). Recent literature has also pointed to the use of alveolar epithelial cells as a potential route of spore egress from the lungs (35).

The resistance of *B. anthracis* to several antibiotics and the capacity to acquire resistance to currently used antibiotics underscores the importance of identifying new antimicrobials and therapies that can be utilized against anthrax. *B. anthracis* demonstrates resistance to bacitracin, cephalosporin, and streptomycin (8, 29). Currently employed antibiotic treatments, primarily ciprofloxacin and doxycycline, caused adverse side effects such as severe gastrointestinal symptoms, such as diarrhea and vomiting, seizures,

hallucinations, and anaphylaxis, which were observed during post-exposure prophylaxis to aerosolized *B. anthracis* endospores (31, 37). *B. anthracis* development of reduced susceptibility to the quinolones occurred in the presence of sub-inhibitory concentrations of ofloxacin or ciprofloxacin(41). Current treatments of endemic anthrax outbreaks in developing countries have resulted in penicillin resistant *B. anthracis* by activating the dormant β -lactamase present in all tested isolates (10). The acquisition of antibiotic resistance gene(s) through horizontal gene transfer is of great concern, originating in part from the ability of *B. anthracis* to become competent for transformation when experiencing nutrient limited conditions (33).

Current antibiotic treatments require that the spore be fully germinated and outgrown into a vegetative cell with functional metabolism for antibiotics to target protein synthesis, cell wall biosynthesis, specific metabolic pathways, or DNA replication. Cell wall and DNA replication inhibition will prevent bacteremia by blocking growth. It is notable that these drugs will not eliminate the effects on the host of bacterial produced toxins. Therefore, ribosomal inhibitors in conjunction with these antimicrobials are required to prevent toxin synthesis to eliminate toxemia (31, 37). The adverse side effects associated with treatment of anthrax infections and the ability of *B. anthracis* to acquire antibiotic resistance underscores the critical need for the development of alternative treatments.

As described in previous chapters, lantibiotics are cationic antimicrobial peptides (9) that provide a unique peptide platform to inhibit infections by spore-forming pathogens such as *B. anthracis*. As discussed in chapter 1, nisin is a

highly post-translationally modified peptide containing non-proteogenic amino acids and (methyl)lanthionine thioether rings, which provides resistance to proteolytic degradation and the necessary structural constraints for target recognition (9). Nisin induces pore formation in lipid membranes (34) and inhibits transglycosylation preventing cell wall biosynthesis via lipid II binding to inhibit vegetative bacteria (28, 43) while preventing germinating spore outgrowth via membrane disruption (27). Interestingly, nisin has been relatively unaffected by the emergence of microbial resistance, despite widespread use in the food industry as a preservative (13, 34).

Because *B. anthracis* spore interactions with macrophages and dendritic cells are important for both the dissemination and control of disease progression, the effects of nisin on spore interactions with these immune cells was investigated. Taking advantage of the *in vitro* infection model discussed in chapter 5 (38), the effects nisin has on spore-immune cell interactions were evaluated utilizing both alveolar and peritoneal cultured macrophage cell lines and a cultured dendritic cell line. The effect nisin has on the survival of both the spore and the immune cell during and post infection was investigated. In addition, any effects nisin would have on binding and phagocytosis of the spore were evaluated. Further interrogation of spore-immune cell interactions centered on whether nisin was able to interact with the spore within a macrophage during and post infection to determine the effect of post exposure treatment. In addition, cytokine expression was used to evaluate whether nisin prevents the establishment of a "normal" infection as well as whether nisin, itself, is immuno-

modulatory. Collectively, the data demonstrated that nisin aids in immune cells clearance of spore infection while reducing the proper establishment of an infection within an *in vitro* infection model and increased immune cell survival.

6.2 Results

6.2.1 Nisin induced dose dependent clearance of viable B. anthracis.

To determine whether nisin would aid in the clearance of bound and phagocytized viable *B. anthracis* associated with macrophages and dendritic cells, immune cells were infected with spores with nisin treatment during the infection. These infections were also performed in the presence or absence of a potent germinant, fetal bovine serum (FBS) (Chapter 5). When nisin was present in both germinating and non-germinating conditions during RAW264.7 (peritoneal macrophage-like cells) infections, nisin was able to significantly reduce the number of recoverable viable organisms within macrophages at 60 min at both 1 and 10 μ M nisin (Figure 6.1 A, B). Furthermore, nisin was effective at reducing the number of viable organisms in germinating and non-germinating conditions through 240 min at 10 μ M (Figure 6.1 A, B). Further investigation identified that nisin was able to reduce the number of recoverable viable organisms from spore infected MH-S (alveolar macrophages) and JAWSII (dendritic cells) for both germinating and non-germinating conditions beginning at 1 h through 4 h (Figure 6.1 C-F). Moreover, nisin was able to reduce the number of viable bacilli beginning at 1 h through 4 h when RAW264.7 macrophages were infected with vegetative bacteria (Figure 6.2). Non-germinating spores (heat treated samples)

were not affected by antibiotic intervention (Figure 6.2). When the activity of nisin was compared to gentamicin within an infection, only nisin was able to eliminate all germinated, heat sensitive, spores in both germinating and non-germinating infections (Figure 6.3). In long term infections, both nisin (0.1-10 μM) and gentamicin were able to prevent visible growth within the cell culture medium (data not shown). Collectively, these data indicate that nisin was a potent inhibitor of *B. anthracis* when cells were treated during an infection.

Figure 6.1

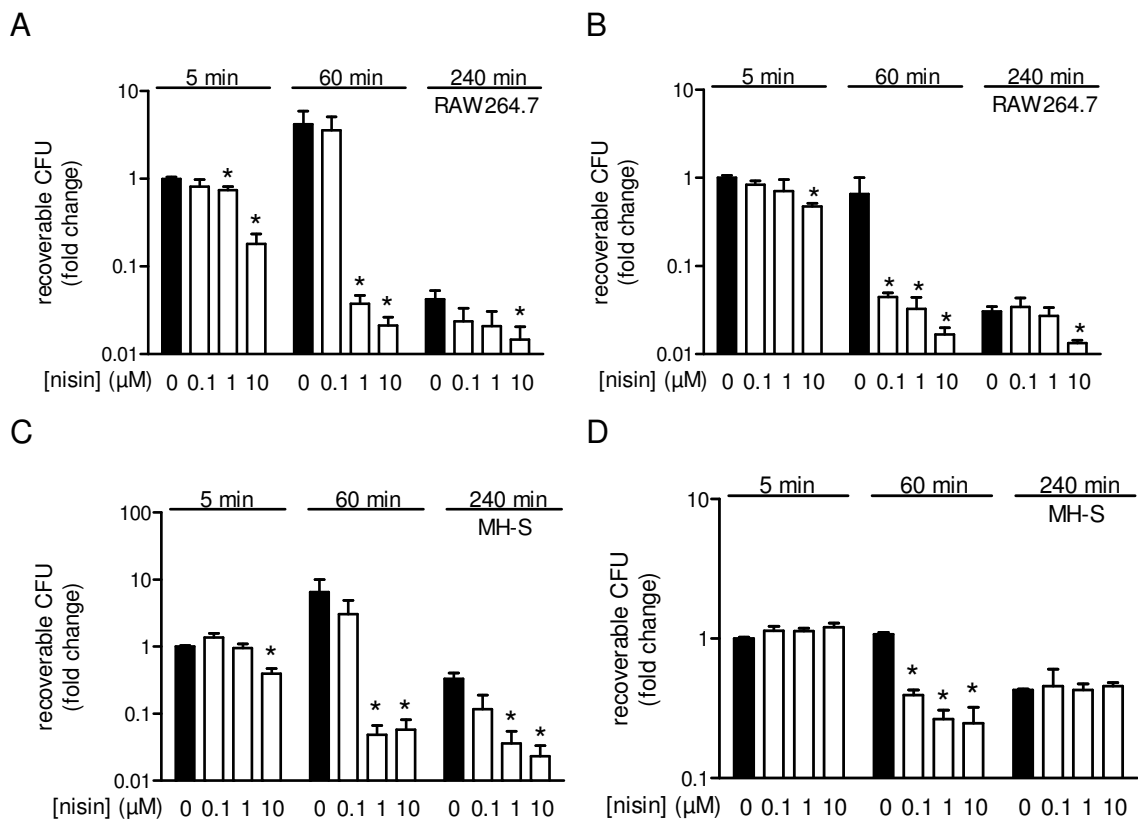
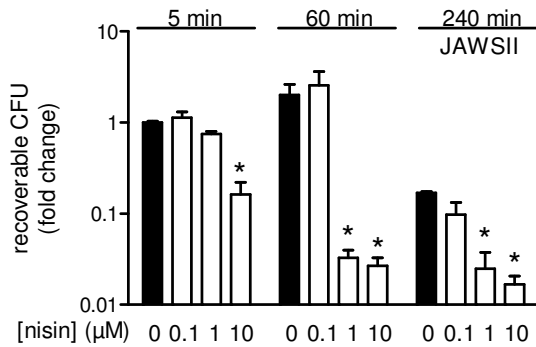


Figure 6.1 (continued)

E



F

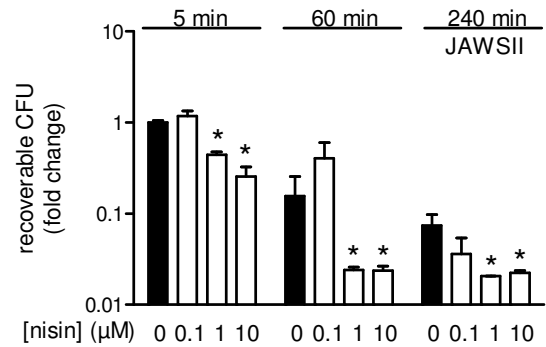


Figure 6.1. Nisin induced dose dependent clearance of viable *B. anthracis*. A,C,E.

Germinating constant infection was performed with FBS as a germinant. B,D, F. B. Non-germinating constant infection was performed in the absence of FBS. A-F. The data are expressed as the fold change of recoverable colony forming units (CFU) at 5, 60, and 240 min from lysed immune cells. * indicates a $P < 0.05$ between control (0 μM nisin, black) and experimental condition (0.1 - 10 μM nisin, white). Error bars indicate standard deviations.

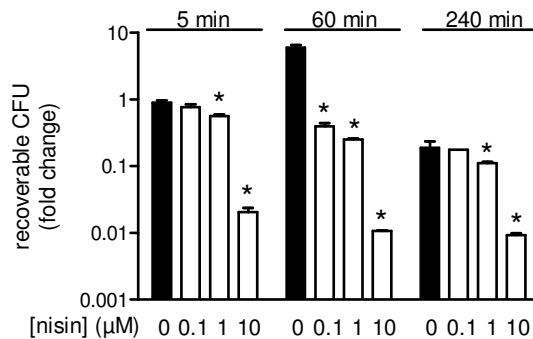


Figure 6.2. Nisin induced dose dependent clearance of viable *B. anthracis* vegetative

cells. Constant infection was performed in the presence of FBS. The data are expressed as the fold change of recoverable colony forming units (CFU) at 5, 60, and 240 min from lysed immune cells. * indicates a $P < 0.05$ between control (0 μM nisin, black) and experimental condition (0.1 - 10 μM nisin, white). Error bars indicate standard deviations.

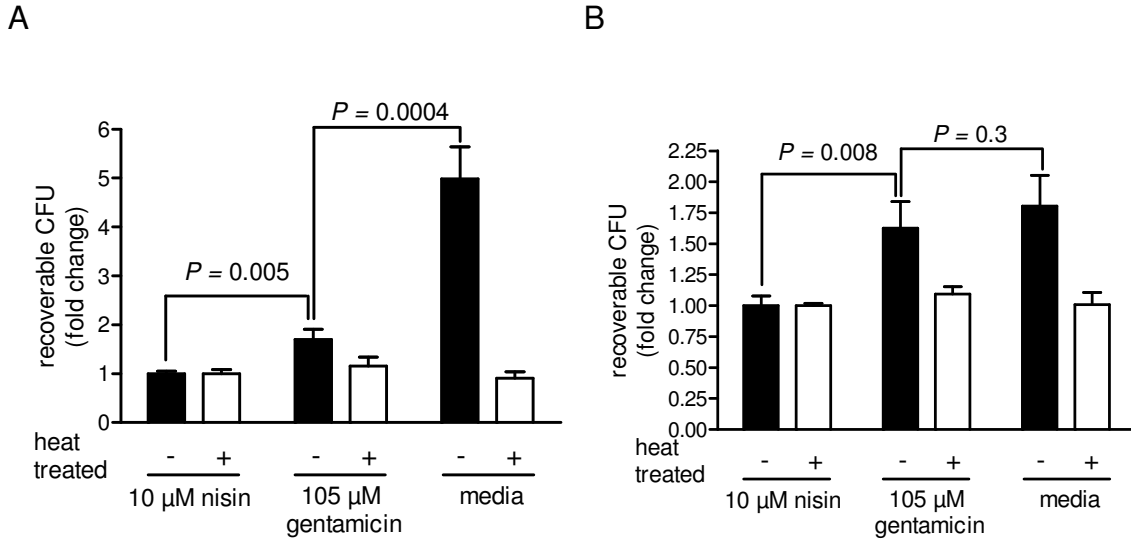


Figure 6.3. Nisin mediated greater clearance of viable *B. anthracis* than gentamicin. A. Germinating constant infection was performed with FBS as a germinant. B. Non-germinating constant infection was performed in the absence of FBS. The data are expressed as the fold change of recoverable colony forming units (CFU) at 60 min from lysed immune cells. Error bars indicate standard deviations.

6.2.2 Nisin prevents *B. anthracis* proliferation in post infection treatments.

Since nisin's presence during an infection was able to reduce the number of viable *B. anthracis*, it was necessary to determine whether nisin would be able to reduce the number of viable organisms within a macrophage post infection. When spores were used to infect RAW264.7 macrophages in germinating conditions followed by nisin addition, nisin was able to significantly reduce the number of viable organisms through 24 h (Figure 6.4 A). In addition, the presence of nisin at all concentrations, even at concentrations below the MIC for *B. anthracis* (27), prevented an increase in the number of viable organisms (Figure 6.4 A). Nisin reduced the number of viable organisms for both MH-S and

JAWSII cell lines in germinating conditions at 1 and 10 μM and prevented an increase in recoverable viable organisms at all concentrations (Figure 6.4 C, E). In the absence of nisin, the number of recoverable viable organisms increased over time for both cell lines (Figure 6.4 C, E). Even during a constant infection where spores were incubated with cells during the entire infection, nisin incubation with peritoneal macrophages prior to, simultaneous with, or post spore infection were able to reduce the number of recoverable CFUs (Figure 6.5).

When evaluating the effect of nisin under germinating conditions, nisin was able to prevent the increase of viable organisms recovered from RAW264.7, MH-S, and JAWSII cell lines (Figure 6.4 A,C,E). However, under non-germinating conditions, nisin at 1 and 10 μM prevented the increase of recoverable CFUs from RAW264.7 and MH-S macrophages (Figure 6.4 B,D) while a reduction was observed for JAWSII dendritic cells (Figure 6.4 F). As a comparator, polymixin B was only able to prevent an increase of recoverable CFU in germinating conditions (Figure 6.4). In addition, the presence of nisin (0.1-10 μM) and polymixin prevented or reduced visible bacterial growth within the cell culture medium for both germinating and non-germinating conditions (data not shown). When added post infection, the presence of nisin prevented an increase, or reduced recoverable CFU.

Figure 6.4

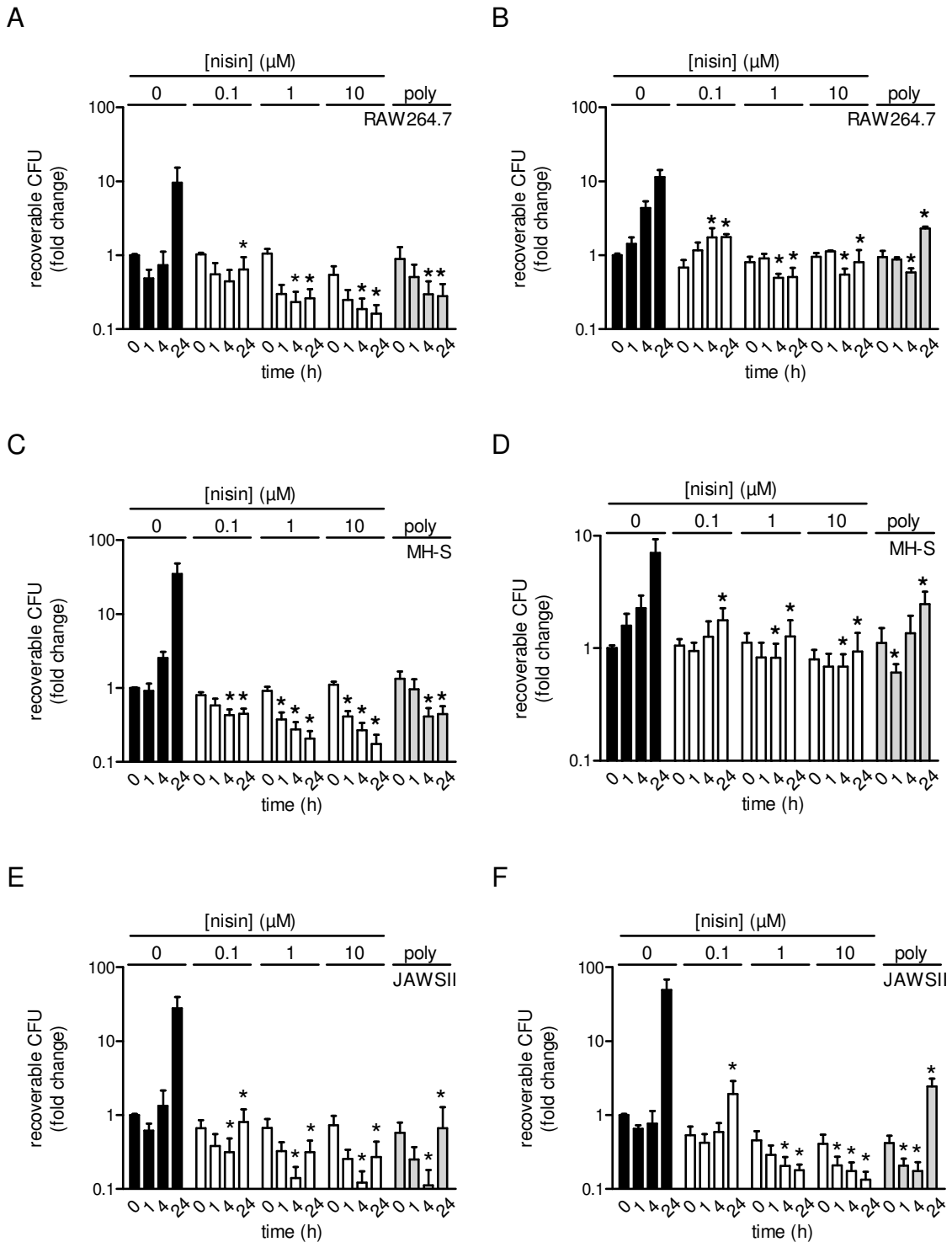


Figure 6.4. Nisin prevented *B. anthracis* proliferation in post infection treatments. A,C,E.

Immune cells were infected with *B. anthracis* spore under germinating conditions followed by gentamicin protection and post infection treatment with nisin in the presence of FBS as indicated

Figure 6.4 (continued)

in the “Materials and Methods”. B,D,F. Immune cells were infected with *B. anthracis* spore under non-germinating conditions followed by gentamicin protection and post infection treatment with nisin in the presence of FBS as indicated in the “Materials and Methods” A-F. The data are expressed as the fold change of recoverable colony forming units (CFU) at 0, 1, 4, and 24 h from lysed immune cells. * indicates a $P < 0.05$ between control (0 μM nisin, black) and experimental condition (0.1 - 10 μM nisin, white; 8 μM polymixin B, gray) at the corresponding time point. Error bars indicate standard deviations

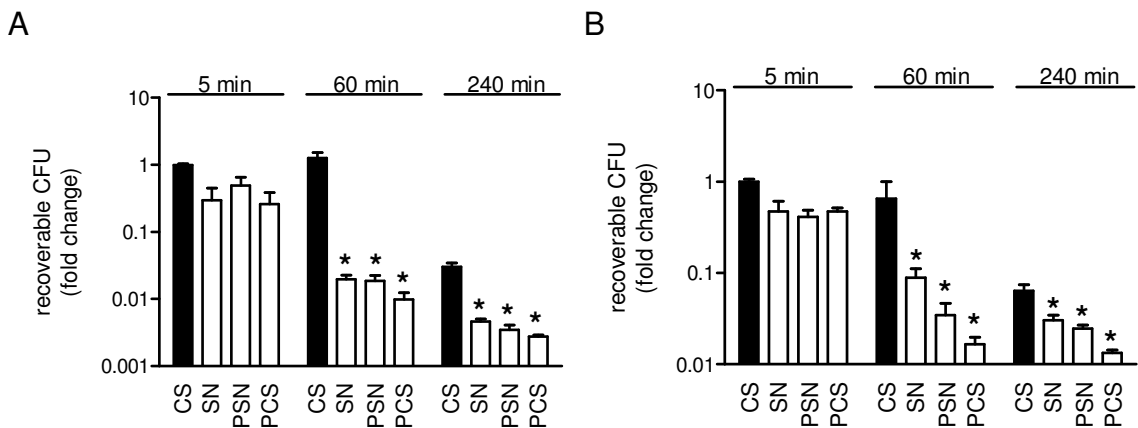


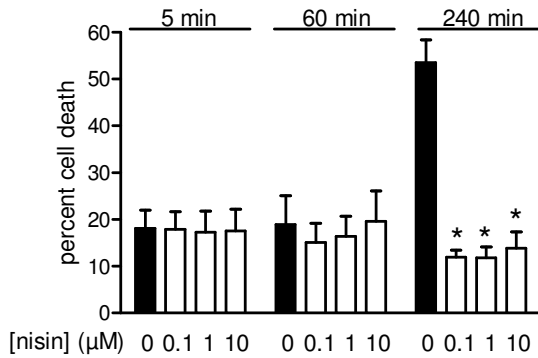
Figure 6.5. Nisin prevented *B. anthracis* proliferation when added prior to, during or post spore infection of macrophages. CS: Spore infection of RAW 264.7 macrophages. SN: Spore infection of RAW 264.7 macrophages in presence of 10 μM nisin. PSN: Spore and 10 μM nisin were pre-incubated prior to RAW 264.7 macrophages infection. PCS: Post infection addition of 10 μM nisin. A. Germinating constant infection was performed with FBS as a germinant. B.

Non-germinating constant infection was performed in the absence of FBS. A,B. The data are expressed as the fold change of recoverable colony forming units (CFU) at 0, 1, 4, and 24 h. * indicates a $P < 0.05$ between control (0 μM nisin, black) and experimental condition (10 μM nisin, white) at the corresponding time point.

6.2.3 Nisin increased the survival of immune cells.

It was unclear whether the nisin-dependent decrease in recoverable CFU discovered when mammalian cells were infected with *B. anthracis* spores would affect the viability of infected cells. Studies to address this issue revealed significantly fewer dead RAW264.7 cells when infected for 4 h in the presence than absence of nisin (Figure 6.6). The presence of nisin was also able to decrease RAW264.7 cell death when infected with *B. anthracis* bacilli (Figure 6.7). The addition of nisin (10 μ M) prior to, simultaneous with, or post an infection increased macrophage survival in either germinating or non-germinating conditions (Figure 6.8). When nisin was present during a 24 h constant infection of RAW264.7 macrophages, nisin (0.1-10 μ M) was able to prevent peritoneal macrophage cell death in both germinating and non-germinating conditions (Figure 6.9). The presence of nisin (0-10 μ M) post infection after gentamicin protection was able to prevent cell death in both germinating and non-germinating conditions (Figure 6.9). Nisin was also able to prevent immune cell death in both the constant and gentamicin protection infections of MH-S and JAWSII cell lines in both germinating and non-germinating conditions (Figure 6.9). These results indicate that the presence of nisin, even at non-inhibitory concentrations in solution, resulted in increased viability of infected mammalian cells during infection with spores.

A



B

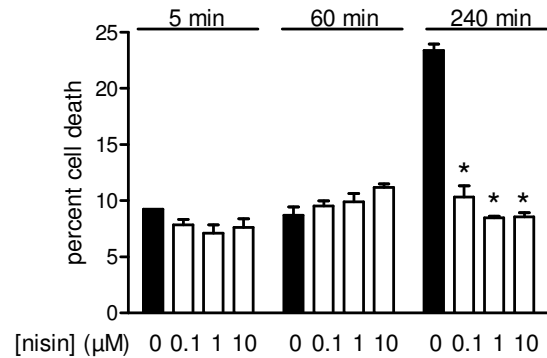


Figure 6.6. Nisin increased the short term survival of immune cells. A. Germinating

constant infection was performed with FBS as a germinant. B. Non-germinating constant infection was performed in the absence of FBS. A, B. Cell death was monitored as a function of PI uptake by immune cell. The data are expressed as percent cell death as a function of PI uptake at 5, 60, and 240 min. * indicates a $P < 0.05$ between control (0 μM nisin, black) and experimental condition (0.1 - 10 μM nisin, white). Error bars indicate standard deviations.

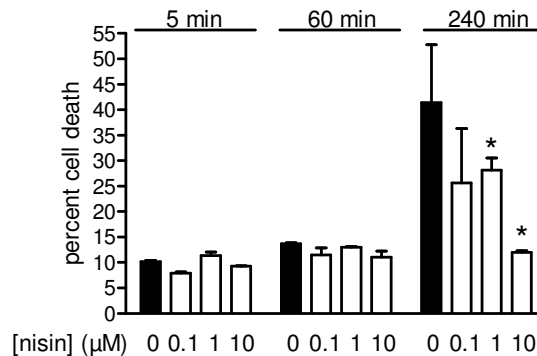


Figure 6.7. Nisin increased the short term survival of immune cells when infected by

vegetative cells. Constant infection was performed in the presence of FBS. Cell death was monitored as a function of PI uptake by immune cell. The data are expressed as percent cell death as a function of PI uptake at 5, 60, and 240 min. * indicates a $P < 0.05$ between control (0 μM nisin, black) and experimental condition (0.1 - 10 μM nisin, white). Error bars indicate standard deviations.

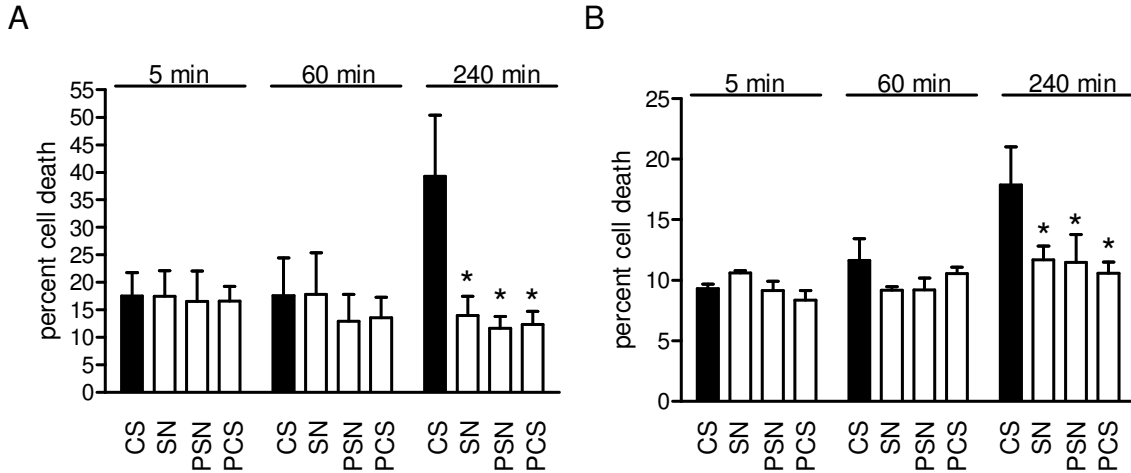


Figure 6.8. Nisin increased the short term survival of immune cells when added prior to, during or post spore infection of macrophages. CS: Spore infection of RAW 264.7 macrophages. SN: Spore infection of RAW 264.7 macrophages in presence of 10 μ M nisin. PSN: Spore and 10 μ M nisin were pre-incubated prior to RAW 264.7 macrophages infection. PCS: Post infection addition of 10 μ M nisin. A. Germinating constant infection was performed with FBS as a germinant. B. Non-germinating constant infection was performed in the absence of FBS. A,B. Cell death was monitored as a function of PI uptake by immune cell. The data are expressed as percent cell death as a function of PI uptake at 5, 60, and 240 min. * indicates a $P < 0.005$ between control (0 μ M nisin, black) and experimental condition (0.1 - 10 μ M nisin, white). Error bars indicate standard deviations.

Figure 6.9

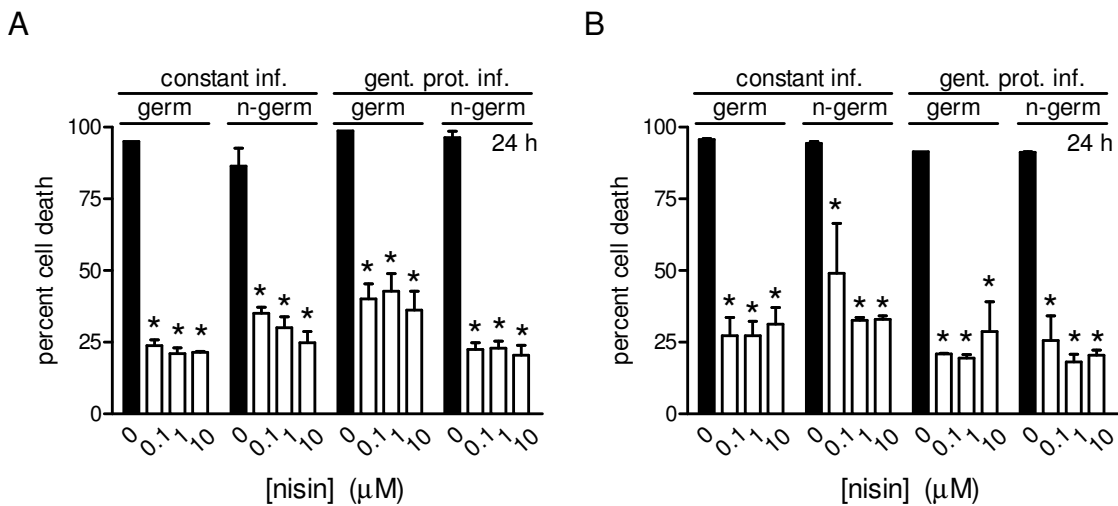


Figure 6.9 (continued)

C

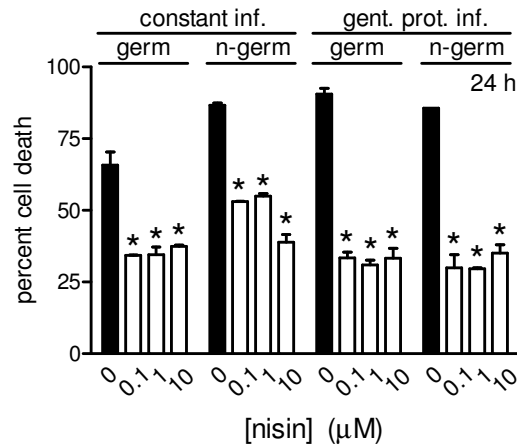


Figure 6.9. Nisin increased the long term survival of immune cells. A. RAW264.7 peritoneal macrophages. B. MH-S alveolar macrophages. C. JAWSII dendritic cells. A-C. Cell death was monitored at 24 h via PI uptake. The data are expressed as percent cell death as a function of PI uptake at 24 h. * indicates a $P < 0.005$ between control (0 μM nisin, black) and experimental condition (0.1 - 10 μM nisin, white). Error bars indicate standard deviations.

6.2.4 The presence of nisin during infection reduced spore association and internalization.

The effects of nisin on both the binding and uptake of Alexa Fluor 488-spores (AF488-spores) by mammalian cells were monitored by flow cytometry. These studies revealed that under both germinating and non-germinating conditions, the presence of nisin resulted in significantly fewer RAW264.7 cells with bound and internalized spores (Figure 6.10). Furthermore, nisin reduced spore binding and uptake in both germinating and non-germinating conditions by MH-S and JAWSII cell lines (data not shown). In addition, microscopic analysis of Alexa-Fluor 568 labeled spore (AF568-spore) infections of RAW264.7 cells in

the presence of 10 μ M nisin significantly reduced the number of spores within infected macrophages for both germinating and non-germinating infections (Figure 6.11). Nisin incubation with RAW264.7 cells prior to or during a constant spore infection was able to reduce the number of internalized spores while the addition of nisin after the infection time slowed the rate of further infection (Figure 6.12). As a control, nisin did not affect AF488-spore fluorescence (Figure 6.13), which indicates that the observed reduction in spore binding and uptake upon nisin addition was not a function of quenching spore fluorescence. When gentamicin protection infections were analyzed by flow cytometry, the addition of nisin as a post infection treatment did not alter extent of infection in germinating and non-germinating conditions for all cell lines (Figure 6.14 and data not shown). Nisin did not reduce the binding and uptake of fluorescent beads in the presence of FBS (germinant), but in the absence of a germinant, nisin increased the uptake of beads (Figure 6.15). Additionally, binding and uptake was reduced in a dose dependent fashion when RAW264.7 macrophages were infected with GFP-expressing bacilli, which suggests the reduction in *B. anthracis* interaction with immune cells is relevant to spores or vegetative cells rather than an inanimate polymer (Figure 6.16).

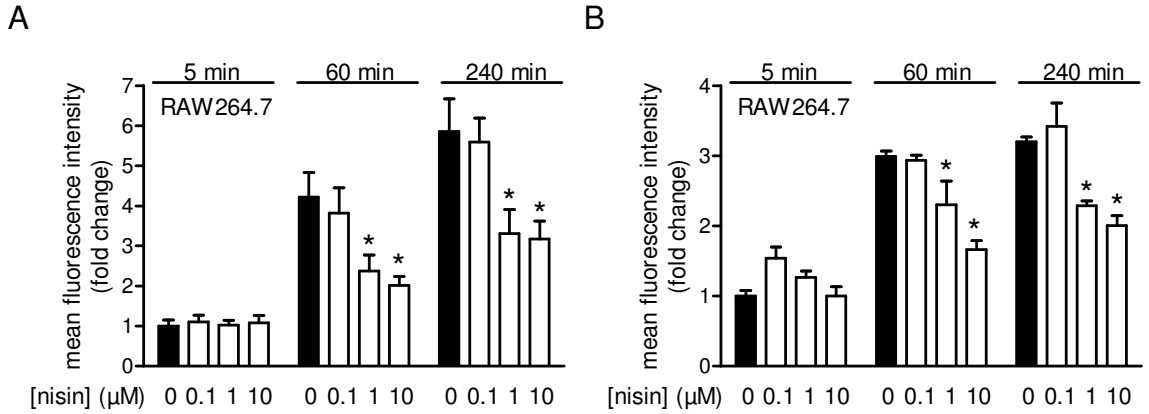


Figure 6.10. Nisin reduced spore interaction with immune cells. A. Germinating

constant infection was performed with FBS as a germinant. B. Non-germinating constant infection was performed in the absence of FBS. A, B. Immune cell binding and internalization of *B. anthracis* spore were monitored via an increase in immune cell fluorescence as a result of the interactions with fluorescently labeled spores. The data are expressed as the fold increase of mean fluorescence intensity of immune cells at 5, 60, and 240 min. * indicates a $P < 0.05$ between control (0 μM nisin, black) and experimental condition (0.1 - 10 μM nisin, white). Error bars indicate standard deviations.

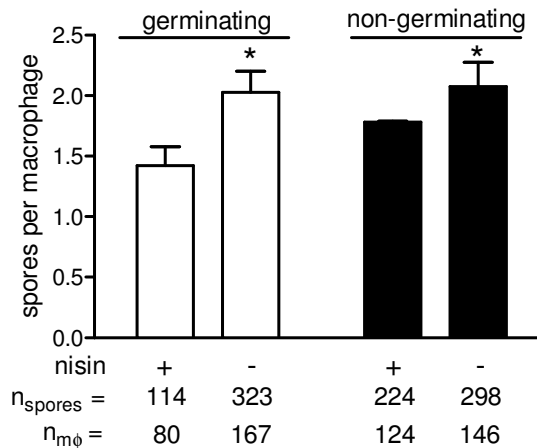


Figure 6.11. Quantification of spore per infected macrophages. The data are expressed as the number of spores per an infected macrophage. * indicates a $P < 0.05$ between an infection performed in the presence of 10 μM nisin and 0 μM nisin. Shown is the mean of a three experiments conducted in duplicate. Error bars indicate standard deviations. + : 10 μM nisin, - : 0 μM nisin.

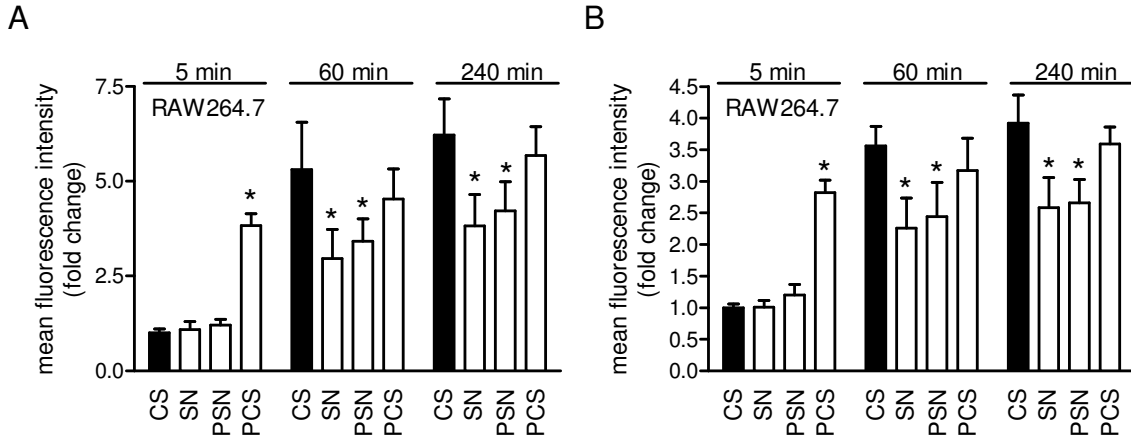


Figure 6.12. Nisin altered spore interaction with immune cells when added prior to, during or post spore infection of macrophages. CS: Spore infection of RAW 264.7 macrophages. SN: Spore infection of RAW 264.7 macrophages in presence of 10 μ M nisin. PSN: Spore and 10 μ M nisin were pre-incubated prior to RAW 264.7 macrophages infection. PCS: Post infection addition of 10 μ M nisin. A. Germinating constant infection was performed with FBS as a germinant. B. Non-germinating constant infection was performed in the absence of FBS. A, B. Immune cell binding and internalization of *B. anthracis* spore were monitored via an increase in immune cell fluorescence as a result of the interactions with fluorescently labeled spores. The data are expressed as the fold increase of mean fluorescence intensity of immune cells at 5, 60, and 240 min. * indicates a $P < 0.05$ between control (0 μ M nisin, black) and experimental condition (0.1 - 10 μ M nisin, white). Error bars indicate standard deviations

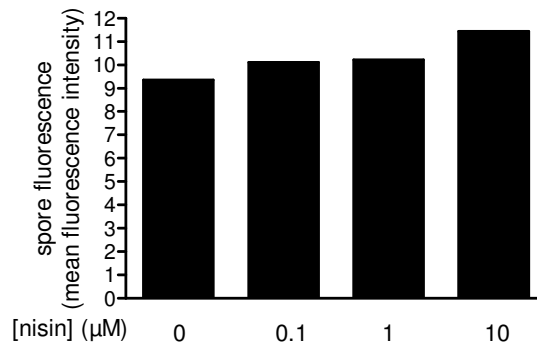
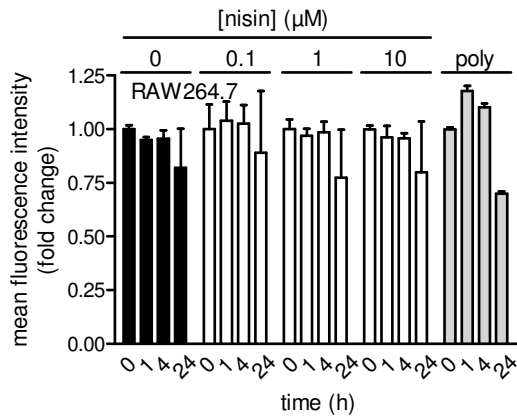


Figure 6.13. Nisin effect on spore fluorescence. AF488-spores were incubated in the presence of nisin (0-10 μ M) for 30 min at 37 $^{\circ}$ C. Flow cytometry was monitored the effect of nisin on spore fluorescence for 10,000 spores.

A



B

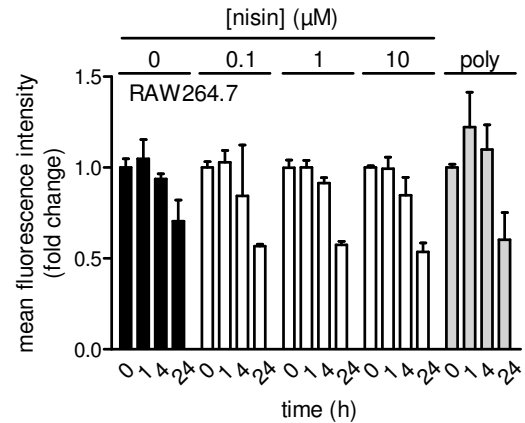


Figure 6.14. Nisin does not alter spore interactions with nisin added after infection of

RAW264.7 cells. A. Immune cells were infected with *B. anthracis* spore under germinating conditions followed by gentamicin protection and post infection treatment with nisin in the presence of FBS as indicated in the “Materials and Methods”. B. Immune cells were infected with *B. anthracis* spore under non-germinating conditions followed by gentamicin protection and post infection treatment with nisin in the presence of FBS as indicated in the “Materials and Methods”. A, B. Immune cell binding and internalization of *B. anthracis* spore were monitored via an increase in immune cell fluorescence as a result of the interactions with fluorescently labeled spores. The data are expressed as the fold increase of mean fluorescence intensity of immune cells at 5, 60, and 240 min. * indicates a $P < 0.05$ between control (0 μM nisin, black) and experimental conditions (0.1 - 10 μM nisin, white; 8 μM polymixin B, gray). Error bars indicate standard deviations.

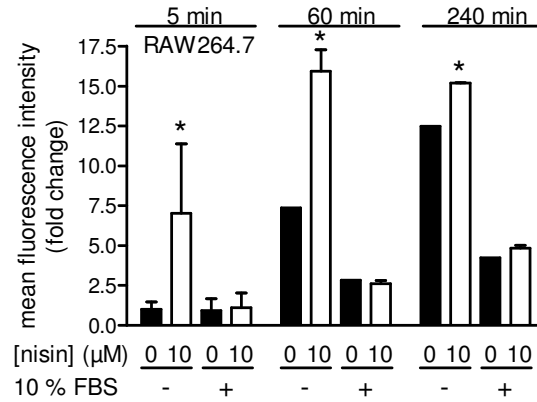


Figure 6.15. Addition of nisin altered the interaction between inert beads and immune cells. Germinating (+) and non-germinating (-) constant infections were performed with FBS as a germinant. Immune cell binding and internalization of *B. anthracis* spore were monitored via an increase in immune cell fluorescence as a result of the interactions with fluorescently labeled spores. The data are expressed as the fold increase of mean fluorescence intensity of immune cells at 5, 60, and 240 min. * indicates a $P < 0.05$ between control (0 µM nisin, black) and experimental condition (10 µM nisin, white). Error bars indicate standard deviations.

Figure 6.16

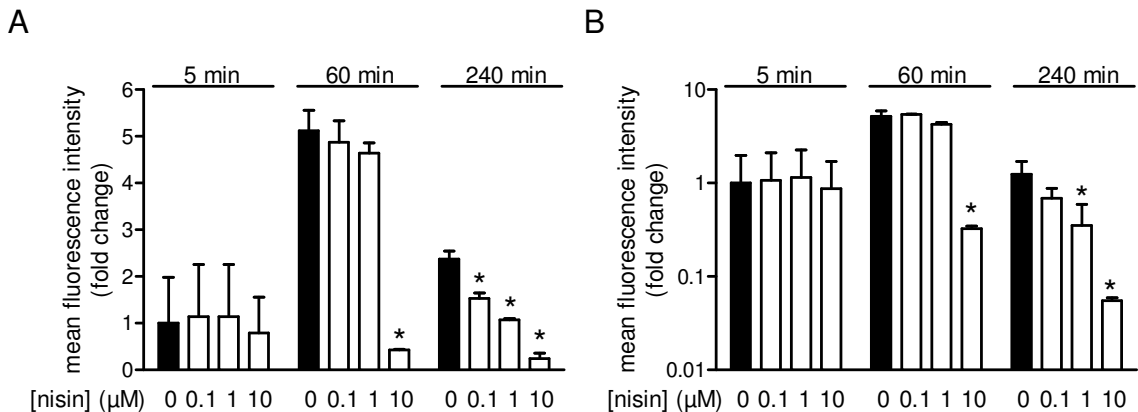


Figure 6.16. Nisin reduced bacilli interaction with immune cells. A. Germinating constant infection was performed with FBS as a germinant. B. Non-germinating constant infection was performed in the absence of FBS. A, B. Immune cell binding and internalization of *B. anthracis* bacilli were monitored via an increase in immune cell fluorescence as a result of the interactions with GFP-expressing bacilli. The data are expressed as the fold increase of mean

Figure 6.16 (continued)

fluorescence intensity of immune cells at 5, 60, and 240 min. * indicates a $P < 0.05$ between control (0 μM nisin, black) and experimental condition (0.1 - 10 μM nisin, white). Error bars indicate standard deviations.

The percentage of cells with internalized spores was significantly reduced in the presence versus absence of nisin (Figure 6.17). In contrast, nisin treatment after spore infection of immune cells did not alter the percentage of cells with internalized spores (Figure 6.18). Incubation of RAW264.7 cells with nisin prior to and simultaneous to further incubation with spores resulted in a significant reduction in the percentage of cells with internalized spores (Figure 6.19). Nisin also reduced the percentage of RAW264.7 macrophages infected with GFP-expressing bacilli (Figure 6.20). However, nisin did not reduce the percentage of cells with intracellular fluorescent beads in the presence or absence of germinant (FBS). Moreover, nisin increased the percentage of cells that took up beads in the absence of FBS (Figure 6.21).

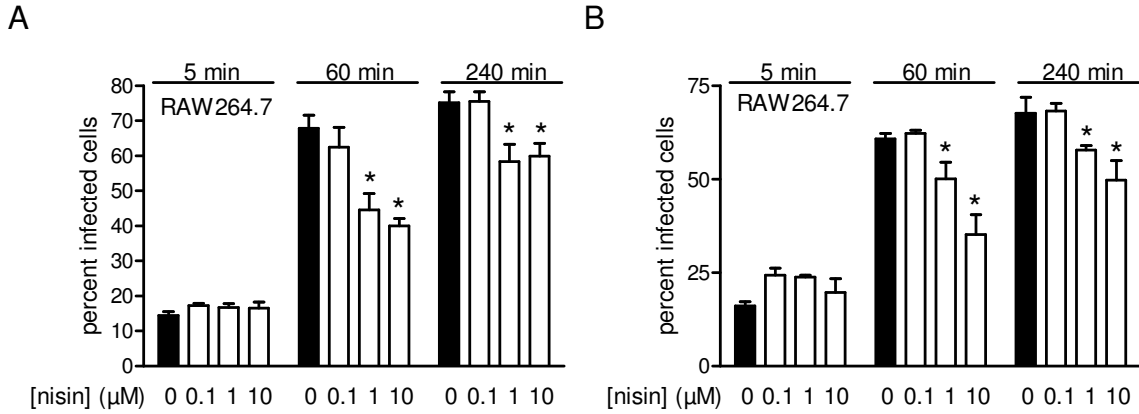


Figure 6.17. Nisin reduced spore infection of immune cells within the population. A.

Germinating constant infection was performed with FBS as a germinant. B. Non-germinating constant infection was performed in the absence of FBS. A, B. Immune cell infection with *B. anthracis* spores was monitored via an increase in immune cell fluorescence as a result of the interactions with fluorescently labeled spores. The data are expressed as the percent of immune cells displaying an increased fluorescence as a function of AF-488 spore interaction at 5, 60, and 240 min. * indicates a $P < 0.05$ between control (0 μM nisin, black) and experimental condition (0.1 - 10 μM nisin, white). Error bars indicate standard deviations.

Figure 6.18

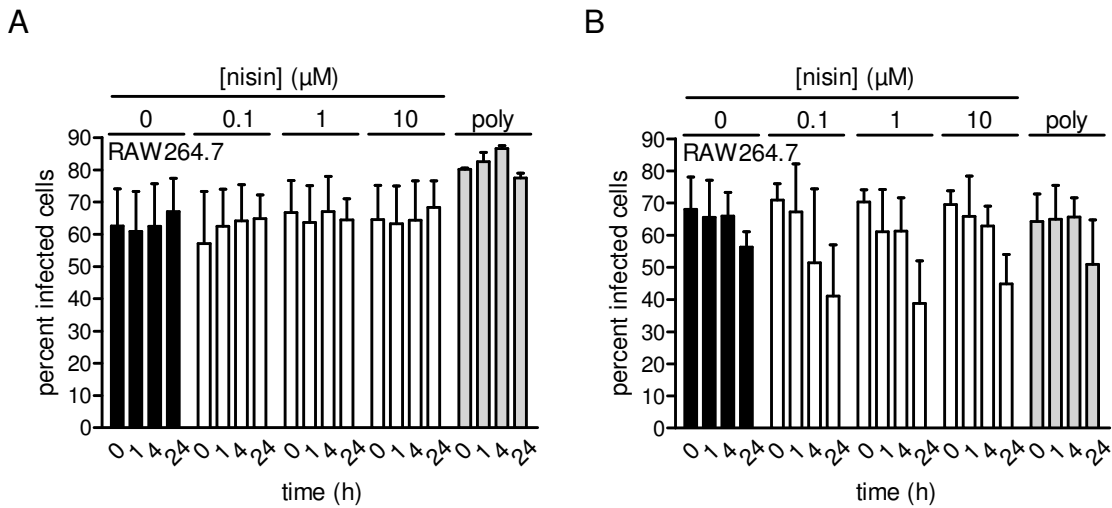


Figure 6.18. Nisin does not spore interaction with nisin post immune cell infection. A.

Immune cells were infected with *B. anthracis* spore under germinating conditions followed by gentamicin protection and post infection treatment with nisin in the presence of FBS as indicated

Figure 6.18 (continued)

in the “Materials and Methods”. B. Immune cells were infected with *B. anthracis* spore under non-germinating conditions followed by gentamicin protection and post infection treatment with nisin in the presence of FBS as indicated in the “Materials and Methods”. A, B. Immune cell infection with *B. anthracis* spores was monitored via an increase in immune cell fluorescence as a result of the interactions with fluorescently labeled spores. The data are expressed as the percent of immune cells displaying an increased fluorescence as a function of AF-488 spore interaction at 5, 60, and 240 min. * indicates a $P < 0.05$ between control (0 μM nisin, black) and experimental conditions (0.1 - 10 μM nisin, white; 8 μM polymixin B, gray). Error bars indicate standard deviations.

Figure 6.19

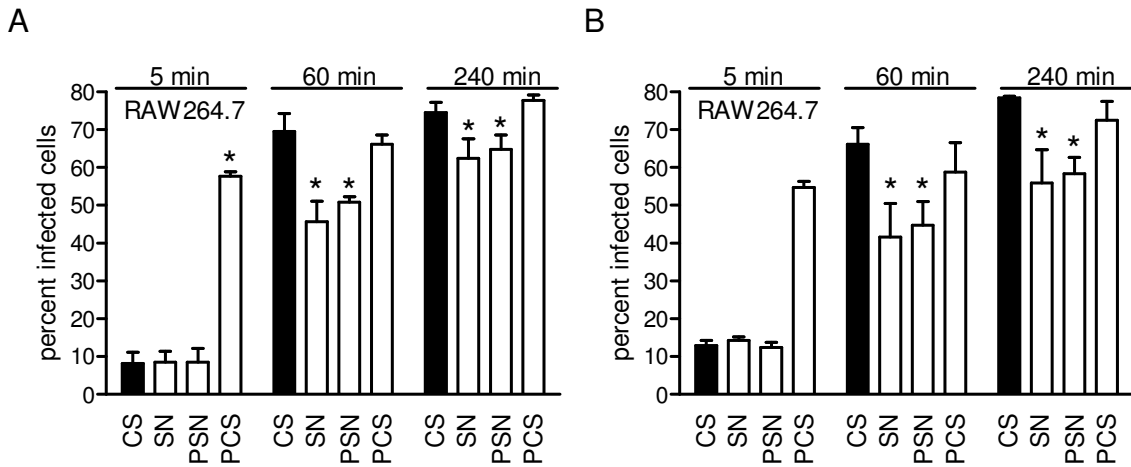


Figure 6.19. Nisin altered spore interaction with immune cells when added prior to, during or post spore infection of macrophages. CS: Spore infection of RAW 264.7 macrophages. SN: Spore infection of RAW 264.7 macrophages in presence of 10 μM nisin. PSN: Spore and 10 μM nisin were pre-incubated prior to RAW 264.7 macrophages infection. PCS: Post infection addition of 10 μM nisin. A. Germinating constant infection was performed with FBS as a germinant. B. Non-germinating constant infection was performed in the absence of FBS. A, B. Immune cell infection with *B. anthracis* spores was monitored via an increase in immune cell fluorescence as a result of the interactions with fluorescently labeled spores. The data are

Figure 6.19 (continued)

expressed as the percent of immune cells displaying an increased fluorescence as a function of AF-488 spore interaction at 5, 60, and 240 min. * indicates a $P < 0.05$ between control (0 μM nisin, black) and experimental condition (0.1 - 10 μM nisin, white). Error bars indicate standard deviations.

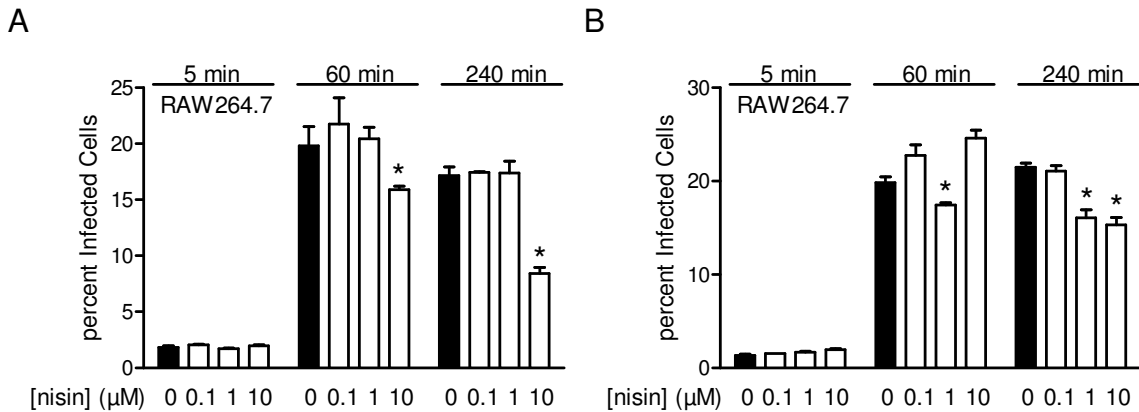


Figure 6.20. Nisin reduced bacilli infection of immune cells within the population. A. Germinating constant infection was performed with FBS as a germinant. B. Non-germinating constant infection was performed in the absence of FBS. A, B. Immune cell infection with *B. anthracis* bacilli was monitored via an increase in immune cell fluorescence as a result of the interactions with fluorescently labeled spores. The data are expressed as the percent of immune cells displaying an increased fluorescence as a function of GFP-expressing bacilli interaction at 5, 60, and 240 min. * indicates a $P < 0.05$ between control (0 μM nisin, black) and experimental condition (0.1 - 10 μM nisin, white). Error bars indicate standard deviations.

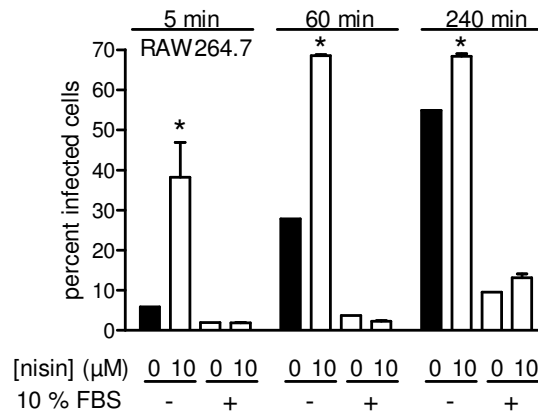


Figure 6.21. Addition of nisin altered immune cells internalization of inert beads.

Germinating (+) and non-germinating (-) constant infections were performed with FBS as a germinant. Immune cell infection with *B. anthracis* spores was monitored via an increase in immune cell fluorescence as a result of the interactions with fluorescently labeled spores. The data are expressed as the percent of immune cells displaying an increased fluorescence as a function of AF-488 spore interaction at 5, 60, and 240 min. * indicates a $P < 0.05$ between control (0 μM nisin, black) and experimental condition (10 μM nisin, white). Error bars indicate standard deviations.

To determine whether the nisin-dependent reduction in internalized spores was due to reduced binding of spores in the presence of nisin, RAW264.7 cells were pre-incubated with 10 μM nisin at 37 °C followed by further incubation of spores (MOI of 10) at 4 °C to prevent uptake, but not binding of spores to the cell surface. These studies revealed a significant reduction in cell-associated spores when incubated in the presence (Figure 6.22A) but not absence of FBS (Figure 6.22B). Additionally when RAW264.7 cells were pre-incubated with 10 μM nisin at 4 °C followed by a germinating spore infection at 37 °C in the absence of nisin, a reduction in binding was not observed for both germinating and non-germinating conditions (Figure 6.22C,D). In cytochlasin D binding experiments,

nisin did not abolish binding, but it induced a dose dependent decrease in spore binding that biologically appears to be a minimal reduction yet was statistically significant for both germinating and non-germinating conditions (Figure 6.23). Furthermore, when the binding effect of nisin was compared to polymixin B or an antibiotic combination of penicillin and streptomycin, all treatments in both germinating infections had a minimal yet statistically significant reduction in spore binding with RAW264.7 macrophages while only polymixin B reduced spore binding in a non-germinating infection (Figure 6.24). Collectively, these data indicate that nisin alters the spore-immune cell interaction resulting in a decrease in the number of infected immune cells when infecting with a biological particle, spore or bacilli. Moreover, immune cell binding of *B. anthracis* spore was implicated as the factor resulting in the decrease in immune cell infection.

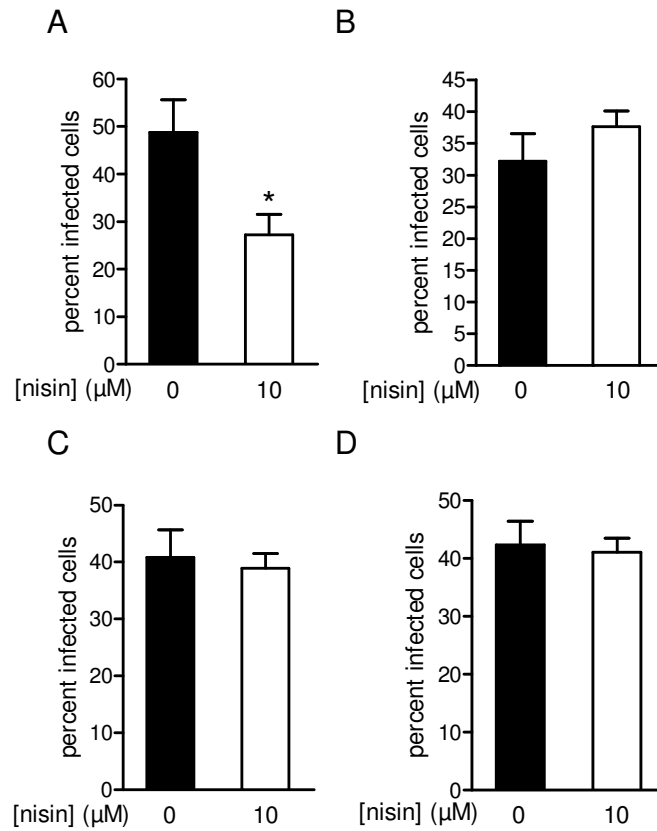


Figure 6.22. Nisin altered spore binding to immune cells. A, C. Germinating constant infection was performed with FBS as a germinant. B, D. Non-germinating constant infection was performed in the absence of FBS. A, B. Spore infection at 4 °C. RAW 264.7 macrophages were pre-incubated in the presence and absence of 10 μM nisin at 37 °C, washed, and infected at 4 °C. C, D. Nisin pre-incubation at 4 °C. RAW 264.7 macrophages were pre-incubated in the presence and absence of 10 μM nisin at 4 °C, washed, and infected at 37 °C. A-D. Immune cell infection with *B. anthracis* spores was monitored via an increase in immune cell fluorescence as a result of the interactions with fluorescently labeled spores. The data are expressed as the percent of immune cells displaying an increased fluorescence as a function of AF-488 spore interaction at 5, 60, and 240 min. * indicates a $P < 0.05$ between control (0 μM nisin, black) and experimental condition (10 μM nisin, white). Error bars indicate standard deviations.

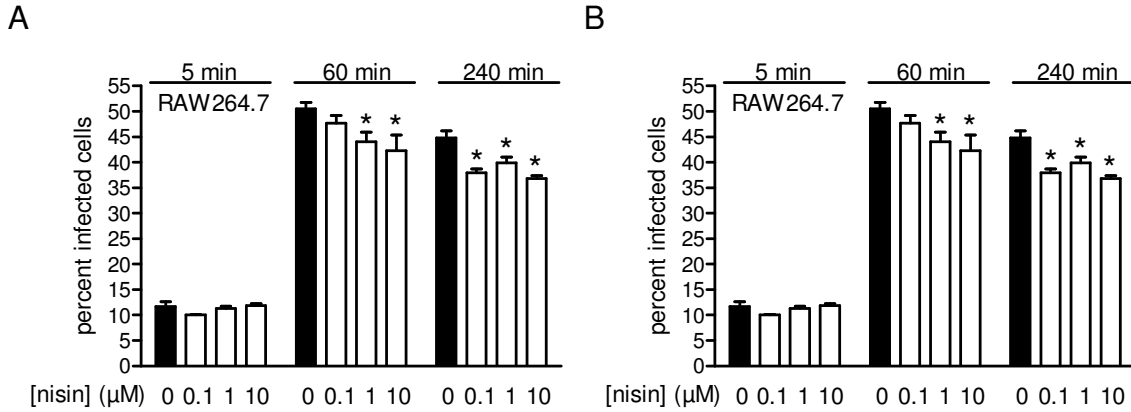


Figure 6.23. Nisin altered spore binding to immune cells - cytochalasin D infection. A.

Germinating constant infection was performed with FBS as a germinant. B. Non-germinating constant infection was performed in the absence of FBS. A, B. Immune cell infection with *B. anthracis* spores was monitored via an increase in immune cell fluorescence as a result of the interactions with fluorescently labeled spores. The data are expressed as the percent of immune cells displaying an increased fluorescence as a function of AF-488 spore interaction at 5, 60, and 240 min. * indicates a $P < 0.05$ between control (0 μM nisin, black) and experimental condition (0.1 - 10 μM nisin, white). Error bars indicate standard deviations.

Figure 6.24

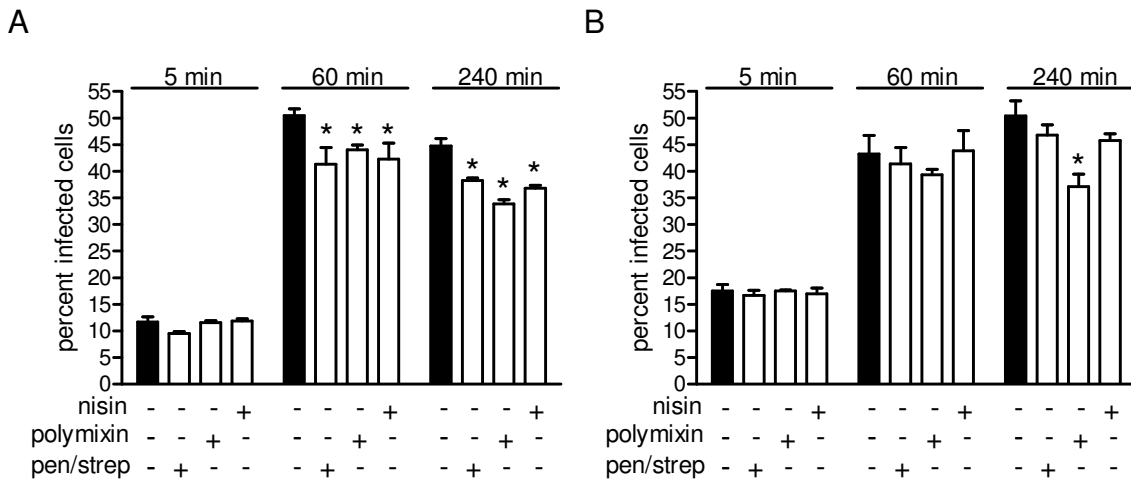


Figure 6.24. Effect of antibiotics on spore binding - cytochalasin D infection. A.

Germinating constant infection was performed with FBS as a germinant. B. Non-germinating constant infection was performed in the absence of FBS. A, B. Immune cell infection with *B. anthracis* spores was monitored via an increase in immune cell fluorescence as a result of the

Figure 6.24 (continued)

interactions with fluorescently labeled spores. The data are expressed as the percent of immune cells displaying an increased fluorescence as a function of AF-488 spore interaction at 5, 60, and 240 min. * indicates a $P < 0.05$ between control (0 μM nisin, black) and experimental condition (10 μM nisin, 8 μM polymixin B, or 100 U penicillin, 0.1 mg streptomycin/ml; white). Error bars indicate standard deviations.

6.2.5 Nisin interacted with spores during an infection.

In an effort to further clarify the conditions that facilitate the interaction of nisin with spores in relation to immune cells, AF568-spores were used to infect RAW264.7 macrophages with the addition 10 μM fluorescein-nisin (f-nisin) either during or post infection in the absence or presence of the germinant FBS. When f-nisin was present during the infection in the presence of a germinant, nisin was determined to co-localize with greater than 85% of the internalized spores (Figure 6.25 A, B). Nisin also localized to intracellular spores when incubated with RAW264.7 cells in the absence of germinants, or after the incubation was completed, but to a lesser degree (< 15%) (Figure 6.25 A, B).

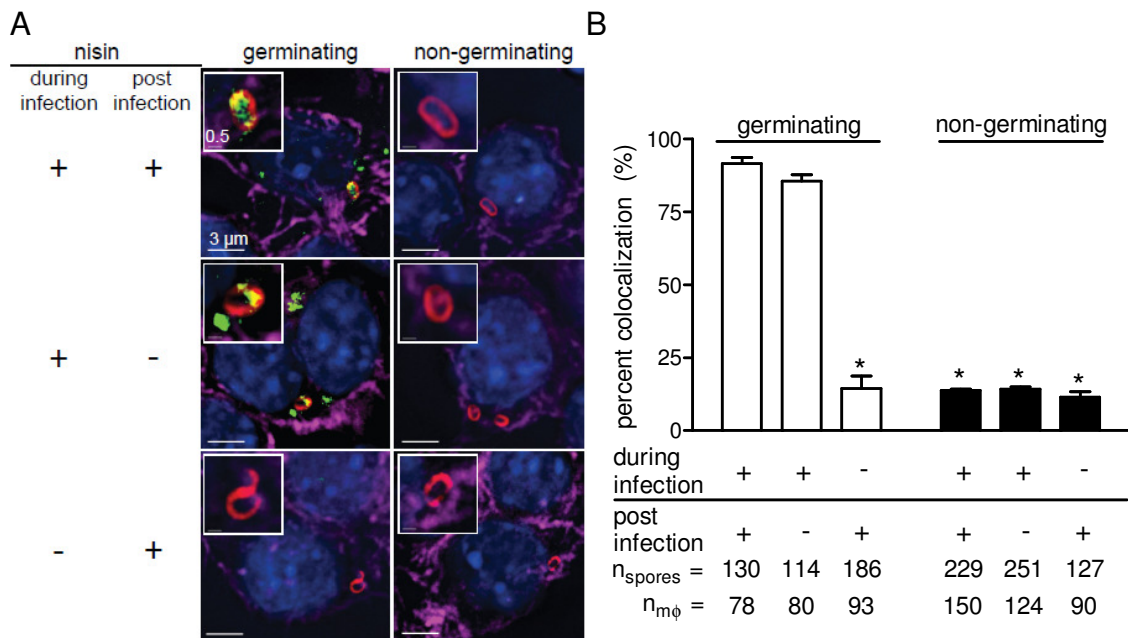


Figure 6.25. Nisin interacted with spores during an infection. A. Microscopy of spore infection and localization of f-nisin. f-nisin: green, spores: red, co-localization: yellow, DNA: blue, actin: purple. The data are representative of three independent experiments. B. Quantification of f-nisin localization with a phagocytized spore. The data are expressed as the percent of spores that were co-localized with f-nisin. * indicates a $P < 0.05$ between nisin present during and post a germination infection and all other conditions. n_{spores} indicates the number of spores that were evaluated. $n_{\text{m}\phi}$ indicates the number of infected macrophages that were evaluated. A,B. + (10 μM nisin) or - (0 μM nisin) are utilized to indicate the presence or absence of nisin either during the infection or post the infection.

6.2.6 Nisin reduced cytokine release during an infection.

In effort to identify whether nisin allows the establishment of a prototypical anthrax infection within immune cells, the expression of 23 cytokines was evaluated with Bio-plex in the presence and absence of nisin (10 μM) during a constant germinating infection of RAW264.7 cells. This screen identified that the

expression of G-CSF, TNF- α , IL-1 β , and IL-6 were significantly reduced in the presence of nisin (data not shown). In addition, it was determined that nisin was not inherently immune stimulating (data not shown), but reduced the expression of MCP1 (CCL2), MIP-1 α (CCL2), and MIP-1 β (CCL2), which are involved with infection associated inflammatory recruitment of monocytes (6, 7, 32) and immune cells as G-CSF. ELISA was used to confirm the Bio-plex results for these four cytokines. Furthermore, vancomycin, a non-pore forming lipid II binding antibiotic, was used a comparator for these analyses to determine whether the reduction in cytokine response was specific to nisin or a function of lipid II binding. The presence of nisin reduced the extracellular levels of all tested cytokines through 24 h (Figure 6.26 A-D), however vancomycin was only able to reduce the extracellular levels of IL-1 β (Figure 6.26 C). The reduction of TNF- α at 24 h (Figure 6.26 B) is the product of immune cell death in the absence of any antibiotic intervention as the cells became rounded and non-adherent, which are regularly observed characteristic of cell death (data not shown). Additional antibiotic controls were performed with chloramphenicol (62 μ M) and polymixin B (8 μ M). The effect on extracellular cytokine levels during an infection in the presence of chloramphenicol closely mimicked the cytokine expression observed with nisin (data not shown). However, the presence of polymixin B had virtually no effect on extracellular cytokine levels and closely mimicked the extracellular cytokine levels of spores alone for all cytokines including the reduction in TNF- α at 24 h as a result of immune cell death (Figure 6.27 A-D). Studies conducted in either the presence or absence of germinant in which nisin was added to

RAW264.7 cells after incubation with spores followed by treatment with gentamicin revealed that extracellular cytokine levels were significantly less in the presence than absence of nisin (Figure 6.27). As above, polymixin B had little effect on extracellular cytokine levels (data not shown). Additionally, nisin did not alter extracellular cytokine levels of RAW264.7 cells when induced by lipopolysaccharide (LPS) isolated from *E. coli* K-12, which was provided by the Richard Tapping laboratory (Figure 6.28). Collectively, these data suggest that in the presence of nisin, the response of RAW264.7 cells to spores was altered as a function of improper infection establishment.

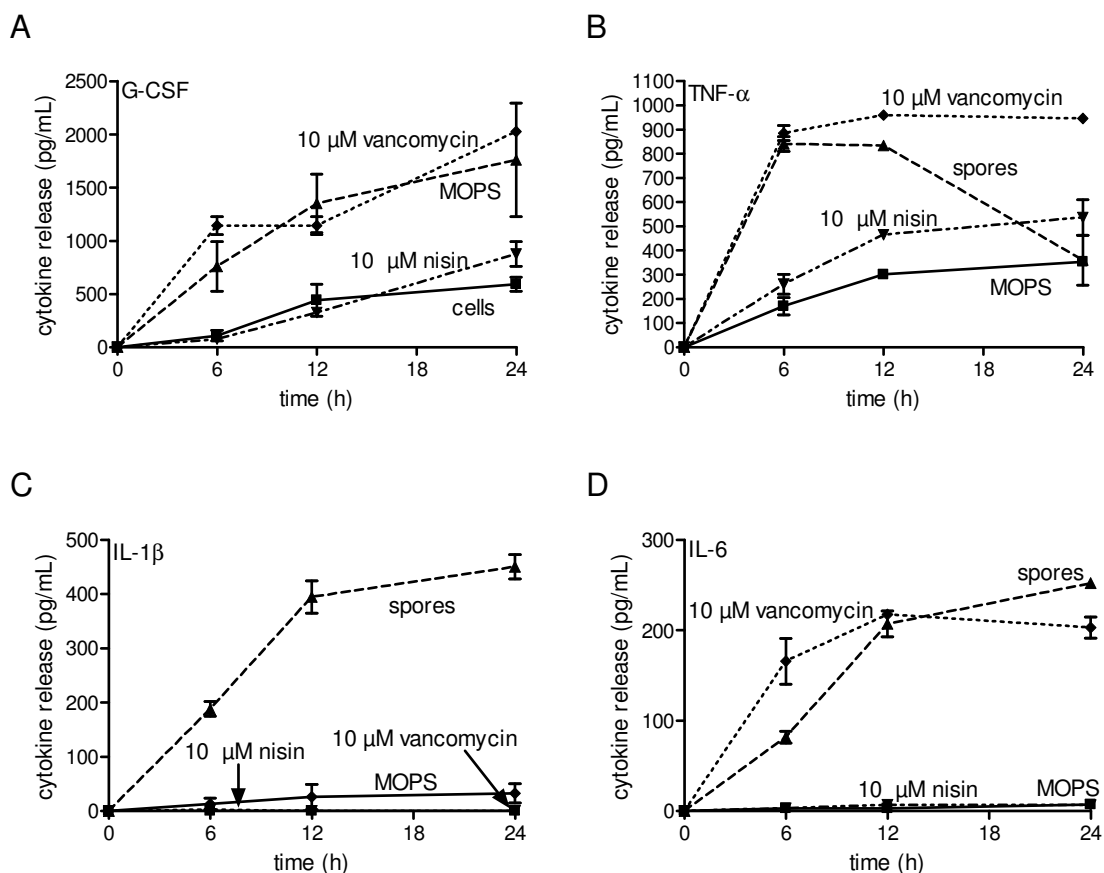
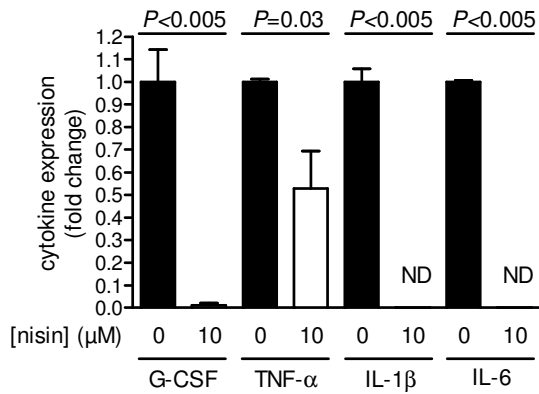


Figure 6.26. Effect of nisin on infection induced cytokine expression - constant infection.

A. G-CSF. B. TNF- α . C. IL-1 β . D. IL-6. The data are representative of three independent constant germinating infections. The data are expressed as cytokine release in pg/ml.

A



B

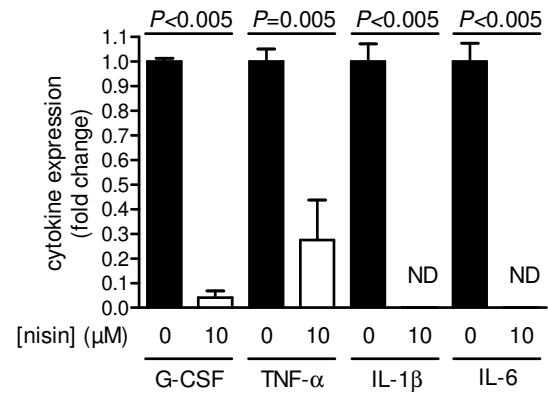


Figure 6.27. Effect of nisin on infection induced cytokine expression - gentamicin

protection. A. Immune cells were infected with *B. anthracis* spore under germinating conditions followed by gentamicin protection and post infection treatment with nisin in the presence of FBS as indicated in the “Materials and Methods”. B. Immune cells were infected with *B. anthracis* spore under non-germinating conditions followed by gentamicin protection and post infection treatment with nisin in the presence of FBS as indicated in the “Materials and Methods”. A, B. Cytokine expression from immune cell infections with *B. anthracis* spores was monitored at 24 h after gentamycin protection via ELISA. The data are expressed as the fold change of cytokine expression during post infection incubations in the presence of nisin relative to the absence of nisin. Error bars indicate standard deviations. ND indicates that cytokine expression was not detectable.

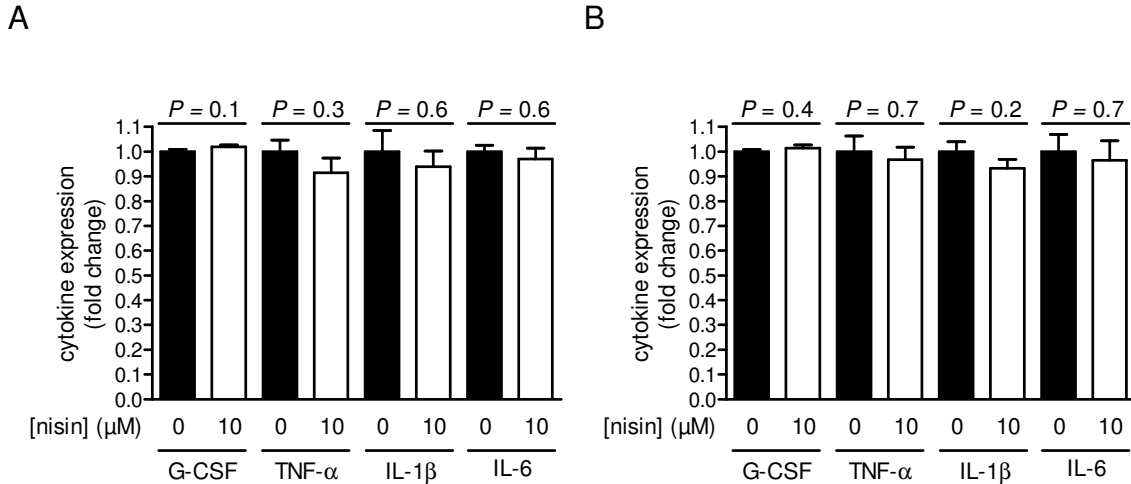


Figure 6.28. Effect of nisin on LPS induced cytokine expression - gentamicin protection.

A. Gentamicin protection infection was performed in the presence of FBS. B. Gentamicin protection infection was performed in the absence of FBS. A, B. Cytokine expression from immune cell infections with LPS was monitored at 24 h after gentamicin protection via ELISA. The data are expressed as the fold change of cytokine expression during post infection incubations in the presence of nisin relative to the absence of nisin. Error bars indicate standard deviations.

6.3 Discussion

With the onset of increasing antimicrobial resistance within bacteria, there must be an effort to identify new antimicrobials and targets that mediate microbial cell death and growth inhibition. In addition to identifying new antibiotics, one could exploit previously used antimicrobials in new ways. In accordance with this point of view, nisin was evaluated for its ability to inhibit the growth of the spore forming bacteria *Bacillus anthracis* within an *in vitro* infection. Nisin has been demonstrated to be a potent inhibitor of bacterial infection *in vivo* utilizing non-spore forming bacteria such as *Staphylococcus aureus* (22). However, *B.*

anthracis has both an intracellular and extracellular phase during the infection process (15). In general, little is known about the effectiveness of antimicrobial compounds on killing or inhibiting the growth of bacteria that are intracellular pathogens (either obligate or intracellular). Unfortunately, antimicrobial compounds are ineffective against dormant spores with germination occurring after uptake into host cells within the alveolar spaces of the lungs (16, 17, 27, 36). Moreover, the rapid onset of bacteremia and toxemia during the disseminated stages of disease (15, 21, 39, 40) limits the therapeutic window during which antimicrobials can effectively clear the infection in a manner that prevents the onset of disease sequelae or fatalities. Evidence indicating that spores germinate and outgrow within the intracellular environment of host cells (15, 21, 39, 40) underscores the challenges associated with therapeutically targeting *B. anthracis* prior to the transition from the intracellular stage of spore outgrowth and replication to the extracellular phase of dissemination.

Several cell lines that serve as *in vitro* models for studying *B. anthracis* infections were employed to evaluate interactions between spores, host cells, and antimicrobial treatments. The studies revealed that nisin was effective at inhibiting the outgrowth of *B. anthracis* spores in the presence of several cell lines, even subsequent to uptake of spores within an intracellular location. Furthermore, in the presence of nisin a greater percentage of immune cells resisted cell death associated with infection through 24 h (Figure 6.6-9), and this increase in survival was witnessed at 0.1 μM of nisin, which is significantly below the IC_{50} for *B. anthracis* in solution reported in chapter 2(27). Interestingly, 0.1

μM nisin was shown in chapter 2 to perturb the establishment of a membrane potential through 30 min without dramatically slowing growth kinetics (27). This suggests that the presence of nisin at non-inhibitory concentrations will slow the establishment of a membrane potential to negatively alter the activation of a metabolism, which would include the expression of virulence factors. This would potentially allow the immune cell to mount an adequate innate and adaptive immune response that can inhibit or kill internalized spores prior to pathogen subversion of an immune response and eventual escape from the macrophage as in the case of inhalation anthrax.

In addition to aiding spore clearance, nisin also altered the interaction between the *B. anthracis* (spore and bacilli) and mammalian cells resulting in a reduction in detectable intracellular spores (Figure 6.10,17). The presence of nisin resulted in a very modest to undetectable decrease in spore binding (Figure 6.22-24). A previous study reported that adhesion of a fungal pathogen, *Candida albicans*, to human gingival cells was decreased in the presence of nisin (1). Overall, these results suggest the possibility that the administration of nisin, either post-exposure or prophylactically if inhalation of spores is suspected, might improve the outcome of infection by decreasing the load of intracellular *B. anthracis*.

The use of lantibiotics like nisin provides a unique addition to treatment of bacterial and spore infection because nisin utilizes two activities, pore formation and inhibiting cell wall biogenesis, to inhibit growth (5, 28, 34, 43). In the case of an infection by *B. anthracis*, antimicrobial intervention must be able to prevent

both the growth of the bacteria and toxin production to prevent death by bacteremia and toxemia, respectively. This means treatment must include two antibiotics that are independently a growth inhibitor and a protein synthesis inhibitor. However, in the presence of a pore forming antimicrobial such as nisin, cell death is accompanied by the lack of protein synthesis due to the disruption of an active metabolism (27). In addition, treatment of a spore infection with nisin would prevent spore outgrowth, in conjunction with inhibiting bacilli, preventing toxin production (2-5, 27, 28, 34). Even though the environment within the lung is not overtly germinating (36), nisin demonstrated the ability to reduce the number of recoverable *B.anthraxis* in non-germinating *in vitro* infections. Nisin should be able to inhibit spores and bacilli released into regional lymph nodes or blood stream from migrating infected immune cells, which are germinant and nutrient rich (20).

Furthermore, nisin has an added advantage in that it has a distinct second activity. Nisin disrupts cell wall biogenesis through lipid II binding, which is a subsequent and distinct mode of action for the inhibition of bacilli and outgrown spores (28). When combined with either ciprofloxacin or doxycycline, the CDC suggested treatment for anthrax (8), three inhibitory activities would be in use to inhibit an anthrax infection. In addition, the use of multiple antibiotics with differing modes of action would prevent the establishment of antibiotic resistance (18, 19).

Nisin is an FDA–approved natural product that has been used for 40 years in food-preservation, due in part to the selective toxicity of this lantibiotic towards

Gram-positive bacteria (12, 13, 42), and this food preservative was evaluated for its potential ability to alter a spore infection of immune cells. Since nisin mediates its inhibition through the interaction with penultimate precursor for cell wall biogenesis, lipid II, nisin could be a relevant treatment option for other spore forming pathogens such as *Clostridia botulinum* and *Clostridia difficile*. Collectively, these results presented here suggest that nisin and similar lantibiotics could be used as relevant treatment option at appropriate concentrations that are non-toxic to the host (30) and have the potential to work in a synergistic fashion with the host immune response to kill both spore forming and non-spore forming pathogenic bacteria.

6.4 Materials and Methods

6.4.1 Spore preparations and fluorescent labeling.

Spores prepared from *B. anthracis* Sterne 7702 were labeled with NHS-AlexaFluor-488 (AF488-spores; Invitrogen, Carlsbad, CA) or NHS-AlexaFluor-568 (AF568-spores, Invitrogen) as previously described (38). Enumeration of spores or bacilli was performed using a Petroff-Hauser hemocytometer under a light microscope at 400x magnification (Nikon Alphaphot YS, Mellville, NY). A typical spore preparation yielded 10 mL of spores at a concentration of 2.0×10^9 spores/mL.

6.4.2 CFU quantification.

Spores were serially diluted and plated on Luria-Bertani (LB; B10 g/L Bacto Tryptone, 5 g/L NaCl, 5 g/L Bacto Yeast Extract, 15 g/L Bacto Agar; BD Biosciences) agar plates. After 12-18 h at 37 °C *B. anthracis* colonies were counted, from which CFU/mL were calculated.

6.4.3 Heat resistance.

Spores were diluted into 0.1 M MOPS pH 6.8 containing D-alanine and D-histidine (both at 10 mM; Sigma), to prevent further germination initiation of dormant spores, and identical aliquots were incubated at either 65 °C or on ice for 30 min. Viable *B. anthracis* were quantified by plating serial dilutions and enumerating CFU. The percentage of heat resistant spores was calculated by dividing CFU recovered from samples heated at 65 °C by CFU recovered from samples incubated on ice.

6.4.4. Nisin purification.

Nisin was purified and assessed according to previously published quality control procedures (27).

6.4.5 Labeling of Nisin.

See Chapter 3 for methods.

6.4.6 Cell culture.

RAW264.7 cells (CRL-2278; ATCC, Manassas, VA) were maintained within a humidified environment at 37 °C and under 5% CO₂ in Dulbecco's modified Eagle's medium (DMEM) (JRH Biosciences) containing penicillin (100 U; Gibco BRL, Grand Island, NY), streptomycin (0.1 mg/ml; Gibco BRL), L-glutamine (2 mM; Sigma), and fetal bovine serum (FBS) (10%; JRH Biosciences, Lenexa, KS). MH-S cells (CRL-2019; ATCC) were maintained within a humidified environment at 37 °C and under 5% CO₂ in containing RPMI-1640 medium (ATCC) penicillin-streptomycin, L-glutamine (4 mM; Sigma, St. Louis, MO), and FBS (10%). JAWSII (CRL-11904; ATCC) were maintained within a humidified environment at 37 °C and under 5% CO₂ in containing modified minimum essential medium alpha modification (MEM) (JRH Biosciences) penicillin-streptomycin, L-glutamine (4 mM; Sigma, St. Louis, MO), and FBS (20%). All tissue culture plasticware was purchased from Corning Incorporated (Corning, NY).

6.4.7 Spore interactions and uptake by mammalian cells.

Cells were seeded into 24-well plates, 96-well plates or 8-well chambered slides (Nalge Nunc International, Rochester, NY) in order to achieve 80 to 95% confluency after 2 days of incubation and were incubated with appropriate media containing penicillin-streptomycin (100 U penicillin, 0.1 mg streptomycin/ml), L-glutamine (4 mM), and FBS (10%) in a humidified environment at 37 °C and under 5% CO₂. To accurately calculate the number of labeled spores needed to

achieve a multiplicity of infection (MOI) of 10, cells from several wells were counted using a hemacytometer immediately before each experiment. The cells were used only if greater than 90% of the cells excluded trypan blue; generally, greater than 95% of the cells within the monolayer excluded trypan blue. Prior to the addition of labeled spores, cells were washed at least three times with HBSS and then incubated in DMEM (RAW264.7 and JAWSII) or RPMI-1460 containing L-glutamine (4 mM) with or without FBS (germinant). To synchronize the exposure of cells to spores, labeled spores were gently centrifuged (600 x *g* for 5 min) onto the surfaces of cells immediately after addition. The plates or slides were incubated within a humidified environment at 37 °C and under 5% CO₂ for the indicated times prior to analysis. In constant infections, spores were incubated with immune cells for the duration of the experiment. For post infection treatments, cells were washed at least three times with HBSS and incubated in appropriate media with 10% FBS and 50 ug/ml gentamicin for 15 min to kill all external germinated spores. Following gentamicin treatment at least three washes with HBSS and incubation in appropriate media with FBS was performed. For binding experiments, cells were pre-incubated with cytochalasin D (10 μM) for 1 h prior to the addition of labeled spores. For cold (on ice) binding experiments, cells were pre-incubated on ice for 15 min prior to the addition of spores or nisin, and the following spore infections or incubations with nisin were performed on ice.

6.4.8 Mammalian cell viability.

Propidium iodide (PI) (1 µg/ml) uptake by RAW264.7, MH-S or JAWSII cells was measured using flow cytometry, as previously described (38).

6.4.9 Fluorescence quenching of Alexa Fluor AF488-spores.

Stock solutions of trypan blue were made in PBS, pH 7.2, and filtered using a 0.22-µm filter prior to use. Where indicated, trypan blue was added (at the indicated final concentration; typically, 0.5% in PBS, pH 7.2) to AF488-spores or to mammalian cells exposed to labeled spores. The samples were incubated for 5 min on ice and analyzed immediately by flow cytometry.

6.4.10 Flow cytometry.

Spore and bacilli infection of mammalian cells assayed and evaluated as previously described (38).

6.4.11 Quantification of cell-associated viable *B. anthracis*.

Cells exposed to *B. anthracis* were washed three times with PBS and then lysed by resuspending and vortexing the cell pellet in sterile tissue culture grade water (Sigma) for 5 min at room temperature. To determine CFU, serial dilutions of the suspensions were plated on LB agar plates as described above.

6.4.12 Epi-Fluorescence microscopy.

After a 30 min infection and a 1 hr post infection treatment within chamber slides, cell were washes 3 times with PBS and fixed during incubation in 4% formaldehyde (Sigma) for 30 min at 37 °C followed by permeabilization with 0.1 % triton X-100 (Sigma) and 0.1% sodium citrate (Sigma). Cells were stained with 4',6-diamidino-2-phenylindole (DAPI, Invitrogen) and Alexa Fluor® 647 phalloidin (Invitrogen) and cured with ProLong® Gold antifade reagent (Invitrogen) according to manufactures protocols. Images were collected using an Applied Precision assembled DeltaVision EpiFluorescence microscope containing an Olympus Plan Apo 100x oil objective with NA 1.42 and a working distance of 0.15 mm, and images were processed using SoftWoRX Explorer Suite (Issaquah, WA).

6.4.13 Cytokine release - cytometric array assay.

At indicated times, cell-culture supernatant of constant *B. anthracis* infections of RAW264.7 were collected and stored at -80°C for analysis using the Bio-Plex suspension array system (Bio-Rad, Hercules, Ca) where 23 biological markers were assayed according to manufacturers protocols: eotaxin, interleukins-1 α , 1 β (IL-1 β), 2, 3, 4, 5, 6 (IL-6), 9, 10, 12p40, 12p70, 13, 17, granulocyte macrophage colony-stimulating factor, granulocyte colony-stimulating factor (G-CSF), interferon- γ , keratinocyte chemoattractant, tumor necrosis factor- α (TNF- α), RANTES, macrophage inflammatory protein-1 α , 1 β , and monocyte chemoattractant protein-1. The biological markers were quantified

using the Bio-Plex protein array reader with data automatically processed and analyzed by Bio-Plex Manager Software 4.1 using the standard curve produced from recombinant cytokine standard.

6.4.14 Cytokine release - ELISA.

At indicated times, cell-culture supernatant of *B. anthracis* infections of RAW264.7 with and without gentamicin protection were collected and stored at -80 °C for analysis using commercial quantitative sandwich enzyme immunoassay kits: interleukins -1 β (Ready-SET-Go!, eBioscience, San Deigo, CA, sensitivity 8 pg/ml), 6 (Ready-SET-Go!, eBioscience, sensitivity 4 pg/ml), TNF- α (Ready-SET-Go!, eBioscience, sensitivity 8 pg/ml), and G-CSF (DuoSet®, R&D Systems, Minneapolis, MN, sensitivity 4 pg/ml).

6.4.15 Statistics.

All data are representative of those from three independent experiments. Error bars represent standard deviations. *P* values were calculated with Student's *t* test using paired, one-tailed distribution. *P* values of <0.05 indicate statistical significance. All statistics, including means, standard deviations, and Student's *t* tests, were calculated using Microsoft Excel (version 11.0).

6.5 References

1. **Akerey, B., C. Le-Lay, I. Fliss, M. Subirade, and M. Rouabhia.** 2009. In vitro efficacy of nisin Z against *Candida albicans* adhesion and transition following contact with normal human gingival cells. *J Appl Microbiol* **107**:1298-307.

2. **Bonev, B. B., E. Breukink, E. Swiezewska, B. De Kruijff, and A. Watts.** 2004. Targeting extracellular pyrophosphates underpins the high selectivity of nisin. *Faseb J* **18**:1862-9.
3. **Breukink, E., and B. de Kruijff.** 2006. Lipid II as a target for antibiotics. *Nat Rev Drug Discov* **5**:321-32.
4. **Breukink, E., P. Ganz, B. de Kruijff, and J. Seelig.** 2000. Binding of Nisin Z to bilayer vesicles as determined with isothermal titration calorimetry. *Biochemistry* **39**:10247-54.
5. **Breukink, E., I. Wiedemann, C. van Kraaij, O. P. Kuipers, H. Sahl, and B. de Kruijff.** 1999. Use of the cell wall precursor lipid II by a pore-forming peptide antibiotic. *Science* **286**:2361-4.
6. **Bystry, R. S., V. Aluvihare, K. A. Welch, M. Kallikourdis, and A. G. Betz.** 2001. B cells and professional APCs recruit regulatory T cells via CCL4. *Nat Immunol* **2**:1126-32.
7. **Carr, M. W., S. J. Roth, E. Luther, S. S. Rose, and T. A. Springer.** 1994. Monocyte chemoattractant protein 1 acts as a T-lymphocyte chemoattractant. *Proc Natl Acad Sci U S A* **91**:3652-6.
8. **CDC.** 2006. **Fact Sheet: Anthrax Information for Health Care Providers.**
9. **Chatterjee, C., Paul, M., Xie, L, van der Donk, W. A.** 2005. Biosynthesis and Mode of Action of Lantibiotics. *Chem Rev* **105**:633-683.
10. **Chen, Y., F. C. Tenover, and T. M. Koehler.** 2004. β -lactamase gene expression in a penicillin-resistant *Bacillus anthracis* strain. *Antimicrob Agents Chemother* **48**:4873-7.
11. **Cleret, A., A. Quesnel-Hellmann, A. Vallon-Eberhard, B. Verrier, S. Jung, D. Vidal, J. Mathieu, and J. N. Tournier.** 2007. Lung dendritic cells rapidly mediate anthrax spore entry through the pulmonary route. *J Immunol* **178**:7994-8001.
12. **Cotter, P. D., C. Hill, and R. P. Ross.** 2005. Bacteriocins: developing innate immunity for food. *Nat Rev Microbiol* **3**:777-88.
13. **Delves-Broughton, J., P. Blackburn, R. J. Evans, and J. Hugenholtz.** 1996. Applications of the bacteriocin, nisin. *Antonie Van Leeuwenhoek* **69**:193-202.
14. **Dixon, T. C., A. A. Fadl, T. M. Koehler, J. A. Swanson, and P. C. Hanna.** 2000. Early *Bacillus anthracis*-macrophage interactions: intracellular survival survival and escape. *Cell Microbiol* **2**:453-63.

15. **Dixon, T. C., M. Meselson, J. Guillemin, and P. C. Hanna.** 1999. Anthrax. *N Engl J Med* **341**:815-26.
16. **Driks, A.** 2002. Maximum shields: the assembly and function of the bacterial spore coat. *Trends Microbiol* **10**:251-4.
17. **Drusano, G. L., O. O. Okusanya, A. Okusanya, B. Van Scoy, D. L. Brown, R. Kulawy, F. Sorgel, H. S. Heine, and A. Louie.** 2008. Is 60 days of ciprofloxacin administration necessary for postexposure prophylaxis for *Bacillus anthracis*? *Antimicrob Agents Chemother* **52**:3973-9.
18. **Evans, H. L., and R. G. Sawyer.** 2009. Preventing bacterial resistance in surgical patients. *Surg Clin North Am* **89**:501-19, x.
19. **Gerding, D. N.** 2000. Antimicrobial cycling: lessons learned from the aminoglycoside experience. *Infect Control Hosp Epidemiol* **21**:S12-7.
20. **Givens, P., and M. Reiss.** 2002. *Human Biology and Health Studies*. Nelson Thornes Ltd, Cheltenham, UK.
21. **Glomski, I. J., F. Dumetz, G. Jouvion, M. R. Huerre, M. Mock, and P. L. Goossens.** 2008. Inhaled non-capsulated *Bacillus anthracis* in A/J mice: nasopharynx and alveolar space as dual portals of entry, delayed dissemination, and specific organ targeting. *Microbes Infect* **10**:1398-404.
22. **Goldstein, B. P., J. Wei, K. Greenberg, and R. Novick.** 1998. Activity of nisin against *Streptococcus pneumoniae*, *in vitro*, and in a mouse infection model. *J Antimicrob Chemother* **42**:277-8.
23. **Guidi-Rontani, C.** 2002. The alveolar macrophage: the Trojan horse of *Bacillus anthracis*. *Trends Microbiol* **10**:405-9.
24. **Guidi-Rontani, C., M. Levy, H. Ohayon, and M. Mock.** 2001. Fate of germinated *Bacillus anthracis* spores in primary murine macrophages. *Mol Microbiol* **42**:931-8.
25. **Guidi-Rontani, C., and M. Mock.** 2002. Macrophage interactions. *Curr Top Microbiol Immunol* **271**:115-41.
26. **Guidi-Rontani, C., M. Weber-Levy, E. Labruyere, and M. Mock.** 1999. Germination of *Bacillus anthracis* spores within alveolar macrophages. *Mol Microbiol* **31**:9-17.
27. **Gut, I. M., A. M. Prouty, J. D. Ballard, W. A. van der Donk, and S. R. Blanke.** 2008. Inhibition of *Bacillus anthracis* spore outgrowth by nisin. *Antimicrob Agents Chemother* **52**:4281-8.

28. **Hasper, H. E., N. E. Kramer, J. L. Smith, J. D. Hillman, C. Zachariah, O. P. Kuipers, B. de Kruijff, and E. Breukink.** 2006. An alternative bactericidal mechanism of action for lantibiotic peptides that target lipid II. *Science* **313**:1636-7.
29. **Jason E. Brouillard, C. M. T., Andreea Tofan, and Mark W. Garrison.** 2006. Antibiotic selection and resistance issues with fluoroquinolones and doxycycline against bioterrorist Agents. *Pharmacotherapy* **26**.
30. **Maher, S., and S. McClean.** 2006. Investigation of the cytotoxicity of eukaryotic and prokaryotic antimicrobial peptides in intestinal epithelial cells *in vitro*. *Biochem Pharmacol* **71**:1289-98.
31. **Martin, S. W., B. C. Tierney, A. Aranas, N. E. Rosenstein, L. H. Franzke, L. Apicella, N. Marano, and M. M. McNeil.** 2005. An overview of adverse events reported by participants in CDC's anthrax vaccine and antimicrobial availability program. *Pharmacoepidemiol Drug Saf* **14**:393-401.
32. **Menten, P., A. Wuyts, and J. Van Damme.** 2002. Macrophage inflammatory protein-1. *Cytokine Growth Factor Rev* **13**:455-81.
33. **Murayama, R., G. Akanuma, Y. Makino, H. Nanamiya, and F. Kawamura.** 2004. Spontaneous transformation and its use for genetic mapping in *Bacillus subtilis*. *Biosci Biotechnol Biochem* **68**:1672-80.
34. **Ruhr, E., and H. G. Sahl.** 1985. Mode of action of the peptide antibiotic nisin and influence on the membrane potential of whole cells and on cytoplasmic and artificial membrane vesicles. *Antimicrob Agents Chemother* **27**:841-5.
35. **Russell, B. H., R. Vasan, D. R. Keene, T. M. Koehler, and Y. Xu.** 2008. Potential dissemination of *Bacillus anthracis* utilizing human lung epithelial cells. *Cell Microbiol* **10**:945-57.
36. **Sanz, P., L. D. Teel, F. Alem, H. M. Carvalho, S. C. Darnell, and A. D. O'Brien.** 2008. Detection of *Bacillus anthracis* spore germination *in vivo* by bioluminescence imaging. *Infect Immun* **76**:1036-47.
37. **Shepard, C. W., M. Soriano-Gabarro, E. R. Zell, J. Hayslett, S. Lukacs, S. Goldstein, S. Factor, J. Jones, R. Ridzon, I. Williams, and N. Rosenstein.** 2002. Antimicrobial postexposure prophylaxis for anthrax: adverse events and adherence. *Emerg Infect Dis* **8**:1124-32.
38. **Stojkovic, B., E. M. Torres, A. M. Prouty, H. K. Patel, L. Zhuang, T. M. Koehler, J. D. Ballard, and S. R. Blanke.** 2008. High-throughput, single-cell analysis of macrophage interactions with fluorescently labeled *Bacillus anthracis* spores. *Appl Environ Microbiol* **74**:5201-10.

39. **Tournier, J. N., A. Quesnel-Hellmann, A. Cleret, and D. R. Vidal.** 2007. Contribution of toxins to the pathogenesis of inhalational anthrax. *Cell Microbiol* **9**:555-65.
40. **Tournier, J. N., S. Rossi Paccani, A. Quesnel-Hellmann, and C. T. Baldari.** 2009. Anthrax toxins: a weapon to systematically dismantle the host immune defenses. *Mol Aspects Med* **30**:456-66.
41. **Turnbull, P. C., N. M. Sirianni, C. I. LeBron, M. N. Samaan, F. N. Sutton, A. E. Reyes, and L. F. Peruski, Jr.** 2004. MICs of selected antibiotics for *Bacillus anthracis*, *Bacillus cereus*, *Bacillus thuringiensis*, and *Bacillus mycoides* from a range of clinical and environmental sources as determined by the Etest. *J Clin Microbiol* **42**:3626-34.
42. **van Kraaij, C., W. M. de Vos, R. J. Siezen, and O. P. Kuipers.** 1999. Lantibiotics: biosynthesis, mode of action and applications. *Nat Prod Rep* **16**:575-87.
43. **Wiedemann, I., E. Breukink, C. van Kraaij, O. P. Kuipers, G. Bierbaum, B. de Kruijff, and H. G. Sahl.** 2001. Specific binding of nisin to the peptidoglycan precursor lipid II combines pore formation and inhibition of cell wall biosynthesis for potent antibiotic activity. *J Biol Chem* **276**:1772-9.

CHAPTER 7: NISIN INTERACTION WITH IMMUNITY PROTEINS AND LOCALIZATION

7.1 Introduction

The immunity to nisin afforded to the native producer, *L. lactis* ATCC 11544, consists of a stoichiometric nisin binding protein, NisI, and an ATP-dependent transporter complex, NisFEG (6, 14). These systems work in a synergistic fashion to facilitate immunity (6, 14). NisI is a constitutively expressed 25.9 kDa protein in its fully modified form. Upon export, NisI undergoes proteolytic removal of a 19-amino acid N-terminal peptide and lipidation of the new N-terminal Cys for membrane anchoring (14).

Approximately 50% of the NisI produced escapes lipidation and is secreted into the surrounding environment (12). Surface plasmon resonance yielded NisI-nisin interactions with a K_D of 0.6 – 2 μ M (19), and this complex has been reported to be unstable and insoluble (14). In terms of function, NisI reduces the amount of soluble nisin able to interact with the membrane thus preventing pore formation (3). Deletion studies have demonstrated that NisI provides the majority of the immunity preventing nisin mediated cell death of the producer strain (14). In addition to NisI, *L. lactis* 11454 also utilizes an ATP-dependent pump to remove nisin from the membrane, and this complex is organized with two NisF proteins, which contain the ATP binding motifs, interacting with the cytosolic portions of the trans-membrane proteins NisEG. The expression of these proteins is controlled by the two-component regulatory system nisRK (3). Through the use of these two systems *L. lactis* acquires the essential immunity for nisin production.

Subtilin is a linear lantibiotic produced by *B. subtilis* ATCC 6633 that contains 5 rings derived from the cyclization of dehydroalanine (Dha) or dehydrobutyrine (Dhb) with Cys. Subtilin shares 63% overall sequence identity with nisin with the first 3 rings in the exact same locations. Similarities between nisin and subtilin continue with both producer strains utilizing an ATP dependent pump, SpaFEG for subtilin, and a stoichiometric binding protein, Spal for subtilin, to prevent lantibiotic interaction with the producer cell (3). The subtilin producer, *B. subtilis* 6633, also has a mechanism to succinylate subtilin resulting in a 10-fold decrease in antimicrobial activity relative to parental subtilin (10). Spal has very little sequence similarity to NisI, and Spal is only 143 amino acids compared to 226 residues for NisI. The presence of either Spal or NisI does not afford cross immunity to nisin and subtilin, respectively, despite high similarity between the lantibiotics (20).

The expression of the structural, biosynthetic, and immunity genes of nisin and subtilin is controlled by a two-component regulatory system, LanRK, to activate expression, which senses the presence of extracellular fully modified lantibiotic. For subtilin, SpaR will bind to Spa boxes located in front of *spaS*, *spaB*, and *spal* to induce preferential expression in the listed order (18). SpaRK also induce their own expression, but their expression has additional regulation through σ^H , which is the first σ factor involved in sporulation. This means that subtilin is expressed in very late logarithmic and stationary phases prior to spore formation while nisin is expressed concurrently in logarithmic phase with lactic

acid production. This chapter describes the efforts to better understand the mechanisms of immunity provided by LanI and LanFEG.

7.2 Results

7.2.1 Cloning and tagging of immunity genes.

In order to investigate the interactions between a lantibiotic and its cognate LanI, as well as its localization within the producing organism, several constructs were made to facilitate affinity purification of LanI and generate fluorescently tagged LanI and LanF. For *in vitro* studies and protein purification, the genes for *nisl* and *spal* were amplified from genomic DNA in a fashion that eliminated the secretion signal from the N-terminus of the protein and resulted in the removal of the first 19 and 22 amino acids, respectively, creating Nisl Δ 1-19 and Spal Δ 1-22. The amplified gene products were inserted in pGEX-6P-1 creating N-terminally glutathione S-transferase (GST) tagged constructs for affinity purification. In addition, Spal Δ 1-22 was inserted into pET15b to provide an N-terminal His₆-tagged variant for cobalt affinity purification.

Fusion constructs were also developed to create C-terminally tagged Spal and SpaF proteins. The genes for *spal* and *spaF* were cloned into pMUTIN and pSG (7, 11) chromosomal integrative plasmids that created a C-terminal fluorescent fusion with either green fluorescent protein (GFP), cyan fluorescent protein (CFP), or yellow fluorescent protein (YFP). pMUTIN will integrate at the gene of interest leaving expression under the control of the native promoter with the rest of the operon under inducible control (11). pSG will integrate within the

amylase gene putting the gene of interest under the control of a xylose inducible promoter (7). Additionally, both Spal and SpaF were independently fused with C-terminal hemagglutinin (HA) and cMYC tags in pMUTIN for immunological detection of these proteins. Moreover, Spal and SpaF were both C-terminally tagged with either a tetra-cysteine or cMyc tag via overlap extension at the 3' end of the gene followed by insertion into a non-integrative *Bacillus* over-expression plasmid, pHCMC05, allowing induction of the gene by IPTG. These series of constructs provide a wide set of options that will facilitate differential expression and multiple visualization options. The utility of these options is discussed further in the discussion section. *Bacillus subtilis* 6633 has been transformed with these plasmids with insertion and expression confirmed by PCR and immunoblot (GFP, CFP, YFP, HA, MYC) or fluorescence gel imaging (TC), respectively (data not shown).

7.2.2 GST purification of Nisl Δ 1-19 and Spal Δ 1-22.

Both Nisl Δ 1-19 and Spal Δ 1-22 were expressed as soluble, recombinant proteins in *E. coli*, each with a N-terminal GST fusion protein to facilitate glutathione affinity chromatography. After a single chromatography step, Nisl Δ 1-19 and Spal Δ 1-22 were purified to greater than 98% purity as determined by SDS-PAGE analysis. The N-terminal GST-tag was removed with the commercially available PreScission protease, and both Nisl Δ 1-19 and Spal Δ 1-22 were purified via glutathione affinity chromatography to high purity as determined by SDS-PAGE analysis (Figure 7.1, 7.2).

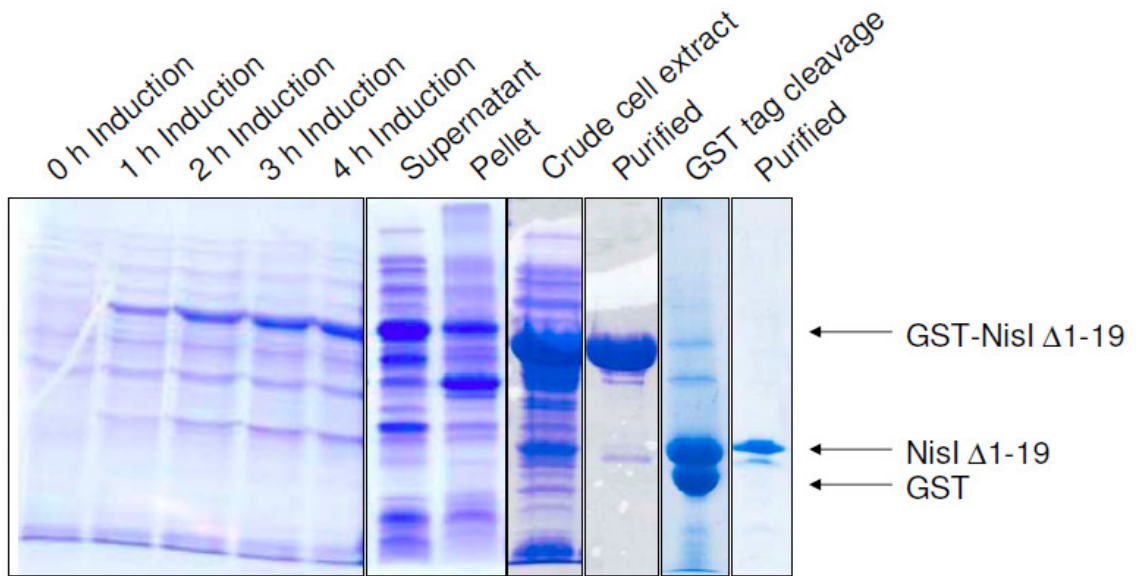


Figure 7.1. Expression and purification of Nisl Δ 1-19. The Nisl Δ 1-19 expression, homogenization fractions, clarified lysates, purified GST-fusion from glutathione affinity chromatography, cleavage reaction, and truncated protein from glutathione affinity chromatography were analyzed by 10% SDS-PAGE, followed by GelCode® Blue staining.

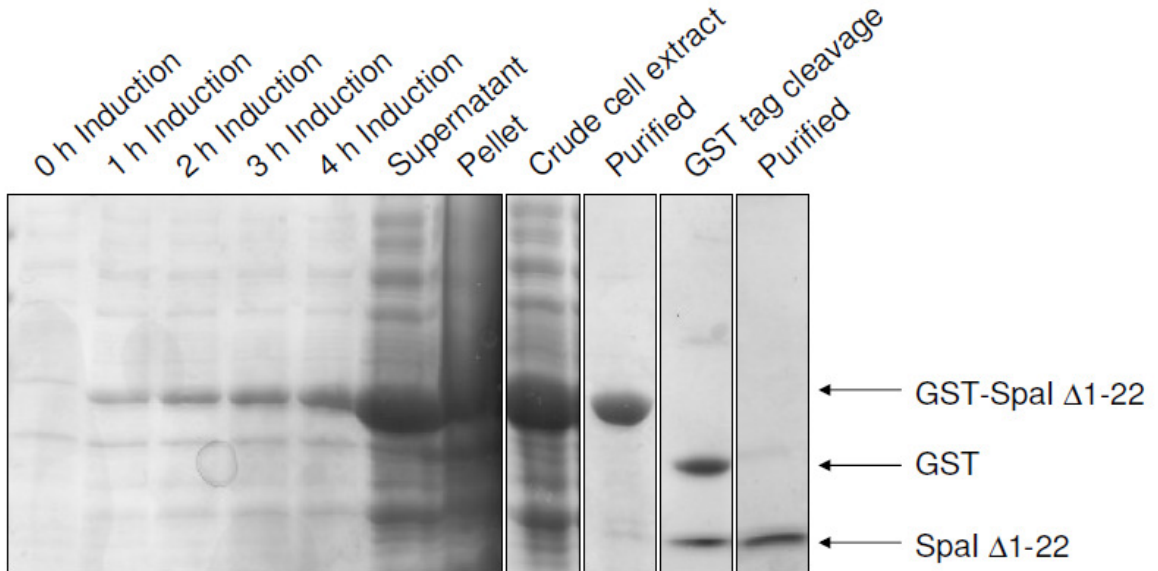


Figure 7.2. Expression and purification of Spal Δ 1-22. The Spal Δ 1-22 over expression, homogenization fractions, clarified lysates, purified GST-fusion from glutathione affinity chromatography, cleavage reaction, and truncated protein from glutathione affinity chromatography were analyzed by 10% SDS-PAGE, followed by GelCode® Blue staining.

7.2.3 Nickel affinity purification of Spal Δ 1-22.

Spal Δ 1-22 was expressed as a soluble, recombinant protein in *E. coli* with an N-terminal hexa-histidine fusion peptide to facilitate purification via cobalt-chelate affinity chromatography. The N-terminal hexa-histidine peptide was removed by thrombin cleavage, and Spal Δ 1-22 was purified to high purity as determined by SDS-PAGE analysis (Figure 7.3).

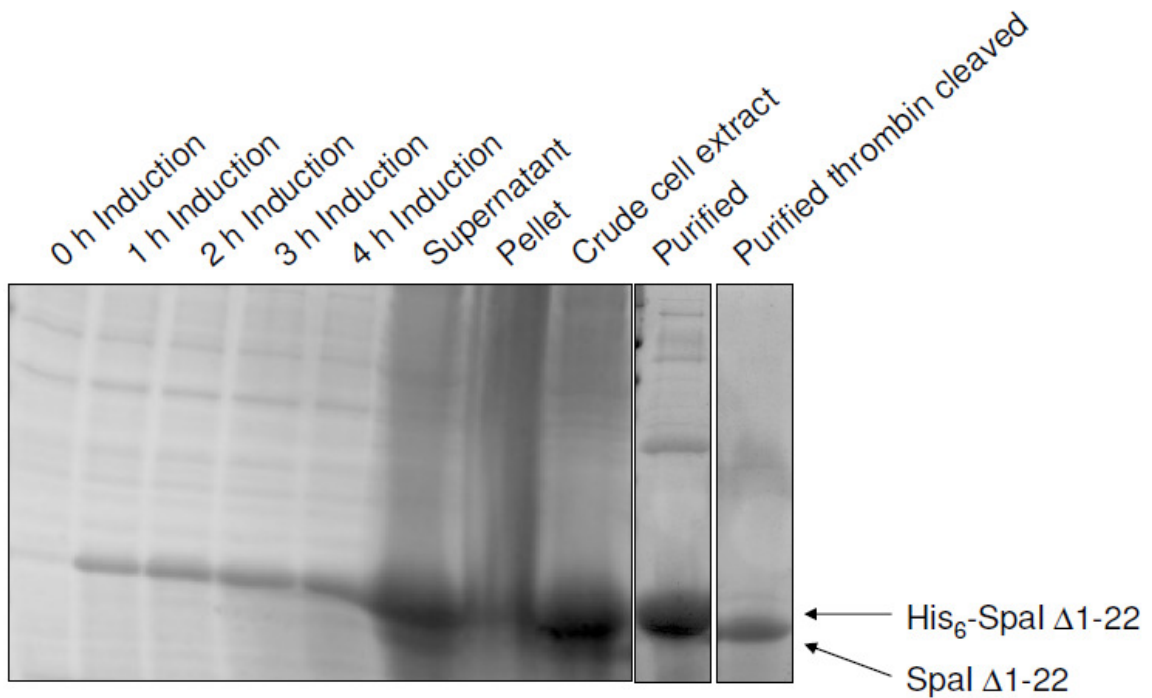


Figure 7.3. Expression and purification of Spal Δ 1-22. The Spal Δ 1-22 expression, homogenization fractions, clarified lysates, purified GST-fusion from cobalt chelate affinity chromatography, and purified thrombin cleaved protein were analyzed by 10% SDS-PAGE, followed by GelCode® Blue staining.

7.2.4 Circular dichroism of nisin and Nisl Δ 1-19.

Investigations were conducted to identify any structural changes accompanying this interaction. First, structure predictions conducted on both

NislΔ1-19 and SpalΔ1-22 identified that both proteins are highly disordered with SpalΔ1-22 predicted to have a significantly more α-helical character than NislΔ1-19 (Table 7.1). However, CD spectra of NislΔ1-19 displayed a significantly higher α-helical character than predicted with 24% of the structure being α-helical compared to the 6.6% that was predicted. Overall, both the predicted and the observed structures of NislΔ1-19 were highly disordered (Table 7.1, Figure 7.4). Interestingly, the observed NislΔ1-19 structure and predicted SpalΔ1-22 are highly similar despite a lack of primary sequence similarity. The addition of nisin to NislΔ1-19 did not significantly alter the CD spectra of NislΔ1-19 with only a minor decrease in the α-helical nature upon the addition of nisin (Table 7.1, Figure 7.4). These results suggest that NislΔ1-19 does not undergo a significant structural change upon nisin addition.

Table 7.1

		Secondary structure characterization of NislΔ1-19 and SpalΔ1-22		
		α-helix	β-strands	Loops/Disordered
NislΔ1-19	predicted ^a	6.6	38.1	55.3
	actual ^b	24.0 ± 2.9	23.8 ± 0.3	53.0 ± 1.9
NislΔ1-19 & nisin	actual ^b	20.3 ± 0.1	24.3 ± 0.2	55.4 ± 0.2
SpalΔ1-22	predicted ^a	25.2	20.3	54.5

Table 7.1. Secondary structure characterization of NislΔ1-19 and SpalΔ1-22. ^a The secondary structures of NislΔ1-19 and SpalΔ1-22 predictions were performed using the consensus prediction method on the NPS@ web server (network protein sequence analysis; http://npsa-pbil.ibcp.fr/cgi-bin/npsa_automat.pl?page=/NPSA/npsa_seccons.html) of the Pôle BioInformatique Lyonnais (4). ^b CD spectra were recorded in the far-UV range utilizing a J-720 CD spectropolarimeter. The spectra were recorded from 190 to 260 nm at a scan rate of 50 nm/s and a 1-nm wavelength step with five accumulations utilizing 5 μM NislΔ1-19 in absence and

Table 7.1 (continued)

presence of 50 μM nisin. The spectra were uploaded onto the DICHROWEB online server and analyzed as described in Materials and Methods.

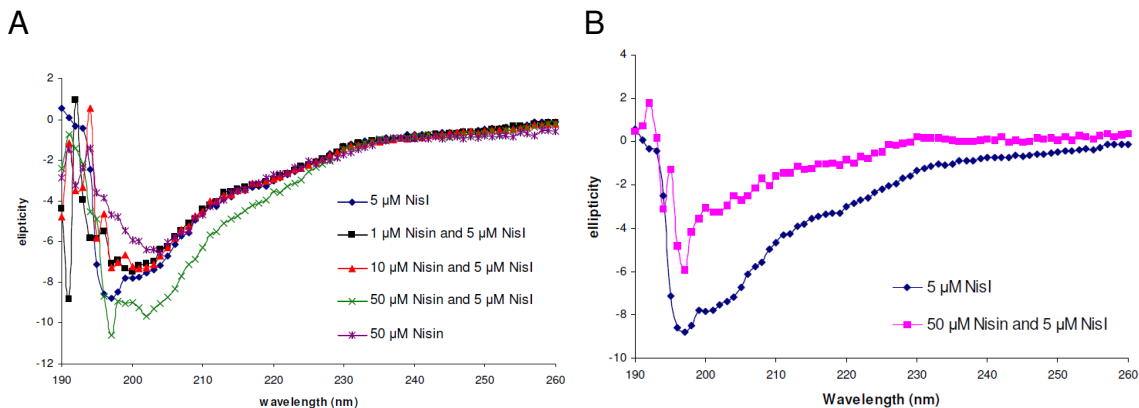


Figure 7.4. Circular dichroism of nisin and NisI Δ 1-19. A. CD spectra of nisin, NisI Δ 1-19 (listed as NisI), and a NisI Δ 1-19 with increasing concentrations. B. CD spectra of nisin and NisI Δ 1-19 with nisin contribution to ellipticity subtracted. A, B. CD spectra were recorded in the far-UV range utilizing a J-720 CD spectropolarimeter. The spectra were recorded from 190 to 260 nm at a scan rate of 50 nm/s and a 1-nm wavelength step with five accumulations.

7.2.5 Oligomerization analysis of NisI Δ 1-19.

In the absence of any dramatic structural changes in NisI Δ 1-19 incubated with nisin, investigations were conducted to determine whether NisI Δ 1-19 attained an altered oligomerization state upon nisin binding. Both size exclusion chromatography and native-PAGE analysis were performed. Size exclusion chromatography demonstrated NisI Δ 1-19 is present in both dimeric and tetrameric states in the presence or absence of nisin (Figure 7.5 A). Native gel analysis supported this result with no observable change in band intensity or location with the addition of nisin (Figure 7.5B). It is important to note that nisin is not efficiently stained with Coomassie protein dyes for visualization (data not

shown). The ratio of oligomeric states was not affected by the addition of nisin; however, a two-fold reduction of solution signal intensity was observed with the addition of nisin (Figure 7.5A). These observations are congruent with previous studies that suggest the NisI-nisin binding renders both proteins insoluble (19). However, no observable precipitate was observed in Nis Δ 1-19 solutions with nisin present (data not shown).

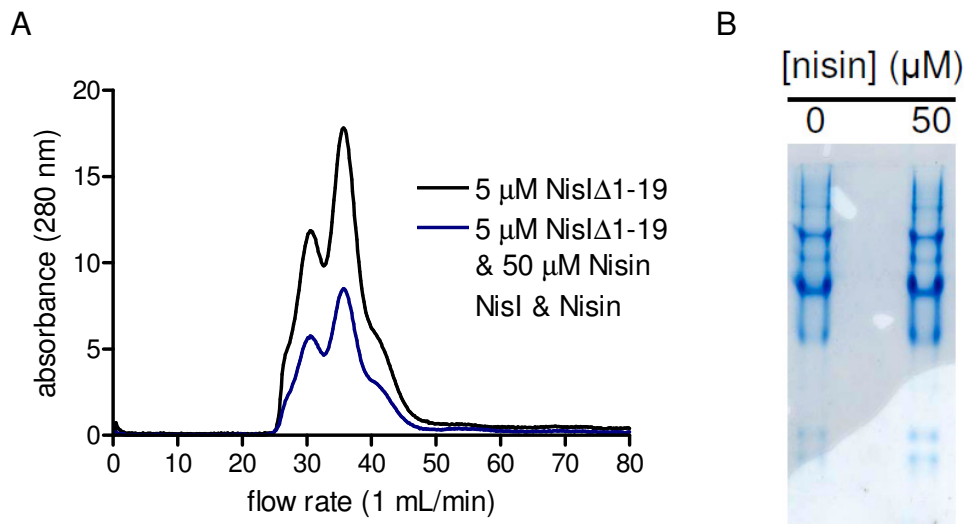


Figure 7.5. Oligomerization analysis of NisI Δ 1-19. A. Size exclusion chromatography was utilized to determine the oligomerization state of NisI Δ 1-19 in the absence (black) and presence (blue) of nisin. The molecular weights of each species were calculated from the retention times of the peak absorbance by comparison with calibration standards having known molecular weights to identify the oligomerization state of NisI Δ 1-19. B. Native-PAGE analysis was utilized to determine the oligomerization state of 5 μ M NisI Δ 1-19 in the absence and presence of nisin.

7.2.6 Lipid II localization within *B. subtilis* ATCC 6633.

The goal of this study was to optimize the staining, mounting, and growth conditions for the observation of lipid II localization in *B. subtilis* 6633. Conditions

tested included live versus fixed (4% formaldehyde) imaging; culturing for 4, 6, 12, or 18 h; use of diverse growth media - Luria-Bertani (LB) broth, tryptone-yeast extract (TY) broth, brain heart infusion (BHI) broth, or Difco™ sporulation medium (DSM); different labeled antibiotic concentrations - 0.1, 0.5 or 1 μM b-vancomycin and b-nisin (see chapter 3); various mounting conditions - Slowfade (antifade reagent), poly-d-lysine, or 0.5% low melt agarose; and the use of epifluorescence versus confocal microscopy. A series of experiments were performed with each condition independently, and the optimal conditions for lipid II viewing were *B. subtilis* 6633 cultures grown in DSM broth for 6-12 h with live imaging and 0.5% agarose immobilization utilizing 0.5 μM b-vancomycin and b-nisin (Figure 7.6 and data not shown). *B. subtilis* 6633 cultured in TY, LB, and BHI broths grew to higher cell numbers, but the lipid II localization was more difficult to observe since cells were significantly shorter in length. The shorter cells prevented the visualization of lipid II along the long axis of the cell (data not shown). Observations at 4 h were hindered by low cell density while cultures at 18 h were affected by sporulation. Released spores were highly labeled and exceptionally bright when present in fields of vision, which hindered accurate observation of lipid II of adjacent bacilli (data not shown). Cells that were treated with 0.1 μM b-vancomycin and b-nisin were not stained sufficiently and required long exposure times to observe lipid II localization, which caused photobleaching of the fluorophore. B-vancomycin at 1 μM stained both the lipid II and the cell wall of the bacilli, which hindered specific localization of only lipid II. The use of 1 μM b-nisin displayed some but minor non-specific labeling of the cell

membrane (data not shown). When mounting slides in Slowfade, the cells were not immobilized or adherent to the slide surface allowing cell movement and causing blurred images. Immobilization with poly-D-lysine caused a significant increase in background fluorescence that prevented accurate visualization of lipid II (data not shown). Fixing of the cells altered membrane physiology to the extent that lipid II localization was also altered resulting in an overall diffuse localization of lipid II (data not shown). Epi-fluorescence microscopy was chosen over confocal microscopy because of high fluorescence sensitivity and reduced transmission energy to prevent photo bleaching. With the optimized conditions identified, high-resolution images were obtained that demonstrated lipid II localization at the poles and across the long axis of the cell. These images correlated with previous studies visualizing lipid II with fluorescently labeled antibiotics (5, 21).

Figure 7.6

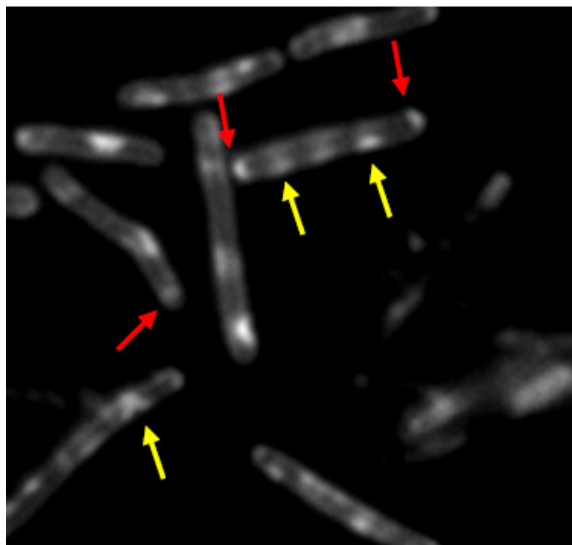


Figure 7.6. Optimized lipid II localization within *B. subtilis* 6633. *B. subtilis* 6633 cells were cultured in DSM for 12 h followed by the addition of b-vancomycin (0.5 μ M) for 5 min.

Figure 7.6 (continued)

Samples were taken and mounted on glass slide in 0.5% agarose for live epi-fluorescence microscopy. The localization of lipid II as a function of b-vanocmycin staining is indicated at the long axis (yellow arrows) and the poles (red arrows) of the cells. The image was obtained using a Applied Precision assembled DeltaVision epi-fluorescence microscope containing an Olympus Plan Apo x100 oil objective with a numerical aperture of 1.42 and a working distance of 0.15 mm.

7.2.7 Purification of subtilin from *B. subtilis* ATCC 6633.

To facilitate *in vitro* investigation into the interaction between Spal Δ 1-22 and subtilin, a purification protocol had to be developed to purify subtilin to high purity from culture supernatants of *B. subtilis* ATCC 6633. Special effort was made to identify conditions to purify N-succinyl-subtilin from wild-type subtilin since the N-terminal modification induces a substantial loss of antimicrobial activity (10). *B. subtilis* ATCC 6633 was cultured at 37 °C for 12, 15, or 18 h in 500 mL of LB broth, and culture supernatants were analyzed by MALDI-TOF mass spectrometry. The data demonstrated that all cultures produced subtilin as the most abundant analyte within the supernatants (Figure 7.7A). However, with increased incubation times an increase in the N-succinyl-subtilin was observed, particularly at 18 h (Figure 7.7A). The culture supernatants were subjected to a two-step purification method utilizing Varian C18 bond-elute chromatography and reverse phase-HPLC with a C4 column to obtain subtilin as a single species from reverse phase-HPLC. MALDI-TOF mass spectrometry analysis identified this species as subtilin and associated salt adducts (Figure 7.7B). Thus, a protocol has been developed utilizing a two-step procedure that effectively purifies subtilin

from cell culture supernatants and most importantly from N-succinyl-subtilin, with no similar protocol developed to date.

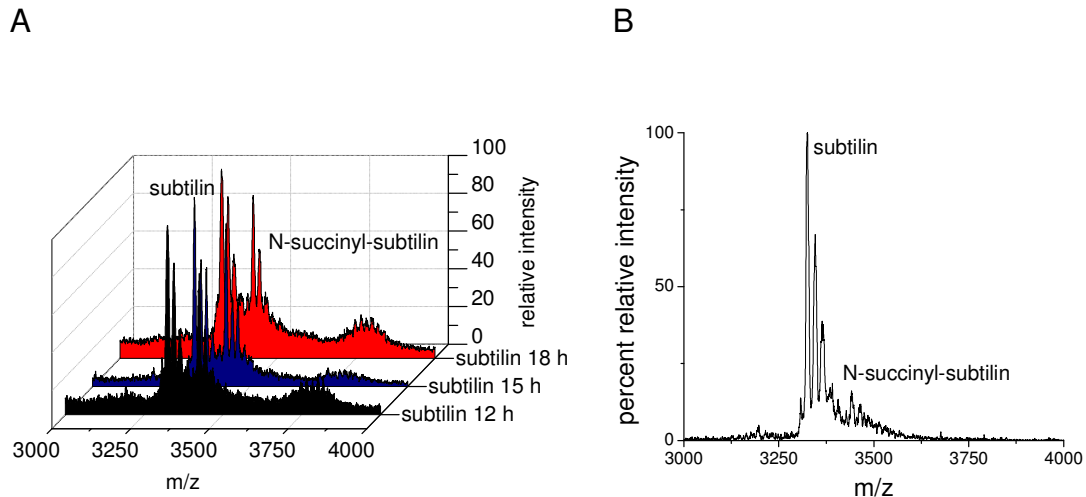


Figure 7.7. Purification of subtilin from *B. subtilis* ATCC 6633. A. *B. subtilis* ATCC 6633 was cultured for 12 (black), 15 (red), and 18 h (blue) in LB broth. Samples were taken at the end of culture to observe the expression of subtilin and n-succinyl-subtilin. B. Cultures were first partially purified with a Varian C18 bond elute chromatography prior to final HPLC purification and analysis by MALDI-TOF mass spectrometry. Subtilin, major peak, with salt adducts and n-succinyl-subtilin, minor peak, were observed.

7.3 Discussion

A series of SpaI and SpaF tagged constructs were generated to facilitate differential expression, multiple visualization options, and differential protein tagging to monitor the interaction of immunity proteins with other prominent cellular structures, specifically cell proteins and peptidoglycan substrates. The 2 types of integrative plasmids, pMUTIN and pSG, were chosen because they facilitate differential expression of the gene of interest. pMUTIN will integrate at the gene of interest via a single crossover event between the chromosomal and

cloned fragments. The transformant will produce a tagged construct of the inserted gene of interest under the native promoter with the remainder of the operon under the control of an isopropyl β -D-1-thiogalactopyranoside (IPTG) inducible promoter (11). pSG integrates into the amylase gene, *amyE*, via a single crossover event with the target gene under the control of a xylose inducible promoter (7). The multiple tags of each protein - CFP, GFP, YFP, cMYC, HA, and tetracysteine - provides several color options to ensure that fluorescence emission and excitation profile do not overlap, especially in experiments designed to simultaneously detect SpaI and SpaF localization as well as with any potential cell wall substrates or proteins. The addition of a tetracysteine tag to SpaI and SpaF allows visualization in live cells with ReAsh in the red visual spectrum (1). The addition of ReAsh extends the available color spectrum to include red to further prevent emission and excitation overlap. The addition of HA and MYC tags facilitate antibody based imaging, which expands the color pallet from blue to far red utilizing a series of AlexaFluor conjugated antibodies instead of being limited to the cyan to red color spectrum presented by current fluorescent protein limitations. The ability to express the tagged proteins under the native promoter or with sugar inducers facilitates controlled expression of the tagged protein. Furthermore, placing the expression of SpaEG under inducible expression enables investigation into pump formation and protein localization as a function of complex formation. Unfortunately, with the IPTG induced expression of SpaEG, the wild type untagged SpaF will also be expressed, which is a consequence of the single crossover insertion that tagged

the gene of interest. The untagged SpaF will compete with natively expressed tagged SpaF for SpaEG interaction and complex formation, which may ultimately affect tagged SpaF localization. In addition to providing a wide set of colors for tagging to prevent overlap of fluorescence properties, the multiple tags of a single protein will be used to determine whether any tag specific alterations in localization occur. Lastly, the multiple tags provide several options in the event that multiple microscopes are required for these studies. Each microscope is accompanied by a set of limitations, and the tractability of multiple color options will help to prevent any delays that may arise as a consequence of limited fluorescence image filter sets or lasers. With these tools and with an optimized protocol for lipid II staining, studies can be initiated to determine the *in vivo* localization of lantibiotic immunity genes and their relationship to membrane bound proteins and structures.

As a part of this chapter, studies were conducted to determine the *in vitro* interaction between NisI Δ 1-19 and nisin as well as performing the necessary ground work to investigate SpaI Δ 1-22 and subtilin interactions. *In vitro* investigations were facilitated by the development of NisI Δ 1-19 expression and purification protocols, and these studies demonstrated that nisin did not induce any changes to the structural or oligomeric state of the immunity protein. Further research is necessary to fully understand the NisI Δ 1-19-nisin interaction particularly with reports that this interaction is highly unstable causing precipitation (19), although thus far such behavior was not observed. For the studies into SpaI Δ 1-22, constructs and protocols were developed for the

expression of both GST- and His₆-tag constructs, and for the first time, a protocol was developed for the purification of subtilin that was also able to separate subtilin from N-succinyl-subtilin. These materials will enable mechanistic investigations into binding interactions between subtilin and Spal Δ 1-22.

A significant number of studies have been performed to identify new lantibiotics, elucidate biosynthetic mechanisms, perform bioengineering, and determine mechanisms of action (2, 3, 8, 16, 17); however, a detailed understanding of how lantibiotic immunity genes interact with their cognate producers have been very limited. *In vitro* and *in vivo* studies have identified general mechanisms of action, predicted protein structure, provided protein specificity for immunity, and in limited cases identified necessary residues or structure characteristics that mediate immunity (6, 14, 20). Significantly more research into these aspects of immunity is required to truly understand how producer organisms create highly specific and effective self-resistance to lantibiotics. The diversity witnessed in antimicrobial peptide structures can potentially be rivaled by the structural diversity and specificity of immunity proteins.

7.4 Materials and Methods

7.4.1 Cloning of immunity genes.

pGEX-6P-1-*nis*/ Δ 1-19 - Genomic DNA was obtained from *L. lactis* ATCC 11454 cultivated at 30°C without aeration in GM17 (3.725% M17 broth, Oxoid, Hampshire, England; Millipore deionized water; 0.5% glucose, Fisher Chemical,

Fairlawn, NJ). DNA was isolated from mid-log-phase cultures and was purified using the DNeasy tissue kit (QIAGEN, Valencia, CA). *L. lactis* 11454 *nisI* was PCR amplified using primers (Integrated DNA Technologies, Coralville, IA) that excluded the first 57 5' nucleotides to develop a deletion of the first 19 N-terminal amino acids (Table 7.2). These primers were engineered such that 5' BamHI and 3' XhoI restriction sites were incorporated. Each PCR product was purified using the PCR purification kit (QIAGEN). The purified amplicons were sequentially incubated with BamHI (New England Biolabs, Ipswich, MA) and XhoI (New England Biolabs) to generate directional annealing sites. The amplicons were then ligated with pGEX-6P-1 (GE Healthcare, Piscataway, NJ) plasmid digested with the same restriction enzymes to replace the BamHI-XhoI fragment within the multiple cloning site. The ligation mixtures were introduced into *E. coli* DH5 α (Novagen, Madison, WI) by electroporation. The integrity of each gene from individual clones was confirmed by DNA sequencing. pGEX-6P-1-*nisI* Δ 1-19 was isolated using the plasmid miniprep kit (QIAGEN) and introduced by electroporation into *E. coli* T7 lysogen BL21 (DE3) (Novagen). Pfx platinum polymerase for PCR amplification was acquired from Stratagene (La Jolla, CA). DNA sequencing was performed at the Roy J. Carver Biotechnology Center (Urbana, IL).

pGEX-6P-1- *spaI* Δ 1-19 - Genomic DNA was obtained from *B. subtilis* ATCC 6633 cultivated at 37 °C with aeration on a rotary shaker in brain heart infusion medium (3.7% Bacto brain heart infusion, BD Diagnostics, Franklin Lakes, NJ; Millipore deionized water; 0.5% glycerol, Fisher Chemical). DNA was

isolated from mid-log-phase cultures and was purified using the DNeasy tissue kit. *B. subtilis* 6633 *spaI* was PCR amplified using primers that excluded the first 66 5' nucleotides of the gene to develop a deletion of the first 22 N-terminal amino acids (Table 7.2). These primers were engineered such that 5' BamHI and 3' XhoI restriction sites were incorporated. Each PCR product was purified using the PCR purification kit. The purified amplicons were sequentially incubated with BamHI and XhoI to generate directional annealing sites. The amplicons were then ligated with pGEX-6P-1 plasmid digested with the same restriction enzymes to replace the BamHI-XhoI fragment within the multiple cloning site. The ligation mixtures were introduced into *E. coli* DH5 α by electroporation. The integrity of each gene from individual clones was confirmed by DNA sequencing. pGEX-6P-1-*spaI* Δ 1-22 was isolated using the plasmid miniprep kit and introduced by electroporation into *E. coli* T7 lysogen BL21 (DE3).

pET15b-*spaI* Δ 1-22 - Genomic DNA was obtained from *B. subtilis* ATCC 6633 cultivated at 37 °C with aeration on a rotary shaker in brain heart infusion medium (3.7% Bacto brain heart infusion, Millipore deionized water, 0.5% glycerol shaker). DNA was isolated from mid-log-phase cultures and was purified using the DNeasy tissue kit. *B. subtilis* 6633 *spaI* was PCR amplified using primers that exclude the first 66 5' nucleotides of the gene to develop a deletion of the first 22 N-terminal amino acids (Table 7.2). These primers were engineered such that 5' NdeI and 3' XhoI restriction sites were incorporated. Each PCR product was purified using the PCR purification kit. The purified amplicons were sequentially incubated with NdeI (New England Biolabs) and

XhoI to generate directional annealing sites. The amplicons were then ligated with pET-15b (Novagen) plasmid to replace the NdeI-XhoI fragment within the multiple cloning site. The ligation mixtures were introduced into *E. coli* DH5 α by electroporation. The integrity of each gene from individual clones was confirmed by DNA sequencing. pET15b-*spa* Δ 1-22 was isolated using the plasmid miniprep kit and introduced by electroporation into *E. coli* T7 lysogen BL21(DE3).

Table 7.2

Primer sequences for cloning LanI immunity proteins							
Gene ^a	Protein ID ^b	Primer	Primer Sequence (5'→3') ^c	Plasmid	Affinity tag ^d	First residue of coding sequence ^e	Last residue of coding sequence ^f
<i>nisI</i>	CAA54209.1	Forward	5'-GCGCGCGGATCCTG TTATCAAACAAGTCAT AAAAAGG-3'	pGEX-6P-1	GST	Cys20	Asn245
		Reverse	5'-ATATATCTCGAGCT AGTTTCTACCTTCGT TGCAAGC-3'				
<i>spaI</i>	AAB91598.1	Forward	5'-GCGCGCGGATCC TGCAATCATTAACA AAGTTTAAAG-3'	pGEX-6P-1	GST	Cys23	Asp165
		Reverse	5'-ATATATCTCGAGTT ATTCTTTTCATTCTT TATTTAAACC-3'				
<i>spaI</i>	AAB91598.1	Forward	5'-GCGCGCCATATGTG TCAATCATTAACAAAG TTTAAAG-3'	pET-15b	His ₆	Cys23	Asp165
		Reverse	5'- ATATATCTCGAGTTAT TCCTTTTCATTCTTTATT AAAACC-3'				

Table 7.2. Primer sequences cloning LanI immunity proteins. ^a *nisI* was cloned from *L.lactis* ATCC 11454. *spaI* was cloned from *B. subtilis* ATCC 6633. ^b Protein and DNA sequences were obtained from Pubmed Nucleotide, National Center for Biotechnology Information, U.S. National Library of Medicine (<http://www.ncbi.nlm.nih.gov/nucleotide/>).

Table 7.2 (continued)

^c Oligonucleotide primers were engineered such that 5' BamHI and 3' XhoI restriction sites were incorporated for genes that were inserted into pGEX-6P-1. Oligonucleotide primers were engineered such that 5' NdeI and 3' XhoI restriction sites were incorporated for the gene inserted into pET-15b. Primers were synthesized by Integrated DNA Technologies (Coralville, IA). Coding sequence was obtained from Pubmed Nucleotide. ^d Indicates the N-terminal that installed by plasmid for affinity purification. ^e Nucleotide sequence for the first 19 amino acids of NisI were excluded to remove the N-terminal secretion signal peptide. Nucleotide sequence for the first 22 amino acids of SpaI was excluded to remove the N-terminal secretion signal peptide. First amino acid of cloned immunity gene is indicated. ^f Indicates the last amino acid of protein.

pHCMC05 constructs - Genomic DNA was obtained from *B. subtilis* ATCC 6633 cultivated at 37 °C with aeration on a rotary shaker in brain heart infusion medium. DNA was isolated from mid-log-phase cultures and was purified using the DNeasy tissue kit. *B. subtilis* 6633 *spaI* and *spaF* were PCR amplified using primers corresponding to the 5' and 3' ends of each gene (Table 7.3 and 7.4). A series of sequential PCR amplification introduced 5' BamHI and 3' EcoRI-AatII restriction sites as well as a 3' tetracysteine (TC) or MYC tag utilizing primer extension (Table 7.3 and 7.4). Each PCR product was purified using the PCR purification kit. The purified amplicons were sequentially incubated with BamHI and EcoRI (New England Biolabs) to generate directional annealing sites. The amplicons were then ligated with pUC-19 plasmid (New England Biolabs) to replace the BamHI-EcoRI fragment within the multiple cloning site. The ligation mixtures were introduced into *E. coli* DH5α by electroporation. The integrity of each gene from individual clones was confirmed by DNA sequencing. The pUC-19 constructs with the correct sequences were

isolated using the plasmid miniprep kit and incubated with BamHI and AatII (New England Biolabs) to isolate the target tagged gene and generate directional annealing sites. The digest fragments were purified via 1% agarose gel purification and Qiaquick gel extraction kit (Qiagen) and ligated with pHCMC05 plasmid (15) to replace the BamHI-AatII (*spaI/F*) or BamHI-ClaI (*nisI*) fragment within the multiple cloning site. The ligation mixtures were introduced into *E. coli* DH5 α by electroporation. The integrity of each gene from individual clones was confirmed by DNA sequencing. pHCMC05-*spaI*-TC, pHCMC05-*spaI*-MYC, pHCMC05-*spaF*-TC, and pHCMC05-*spaF*-MYC were isolated using the plasmid miniprep kit for transformation of *B. subtilis* ATCC 6633.

Table 7.3

Cloning of <i>B. subtilis</i> ATCC 6633 <i>SpaI</i> and addition of a C-terminal tag						
Gene	Protein id ^a	Primer	Primer Sequence (5'→3') ^b	Plasmid	Tag ^c	First residue of coding sequence ^e
<i>spaI</i>	AAB91598.1	Forward	5'-GCGCGCGGATCCAT GTTGTTTTTGAAAAGA AGTGTTAC-3'	pHCMC05	tetra- Cys/cMyc	Met1
		Reverse 1	5'-GCAGCAGCCCGGGC AGCATTCTTTTCATT TTATTAAAACC-3'		tetra-Cys	
		Reverse 2	5'-ATATATGAATTGAC GTCCTAGCAGCAGCC CGGGCAGCA-3'			
		Reverse 1	5'-ACTTATTAATTTTTG CTCTCCTTTTCATTCT TTATTAAAACC-3'			
		Reverse 2	5'-GACGTCCTATAAA TCCTCCTCACTTATT AATTTTTGCTC-3'		cMyc	
		Reverse 3	5'-ATATATGAATTG ACGTCCTATAAATC CTCCTC-3'			

Table 7.3. Cloning of *B. subtilis* ATCC 6633 *SpaI* and addition of a C-terminal tag. ^a DNA sequence was obtained from Pubmed Nucleotide, National Center for Biotechnology Information,

Table 7.3 (continued)

U.S. National Library of Medicine (<http://www.ncbi.nlm.nih.gov/nucleotide/>). ^b Oligonucleotide primers were engineered such that 5' BamHI and 3' EcoRI-AatII restriction sites were incorporated. Primers were synthesized by Integrated DNA Technologies (Coralville, IA). Coding sequence was obtained from Pubmed Nucleotide. ^c Primers utilized to create the indicated c-terminal tag that was added via overlap extension. ^d Indicates the first amino acid of cloned immunity gene.

Cloning of <i>B. subtilis</i> ATCC 6633 SpaF and addition of a C-terminal tag						
Gene	Protein id ^a	Primer	Primer Sequence (5'→3') ^b	Plasmid	Tag ^c	First residue of coding sequence ^e
<i>spaF</i>	AAB91598.1	Forward	5'-GCGCGCGGATCC ATGAAAAGGAATAAG GGAGAGTGTGAC-3'	pHCMC05	tetra- Cys/cMyc	Met1
		Reverse 1	5'-GCAGCAGCCCGGG CAGCATCTTTTACAC CTTCTTTTTCACGAG-3'		tetra-Cys	
		Reverse 2	5'-ATATATGAATTCGAC GTCCTAGCAGCAGCC CGGGCAGCA-3'			
		Reverse 1	5'-ACTTATTAATTTTTG CTCTCTTTTACACCTT CTTTTTCACGAG-3'			
		Reverse 2	5'-GACGTCCTATAAATC CTCCTCACTTATTAATT TTTGCTC-3'		cMyc	
		Reverse 3	5'-ATATATGAATTCGA CGTCCTATAAATCCT CCTC-3'			

Table 7.4. Cloning of *B. subtilis* ATCC 6633 SpaF and addition of a C-terminal tag.

^a DNA sequence was obtained from Pubmed Nucleotide, National Center for Biotechnology Information, U.S. National Library of Medicine (<http://www.ncbi.nlm.nih.gov/nucleotide/>).

^b Oligonucleotide primers were engineered such that 5' BamHI and 3' EcoRI-AatII restriction sites were incorporated. Primers were synthesized by Integrated DNA Technologies (Coralville, IA). Coding sequence was obtained from Pubmed Nucleotide. ^c Primers utilized to create the indicated c-terminal tag that was added via overlap extension. ^d Indicates the first amino acid of cloned immunity gene.

pSG constructs - Genomic DNA was obtained from *B. subtilis* ATCC 6633 cultivated at 37 °C with aeration on a rotary shaker in brain heart infusion medium. DNA was isolated from mid-log-phase cultures and was purified using the DNeasy tissue kit. *B. subtilis* 6633 *spaI* and *spaF* were PCR amplified using primers corresponding to the 5' and 3' ends of each gene (Table 7.5 and 7.6). These primers were engineered such that 5' KpnI (*spaI*) or ClaI (*spaF*) and 3' XhoI (*spaI* and *spaF*) restriction sites were incorporated. Each PCR product was purified using the PCR purification kit. The purified amplicons were sequentially incubated with KpnI (*spaI*; New England Biolabs) or ClaI (*spaF*) and XhoI (*spaI* and *spaF*) to generate directional annealing sites. The amplicons were then ligated with pSG (GFP, CFP, YFP) (7) plasmids to replace the KpnI-EcoRI (*spaI*) or XhoI-EcoRI (*spaF*) fragment within the multiple cloning site. The ligation mixtures were introduced into *E. coli* DH5 α by electroporation. The integrity of each gene from individual clones was confirmed by DNA sequencing. pSG-*spaI*-GFP, pSG-*spaI*-CFP, pSG-*spaI*-YFP, pSG-*spaF*-GFP, pSG-*spaF*-CFP, and pSG-*spaF*-YFP were isolated using the plasmid miniprep kit for transformation of *B. subtilis* ATCC 6633.

Cloning of <i>B. subtilis</i> ATCC 6633 Spal and addition of a fluorescent C-terminal tag						
Gene	Protein id ^a	Primer	Primer Sequence (5'→3') ^b	Plasmid ^c	Tag ^d	First residue of coding sequence ^e
<i>spal</i>	AAB91598.1	Forward	5'-GCGCGCGGTACC ATGTTGTTTTGAAA AGAAGTGTAAAC-3'	pSG1154	GFP	Met1
		Reverse	5'-ATATATGAATTCTT CCTTTTCATTCTTTAT TAAAAC-3'	pSG1192 pSG1193	CFP YFP	

Table 7.5. Cloning of *B. subtilis* ATCC 6633 Spal and addition of a fluorescent C-terminal tag. ^a DNA sequence was obtained from Pubmed Nucleotide, National Center for Biotechnology Information, U.S. National Library of Medicine (<http://www.ncbi.nlm.nih.gov/nucleotide/>). ^b Oligonucleotide primers were engineered such that 5' KpnI and 3' EcoRI restriction sites were incorporated. Primers were synthesized by Integrated DNA Technologies (Coralville, IA). Coding sequence was obtained from Pubmed Nucleotide. ^c Plasmid used will insert into *amyE* within the chromosome inactivating the gene. The expression of *spal* will be under the control of a xylose inducible promoter. ^d Indicates the transcriptional c-terminal tag added to Spal. ^e Indicates the first amino acid in Spal.

Table 7.6

Cloning of <i>B. subtilis</i> ATCC 6633 SpaF and addition of a fluorescent C-terminal tag						
Gene	Protein id ^a	Primer	Primer Sequence (5'→3') ^b	Plasmid ^c	Tag ^d	First residue of coding sequence ^e
<i>spaF</i>	AAB91597.1	Forward	5'-GCGCGCCTCGA GATGAAAAGGAATA AGGGAGAGTGTG-3'	pSG1154	GFP	Met1
		Reverse	5'-ATATATGAATTCTC TTTTTACACCTTCTTT TTCACGAGTTG-3'	pSG1192 pSG1193	CFP YFP	

Table 7.6. Cloning of *B. subtilis* ATCC 6633 SpaF and addition of a fluorescent C-terminal tag. ^a DNA sequence was obtained from Pubmed Nucleotide, National Center for Biotechnology Information, U.S. National Library of Medicine (<http://www.ncbi.nlm.nih.gov/nucleotide/>).

Table 7.6 (continued)

^b Oligonucleotide primers were engineered such that 5' XhoI and 3' EcoRI restriction sites were incorporated. Primers were synthesized by Integrated DNA Technologies (Coralville, IA). Coding sequence was obtained from Pubmed Nucleotide. ^c Plasmid used will insert into *amyE* within the chromosome inactivating the gene. The expression of *spaF* will be under the control of a xylose inducible promoter. ^d Indicates the transcriptional c-terminal tag added to SpaF. ^e Indicates the first amino acid in SpaF.

pMUTIN constructs -Genomic DNA was obtained from *B. subtilis* ATCC 6633 cultivated at 37 °C with aeration on a rotary shaker in brain heart infusion medium. DNA was isolated from mid-log-phase cultures and was purified using the DNeasy tissue kit. *B. subtilis* 6633 *spaI* and *spaF* were PCR amplified using primers corresponding to the 5' and 3' ends of each gene (Table 7.7 and 7.8). These primers were engineered such that 5' HindIII (*spaI* and *spaF*) and 3' KpnI (*spaI*) or ClaI (*spaF*) restriction sites were incorporated. Each PCR product was purified using the PCR purification kit. The purified amplicons were sequentially incubated with HindIII (New England Biolabs) and KpnI (*spaI*) or ClaI (*spaF*) to generate directional annealing sites. The amplicons were then ligated with pMUTIN (GFP, CFP, YFP, HA, MYC) (11) plasmids to replace the HindIII-KpnI (*spaI*) or HindIII-ClaI (*spaF*) fragment within the multiple cloning site. The ligation mixtures were introduced into *E. coli* DH5α by electroporation. The integrity of each gene from individual clones was confirmed by DNA sequencing. pMUTIN-*spaI*-GFP, pMUTIN-*spaI*-CFP, pMUTIN-*spaI*-YFP, pMUTIN-*spaI*-HA, pMUTIN-*spaI*-MYC, pMUTIN-*spaF*-GFP, pMUTIN-*spaF*-CFP, pMUTIN-*spaF*-YFP,

pMUTIN-*spaF*-HA, and pMUTIN-*spaF*-MYC were isolated using the plasmid miniprep kit for transformation of *B. subtilis* ATCC 6633.

Cloning of <i>B. subtilis</i> ATCC 6633 <i>Spal</i> and addition of a fluorescent C-terminal tag						
Gene	Protein id ^a	Primer	Primer Sequence (5'→3') ^b	Plasmid ^c	Tag ^d	First residue of coding sequence ^e
<i>spaI</i>	AAB91598.1	Forward	5'-GCGCGAAGCTT ATGTTGTTTTTGA AGAAGTGTTAAC-3'	pMutin-GFP	GFP	Met1
				pMutin-CFP	CFP	
		Reverse	5'-ATATATCCATGGT TCCTTTCATTCTT ATTAAAAC-3'	pMutin-YFP	YFP	
				pMutin-cMyc	cMyc	
			pMutin-HA	HA		

Table 7.7. Cloning of *B. subtilis* ATCC 6633 *Spal* and addition of a fluorescent C-terminal tag. ^a DNA sequence was obtained from Pubmed Nucleotide, National Center for Biotechnology Information, U.S. National Library of Medicine (<http://www.ncbi.nlm.nih.gov/nucleotide/>). ^b Oligonucleotide primers were engineered such that 5' HindIII and 3' KpnI restriction sites were incorporated. Primers were synthesized by Integrated DNA Technologies (Coralville, IA). Coding sequence was obtained from Pubmed Nucleotide. ^c Plasmid used will insert into the chromosome at the gene of interest via double crossover tagging chromosomal copy of the gene with the indicated tag under the control of the native promoter and placing the downstream genes of the operon under the control of a IPTG inducible promoter. ^d Indicates the transcriptional c-terminal tag added to *Spal*. ^e Indicates the first amino acid in *Spal*.

Cloning of <i>B. subtilis</i> ATCC 6633 SpaF and addition of a fluorescent C-terminal tag						
Gene	Protein id ^a	Primer	Primer Sequence (5'→3') ^b	Plasmid ^c	Tag ^d	First residue of coding sequence ^e
<i>spaF</i>	AAB91597.1	Forward	5'-GCGCGCAAGCT TATGAAAAGGAATA AGGGAGAGTGTG-3'	pMutin-GFP	GFP	Met1
				pMutin-CFP	CFP	
		Reverse	5'-ATATATTAGCTATC TTTTTACACCTTCTTT TTCACGAGTTG-3'	pMutin-YFP	YFP	
				pMutin-cMyc	cMyc	
				pMutin-HA	HA	

Table 7.8. Cloning of *B. subtilis* ATCC 6633 SpaF and addition of a fluorescent C-terminal tag. ^a DNA sequence was obtained from Pubmed Nucleotide, National Center for Biotechnology Information, U.S. National Library of Medicine (<http://www.ncbi.nlm.nih.gov/nucleotide/>). ^b Oligonucleotide primers were engineered such that 5' HindIII and 3' Clal restriction sites were incorporated. Primers were synthesized by Integrated DNA Technologies (Coralville, IA). Coding sequence was obtained from Pubmed Nucleotide. ^c Plasmid used will insert into the chromosome at the gene of interest via double crossover tagging chromosomal copy of the gene with the indicated tag under the control of the native promoter and placing the downstream genes of the operon under the control of a IPTG inducible promoter. ^d Indicates the transcriptional c-terminal tag added to SpaF. ^e Indicates the first amino acid in SpaF.

7.4.2 Transformation of *Bacillus subtilis*: starvation.

The recipient strain, *B. subtilis* ATCC 6633, was streaked on solid Luria-Bertani broth (LB, 1.0% Bacto Trypton, BD Diagnostics; 0.5% Bacto yeast extract, BD Diagnostics; 0.5% NaCl, Fisher Chemical; Millipore deionized water) and incubated overnight (18 hr) at 37 °C. Colonies were selected and used to 4.5 mL of medium A (0.1% yeast extract, BD Diagnostics; 0.02% casamino

acids, Fisher Chemical; 0.5% glucose; 0.2% $(\text{NH}_4)_2\text{SO}_4$, Fisher Chemical; 0.183% K_2HPO_4 , Fisher Chemical; 0.6% KH_2PO_4 , Fisher Chemical; 0.1% sodium citrate, Fisher Chemical; 0.02% MgSO_4 , Fisher Chemical) in a sterile test tube. Contents of the tube were mixed thoroughly and optical density (OD) was measured at 600 nm with a spectrophotometer (Genesys 20 spectrophotometer, Thermo Fisher Scientific, Waltham, MA). The OD_{600} was adjusted 0.1-0.2 while maintaining the volume at 4.5 ml. The cultures were incubated at 37 °C with vigorous aeration. The optical density was measured at 600 nm every 20 min and OD_{600} plotted against time on semi-log paper. After a brief lag, the OD increased logarithmically. The point at which the culture leaves log growth is known as t_0 in *Bacillus* genetics. The incubation was continued for 90 minutes after the cessation of log growth (t_{90}). The cultures (0.05 mL) were back diluted into 0.45 mL of pre-warmed medium B (medium A; 0.5 mM CaCl_2 , Fisher Chemical; 2.5 nM MgCl_2) with in a clean and sterile test tube for each transformation plus an extra tube for a DNA-free control. The diluted cultures were incubated at 37 °C with vigorous aeration. After 90 min, DNA (1 µg) was added to the competent cells and incubated at 37 °C with aeration for 30 minutes. Aliquots of the transformed cells were plated onto selective agar and incubated overnight at 37 °C.

7.4.3 GST purification of *Nisl*Δ1-19 and *Spal*Δ1-22.

E. coli BL21 (DE3) transformed with either pGEX-6P-1-*nisl*Δ1-19 or pGEX-6P-1-*spal*Δ1-22 was grown in Luria-Bertani broth (LB, 5 mL)

supplemented with ampicillin (100 µg/mL, Fisher Chemical) at 37 °C and with aeration. After 8 h, the initial culture was back-diluted into fresh LB broth (50 mL) supplemented with ampicillin (100 µg/mL) at 37 °C and grown overnight with aeration. After 12 h, the starter culture was back diluted into fresh LB broth (2000 mL) supplemented with ampicillin (100 µg/mL) at 37 °C and grown with aeration until the optical density at 600 nm reached 0.7. Expression of *nislΔ1-19* or *spalΔ1-22* was induced by addition of IPTG (0.25 mM, Fisher Chemical). The cultures were grown for an additional 4 h and then harvested by centrifugation at 8,000 x g for 10 min at 4 °C (Beckman JA-10 rotor, Brea, CA). The pellets were resuspended in 25 mL of binding buffer (500 mM KCl, 140 mM NaCl, 10 mM Na₂PO₄, 1.8 mM KH₂PO₄; pH 7.3; Sigma Aldrich, St. Louis, MO) with 20% glycerol and lysed by sonication (35% amplitude, 4.4 s pulse, 9.9 s pause for total 25 min; Sonics & Materials, Inc., Newtown, CT). The sample was centrifuged at 23,700xg for 30 min at 4 °C. The supernatant was loaded onto 10 mL (bed volume) glutathione affinity resin (glutathione sepharose 4 fast flow resin, GE Healthcare) pre-equilibrated with binding buffer. After 1 hour of gentle agitation at 4 °C, the bound protein was washed with twenty 10 mL volumes of binding buffer, three 10 mL volumes of equilibration buffer (50 mM Tris ,100 mM NaCl; pH 8; Sigma Aldrich, St. Louis, MO), and eluted with three 10 mL volumes of elution buffer (50 mM Tris ,100 mM NaCl, 20 mM glutathione; pH 8; Sigma Aldrich). The column eluant was then exchanged into PreScission protease cleavage buffer (50 mM Tris-HCl, 100 mM NaCl, 1 mM EDTA, 1 mM DTT; pH 8.0; Sigma Aldrich) utilizing an Amicon centrifugal filter device. GST tagged

proteins were incubated with 150 μ L of PreScission protease overnight at 4 $^{\circ}$ C with gentle agitation. After 12 h, the cleavage reaction was loaded onto 10 mL (bed volume) glutathione affinity resin (GE Healthcare) pre-equilibrated with binding buffer. After 1 hour of gentle agitation at 4 $^{\circ}$ C, the untagged NisI Δ 1-19 and SpaI Δ 1-22 were eluted with twenty 10 mL volumes of binding buffer. The column eluant was then exchanged into 50 mM HEPES (EMD Biosciences, Inc., La Jolla, CA) with 20% glycerol utilizing an Amicon centrifugal filter device. Proteins were quantified utilizing the Bradford protein quantification assay.

The glutathione resin was prepared for protein binding by washing 10 mL (bed volume) of resin with six 10 mL volumes of 6 M guanidine HCl (Sigma Aldrich), ten 10 mL volumes of deionized water, three 10 mL volumes of 1 mM dithiothreitol (DTT, Sigma Aldrich), and twenty 10 mL volumes of binding buffer.

7.4.4 Nickel affinity purification of *SpaI* Δ 1-22.

E. coli BL21(DE3) transformed with either pET-15b-*spaI* Δ 1-22 was grown in LB broth (5 mL) supplemented with ampicillin (100 μ g/mL) at 37 $^{\circ}$ C and with aeration. After 8 h, the initial culture was back-diluted into fresh LB broth (50 mL) supplemented with ampicillin (100 μ g/mL) at 37 $^{\circ}$ C and grown overnight with aeration. After 12 h, the starter culture was back-diluted into fresh LB broth (2000 mL) supplemented with ampicillin (100 μ g/mL) at 37 $^{\circ}$ C and grown with aeration until the optical density at 600 nm reached 0.7. Expression of *nisl* Δ 1-19 or *spaI* Δ 1-22 was induced by addition of IPTG (0.25 mM, Fisher Chemical). The cultures were grown for an additional 4 h and then harvested by centrifugation at

8,000 x g for 10 min at 4 °C (Beckman JA-10 rotor, Brea, CA). The pellets were resuspended in 25 mL of GST binding buffer (500 mM KCl, 140 mM NaCl, 10 mM Na₂PO₄, 1.8 mM KH₂PO₄; pH 7.3; Sigma, St. Louis, MO) with 20% glycerol and lysed by sonication (35% amplitude, 4.4 s pulse, 9.9 s pause for total 25 min; Sonics & Materials, Inc., Newtown, CT). The sample was centrifuged at 23,700xg for 30 min at 4 °C. The supernatant was loaded onto 5 mL (bed volume) of Talon® cobalt affinity resin (Clontech, Mountain View, CA) pre-equilibrated with start buffer. After 1 hour of gentle agitation at 4 °C, the bound protein was washed with two 10 mL volumes of binding buffer, one 10 mL volumes of wash buffer (500 mM KCl, 140 mM NaCl, 10 mM Na₂PO₄, 1.8 mM KH₂PO₄, 5 mM imidazole; pH 7.3; Sigma Aldrich), and eluted with two 10 mL volumes of elution buffer (500 mM KCl, 140 mM NaCl, 10 mM Na₂PO₄, 1.8 mM KH₂PO₄, 200 mM imidazole; pH 7.3). The column eluant was then exchanged into 50 mM HEPES (EMD Biosciences, Inc., La Jolla, CA) with 20% glycerol utilizing an Amicon centrifugal filter device.

For His₆-tag removal, the Novagen thrombin cleavage kit and protocol were utilized. Briefly, purified protein was exchanged into thrombin protease cleavage buffer (200 mM Tris-HCl pH 8.4, 1.5 mM NaCl, 2.5 mM CaCl₂, 10 mM DTT) utilizing an Amicon centrifugal filter device. The tagged protein was incubated for 18 h with gentle shaking at 4 °C. Streptavidin agarose beads bound biotinylated thrombin during a 30 min incubation at room temperature. Beads were removed via spin column filtration at 500 x g using a bench top microcentrifuge (Thermo Electron Corporation, Waltham, MA) provided with the

kit. The column eluant was then exchanged into 50 mM HEPES (EMD Biosciences, Inc., La Jolla, CA) with 20% glycerol utilizing an Amicon centrifugal filter device. Proteins were quantified utilizing the Bradford protein quantification assay.

7.4.5 Purification of nisin and subtilin.

Nisin was purified and characterized as described previously (9). Subtilin was purified from spent media of *B. subtilis* ATCC 6633 cultures. *B. subtilis* ATCC was cultured at 37 °C for 12, 15, or 18 h in 500 mL of LB broth. The culture was centrifuged at 8,000 xg for 20 min at 4 °C, and supernatants were filter sterilized and loaded onto a Varian C18 bond-elute column twice (Agilent Technologies, Santa Clara, CA) pre-equilibrated with 50% acetonitrile (Fisher Chemical). Bound peptide was washed and then eluted with a gradient of 0-100% acetonitrile utilizing a 10% step-wise increase of 50 mL fractions. Matrix Assisted Laser Desorption/Ionization – Time Of Flight (MALDI-TOF) mass spectrometry (General Electric, NY) was performed to identify the fractions that contained purified subtilin. Fractions containing subtilin were pooled and lyophilized. Dried peptide was resuspended in 30% acetonitrile with 0.1% trifluoroacetic acid (TFA, Sigma Aldrich), and Reverse Phase-High Performance Liquid Chromatography (RP-HPLC, Waters, Milford, MS) was performed with a PrePack C4 semi-preparative column (Waters, Milford, MS, diameter 25 mm, length 100 mm) with a gradient of 0-100% acetonitrile. Under these conditions, subtilin had a retention time of 29 min. Acetonitrile and TFA were removed from

fractions containing subtilin by rotary evaporation followed by lyophilization to remove water. The identity of purified subtilin was confirmed by MALDI-TOF mass spectrometry. Prior to use, lyophilized nisin was weighed on an analytical balance and dissolved in 0.1 M MOPS pH 6.8 to yield the desired concentration.

7.4.6 Labeling of nisin and vancomycin.

See Chapter 3 for methods.

7.4.7 Epi-Fluorescence microscopy.

Samples of *B. subtilis* 6633 cultured in Difco sporulation media (DSM , 0.8% Bacto nutrient broth, BD Diagnostics; 0.1% KCl, Fisher Chemical; 0.025% MgSO₄, Fisher Chemical; Millipore deionized water), TY broth (0.8% Tryptone, 0.5% yeast extract, 0.5% NaCl, Millipore dionized water) for 12 h were incubated with 0.1, 0.5, 1 μ M b-vancomycin or b-nisin for 5 min. Samples were fixed by incubation in 4% formaldehyde (Sigma) for 30 min at 37 °C followed by mounting on glass slides in 20% glycerol (Sigma) or Slow-Fade[®] antifade reagent (Invitrogen) under glass cover slips for epi-fluorescence microscopy. Live epi-fluorescence microscopy was also performed by mounting samples on glass slides in 0.5% agarose under cover slips. Differential interference contrast (DIC) and fluorescence microscopy images were collected with an Applied Precision assembled DeltaVision epi-fluorescence microscope containing an Olympus Plan Apo x100 oil objective with a numerical aperture of 1.42 and a working distance of 0.15 mm using CFP (Ex. 430/24, Em.470/24), FITC (Ex. 490/20, Em. 528/38),

rhodamine (Ex. 555/28, Em. 617/73), and CY-5 (Ex. 640/20, Em. 685/40) filter sets, and the images were processed with the SoftWoRX (Issaquah, WA) Explorer Suite program.

7.4.8 Circular dichroism.

Circular dichroism (CD) spectra was collected for Nisl Δ 1-19 with increasing concentrations of nisin (0, 5, 10, and 50 μ M) in the far-UV range utilizing a J-720 CD spectropolarimeter from JASCO (Easton, MD). A cylindrical cuvette with a total volume of 350 μ L and a path length of 0.1 cm was used for each assay. The CD spectra of Nisl Δ 1-19 (5.0 μ M) in optically clear borate buffer (50 mM potassium borate, pH 8.0) was recorded from 190 to 260 nm at a scan rate of 50 nm/s with a 1-nm wavelength step and with five accumulations.

Data acquisition was coordinated using the JASCO Spectra Manager v1.54A software. Raw data files were uploaded onto the DICHROWEB online server (<http://www.cryst.bbk.ac.uk/cdweb/html/home.html>) and analyzed using the CDSSTR algorithm with reference set 4, which is optimized for the analysis of data recorded in the range from 190 to 240 nm (13).

7.4.9 Oligomerization analysis - size exclusion chromatography and native gel electrophoresis.

Size exclusion chromatography was conducted using an AKTA Purifier 900 fast protein liquid chromatography (FPLC) system (GE Healthcare) equipped with a Superdex 200 10/300 GL size exclusion column (GE Healthcare) and a

UV detector (GE Healthcare). Nisl Δ 1-19 (5 μ M; 100 μ l) or a gel filtration standard mixture was injected onto the column pre-equilibrated with 0.1 M MOPS (Fisher Chemical, pH 6.8) liquid phase at a flow rate of 0.5 mL/min. Standard curves were generated by plotting the log of the molecular weights (provided by the supplier) of the gel filtration standards versus retention times. Experimental retention times were used to calculate the apparent molecular weights of Nisl Δ 1-19 in the presence and absence of 50 μ M nisin from the standard curve. To confirm FPLC results native-PAGE was performed.

7.4.10 Immunoblot analysis.

Samples removed from *B. subtilis* ATCC 6633 cultures were mixed with an equal volume of 2x sodium dodecyl sulfate (SDS) sample buffer (4% SDS, 100 mM Tris, 0.4 mg bromophenol blue/ml, 0.2 M dithiothreitol, 20% glycerol). The samples were boiled for 5 min and were resolved by SDS-PAGE (10% acrylamide). The contents of the gels were electrotransferred to nitrocellulose membranes (Pierce, Rockford, IL). The membranes were probed for the presence of GFP, MYC, HA, and TC using anti-GFP mouse monoclonal antibody (Sigma Aldrich), anti-MYC mouse monoclonal antibody (Invitrogen), anti-HA rabbit monoclonal antibody (Sigma Aldrich), and ReAsh (Invitrogen), respectively. Goat horseradish peroxidase-conjugated anti-mouse or rabbit immunoglobulin G (Abcam Inc., Cambridge, MA) was used as the secondary antibody, and cross-reacting material was visualized after the blots were exposed to X-ray film (Denville Scientific Inc., Metuchen, NJ) in the

presence of the enhanced chemiluminescence immunoblotting reagent (Pierce, Rockford, IL). ReAsH was detected using a Typhoon gel scanner (GE healthcare).

7.4.11 Structure prediction.

The secondary structures of Nisl Δ 1-19 and Spal Δ 1-22 predictions were performed using the consensus prediction method on the NPS@ web server (network protein sequence analysis; http://npsa-pbil.ibcp.fr/cgi-bin/npsa_automat.pl?page=/NPSA/npsa_seccons.html) of the Pôle BioInformatique Lyonnais (4).

7.4.12 Statistics.

All data are representative of those from three or more independent experiments. Error bars represent standard deviations. *P* values were calculated with Student's *t* test using paired, one-tailed distribution. *P* values of <0.05 indicate statistical significance. All statistics, including means, standard deviations, and Student's *t* tests, were calculated using Microsoft Excel (version 11.0).

7.5 References

1. **Adams, S. R., and R. Y. Tsien.** 2008. Preparation of the membrane-permeant biarsenicals FIAsH-EDT2 and ReAsH-EDT2 for fluorescent labeling of tetracysteine-tagged proteins. *Nat Protoc* **3**:1527-34.
2. **Asaduzzaman, S. M., and K. Sonomoto.** 2009. Lantibiotics: diverse activities and unique modes of action. *J Biosci Bioeng* **107**:475-87.

3. **Chatterjee, C., Paul, M., Xie, L, van der Donk, W. A.** 2005. Biosynthesis and Mode of Action of Lantibiotics. *Chem Rev* **105**:633-683.
4. **Combet, C., C. Blanchet, C. Geourjon, and G. Deleage.** 2000. NPS@: network protein sequence analysis. *Trends Biochem Sci* **25**:147-50.
5. **Daniel, R. A., and J. Errington.** 2003. Control of cell morphogenesis in bacteria: two distinct ways to make a rod-shaped cell. *Cell* **113**:767-76.
6. **Draper, L. A., R. P. Ross, C. Hill, and P. D. Cotter.** 2008. Lantibiotic immunity. *Curr Protein Pept Sci* **9**:39-49.
7. **Feucht, A., and P. J. Lewis.** 2001. Improved plasmid vectors for the production of multiple fluorescent protein fusions in *Bacillus subtilis*. *Gene* **264**:289-97.
8. **Field, D., C. Hill, P. D. Cotter, and R. P. Ross.** 2010. The dawning of a 'Golden era' in lantibiotic bioengineering. *Mol Microbiol* **78**:1077-87.
9. **Gut, I. M., A. M. Prouty, J. D. Ballard, W. A. van der Donk, and S. R. Blanke.** 2008. Inhibition of *Bacillus anthracis* spore outgrowth by nisin. *Antimicrob Agents Chemother* **52**:4281-8.
10. **Heinzmann, S., K. D. Entian, and T. Stein.** 2006. Engineering *Bacillus subtilis* ATCC 6633 for improved production of the lantibiotic subtilin. *Appl Microbiol Biotechnol* **69**:532-6.
11. **Kaltwasser, M., T. Wiegert, and W. Schumann.** 2002. Construction and application of epitope- and green fluorescent protein-tagging integration vectors for *Bacillus subtilis*. *Appl Environ Microbiol* **68**:2624-8.
12. **Koponen, O., T. M. Takala, U. Saarela, M. Qiao, and P. E. Saris.** 2004. Distribution of the NisI immunity protein and enhancement of nisin activity by the lipid-free NisI. *FEMS Microbiol Lett* **231**:85-90.
13. **Lobley, A., L. Whitmore, and B. A. Wallace.** 2002. DICHROWEB: an interactive website for the analysis of protein secondary structure from circular dichroism spectra. *Bioinformatics* **18**:211-2.
14. **Lubelski, J., R. Rink, R. Khusainov, G. N. Moll, and O. P. Kuipers.** 2008. Biosynthesis, immunity, regulation, mode of action and engineering of the model lantibiotic nisin. *Cell Mol Life Sci* **65**:455-76.

15. **Nguyen, H. D., Q. A. Nguyen, R. C. Ferreira, L. C. Ferreira, L. T. Tran, and W. Schumann.** 2005. Construction of plasmid-based expression vectors for *Bacillus subtilis* exhibiting full structural stability. *Plasmid* **54**:241-8.
16. **Piper, C., P. D. Cotter, R. P. Ross, and C. Hill.** 2009. Discovery of medically significant lantibiotics. *Curr Drug Discov Technol* **6**:1-18.
17. **Ross, A. C., and J. C. Vederas.** 2010. Fundamental functionality: recent developments in understanding the structure-activity relationships of lantibiotic peptides. *J Antibiot (Tokyo)*.
18. **Stein, T., S. Heinzmann, P. Kiesau, B. Himmel, and K. D. Entian.** 2003. The spa-box for transcriptional activation of subtilin biosynthesis and immunity in *Bacillus subtilis*. *Mol Microbiol* **47**:1627-36.
19. **Takala, T. M., O. Koponen, Q. Mingqiang, and P. E. Saris.** 2004. Lipid-free NisI: interaction with nisin and contribution to nisin immunity via secretion. *FEMS Microbiol Lett* **237**:171-177.
20. **Takala, T. M., and P. E. Saris.** 2006. C-terminus of NisI provides specificity to nisin. *Microbiology* **152**:3543-9.
21. **Tiyanont, K., T. Doan, M. B. Lazarus, X. Fang, D. Z. Rudner, and S. Walker.** 2006. Imaging peptidoglycan biosynthesis in *Bacillus subtilis* with fluorescent antibiotics. *Proc Natl Acad Sci U S A* **103**:11033-8.

CHAPTER 8: CONCLUSIONS AND FUTURE DIRECTIONS

8.1 Introduction

Nisin is most effective against Gram-positive bacteria, and few strains have developed resistance in spite of unregulated worldwide use in the food industry due to the three distinct activities (3). Nisin exerts its bactericidal effects through pore formation (11) and/or disruption of cell wall biosynthesis functioning as a transglycosylase inhibitor by binding to lipid II (4, 13). A third activity attributed to nisin is the prevention of spore outgrowth (2). Previous studies demonstrated through phase contrast microscopy that nisin prevents the outgrowth of both *Bacillus* and *Clostridia* spores (2, 7). The exact manner in which nisin alters *Bacillus* spores to inhibit outgrowth had not been characterized. Dha5 was reported to be essential for outgrowth inhibition and postulated to form a covalent bond with a Cys in a spore protein (8).

In the studies presented this thesis, *Bacillus anthracis* Sterne 7702 was used as a model organism to determine the mechanism by which nisin inhibits outgrowth, to identify nisin's target(s), and to determine the requirement of pore formation for outgrowth inhibition. In addition, an *in vitro* infection model was developed and used to demonstrate that nisin is protective against spore infection of immune cells. Finally, constructs and protocols have been developed to monitor the localization of the immunity proteins of a lantibiotic producer.

8.2 Summary of Results

8.2.1 Characterization of the consequences of *Bacillus anthracis* exposure to nisin.

First, it was determined that nisin inhibits spore outgrowth with IC_{50} and IC_{90} values of 0.60 μM and 0.95 μM , respectively. Colony forming unit (CFU) analysis revealed that no recoverable spores were observed after incubation with nisin concentrations $\geq 1 \mu\text{M}$ in brain heart infusion broth. Differential interference contrast microscopy experiments provided congruent data illustrating outgrowth inhibition at nisin concentrations $\geq 1 \mu\text{M}$. These observations were confirmed via spectrophotometric analysis at O.D. $_{600 \text{ nm}}$ and with scanning electron microscopy. These data taken as a whole demonstrated that nisin has the ability to inhibit outgrowth of *Bacillus anthracis* spores.

When spores were incubated with nisin, the inability to detect recoverable CFUs could be due to irreversible inhibition of germination initiation by nisin or spore killing post germination initiation. Loss of refractility, which signifies spore hydration, and loss of heat resistance are two classical determinants of germination (5, 12). Spores were able to initiate germination in the presence of BHI in all nisin concentrations (0-100 μM). In fact, nisin required the initiation of germination to inhibit spores, and the inhibition was irreversible. This later point was demonstrated by incubating spores with 10 μM nisin in the presence or the absence of BHI followed by washing and resuspension in nisin free BHI and monitoring growth after 18 h. Further confirmation that nisin requires germination was provided by the observation that only spores incubated with BODIPY-nisin in

the presence of BHI exhibited nisin associated fluorescent labeling of spores. Collectively, these data demonstrated that nisin requires germination initiation allowing spore-nisin interaction to induce irreversible inhibition.

Previous data demonstrated that early events of germination, loss of refractility and heat resistance, occurred while a late event of germination, outgrowth, was inhibited. Nisin was then evaluated for its ability to modulate other hallmarks of germination. Since toxin expression is essential for anthrax infection and disease, lethal toxin (LT), which is composed of lethal factor (LF) and protective antigen (PA), was assayed for expression by immunoblot when spores were incubated in the presence of 10 μM nisin in BHI. After 7 h and 10 h, expression of either component of LT was not observed. Additionally, spores and bacilli were homogenized and assayed for the components of LT. LF and PA were only observed in association with bacilli. Subsequently, oxidative metabolism was assayed by monitoring the conversion of tetrazolium to formazan. Spores germinated in nisin concentrations $\geq 1 \mu\text{M}$ were devoid of oxidative metabolism. Under these conditions nisin inhibited membrane potential establishment through 10 h. Additional flow cytometric analysis using propidium iodide (PI) demonstrated a dose dependent increase in spore fluorescence. This increase in fluorescence was due to membrane permeabilization allowing PI to interact with spore DNA. Another event of germination is the release of dipicolinic acid (DPA) chelated to calcium. The release of DPA in solution can be monitored utilizing DPA-terbium energy transfer interactions in solution. Endospores germinated in the presence of nisin (0-100 μM) were able to release

DPA at similar rate and magnitude. These data also suggested indirectly that nisin does not inhibit the release of calcium. Further analysis of germination utilizing transmission electron microscopy demonstrated that nisin did not inhibit the shedding of the sporecoat, exosporium, or cortex during germination.

Additional research of the nisin pore demonstrated that the pore allows the efflux of Cl^- and K^+ ions and the influx of PicoGreen DNA dye while not releasing spore DNA and cytosolic proteins through lysis of the spore. Nisin-mediated membrane disruption can be inhibited with ion channel blockers or polyethylene glycol in a manner that suggests that the membrane perturbations are approximately 2 nm in diameter and slightly anion selective. These data taken as a whole demonstrate nisin inhibition of spore outgrowth and metabolic function through membrane potential dissipation via cell membrane permeabilization.

8.2.2 Nisin inhibits outgrowth via membrane disruption.

BODIPY-nisin and fluorescein-vancomycin were used to identify lipid II as a target for outgrowth inhibition demonstrated via co-localization studies with epifluorescence microscopy. Competition assays between vancomycin and nisin revealed that vancomycin blocked nisin binding and visa versa, which confirms nisin binding of lipid II for spore outgrowth inhibition. In an effort to identify a covalently bound protein target for outgrowth inhibition, biotin- and fluorescent-nisin were used as probes, however such a target was not isolated. The activity of wt nisin was compared against vancomycin (lipid II binding), nisin 1-21 (non-pore forming, but lipid II binding), nisin N20P/M21P (non-pore forming, but lipid II

binding), nisin M21P/K22P (non-pore forming, but lipid II binding), and ciprofloxacin (DNA gyrase inhibitor). These studies revealed that lipid II binding is not sufficient for outgrowth inhibition, and that the pore forming activity of wt nisin is essential to prevent membrane potential establishment resulting in outgrowth inhibition. However, the nisin S5A mutant still retains the ability to inhibit membrane potential establishment and outgrowth while disrupting the membrane, which demonstrates that Dha5 is not essential for inhibition of germinating spores.

8.2.3 Nisin is protective with respect to in vitro infection of mammalian immune cells.

Next, the effectiveness of nisin in an *in vitro* infection model was evaluated. First, a completely non-germinating infection model had to be developed. These investigations identified an *in vitro* infection model that was devoid of fetal bovine serum and utilizing either DMEM or RPMI as cell culture media that did not induce spore germination within 4 h while maintaining the health of the immune cells. Utilizing this infection model it was determined that nisin aided, in a dose dependent manner, clearance of spores while increasing immune cell survival with continuous spore infection of cultured peritoneal and alveolar macrophages and dendritic cells. In addition, nisin also reduced the uptake of spores for all cell lines in germinating conditions while not affecting spore binding assays. The use of fluorescein-nisin demonstrated spore-nisin localization within a phagosome of a peritoneal macrophage illustrating that nisin

can interact with a spore within a phagosome. In addition, nisin reduced spore-induced expression of IL-1 β , IL-6, TNF- α , and G-CSF.

8.2.4 Localization and activity of immunity proteins for protection against lantibiotics in producing organisms.

Immunity to nisin and subtilin by the native producer is derived via the synergistic cooperation between LanI, to bind and reduce the concentration of the lantibiotic, and an ATP- dependent transporter, LanFEG, to remove it from the membrane (2). NisI was cloned, purified, and over-expressed. Native gel and gel filtration data indicate that NisI remains in a dimer with no significant structural changes observed by circular dichroism, and NisI retains a highly disordered secondary structure in the presence of nisin. To monitor the localization of the immunity genes the subtilin equivalent of LanF, which is SpaF, has been tagged on the chromosome with GFP or HA tags while SpaI was tagged with tetra-cysteine or cMYC expressed from plasmids in *B. subtilis* 6633 and 168. A protocol has been optimized for lipid II localization using Bodipy-633-vancomycin.

8.3 Conclusions and Future Directions

In this thesis the mechanism and target for nisin inhibition of spore outgrowth has been identified, and a model for the mode of action has been developed (Figure 8.1). Upon germination of *B. anthracis* spores, nisin will interact with spore lipid II to disrupt the membrane, presumably by pore

formation. This disruption of the membrane will allow the flow of small molecules and ions, most importantly H^+ , thus preventing the establishment of a membrane potential. The data suggest that the nisin-lipid II interaction could facilitate the inhibition of other spore-forming bacteria from the genera *Bacillus* and *Clostridium*, including those of medical relevance such as *C. botulinum* and *C. difficile*. Further investigation is necessary to confirm the potential universal nature of this mechanism. It is anticipated that other lantibiotics such as subtilin (6, 10), epidermin (1), and haloduracin (9) would also inhibit spore outgrowth utilizing the same mechanism. Furthermore, any antimicrobial that either specifically dissipates a membrane potential, FCCP for example, or is membrane disrupting would inhibit spore outgrowth. However, the interaction of nisin with lipid II provides specificity to nisin-mediated membrane disruption preventing non-specific killing of mammalian cells as would be observed with a non-specific inhibitor. Further investigation is required to determine whether the above listed lantibiotics as well as other membrane acting antimicrobials would also inhibit spore outgrowth.

Upon the development of an entirely non-germinating *in vitro* infection model, nisin was evaluated for its ability to alter the outcome of spore infections of mammalian cells. Nisin significantly tipped the scale in the favor of the immune cell. The addition of nisin reduced the number of viable *B. anthracis* recovered from immune cells while increasing immune cell survival and reducing infection mediated cytokine expression in both germinating and non-germinating conditions. Spore uptake was decreased as a result of reduced spore binding to

immune cells. However, the mechanism by which nisin inhibits spore attachment to immune cells is not understood and requires further investigation. The ability of nisin or another pore-forming lantibiotic such as haloduracin, which is more stable (9), to clear a *B. anthracis* infection would be accurately assessed in an *in vivo* mouse infection model utilizing *B. anthracis* Ames (which expresses toxins and capsule). The results from an *in vivo* infection would determine whether nisin or lantibiotics as a group of antimicrobials could function as a relevant treatment option for spore-forming bacterial infections.

Figure 8.1

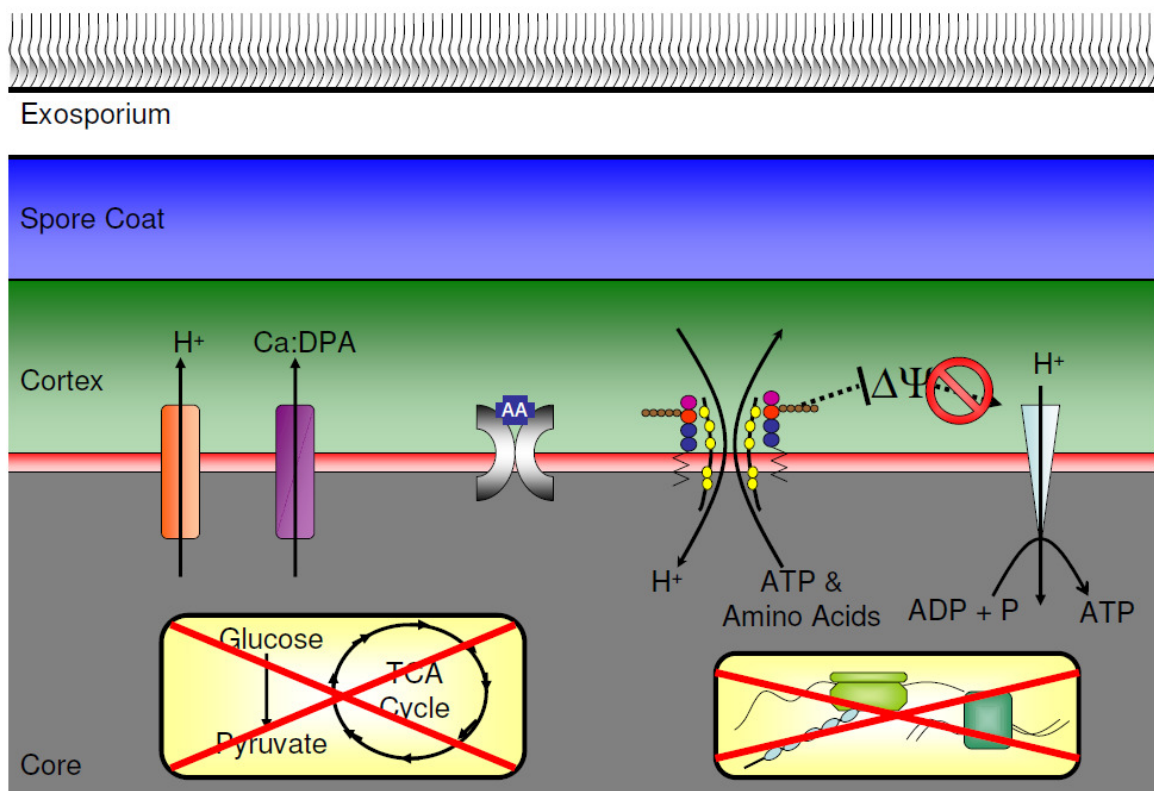


Figure 8.1. Model of nisin mode of action. Upon binding of an amino acid germinant (AA), spores will efflux H⁺ and Ca²⁺ chelated to dipicolinic acid (DPA), hydrate the core, and degrade and shed the cortex, spore coat, and exosporium. Concurrently, nisin will hydrogen bond to lipid II inserted into the membrane forming pores preventing membrane potential

Figure 8.1 (continued)

establishment and allowing the efflux of small molecules without inducing lysis. Nisin renders the spore metabolically inactive and unable to synthesize macromolecules such as RNA and protein. The nisin-lipid II interaction also suggest that nisin will inhibit transglycosylation as a second mode of action against spores.

8.4 References

1. **Brotz, H., M. Josten, I. Wiedemann, U. Schneider, F. Gotz, G. Bierbaum, and H. G. Sahl.** 1998. Role of lipid-bound peptidoglycan precursors in the formation of pores by nisin, epidermin and other lantibiotics. *Mol Microbiol* **30**:317-27.
2. **Chan, W. C., H. M. Dodd, N. Horn, K. Maclean, L. Y. Lian, B. W. Bycroft, M. J. Gasson, and G. C. Roberts.** 1996. Structure-activity relationships in the peptide antibiotic nisin: role of dehydroalanine 5. *Appl Environ Microbiol* **62**:2966-9.
3. **Delves-Broughton, J., P. Blackburn, R. J. Evans, and J. Hugenholtz.** 1996. Applications of the bacteriocin, nisin. *Antonie Van Leeuwenhoek* **69**:193-202.
4. **Hasper, H. E., N. E. Kramer, J. L. Smith, J. D. Hillman, C. Zachariah, O. P. Kuipers, B. de Kruijff, and E. Breukink.** 2006. An alternative bactericidal mechanism of action for lantibiotic peptides that target lipid II. *Science* **313**:1636-7.
5. **Levinson, H. S., and M. T. Hyatt.** 1966. Sequence of events during *Bacillus megaterim* spore germination. *J Bacteriol* **91**:1811-8.
6. **Liu, W., and J. N. Hansen.** 1992. Enhancement of the chemical and antimicrobial properties of subtilin by site-directed mutagenesis. *J Biol Chem* **267**:25078-85.
7. **Mazzotta, A. S., A. D. Crandall, and T. J. Montville.** 1997. Nisin Resistance in *Clostridium botulinum* Spores and Vegetative Cells. *Appl Environ Microbiol* **63**:2654-2659.
8. **Morris, S. L., R. C. Walsh, and J. N. Hansen.** 1984. Identification and characterization of some bacterial membrane sulfhydryl groups which are targets of bacteriostatic and antibiotic action. *J Biol Chem* **259**:13590-4.

9. **Oman, T. J., and W. A. van der Donk.** 2009. Insights into the mode of action of the two-peptide lantibiotic haloduracin. *ACS Chem Biol* **4**:865-74.
10. **Parisot, J., S. Carey, E. Breukink, W. C. Chan, A. Narbad, and B. Bonev.** 2008. Molecular mechanism of target recognition by subtilin, a class I lanthionine antibiotic. *Antimicrob Agents Chemother* **52**:612-8.
11. **Ruhr, E., and H. G. Sahl.** 1985. Mode of action of the peptide antibiotic nisin and influence on the membrane potential of whole cells and on cytoplasmic and artificial membrane vesicles. *Antimicrob Agents Chemother* **27**:841-5.
12. **Vary, J. C., and H. O. Halvorson.** 1965. Kinetics of germination of *Bacillus* spores. *J Bacteriol* **89**:1340-7.
13. **Wiedemann, I., E. Breukink, C. van Kraaij, O. P. Kuipers, G. Bierbaum, B. de Kruijff, and H. G. Sahl.** 2001. Specific binding of nisin to the peptidoglycan precursor lipid II combines pore formation and inhibition of cell wall biosynthesis for potent antibiotic activity. *J Biol Chem* **276**:1772-9.

CURRICULUM VITAE

Ian M. Gut

Education

Master's Degree in Microbiology
University of Illinois - Urbana/Champaign
Overall GPA 3.74
October 2008

Bachelor of Arts and Sciences in Biology
Benedictine University, Lisle, IL
Overall GPA 3.651
Dean's List
May 2003

Emergency Medical Technician - Basic
Northwest Community Hospital and
William R. Harper College
May 2003

Experience

Cell Structure and Function Teacher's Assistant
Molecular Biology Teacher's Assistant
Microbiology Lab Teacher's Assistant
Chemistry Lab Teacher's Assistant
Aug. 2008 – Dec. 2008
Jan. 2006 – May 2006
Jan. 2003 – May 2003
Jan. 2001 – May 2002

Lawrence Food, Inc.
Research and development scientist
Nov. 2004 – July 2005

Hospital Observation
Benedictine University and Edward Hospital
Jan. 2002 – May 2002

Surgical Sales Internship
Smith & Nephew, Chicago, IL
May 2001 – Aug. 2001

Honors

Catherine Connor Outstanding Dissertation
in Biotechnology
University of Illinois – Urbana/Champaign:
Roy J. Carver Biotechnology Center
2011

James R. Beck Microbiology Graduate Fellowship
University of Illinois – Urbana/Champaign
2010, 2009

Graduate College Travel Award
University of Illinois – Urbana/Champaign
2009

Corporate Activities Program Student Travel Grant for ASM General Meeting American Society of Microbiology	2008
Chemical Biology Interface Fellowship funded by the NIH University of Illinois – Urbana/Champaign	Aug. 2006 – July 2008
Tri-Beta Biological Honor Society Benedictine Univeristy	2002

Affiliations

Faculty of 1000 Associate Faculty Member	Dec. 2009 - 2010
American Society of Microbiology	2006 – 2010

Publications

Ian M. Gut, Batcha Tamilselvam, Angela M. Prouty, Bojana Stojkovic, Stephanie Czeschin, Wilfred A. van der Donk, and Steven R. Blanke. *Bacillus anthracis* spore interactions with mammalian cells: Relationship between medium composition, germination state, and the outcome of *in vitro* infections. *BMC Microbiology*. 2011 Feb;11(46).

Ian M. Gut and Steven R. Blanke, Faculty of 1000 evaluations, dissents and comments for[Kolodkin-Gal I et al. D-amino acids trigger biofilm disassembly. *Science*. 2010 Apr 30; 328(5978):627-9; doi: 10.1126/science.1188628]. Faculty of 1000, 06 Oct 2010. F1000.com/3213956.

I. Gut, A. Prouty, W. A. van der Donk, and S. R. Blanke. Cellular effects of nisin inhibition against *Bacillus anthracis* Sterne 7702. *Antimicrobial Agents and Chemotherapy*. 2008 Dec;52(12):4281-8.

Ian M. Gut, Steven R. Blanke, and Wilfred A. van der Donk . Mechanism of Nisin Inhibition of *Bacillus anthracis* Spore Outgrowth. Submitted.

Ian M. Gut, Batcha Tamilselvam, Wilfred A. van der Donk, and Steven R. Blanke. Nisin modulation of *Bacillus anthracis* spore and immune cell interactions and survival. Submitted - Revisions.

Scholarly Activities - Oral Presentations

Understanding the cellular effects of nisin inhibition of spore outgrowth.	October 2, 2010
Department of Microbiology Annual Conference - University of Illinois - Urbana/Champaign	

Nisin inhibition of germinated *Bacillus* spores. March 30, 2010
 Department of Microbiology Student Seminar - University of Illinois -
 Urbana/Champaign

Nisin inhibitory interactions and immunity. March 10, 2009
 Department of Microbiology Student Seminar - University of Illinois -
 Urbana/Champaign

Nisin Localization and Inhibition of *Bacillus anthracis* November 14, 2008
 Spore Outgrowth.
 Cell and Molecular Biology & Molecular Biophysics Training Grants - 21th Annual
 Research Symposium - Invited Presentation - University of Illinois -
 Urbana/Champaign

Inhibitory Interactions of Nisin Prevent *Bacillus anthracis* September 5, 2008
 Spore Outgrowth.
 Chemical Biology Interface 4th Annual Research Symposium – Univeristy of
 Illinois – Urbana/Champaign

Effects of Nisin Against *Bacillus anthracis* During April 8, 2008
 Endospore Germination.
 Department of Microbiology Student Seminar - University of Illinois -
 Urbana/Champaign

Elucidating the Effects of Nisin Against *Bacillus anthracis*. October 18, 2007
 Chemical Biology Interface - University of Illinois - Urbana/Champaign

Characterizing an Alternative Function of Nisin against October 17, 2007
Bacillus anthracis.
 Chemical Biology Interface - University of Illinois - Urbana/Champaign

Characterizing the Third Function of Nisin against October 11, 2007
Bacillus anthracis.
 Chemical Biology Interface - University of Illinois - Urbana/Champaign

The Small Protein Inhibition of *Bacillus anthracis*. August 31, 2007
 Chemical Biology Interface - University of Illinois - Urbana/Champaign

Lantibiotic Inhibition of *Bacillus anthracis*. April 12, 2007
 Chemical Biology Interface - University of Illinois - Urbana/Champaign

The Lantibiotic Nisin Inhibition of *Bacillus anthracis*. March 15, 2007
 Chemical Biology Interface - University of Illinois - Urbana/Champaign

Scholarly Activities - Poster Presentations

Lantibiotics, expanding the classes of clinically relevant antimicrobial agents that inhibit *Bacillus anthracis* spore outgrowth. October 22, 2010

Cell and Molecular Biology & Molecular Biophysics Training Grants - 23rd Annual Research Symposium University of Illinois - Urbana/Champaign

Lysosomal remodeling and escape of *Bacillus anthracis* from infected immune cells. October 22, 2010

Cell and Molecular Biology & Molecular Biophysics Training Grants - 23rd Annual Research Symposium University of Illinois - Urbana/Champaign

Dynamic remodeling and escape of *Bacillus anthracis* containing intracellular vesicles from infected immune cells. October 2, 2010

Department of Microbiology Annual Conference - University of Illinois - Urbana/Champaign

Lantibiotics, expanding the classes of clinically relevant: antimicrobial agents Nisin-dependent *Bacillus anthracis* spore outgrowth inhibition. September 11, 2010

Midwest Microbial Pathogenesis Conference - Washington University, St. Louis

Novel mechanism of spore-mediated dynamic remodeling and escape of intracellular *Bacillus anthracis* containing vesicles (BCVs) from infected immune cells. September 11, 2010

Midwest Microbial Pathogenesis Conference - Washington University, St. Louis

Brothers in arms: synergistic interactions between host immune cells and antibiotics in control of bacterial infections. October 16, 2009

Cell and Molecular Biology & Molecular Biophysics Training Grants - 22nd Annual Research Symposium University of Illinois - Urbana/Champaign

A novel mechanism of anthrax spore dissemination: Intracellular remodeling and escape of bacillus anthracis spores for immune cells. October 16, 2009

Cell and Molecular Biology & Molecular Biophysics Training Grants - 22nd Annual Research Symposium University of Illinois - Urbana/Champaign

Nisin modulation of *B. anthracis* spore and immune cell interactions and survival. September 26, 2009

Department of Microbiology Annual Conference - University of Illinois - Urbana/Champaign

Remodeling and escape of *Bacillus anthracis* spores from immune cells. September 26, 2009

Department of Microbiology Annual Conference - University of Illinois - Urbana/Champaign

Lantibiotics as an expanding class of antimicrobial agents September 2, 2009
refractive to resistance: Nisin- dependent *Bacillus anthracis* spore outgrowth
inhibition.

Bacillus-ACT 2009 The International *B. anthracis*, *B. cereus*, and *B.*
thuringiensis Conference - Santa Fe, New Mexico

Nisin interactions with *Bacillus anthracis* spores to inhibit May 19, 2009
outgrowth.

109th American Society of Microbiology General Meeting – Philadelphia, PA

Pathogen-Induced exocytosis of *Bacillus anthracis* November 14, 2008
spores from within infected host immune cells.

Cell and Molecular Biology & Molecular Biophysics Training Grants - 21st Annual
Research Symposium University of Illinois - Urbana/Champaign

Nisin Targeting and Activity Against *Bacillus anthracis* September 20, 2008
Spores.

Department of Microbiology Annual Conference - University of Illinois -
Urbana/Champaign

The Great Escape: Egress of *B. anthracis* from host cells September 20, 2008
as a mechanism for dissemination during inhalational anthrax.

Department of Microbiology Annual Conference - University of Illinois -
Urbana/Champaign

Small Protein Effects on Spores. April 18, 2008

New and Reemerging Infectious Disease Conference

Department of Veterinary Medicine- University of Illinois - Urbana/Champaign

Inhibitory Effects of Nisin Against *Bacillus anthracis* June 8, 2008
Spores.

108th American Society of Microbiology General Meeting – Boston, MA

Nisin effects on *Bacillus anthracis* germination. November 2, 2007

Cell and Molecular Biology & Molecular Biophysics Training Grants - 20th Annual
Research Symposium

University of Illinois - Urbana/Champaign

Department of Microbiology Annual Conference Co-Chair October 13, 2007

University of Illinois - Urbana/Champaign

Effect of Nisin on *Bacillus anthracis* Germination and October 13, 2007
Growth.

Department of Microbiology Annual Conference - University of Illinois -
Urbana/Champaign

Nisin Inhibition of *Bacillus anthracis* Growth. September 29, 2007
Midwest Microbial Pathogenesis Conference - Northwestern University

Characterization of the Inhibitory Effects of Nisin Against *Bacillus anthracis*. April 20, 2007
New and Reemerging Infectious Disease Conference
Department of Veterinary Medicine- University of Illinois - Urbana/Champaign

Characterization of the Inhibitory Effects of Nisin Against *Bacillus anthracis*. October 15, 2006
Department of Microbiology Annual Conference - University of Illinois -
Urbana/Champaign

Mentoring

Isabel Neacato, Microbiology Graduate Student, Univeristy of Illinois - Urbana/Champaign	2010-2011
Stephanie Czeschin, Molecular and Cellular Biology Undergraduate, University of Illinois - Urbana/Champaign	2009-2011
Katie Whalen, Biochemistry Graduate Student, Univeristy of Illinois - Urbana/Champaign	2009
Christian Dewan, Molecular and Cellular Biology Undergraduate, University of Illinois - Urbana/Champaign	2008-2010
Paul Dilfer, Molecular and Cellular Biology Undergraduate, University of Illinois - Urbana/Champaign	2008-2009
Mychal Kelly, Molecular and Cellular Biology Undergraduate, University of Illinois - Urbana/Champaign	2008
Lindsey Johnstone, Chemical Biology Graduate Student, University of Illinois - Urbana/Champaign	2007
Brett Chrobot, Molecular and Cellular Biology Undergraduate, University of Illinois - Urbana/Champaign	2007-2008

Skills

Boiling Point	Recrystallization	Filtration
Aseptic Technique	Distillation	Gas Chromatography
Melting Point	Gel-Electrophoresis	PCR
Subcellular Fractionation	Gram Staining	Column Chromatography
Bacterial Plating	Titration	Flow Cytometry
HPLC	Molecular Biology	Mass Spectrometry
Radioactivity	Protein Purification	Cell Culture
BSL-2 Organisms	Western Blotting	Protein Modification
ELISA	FPLC	ITC-Titrations
LC-MS/MS	Circular Dichroism	Confocal Microscopy
Epi-fluorescence Microscopy		
Transmission Election Microscopy		
Scanning Electron Microscopy		

Relevant

Coursework

General Chemistry	General Biology	Organic Chemistry & Lab
Physics	Human Anatomy	Cell Biology & Lab
Human Physiology	Nutrition	Genetics
Microbiology	Environmental Toxicology	Biometry
Microbial Genetics	Molecular Microbiology	Bacterial Pathogenesis
Physical Biochemistry	Enzyme Mechanisms and Reactions	
Advanced Biochemistry	Advanced Molecular Biology	
Natural Science Labs		

Specialized

Coursework

NCBI Mini Course: Identification of Disease Genes, University of Illinois	2007
NCBI Mini Course: Making Sense of DNA and Protein Sequences, University of Illinois	2007
NCBI Mini Course: Blast Quick Start, University of Illinois	2007
NCBI Mini Course: Structural Analysis Quick Start, University of Illinois	2007

Computers

Microsoft Word, Microsoft Excel, Microsoft PowerPoint, Microsoft Access, Internet, All Windows and OSX (Macintosh) Based Machines, ChemDraw, Summit (Flow Cytometry), FCS Express (Flow Cytometry), Graphpad Prism, KaleidaGraph, and Adobe Illustrator.